Remote activation of Frizzled receptors using magnetic nanoparticles for bone tissue engineering

Michael Rotherham

Thesis submitted for the degree of Doctor of Philosophy

October 2016

Keele University

SUBMISSION OF THESIS FOR A RESEARCH DEGREE

Part I. DECLARATION by the candidate for a research degree. To be bound in the thesis

Degree for which thesis being submitted: Doctor of Philosophy
Title of thesis: Remote activation of Frizzled receptors using magnetic nanoparticles for bone tissue engineering
This thesis contains confidential information and is subject to the protocol set down for the submission and examination of such a thesis.
NO
Date of submission: 17/6/16 Original registration date: 31/10/11
(Date of submission must comply with Regulation 2D)
Name of candidate: Michael Rotherham
Research Institute: ISTM Name of Lead Supervisor: Prof. Alicia El Haj

I certify that:

(a) The thesis being submitted for examination is my own account of my own research
(b) My research has been conducted ethically. Where relevant a letter from the approving body confirming that ethical approval has been given has been bound in the thesis as an Annex
(c) The data and results presented are the genuine data and results actually obtained by me during the conduct of the research
(d) Where I have drawn on the work, ideas and results of others this has been appropriately acknowledged in the thesis
(e) Where any collaboration has taken place with one or more other researchers, I have included within an 'Acknowledgments' section in the thesis a clear statement of their contributions, in line with the relevant statement in the Code of Practice (see Note overleaf).
(f) The greater portion of the work described in the thesis has been undertaken subsequent to my registration for the higher degree for which I am submitting for examination
(g) Where part of the work described in the thesis has previously been incorporated in another thesis submitted by me for a higher degree (if any), this has been identified and acknowledged in the thesis
(h) The thesis submitted is within the required word limit as specified in the Regulations

Total words in submitted thesis (including text and footnotes, but excluding references and appendices) …45,393……

Signature of candidate:…….. Date……..

Note

Extract from Code of Practice: If the research degree is set within a broader programme of work involving a group of investigators – particularly if this programme of work predates the candidate's registration – the candidate should provide an explicit statement (in an 'Acknowledgments' section) of the respective roles of the candidate and these other individuals in relevant aspects of the work reported in the thesis. For example, it should make clear, where relevant, the candidate's role in designing the study, developing data collection instruments, collecting primary data, analysing such data, and formulating conclusions from the analysis. Others involved in these aspects of the research should be named, and their contributions relative to that of the candidate should be specified (*this does not apply to the ordinary supervision, only if the supervisor or supervisory team has had greater than usual involvement*).

Abstract

The Wnt signalling pathways play crucial roles in development, tissue patterning, and stem cell fate determination. These pathways are therefore an attractive therapeutic target in the field of regenerative medicine and tissue engineering. Magnetic nanoparticles (MNP) are useful tools in bio-engineering. Previous work from our group has demonstrated the efficacy of targeting and activating cell signalling pathways using MNP functionalised with targeting proteins coupled with magnetic fields to remotely torque the MNP. Using this approach, in this work MNP were functionalised with ligands targeted to cell surface Frizzled receptors which are involved in Wnt signal transduction. The effects of remote stimulation with MNP on Wnt pathway activity were then assessed in human mesenchymal stem cells (hMSC). Results demonstrated that targeting of Frizzled receptors with MNP and remote stimulation using magnetic fields remotely activated Wnt signalling pathways. This was indicated by nuclear mobilisation of β-catenin and activation of a TCF/LEF luciferase reporter. The effect of remote Wnt pathway activation on hMSC osteogenesis was subsequently assessed. Activation was shown to augment hMSC differentiation in monolayer experiments where expression of osteogenic markers increased. This strategy also had beneficial effects on bone formation in an *ex vivo* foetal chick femur model as indicated by μCT and histology. The role of spatial Wnt gradients on bone formation is also important in development and was investigated using a tissue engineering platform utilising immobilised Wnt protein. In conclusion, these studies demonstrate the use of MNP to remotely activate Wnt signalling pathways and have shown potential in directing hMSC differentiation. This provides proof of concept for new injectable therapies that modulate cell signalling pathways with applications in regenerative medicine.

Key Words:

Wnt, Frizzled, MSC, Bone, MNP

Table of Contents

List of Tables

List of Figures

Chapter 1

Chapter 2

Chapter 3

Chapter 4

Chapter 5

Appendix

Abbreviations

4-MUP	= 4-Methylumbelliferyl phosphate
ACI	= Autologous Chondrocyte implantation
AER	= Apical Ectodermal Ridge
ALP	= Alkaline Phosphatase
APC	= Adenomatous polyposis coli
ATP	= Adenosine triphosphate
β-GP	=β-Glycerophosphate
BIO	= 6-Bromoindirubin-3’ -oxime
BMP	= Bone Morphogenetic protein
BSA	= Bovine Serum Albumin
CAMK	= Calcium/calmodulin-dependent kinase
cDNA	= complimentary Deoxyribonucleic Acid
CFU-F	= Colony forming units-Fibroblasts
CK1	= Casein kinase 1
CO_2	= Carbon Dioxide
COX	= Cyclooxygenase
CRD	= Cysteine rich domain
DAB	= 3,3 –diaminobenzidine
DAPI	= 4',6-diamidino-2-phenylindole
DEA	= Diethanolamine
Dkk	= Dickkopf WNT Signalling Pathway Inhibitor
DMEM	= Dulbecco's Modified Eagle's medium
DMSO	=Dimethyl sulfoxide
DNA	= Deoxyribonucleic Acid
Dsh	= Dishevelled
ECM	= Extracellular matrix
EDAC	= N-(3-Dimethylaminopropyl)-N’-ethylcarbodiimide hydrochloride
EGF	= Epidermal growth factor
ERK	= Extracellular signal regulated kinases
ES	= Embryonic stem cell
FBS	= Foetal bovine serum
FGF	= Fibroblast growth factor
FITC	= Fluorescein isothiocyanate
Fz	= Frizzled
GAPDH	= Glyceraldehyde 3-phosphate dehydrogenase
GPCR	= G-protein coupled receptor
GSK-3β	= Glycogen synthase kinase 3 beta
GTP	= Guanosine-5'-triphosphate
HLA-DR	= Human Leukocyte Antigen - antigen D Related
HOX	= Homeotic gene
IgG	= Immunoglobulin G
JNK	= c-Jun N-terminal kinase
LEF	= Lymphoid enhancer factor
LiCl	= Lithium Chloride

LRP = Low-density lipoprotein receptor-related protein
hMSC = human Mesenchymal Stem Cell
HUVEC = Human Umbilical Vein Endothelial Cells
IMS = Industrial methylated spirits
iPS = induced Pluripotent stem cells
MAP = Mitogen associated protein
α-MEM = alpha--Minimum Essential Medium
MFB = Magnetic Force Bioreactor
MNP = Magnetic Nanoparticle
MRI = Magnetic Resonance Imaging
mRNA = messenger Ribonucleic Acid
MSC = Mesenchymal Stem Cell
MTT = 3-(4,5-Dimethylthiazol-2-yl)-2,5-Diphenyltetrazolium Bromide
NdFeB = Neodymium Iron Boron
NF-κB = Nuclear factor kappa-light-chain-enhancer of activated B cells
NHS = N-Hydroxysuccinimide
NO = Nitric Oxide
OCN = Osteocalcin
OPN = Osteopontin
PBS = Phosphate buffered saline
PCP = Planar cell polarity
PCR = Polymerase Chain Reaction
PDGF = Platelet derived growth factor
PDGFRα = Platelet derived growth factor receptor alpha
PEG = Polyethylene glycol
PGA = Polyglycolic acid
PGE_2 = Prostaglandin E_2
PKC = Protein kinase C
PLA = Polylactic acid
pN = piconewton
PTH = Parathyroid hormone
RGD = Arg-Gly-Asp
RNA = Ribonucleic Acid
ROR = Rho-associated protein kinase
RT = Reverse Transcription
RTK = Receptor Tyrosine Kinase
RUNX2 = Runt-Related Transcription Factor 2
SDS = Sodium dodecyl sulphate
sFRP2 = secreted Frizzled related protein 2
Shh = Sonic hedgehog
SPION = Superparamagnetic iron oxide nanoparticle
TCF = T-cell factor
TCP = Tricalcium phosphate
TERM = Tissue Engineering and Regenerative Medicine
TGF = Transforming growth factor
TREK = TWIK-related K^+ channel
μCT = micro Computed Tomography

VEGF = Vascular endothelial growth factor
WIF1 = Wnt inhibitory factor 1
Wnt = Wingless-related integration site

Acknowledgements

I wish to express my gratitude to my supervisor Alicia, who has not only afforded me the opportunity to work with her but also pushed me towards studying for a higher degree in a fascinating topic. I sincerely appreciate the time, guidance and enthusiasm that you have provided throughout the past few years. I also thank my fellow members of Alicia's group: Hari, Katie, Yvonne, Josh and Yanny. I've really enjoyed working with such a diverse and interesting group of people. I also wish to state my gratitude to the numerous collaborators who have contributed to parts of this work. In particular I wish to thank Dr James Henstock who was involved in the chick femur studies and my fellow LOLA collaborators at Southampton University (Dr's Smith, Gothard and Kanczler and Prof. Oreffo) who provided training and guidance in the chick femur work. At the University of Nottingham I thank Dr's Rashidi and Qutachi and Prof. Shakesheff who provided the BMP2 releasing microparticles. I wish to thank Dr Shukry Habib at Kings College London who provided the immobilised Wnt slides. To my friends and colleagues at the ISTM I express my gratitude to Dr Roach, Dr Farrow and Dr Hu Bin who were involved in sourcing the UM206 peptides and provided the TCF/LEF reporter respectively. I also thank Dr Telling for useful discussions on magnetic particles and Dr Richardson and Dr Robinson for their advice on western blotting. A special thanks goes to my fellow lab mates at the Guy Hilton including Tina, James, Anthony, Abi, Natalie, Sandhya, Kaarjel and our Iraqi friends. I also thank past lab members Kim, Rupert, Antonella, Kiren, Khondoker, Angeliki, Ian, Richard, Alex and Deepz. I appreciate your advice, discussions, encouragement and of course the banter over the past few years! I'd also like to thank Prof. David Smith for his company and encouragement throughout my project and of

course the Saturday morning breakfasts! I wish to thank my family who have always supported me during my studies. Mum, Dad, Tim, Zita, Becky, Andy, Linsey, Amaan, Anne and Carl, you have all constantly supported me in different ways throughout and have helped me find perspective on things. A cheers goes to my university friends Dan, DW and Big Dave, I've really appreciated our weekend meet up's. Finally I wish to thank my partner Alison and her parents Ann and Richard who have welcomed me to their home. To Alison, I know living with a scientist can be 'challenging' at times but I know I am very lucky to have found such a beautiful and grounded individual, so thank you for your patience. I wish to dedicate this thesis to my grandparents and Private Gareth Bellingham, who would've been proud of the path I have chosen.

Funding

I extend my gratitude towards the funding bodies which supported this work. This project was generously supported by grants from the BBSRC (Grant BB/G010560/1), EPSRC and MRC.

Related Publications

Published articles

M Rotherham, AJ El Haj (2015), Remote Activation of the Wnt/β-Catenin Signalling Pathway Using Functionalised Magnetic Particles, PloS one 10 (3), e0121761

JR Henstock, **M Rotherham**, H Rashidi, KM Shakesheff, AJ El Haj (2014), Remotely activated mechanotransduction via magnetic nanoparticles promotes mineralization synergistically with bone morphogenetic protein 2: applications for injectable cell therapy Stem cells translational medicine 3 (11), 1363-1374

D Gothard, EL Smith, JM Kanczler, H Rashidi, O Qutachi, J Henstock, **M Rotherham**, A El Haj, KM Shakesheff, ROC Oreffo (2014), Tissue engineered bone using select growth factors: a comprehensive review of animal studies and clinical translation studies in man. European Cells and Materials 28, 166-208

H Markides, **M Rotherham**, AJ El Haj (2012), Biocompatibility and toxicity of magnetic nanoparticles in regenerative medicine, Journal of Nanomaterials 2012, 13

Published conference abstracts

AJ El Haj, **M Rotherham**, H Bin, J Price, J Henstock (2015), Spatial Control of Wnt signalling for Orthopaedic Tissue Engineering, TISSUE ENGINEERING PART A 21, S132-S132

M Rotherham, JR Henstock, O Qutachi, KM Shakesheff, AJ El Haj (2015), Regulation of Wnt signalling and promotion of bone mineralisation using peptide-conjugated magnetic nanoparticles, European Cells and Materials Vol. 29. Suppl. 3, (page 95).

J Henstock, **M Rotherham**, A El Haj (2014), Targeted magnetic nanoparticles-remotely controlled mechanotransduction for injectable cell therapy, JOURNAL OF TISSUE ENGINEERING AND REGENERATIVE MEDICINE 8, 50-50

M Rotherham, AJ El Haj (2014), Remote activation of wnt signalling pathways in human mesenchymal stem cells using magnetic nanoparticle technology, J Tissue Eng Regen Med 8 (S1), 51

M Rotherham, M Worrallo, AJ El Haj (2012), Remote activation of Wnt signalling pathways in human mesenchymal stem cells using magnetic nanoparticle technology, JOURNAL OF TISSUE ENGINEERING AND REGENERATIVE MEDICINE 6, 242-242

Rotherham M, Cheema PMS, Bowen W, Dale T, Hu B, Forsyth NR, El Haj AJ (2011), MAGNETIC NANOPARTICLE TECHNOLOGY FOR USE IN CONTROLLING DIFFERENTIATION OF EMBRYONIC STEM CELLS, HISTOLOGY AND HISTOPATHOLOGY 26 (supplement 1)

Introduction

Increasing life expectancy has resulted in a shift in the world's demography towards an ageing population. This is a testament to the success of medical advancements but has also led to increased incidence of chronic disease which is now putting increasing strain on healthcare systems. A major part of this problem is the incidence of bone fractures. Current treatments often involve fixing afflicted limbs for prolonged periods or performing bone transplants. One particular problem is that these interventions often require multiple rounds of invasive surgery which can have long-term effects on patient outcome.

As such there is growing interest in the development of novel therapies to improve the clinical outcome for patients afflicted with orthopaedic pathologies. One area of research that strives to meet the developing need for new orthopaedic healthcare treatments is tissue engineering and regenerative medicine (TERM). The aims of TERM are to develop new tissue engineered constructs that utilise stem cells in combination with advanced materials which can be implanted into the patient to promote tissue regeneration. There are many such systems in development that are geared towards driving stem cell differentiation towards lineages that are involved in tissue formation.

One novel approach which has gained interest over recent years is the use of magnetic nanoparticles to condition stem cells. This can be achieved by tailoring the functionality of the nanoparticle surface to enable control over where the nanoparticles bind. Magnetic fields can then be used to remotely induce direct mechanical forces to the cells via twisting of the nanoparticles. Recent work has demonstrated the feasibility of using nanoparticle targeted to specific cell receptors and ion channels to remotely stimulate

cell signalling pathways in order to influence stem cell behaviour. This strategy has been demonstrated to have beneficial effects on stem cell differentiation towards bone forming osteoblasts that results in putative bone formation.

One signalling pathway that is known to regulate stem cell differentiation towards the bone lineage is Wnt signalling. This pathway is therefore an attractive target for modulation in a bone tissue engineering context. To date, the potential for targeting Wnt signalling pathways in stem cells using nanoparticles has not been investigated. Neither have the effects of mechanoactivation of these pathways on stem cell behaviour or osteogenesis.

Aims of this thesis

The primary aim of this thesis was to determine the feasibility of targeting the Wnt signalling pathway for remote activation in a clinically relevant stem cell type, human mesenchymal stem cells (hMSC). Wnt signalling pathways are involved in the regulation of stem cell fate including hMSC, therefore novel strategies for the modulation of this pathway are of particular relevance to stem cell biology and tissue engineering. This aim was explored with the use of magnetic nanoparticles (MNP) that were functionalised with ligands targeted to the Wnt receptor Frizzled. This is a novel way of targeting and controlling cell signalling pathways in order to influence cell behaviour.

The secondary aim was to assess the effects of functionalised MNP mediated Wnt pathway activation on the osteogenic differentiation of hMSC. This is particularly relevant to bone tissue engineering where new treatments are currently needed. With this in mind, the aim was to demonstrate the feasibility of a magnetic stem cell activation approach which can inform the development of future injectable cell therapies. This aim was assessed in two ways. Firstly the osteogenic response of hMSC to MNP *in vitro* was assessed in monolayer cell culture experiments. Secondly, the translational applications of this strategy was assessed using an *ex vivo* foetal chick femur model of bone development. The third aim of this thesis was to introduce and briefly explore the role of Wnt gradients presented in a spatial manner in maintaining the MSC niche. This facet of cell signalling is often overlooked but plays critical roles in regulating tissue development. This aim was investigated with the use of a novel tissue engineering platform featuring immobilised Wnt protein overlaid with cells and collagen hydrogel.

Chapter 1: Literature Review

This thesis will be focusing on the osteogenic differentiation of stem cells and bone formation strategies in tissue engineering. An understanding of bone structure, re-modelling and repair is therefore required and will be provided in the following sections.

1.1 Bone

1.1.1 Role and components of bone

Bone is a specialised form of connective tissue which has multiple roles in the body. The principle role of bone is to provide support and stability for the body; it also provides protection for vital organs and acts as a framework that allows movement. Bone also acts as a store for ions such as calcium, magnesium and phosphorus (Hull, 2011). Bone tissue is mainly composed of collagen fibres which constitute around 85% of bone protein and a crystalline matrix of calcium phosphate (Currey, 2013). Together these constituents enable bone to resist externally applied tensile stresses and compressional forces (Khan, 2001). Other constituents of bone include proteoglycans and non-collagenous proteins such as osteopontin and osteocalcin which play a number of roles in regulating bone formation. These constituents act as nucleators for calcium phosphate deposition, bind to and control the bio-availability and activity of growth factors and regulate cellular processes which control bone metabolism. Bone also contains multiple cell types which control tissue development, these cell types include osteoblasts, osteoclasts, osteocytes as well as osteoprogenitor and stem cells (Bilezikian et al., 2008), (Hollinger et al., 2004).

1.1.2 Structure of bone

Bone is categorised into four classes: long, short, flat and irregular bone. Examples of these four types include the femur, carpals, cranium and vertebrae respectively. On a macro scale bone is broadly organised into two types, cortical and cancellous bone. These

bone types are classified according to their strength, structure and porosity. Cortical bone, also known as compact bone is much denser, less porous (less than 5%) and stronger than cancellous bone. Cortical bone is mainly found along the shafts of long bones and covering cancellous bone at the epiphyseal ends of long bones. The micro structure of cortical bone consists of tightly packed Haversian systems which contain blood vessels and are surrounded by canaliculi and concentric lamellae which all together form osteons. Cancellous bone, which is also known as trabecular bone is more porous in structure and mechanical weaker than cortical bone. Cancellous bone consists of an interconnected matrix of mineralised rods and plates which together form an inter-connected network known as a trabecular network. The pores in between the trabeculae contain the bone marrow. Cancellous bone is mainly found in the centre of long bones and makes up approximately 20% of the human skeleton. Bones are lined by a periosteal layer which is involved in bone repair and consists of a cell layer which harbours osteoblasts, osteoclasts and osteoprogenitor cells and an outer fibrous layer mainly consisting of collagen fibres as well as vasculature and nerve fibres (Clarke, 2008), (Mortensen, 2006), (Steele and Bramblett, 1988), (Singh, 2014). The macro- and microscopic structure of bone is illustrated in Figure 1.1.

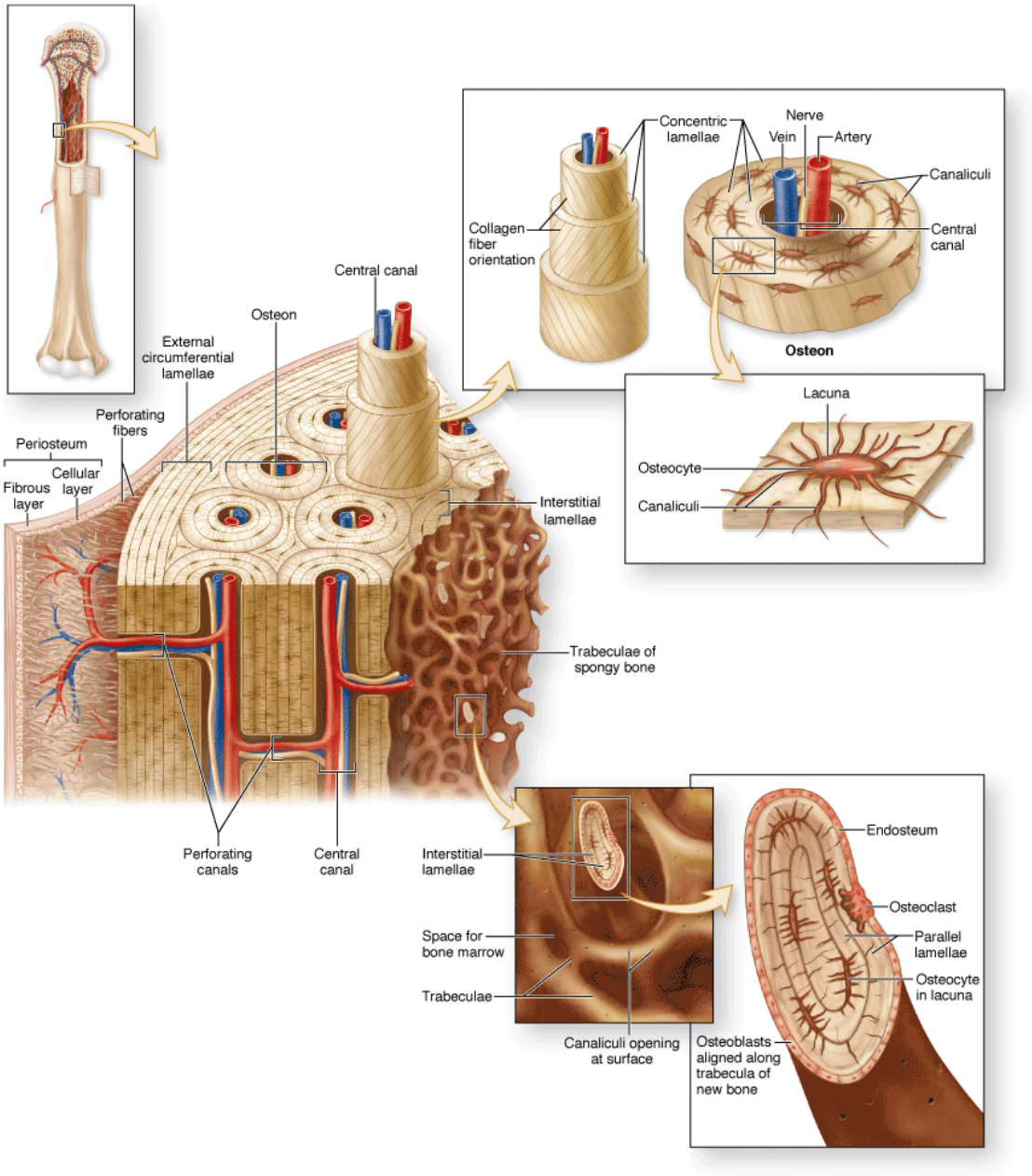

Figure 1.1. Structure of bone.
Illustration depicting the micro- and macroscopic structure and components of long bones. Image reproduced with permission from Mescher 2009 (Mescher, 2009)

1.1.3 Bone formation mechanisms

There are two mechanisms of bone formation, these are known as intramembranous and endochondral ossification. Intramembranous formation describes bone that is directly synthesised by differentiated mesenchyme tissue and is the prominent process behind flat bone formation. This process is controlled by mesenchymal stem cells (MSC) which first proliferate, form aggregations, then differentiate down the osteogenic lineage to become bone forming osteoblasts. These cells are responsible for synthesis of new bone matrix (Gilbert, 2000). The second mechanism of bone formation, endochondral ossification, is a multi-step process that involves deposition of new bone by osteoblasts over a pre-established cartilaginous matrix. This matrix is deposited by chondrocytes. This mechanism of bone formation plays a major role in the formation of long bones (Claes and Willie, 2007), (Gilbert, 2000). An important part of later bone formation is angiogenesis which initiates vascularisation of the developing tissue and allows nutrient transfer for the propagation of bone formation (Wohl et al., 2009).

1.1.4 Limb bud formation during development

In vertebrate embryogenesis, limb development begins with cell outgrowths from the embryonic body wall. These outgrowths are known as limb buds and consist of a condensation of mesenchymal cells belonging to the mesoderm lineage. At their distal ends, the limb bud is covered by an epithelial layer of the ectoderm lineage known as the apical ectodermal ridge (AER) (Pownall and Isaacs, 2010). The cells of the AER are involved in maintaining the development and outgrowth of the limb bud by creating temporal and spatial signalling gradients of fibroblast growth factor (FGF) members which orchestrate limb development (Martin, 1998), (Niswander et al., 1993). The cells proximal to the AER, under the influence of FGFs, remain in an undifferentiated state during

outgrowth. Conversely, the mesenchymal cells distal to the AER and proximal to the body wall fall under the influence of Retinoic acid and begin to form condensations. Mesenchymal condensation is followed by specification and differentiation of these mesenchymal cells distal from the AER progress zone (Yashiro et al., 2004), (Mercader et al., 2000). The next stage of development involves limb patterning. This process is fine-tuned by expression of a variety of other signalling factors including members of the Sonic hedgehog (Shh), Wingless related integration site (Wnt), Homeotic (HOX) gene family members (Ahn and Joyner, 2004), (Riddle et al., 1995), (Kengaku et al., 1998). At later stages of development members of the Bone morphogenetic protein family (BMP), such as BMP2 and 7, are involved in inducing differentiation of stem cell progenitors towards the bone and cartilage forming lineage. This process is required for bone formation to progress through endochondral ossification (Kang et al., 2004), (Hogan, 1996).

1.1.5 Bone remodelling

Bone remodelling is a continual and crucial process throughout life. This process adapts the architecture of bone structure according to the magnitude of mechanical forces applied to the tissue. This phenomenon was first suggested by Julius Wolff in the 19th century and is known as Wolff's law. The bone remodelling process helps to preserve bone integrity by enabling the tissue to withstand increased loads (Maquet et al., 2012). Bone remodelling ultimately ensures appropriate bone turnover and maintains tissue homeostasis by removing old or damaged bone and depositing new bone to load-bearing regions. The bone remodelling process consists of three phases: resorption, reversal and synthesis. Bone resorption involves the removal of old bone and is mediated by osteoclast cells, which release hydrogen ions and lysosomal enzymes to break down and remove old bone. The resorption phase may last for up to two weeks. The second phase

is known as the reversal stage. During this time mononuclear cells prime the bone surface and secrete signals that cause the recruitment and differentiation of osteoblast cells; this stage last for around five weeks. The final stage of remodelling is the bone formation stage, this is where new bone is synthesised by osteoblasts. Osteoblasts synthesize and secrete new matrix which is eventually mineralised. The formation stage may continue for months (Hadjidakis and Androulakis, 2006). At the cellular level, bone remodelling is controlled by the action of bone resorbing osteoclasts and bone forming osteoblasts. The remodelling process is delicately balanced and tightly regulated by multiple factors. The action and activity of osteoblasts and osteoclasts is regulated by many signals such as growth, hormonal and cytokines as well as the genetic, nutritional and mechanical environment. Imbalances in the activity between these cells has serious consequences on tissue integrity and mechanical stability. If the action of osteoclasts is higher than osteoblasts, this inevitably leads to lower bone mass and is the major pathology behind Osteoporosis and Paget's disease (Tanaka et al., 2005), (Kini and Nandeesh, 2012), (Raisz, 1999), (Fraher, 1993). In the opposite scenario, where osteoblast activity is higher than osteoclast activity, this leads to a high bone mass phenotype and is seen in conditions such as Sclerosteosis and Van Buchem disease (Ahituv, 2012).

1.1.5.1 Mechanical forces in bone remodelling

The bone remodelling process is particularly sensitive to environmental factors, especially externally applied forces which are present during normal activities such as exercise. Mechanical forces cause small deformations in the shape of bone which results in pressure changes and oscillatory fluid flow in the canaliculi network (Klein-Nulend et al., 2005). These changes are sensed by osteocytes embedded in bone matrix which release numerous signalling factors such as Nitric Oxide (NO), BMPs, Wnts and Prostaglandin E_2

(PGE_2). These signalling factors direct the activation and differentiation of osteoblasts and Osteoprogenitor cells and regulate the behaviour of osteoclasts (Robling et al., 2008), (Tan et al., 2007), (You et al., 2008), (Santos et al., 2009), (Santos et al., 2011), (Jiang and Cheng, 2001), (Kitase et al., 2010). Osteoblasts are also mechanosensitive and respond to external forces by proliferating and increasing matrix protein production (Liedert et al., 2006). Ultimately, external forces have profound effects on bone homeostasis, remodelling and the load bearing capacity of the tissue (Chen et al., 2008), (Knothe Tate et al., 2008).

1.1.6 Bone repair mechanism

Bone tissue can be damaged through many mechanisms such as disease or trauma. The bone repair process is divided into three main phases and is depicted in Figure 1.2. Phase one is known as the inflammatory phase which lasts for approximately one week and is characterised according to the inflammatory response caused by an injury. This stage involves formation of a haematoma and recruitment of immune cells and subsequent initiation of angiogenesis which precedes the repair phase. The next phase is the repair phase and commences within days after injury and lasts for several weeks. This phase involves callous tissue formation which consists of fibrous connective tissue that provides support and stability for the injury site. This stage also sees the recruitment and differentiation of mesenchymal stem cells which eventually differentiate into osteoblast cells which synthesis new bone via intramembranous ossification. At the callous periphery, mesenchymal cells differentiate towards the chondrocyte lineage and form a cartilaginous matrix. New bone is synthesized over the cartilaginous matrix through the process of endochondral ossification. By this point the calcified callous becomes more rigid, is invaded by blood vessels and begins to resemble woven bone. The final stage of

bone repair is known as the remodelling phase and involves resorption of excess bone and conversion of woven bone to lamellar bone. This process may be active for several years and is fine-tuned according to the mechanical stability of the remodelled bone at the fracture site (Sfeir et al., 2005).

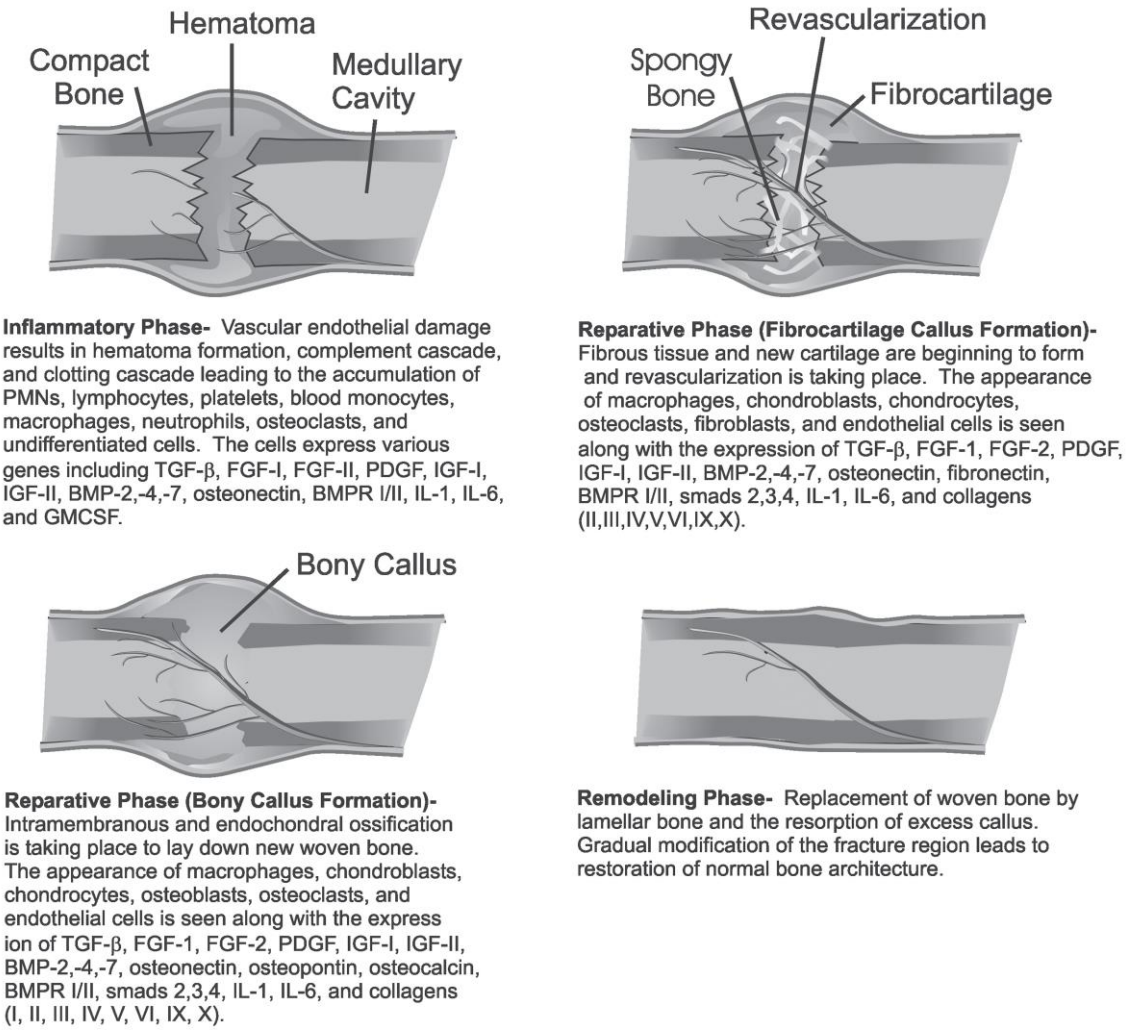

Figure 1.2. Fracture repair mechanism.
Illustration of the fracture repair process. The repair process consists of three distinct phases, an inflammatory phase, a reparative phase and a final remodelling phase. Image reproduced with permission from Sfeir et al. 2005 (Sfeir et al., 2005)

The bone repair process is also affected by the mechanical environment present during healing. If a fractured bone is given the correct support and fixed in place then callous formation and intramembranous bone formation leads to properly mineralised and repaired tissue. However complications can occur during the healing process that can lead to extended healing times, inadequate re-mineralisation, tissue regeneration and mechanical instability (Gomez-Benito et al., 2011). This is exemplified by the observation that healing is delayed when load is applied to fractured limbs too soon after injury (Gardner et al., 2006).

1.2 The embryonic chick as a model of bone formation

One well studied model of limb development that has been prominently used in research is the chick embryo. Later models of post-natal chick bone development have also been adopted to study the processes underpinning bone development. One example here is the embryonic femur which is now a well-established tool for studying bone development *in vitro* and *ex vivo*. Due to the ease of isolation and capability for high throughput experiments, this model is especially useful as a screening tool in the development of new therapies. Another advantage of this model is that the underlying developmental similarities, particularly in the signalling process, between vertebrate species means that the knowledge gained from these models can inform the developmental process in humans. Many groups have applied the embryonic chick model to study the process of embryonic bone and cartilage formation and repair (Anderson and Reynolds, 1973), (Todt and Fallon, 1984), (Roach, 1990), (Takahashi et al., 1991). Subsequent work has revealed the network of signalling processes such as Wnt and FGF signalling that underpin limb

growth, patterning and bone formation in vertebrates (Satoh et al., 2010), (Yonei-Tamura et al., 1999), (Maruyama et al., 2010), (Jin et al., 2012). The foetal chick model has remained an invaluable research tool today where it is used as a screening tool to inform the development of new treatments, especially in the field of bone tissue engineering (Smith et al., 2012), (Smith et al., 2015), (Smith et al., 2014a), (Smith et al., 2014b), (Kanczler et al., 2012).

1.3 Orthopaedic pathologies

The advances of modern medicine have continued to extend life expectancy and have subsequently led to an ageing population. Unfortunately quality of life has not kept pace with this extension in lifespan. One of the major impactors on this is mobility, which is compromised by orthopaedic pathologies. Osteoarthritis is a major problem caused by a loss of articular cartilage and friction between bones. This causes significant pain and discomfort in affected joints and affects 13.9% of adults aged 25+ and 33.6% (12.4 million) of people aged 65+ in the US (Helmick et al., 2008). Bone can also be damaged as a result of malignancies such as Ewing sarcoma, Osteosarcomas and Multiple Myeloma (Li and Siegal, 2010). Bone fractures are also particular problems. Fractures are caused by trauma or arise as a result of Osteoporosis, and are the most common bone pathology in adults. In the US there are approximately 58 million people considered to be at risk of Osteoporosis and over 6 million cases are reported annually. 5-10% of these cases result in complications in healing that frequently require multiple surgical interventions. Orthopaedic pathologies such as osteoporosis are particular problems in the elderly and women especially. This is due to many factors; the bone formation and repair

mechanisms become less efficient with age due to physiological changes in hormone production. Decreased osteoblast activity and decline of stem cell populations or differentiation is also observed. As such, bones gradually lose mass, become more porous, the healing process takes considerably longer and is less efficient (Gruber et al., 2006), (Claes and Willie, 2007), (Saxon et al., 2014). An added complication of bone fractures is the incidence of delayed and non-union fractures which have been reported to affect between 4-48% of Tibial fractures (Bhandari et al., 2001) and 1.7-7.5% of Femoral shaft fractures depending on treatment (Canadian Orthopaedic Trauma, 2003). All of these pathologies require extensive and expensive surgical intervention.

1.3.1 Current treatments

The optimal treatment for orthopaedic conditions depends on the causes, site and extent of the injury to the tissue. The risk of bone fractures due to osteoporosis can be mitigated to a certain extent by altering life style factors such as increasing physical activity and by administering calcium supplements or hormone replacement therapy (in post-menopausal women) in order to reduce bone loss (Saxon et al., 2014). However, when fractures do occur, the current gold standard treatments involve immobilisation of the afflicted limb using internal or external fixators and / or some form of reparative surgery. This may be achieved through bone grafts or implants which may consist of steel or titanium screws and plates which are used to stabilise damaged limbs. However, these treatments involve invasive surgery, usually require replacement or refinement at some stage and frequently lead to unsatisfactory clinical outcome for the patient (Stannard et al., 2007), (Park, 2012). With increasing cases of bone pathologies there is now a clear need for new scalable, effective and affordable treatments in order to meet the growing clinical need. These treatments will now be discussed.

1.3.2 Tissue engineering strategies

One thriving area of research for the development of new clinical treatments is Tissue engineering and regenerative medicine (TERM). The aim of TERM is to develop new treatments that recreate the *in vivo* environment and developmental niche in order to provide the optimal conditions for tissue repair. The tools for TERM include the use of stem cells, biomaterials and growth factors. These tools can also be combined with bioreactor systems in order to provide an optimal growth environment for specific tissues. A crucial and central aim of TERM is to develop treatments that promote integration of grafts or implanted scaffolds and newly formed tissue with existing host tissue (El Haj et al., 2005).

1.3.2.1 Growth factor delivery

One aspect of TERM based treatments involves the application of growth factors to injured tissue in order to enhance host tissue formation. Growth factors provide biochemical cues to cells and are instrumental in guiding cell function and fate by influencing cell proliferation and differentiation. This strategy has shown promise in fracture and spinal injury repair where delivery of growth factors belonging to the Bone Morphogenetic protein (BMP) family e.g. BMP2 and BMP7 in conjunction with a collagen carrier have been shown to enhance bone repair and induce new bone formation. BMP based treatments have since been translated to the clinic and commercialised as a treatment for non-union fractures (Laursen et al., 1999), (White et al., 2007). Other growth factor treatments include Parathyroid hormone (PTH) which has been used in a number of models and translated to the clinic where it was shown to enhance bone repair for fracture healing (Barnes et al., 2008), (Ellegaard et al., 2010). A comprehensive

review of the growth factors used for in vivo bone repair in animal and clinical studies is discussed further by Gothard et al. (Gothard et al., 2014).

1.3.2.2 Scaffolds

Lots of current research has focused on the development and application of biocompatible biomaterials in tissue engineering. Biomaterials are defined as non-toxic, inert substances that can be implanted into living systems. A primary requirement for biomaterials is that they must have the capacity to integrate with host tissue; it is also advantageous if the materials are mechanically stable and easy to fabricate (Park, 2012). Biomaterials are especially useful as scaffolds which can be used to support and bridge damaged tissue that enable or enhance tissue repair by the host. In the context of bone tissue engineering, common scaffold materials that are used to support bone repair include inorganic materials such as tricalcium phosphate (TCP), hydroxyapatite based materials or bio-active glasses. Synthetic polymers such as Polylactic acid (PLA), Polyglycolic acid (PGA) or combinations of polymer materials are also popular due to their versatility. These materials are also relatively cheap and easy to fabricate and their shape and surface characteristics can be modified according to the desired application. Hydrogels such as polyethylene glycol (PEG) are also useful due to their elastic properties which mean they can be tailored to fit different defects. Also, their high water content means they can be delivered easily. Natural polymers such as collagen are also of interest in bone tissue engineering. Collagen is a major component of bone, and provides optimal cell attachment motifs although sourcing large scale amounts can be problematic (Stevens, 2008), (Bose et al., 2012), (Hutmacher, 2000).

1.3.2.3 Cell therapies

Another key element of TERM therapies revolves around the expansion and delivery of cells to the sites of injury. Indeed there are established treatments already available in orthopaedics that utilise cell populations which can be directly injected to the site of injury or diseased tissue. An example here is cartilage repair by autologous chondrocyte implantation (ACI). Here chondrocytes are extracted from a patient, expanded in vitro and re-transplanted into the site of repair to promote new hyaline articular cartilage synthesis (Kon et al., 2012), (Roberts et al., 2003). This treatment has been extensively evaluated in high impact joints such as the knee, where ACI has been shown to be effective in restoring joint function and reducing pain (Macmull et al., 2012), (Beris et al., 2012), (Bhosale et al., 2009). Bone tissue engineering cell therapies tend to focuses on the use of adult stem cells, such as the mesenchymal stem cell (MSC) derived from bone marrow or adipose tissue. Both sources of MSC have been shown to promote new bone growth for the repair of bone defects and necrotic bone tissue (Quarto et al., 2001), (Lendeckel et al., 2004), (Pak, 2012). The use of stem cells and mesenchymal stem cells will be discussed in the following sections.

1.4 Stem Cells

By definition Stem cells are undifferentiated cells that are capable of self-renewal, which preserves the stem cell population, or differentiation into other cell types, which gives rise to new tissue. Stem cells can be further classified according to their potency. In this regard embryonic stem cells, which can be isolated from the inner cell mass of a 5-6 day old blastocyst, are considered to be the archetypal stem cell due to their pluripotent

nature. Embryonic stem cells have the capacity to differentiate into any cell type from the three germ layers (Lanza and Atala, 2013), (Bongso and Lee, 2005). In contrast adult stem cells are more differentiated stem cell types that express characteristic surface markers and retain capacity for self-renewal but have limited multipotency. In this respect adult stem cells are more limited in their differentiation capacity and so are committed to cell types of certain lineage. One such example of an adult stem cell is the mesenchymal stem cell which forms tissue of the mesenchyme lineage (Lanza et al., 2004).

1.4.1 Mesenchymal stem cells

Mesenchymal stem cells (MSC) are stromal cells with fibroblastic morphology and are derived from the mesoderm germ layer (Vodyanik et al., 2010). MSC were first isolated from bone marrow but have since been isolated from other tissues such as muscle, umbilical cord and adipose tissue. When MSC are isolated and expanded *in vitro* they form colonies, this led to the term attribution of the term Colony forming units-Fibroblasts (CFU-F). MSC are multipotent in nature, with a capacity for self-renewal or differentiation into other cell types. According to the Mesenchymal and Tissue Stem Cell Committee of the International Society for Cellular Therapy, in order to be classified as MSC cells must be adherent and express surface markers CD105, CD90, CD73. Conversely, MSC populations must also be negative for haematopoietic lineage surface markers CD45, CD34, CD14, CD19 and HLA-DR. Other recently suggested markers for MSC include STRO1, VCAM1 and CD106. Cells expressing these markers can be detected and isolated using fluorescent cell sorting techniques. The final requirement for MSC classification is that cells must be capable of tri-lineage differentiation down the osteogenic, chondrogenic and adipogenic lineages by forming osteoblasts, chondrocytes and adipocytes respectively (Dominici et al., 2006), (Boxall and Jones, 2012), (Oreffo et al., 2005). Interest

around MSC has grown since their stem cell and differentiation capacities were discovered. Previous work has demonstrated the capacity for MSC to form putative cartilage, bone and other connective tissues (Castro-Malaspina et al., 1980), (Prockop, 1997), (Caplan and Bruder, 2001). More recently, MSC have been shown capable of differentiating into a wider range of cell types such as endothelium and myogenic cell lineages (Wu et al., 2013), (Gang et al., 2004), (Oswald et al., 2004). The tissue forming potential of MSC is illustrated in Figure 1.3. The bone and cartilage forming capabilities of MSC's as well as their ease of isolation from a range of tissues makes them a particularly attractive cell type for orthopaedic tissue engineering. In this context MSC already have a proven potential to be utilised as cell therapies particularly in orthopaedics and connective tissue repair (Oreffo et al., 2005), (Ling et al., 2009).

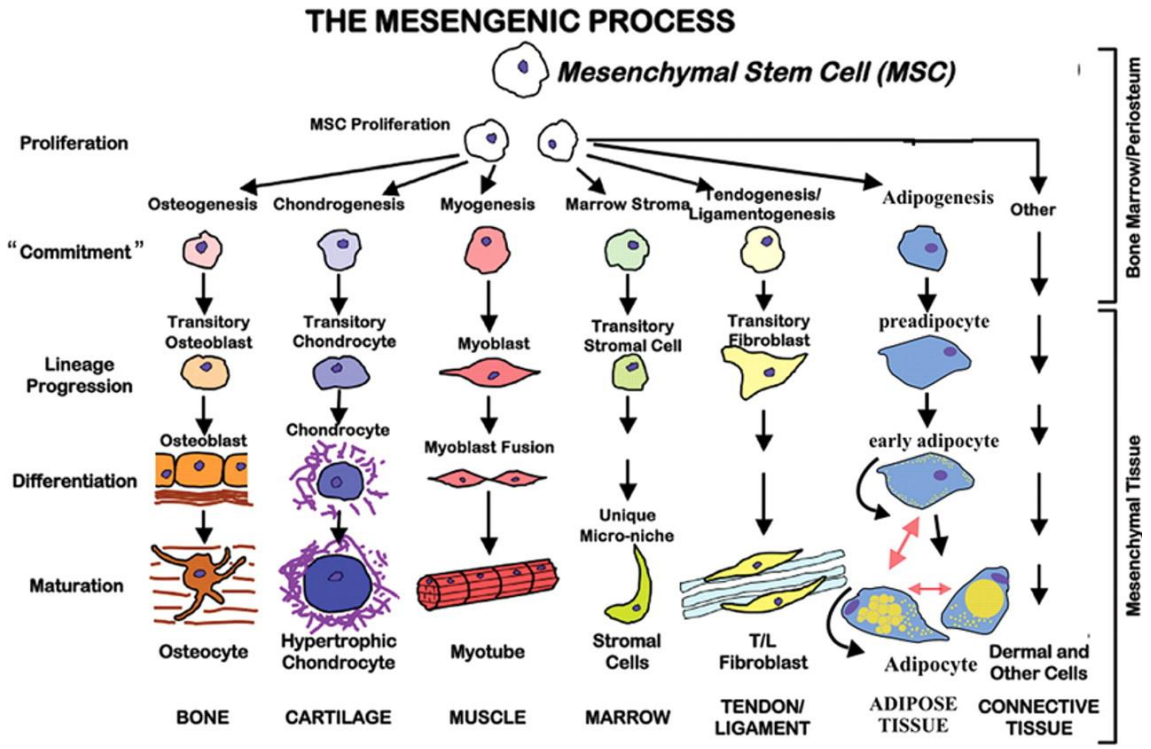

Figure 1.3. The mesenchymal lineage.
Mesenchymal stem cells (MSC) arise from the mesenchyme lineage. MSC can self-renew or differentiate into cells that give rise to connective tissue including bone, cartilage and adipose tissue. Image reproduced with permission from Caplan 2010, (Caplan, 2010).

1.4.2 The MSC Niche

The Stem cell niche was a concept first introduced by Schofield in 1978 and refers to the cellular, extracellular and molecular microenvironment that governs stem cell maintenance and differentiation (Ehninger and Trumpp, 2011), (Schofield, 1978). MSC reside in a number of anatomical locations but are typically located in the endosteum and in the blood vessels that line the bone marrow (Gronthos et al., 2003), (Shi and Gronthos, 2003). The stem cell niche is composed of multiple cell types including stem cells, progenitor and differentiated cells. In the case of bone marrow this includes cells of the haematopoietic lineage as well as differentiated mesenchymal progenitors (Ehninger and Trumpp, 2011), (Kolf et al., 2007). These different cell populations interact with each

other and secrete many signalling factors such as Wnt and FGF which regulate stem cell differentiation and proliferation. Another important aspect of the stem cell niche is the extracellular matrix (ECM), this consists of proteins such as Collagen 1 and Fibronectin. These proteins not only provide points of attachment for cells but also present signalling molecules in a spatially specific manner. The main function of the niche micro-environment is to maintain the stem cell populations that reside there (Kolf et al., 2007), (Lichtman, 1981), (Gattazzo et al., 2014). An illustration showing the different components of the niche environment is shown in Figure 1.4.

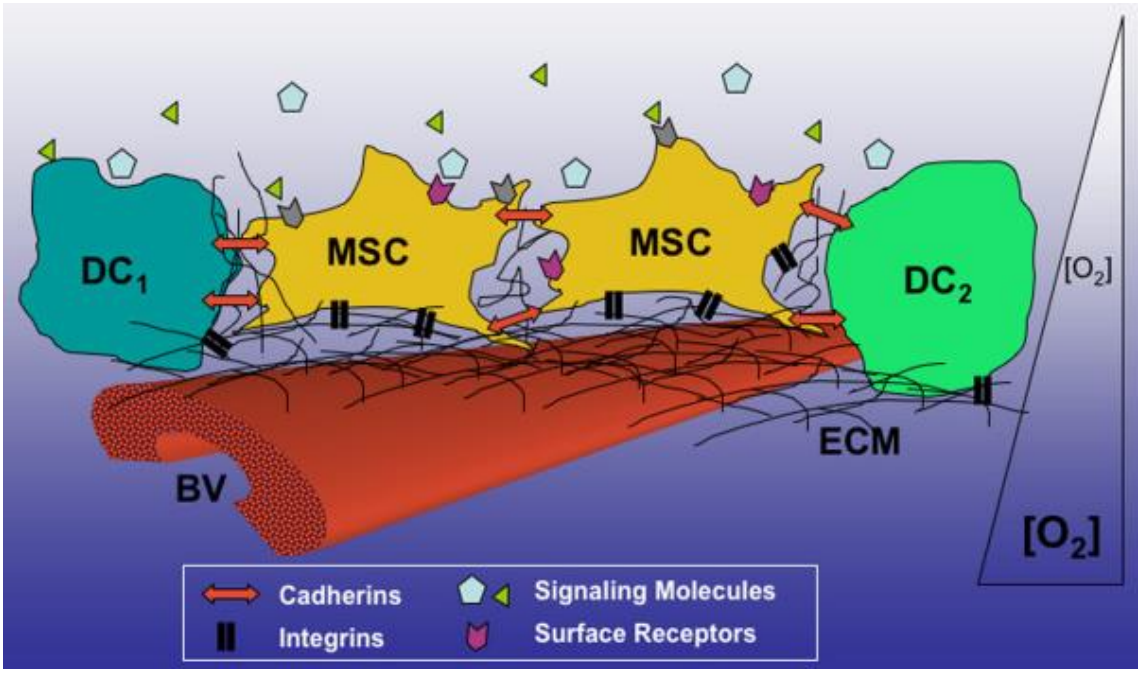

Figure 1.4. The MSC niche.
Illustration of the MSC niche. This consists of multiple differentiated cells (DC1, DC2), Blood vessels (BV), Extracellular matrix components (ECM) as well as soluble signalling factors. Image reproduced from Kolf et al. 2007 (Kolf et al., 2007), (Published by BioMed central).

1.4.3 MSC osteogenic differentiation

The bone forming capabilities of MSC are of particular interest in the development of new orthopaedic treatments. The process of osteogenic differentiation of MSC has been

extensively studied *in vitro* and can be initiated with culture media supplemented with Dexamethasone, Ascorbic acid and β-Glycerophosphate (Pittenger et al., 1999), (Jaiswal et al., 1997). *In vivo,* the commitment and regulation of MSC differentiation to the osteogenic lineage is controlled by multiple growth factor signalling pathways. Amongst these, BMP, Wnt, and Platelet Derived Growth Factor (PDGF) signalling pathways have all been shown to play prominent roles in this process (Rickard et al., 1994), (Liu et al., 2009), (Quarto et al., 2010), (Kratchmarova et al., 2005), (Ng et al., 2008). Integration of these signalling pathways leads to expression of many transcription factors which regulate the expression of bone related genes. With regards to osteogenic differentiation, Runt-Related Transcription Factor 2 (RUNX2), a member of the runt domain family and Osterix (SP7), a zinc-finger containing transcription factor both behave as master regulators of osteogenic differentiation (Schroeder et al., 2005), (Sinha and Zhou, 2013). These transcription factors regulate the expression of multiple bone-related and matrix associated genes such as Collagen 1 (COL1), Osteopontin (SPP1), Osteocalcin (BGLAP) and Alkaline Phosphatase (ALP). The proteins encoded by these genes are all components of bone and play roles in matrix maturation and mineralisation. The changes in gene expression during osteogenesis lead to changes in cell phenotype, lineage commitment and differentiation of osteoblasts (Ziros et al., 2008), (Ducy et al., 1997), (Langenbach and Handschel, 2013), (Kulterer et al., 2007). The osteogenic differentiation process in MSC is shown in Figure 1.5.

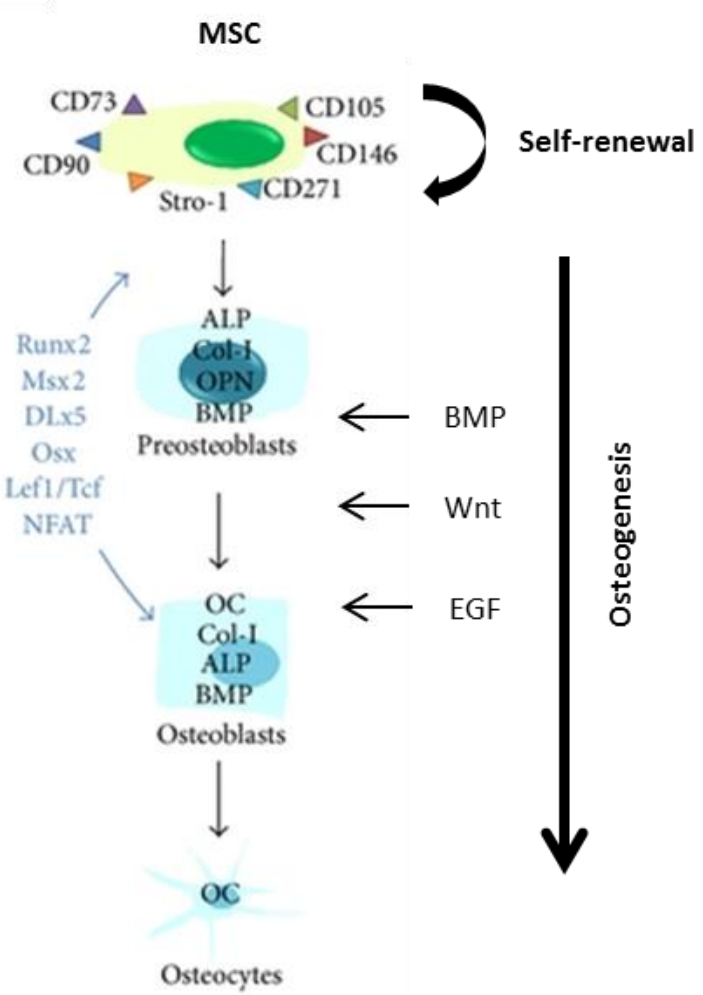

Figure 1.5. Osteogenic differentiation pathway of MSC.
Osteogenic differentiation of MSC to osteocytes is controlled by multiple signalling pathways such as the BMP, Wnt and EGF pathways. These pathways regulate expression of osteogenic transcription factors such as RUNX2 and Osterix (Osx) and up-regulate bone markers such as alkaline phosphatase (ALP), Collagen 1 (Col1), Osteopontin (OPN) and Osteocalcin (OCN). Image adapted from Giuliani et al. 2013 (Giuliani et al., 2013).

1.4.3.1 Markers of MSC osteogenic differentiation

Osteogenic differentiation of MSC leads to characteristic changes in cell phenotype. As differentiation progresses the cells begin to resemble mature osteoblasts. Enhanced matrix synthesis and subsequent mineralisation are typical indicators of differentiation and can be easily identified using histological stains such as Alizarin red which reveals

mineralised matrix by binding to the calcium ions present in the matrix (Puchtler et al., 1969). Collagen production can also be visualised using Picro-Sirius red which binds to basic groups in collagen fibrils via sulphonic acid groups (Junqueira et al., 1979), (Junqueira et al.), (Tullberg-Reinert and Jundt, 1999). The expression of other matrix protein markers such as osteopontin and osteocalcin, which indicate late-stage osteogenic differentiation, can also be investigated using Immunofluorescent techniques (Marom et al., 2005). Another well-established marker of osteogenic potential is the enzyme alkaline phosphatase (ALP). The role of ALP in bone formation is not fully understood but is thought to be involved in initiating mineralisation by cleaving inorganic pyrophosphate, an inhibitor of mineralisation, whilst providing a source of inorganic phosphate for mineralisation (Orimo, 2010), (Harmey et al., 2004). ALP expression can be simply determined using biochemical assays that assess enzyme activity (Bednarska et al., 2006).

1.4.4 MSC in cell therapies

MSC have many useful properties that have prompted interest in developing them as cell based therapies. MSC have been shown to be immune privileged cells that do not elicit a response from the host immune system. The immune privileged nature of MSC can be partly attributed to their secretion of soluble factors including transforming growth factor beta 1 (TGF-β1) and hepatocyte growth factor (HGF) that are thought to regulate immune cell activity and proliferation. As such, the immune regulatory role of MSC is particularly advantageous in allogeneic cell therapies (Bartholomew et al., 2002), (Di Nicola et al., 2002). The most exciting property of MSC stems from their multipotent nature and tissue forming capabilities. Added to this is their relative ease of isolation and expandability which presents MSC as an attractive cell type for new cell therapy treatments. The

multipotent nature of MSC endows the capability of directing their differentiation into multiple useful cell types such as osteoblasts, chondrocytes as well as cells of other mesenchymal lineages including tendon and muscle (Krampera et al., 2006), (Pittenger et al., 1999). In the clinic, implantation of bone marrow which contains MSC, or isolated bone marrow stromal cells in conjunction with biocompatible scaffolds has been shown to be a promising treatment of non-union fractures and bone defects (Quarto et al., 2001), (Connolly, 1995), (Bajada et al., 2007). MSC have also been applied in the treatment of osteoarthritis where injection of MSC into articular cartilage has been shown to enhance cartilage regeneration (Baghaban Eslaminejad and Malakooty Poor, 2014), (Horie et al., 2012). Furthermore, transplants of bone marrow derived osteoprogenitor cells into children with osteogenesis imperfecta has been shown to increase bone formation as a result of MSC differentiation to osteoblasts (Horwitz et al., 1999). A further example is the treatment of spinal cord injuries where MSC have been shown to promote neural regeneration (Dasari et al., 2014). In conclusion, this highlights the promise of stem cells such as MSC, Regenerative medicine and tissue engineering based approaches in addressing current clinical challenges in orthopaedic medicine.

1.5 Wnt signalling components and mechanisms

1.5.1 The Wnt family of proteins

Wnt proteins are an evolutionary conserved class of proteins of which there currently 19 known members in mammals. The broad range of Wnt ligands is an indicator of the degree of complexity of the Wnt signalling pathway and infers how specificity between Wnt signalling pathways is obtained. Wnt proteins are between 350-400 amino acids in

length with a notable occurrence of conserved cysteine rich domains (MacDonald et al., 2009), (Logan and Nusse, 2004). The N-terminus contains a signalling peptide which targets the protein for secretion and there are numerous post translational modifications including glycosylation's and lipid modifications (e.g. palmitoylation) which aids binding of Wnt ligands to the Wnt receptors (Cong et al., 2004), (Komekado et al., 2007). These lipid modifications also confer the distinctive hydrophobic properties of Wnts which, incidentally, also present problems when trying to obtain biochemically active Wnt proteins (MacDonald et al., 2009), (Logan and Nusse, 2004). Of the 19 known Wnt ligand's Wnt 3A and Wnt 5A have been the most extensively studied. Wnt 3A is generally considered to mediate β-catenin activation via Low-density lipoprotein receptor-related proteins (LRP) co-receptors and promote canonical Wnt signalling. In contrast Wnt 5A has been extensively associated with β-catenin independent non-canonical signalling pathways which are transduced through other co-receptors such as Rho-associated protein kinase 2 (ROR2) (Grumolato et al., 2010).

1.5.2 Wnt receptors

1.5.2.1 Frizzled

Wnt signalling has been shown to be mediated through a multitude of different receptors of different classes as well as a multitude of Wnt ligands. The signalling plasticity of Wnt receptors underlines the scale of pleiotropy in Wnt signalling (Logan and Nusse, 2004). The principal class of receptors that Wnt proteins signal through are known as Frizzled receptors. Frizzleds are 7 transmembrane spanning proteins that together form a separate class of G-protein coupled receptors. There are 10 members of the Frizzled family currently identified in mammals. Most Frizzleds show varied capabilities in

activating canonical Wnt signalling, especially when co-expressed with LRP5/6 (Binnerts et al., 2007) although it is thought that there is a degree of functional redundancy amongst the Frizzled family in respect to Wnt signalling activation. Structurally, Frizzleds have an extended N-terminal region that contains a cysteine rich domain (CRD); it is to this CRD domain that the Wnts primarily bind in order to initiate signalling (Logan and Nusse, 2004), (MacDonald et al., 2009), (Wang et al., 2006). Propagation of Wnt signals is mediated through the intracellular c-terminus of most Frizzled receptors. This process involves the interaction between conserved KTXXXW motifs located at the c-terminus of frizzled and PDZ domains contained within intracellular mediators such as Dishevelled. This leads to localisation of these mediators to Frizzled at the cell membrane and activation of downstream signalling (Wong et al., 2003), (Umbhauer et al., 2000). An illustration depicting the structural domains of Frizzled receptors is shown in Figure 1.6.

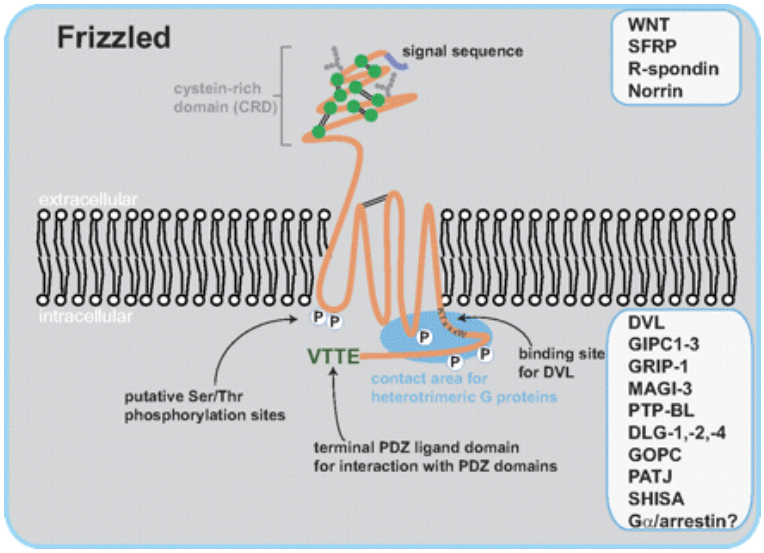

Figure 1.6. Schematic of the Frizzled receptor.
Illustration depicting the structural domains of Frizzled receptors. The extracellular Cysteine rich domain is involved with Wnt reception. The transmembrane domains span the lipid bilayer. The intracellular terminus has binding sites for interaction with intracellular mediators such as Dishevelled (Dvl). Image reproduced with permission from Schulte 2010 (Schulte, 2010).

1.5.2.2 LRP

Besides Frizzled receptors, Wnt reception has also been shown to require recruitment and dimerisation of various co-receptors in order to initiate signalling. Chief amongst these co-receptors are members of the single-pass transmembrane low density lipo-protein receptor-related proteins (LRP) family, namely LRP5/6. It is widely thought that Wnt molecules form a trimeric complex with a Frizzled receptor and a LRP5/6 receptor to signal pathway activation (Logan and Nusse, 2004). In the presence of a Wnt ligand and dimerisation with Frizzled, the LRPs become phosphorylated at a number of sites at their C-terminal. During activation LRP6 becomes phosphorylated at Thr1479, Ser1490, and Thr1493 by kinases such as Glycogen synthase kinase 3 (GSK-3) and Casein Kinase 1 (CK1) upon stimulation by Wnt (Tamai et al., 2004), (Zeng et al., 2005), (Davidson et al., 2005). LRP6 seems to be more prevalent in Wnt signalling, particularly during embryogenesis whereas LRP5 has been shown to be crucial for the maintenance of adult bone (MacDonald et al., 2009).

1.5.2.3 Other related receptors

In addition to Frizzled and LRP5/6, there is an array of other cell surface receptors that play roles in Wnt signalling. A number of these receptors belong to the receptor tyrosine kinase (RTK) family of receptors. One such example is Receptor Tyrosine Kinase-Like Orphan Receptor 2 (ROR2), a transmembrane receptor that is primarily associated with non-canonical Wnt signalling. Like the Frizzled receptors, ROR2 contains a CRD in the extracellular portion of the receptor that is involved in Wnt protein reception. The intracellular C-terminal domain contains the tyrosine kinase domain required for signal

transduction (Oishi et al., 2003), (Kani et al., 2004). ROR2 has been shown to interact with Wnt5A and transduce non-canonical Wnt signalling whilst at the same time antagonising canonical Wnt signalling via Wnt3A (Oishi et al., 2003). RYK is another single pass transmembrane RTK receptor. The extracellular domain of RYK contains a Wnt inhibitory factor (WIF) sequence to which Wnt proteins are presumed to bind. RYK is involved in canonical Wnt signalling and has been shown to play roles in pattern formation and axon guidance (Yoshikawa et al., 2003), (Inoue et al., 2004).

Another Wnt pathway related receptor family are the leucine-rich repeat-containing G protein-coupled receptors (LGR). LGRs are a subgroup of receptors that belong to the Rhodopsin family. They are characterised by their large leucine rich extracellular domains and have been shown to be a receptors for R-spondin. LGR5 is known to be expressed in stem cells and is associated with cell proliferation and has been implicated in numerous cancers (Carmon et al., 2011), (Van Hiel et al., 2012), (Van Loy et al., 2008).

1.5.3 Inherent complexity of Wnt signalling pathways

Wnt signalling is a complex web of inter-connected pathways all of which show cross-talk with each other. The first layer of complexity can be found with Wnt proteins. Some Wnt proteins (e.g. *Drosophila* Wnt) are capable of binding to multiple frizzled receptors with different affinities (Hsieh et al., 1999). Despite there being evidence of Wnt promiscuity in terms of signal specificity, there is also evidence to suggest that certain Wnt proteins have a tendency for signal preference. For example, Wnt 3a is commonly associated with canonical signalling whereas Wnt 5a is usually associated with non-canonical signalling (Grumolato et al., 2010). It is also apparent that most frizzled receptors are capable of signalling through the canonical or non-canonical pathways (MacDonald et al., 2009). The

current model of Wnt signalling indicates that the expression of different co-receptors is the most important factor determining signal specificity and pathway activation (van Amerongen et al., 2008).

1.5.4 Canonical Wnt signalling

In Canonical signalling Wnt proteins interact with target cells by binding to a receptor complex comprised of Frizzled and LRP5/6 located at the cell surface. Wnt is critical in initiating formation of this complex and previous work has demonstrated that an engineered complex of Frizzled and LRP5/6 is sufficient to activate canonical signalling (Cong et al., 2004), (Holmen et al., 2005), (Tolwinski et al., 2003). The complex of Fz/LRP and Wnt transduces the Wnt signal to the scaffold protein Dishevelled (Dvl). Dvl functions by binding to and sequestering several other intracellular proteins including glycogen synthase kinase-3β (GSK-3β), Axin and Adenomatous Polyposis Coli (APC) to the cell membrane. This complex of proteins form what is termed the 'destruction complex' and serves to regulate the cytoplasmic pool of a signalling protein known as β-catenin, which is a transcriptional regulatory factor in the nucleus (Logan and Nusse, 2004). β-catenin is a large multifunctional signalling molecule that consists of a central region of twelve repeats of three helices, this structure allows binding of a wide range of proteins besides GSK-3β including T-Cell Factor (TCF), APC, Axin and cadherin (Bullions and Levine, 1998), (Huber et al., 1997), (Kimelman and Xu, 2006). In the absence of a Wnt signal, the destruction complex successively phosphorylates β-catenin at its N-terminal residues Ser33, Ser37 and a neighbouring aspartate residue. This provides a docking site for E3 ubiquitin ligases which in turn labels Lys19 and Lys49 residues of β-catenin with ubiquitin.

This marks β-catenin for proteasome degradation and thereby prevents Wnt signalling activation (Wu et al., 2003), (Kimelman and Xu, 2006).

In the presence of a Wnt signal the destruction complex is sequestered by Dvl, and as a result becomes deactivated. This results in accumulation of the active, hypo-phosphorylated form of β-catenin in the cell cytoplasm and nucleus. In the nucleus β-catenin acts as a transcriptional regulator and interacts with the T-cell factor / lymphoid enhancer factor 1 (TCF/LEF) family of transcription factors (Logan and Nusse, 2004). These transcription factors bind to and activate transcription of Wnt responsive genes that harbour TCF/LEF responsive elements. β-catenin propagates this process by replacing transcriptional co-repressors such as Groucho and CtBP which associate with TCF/LEF and aids the recruitment of transcriptional activators such as Swi/SNF (Rao and Kuhl, 2010). A schematic of canonical Wnt signalling is shown in Figure 1.7.

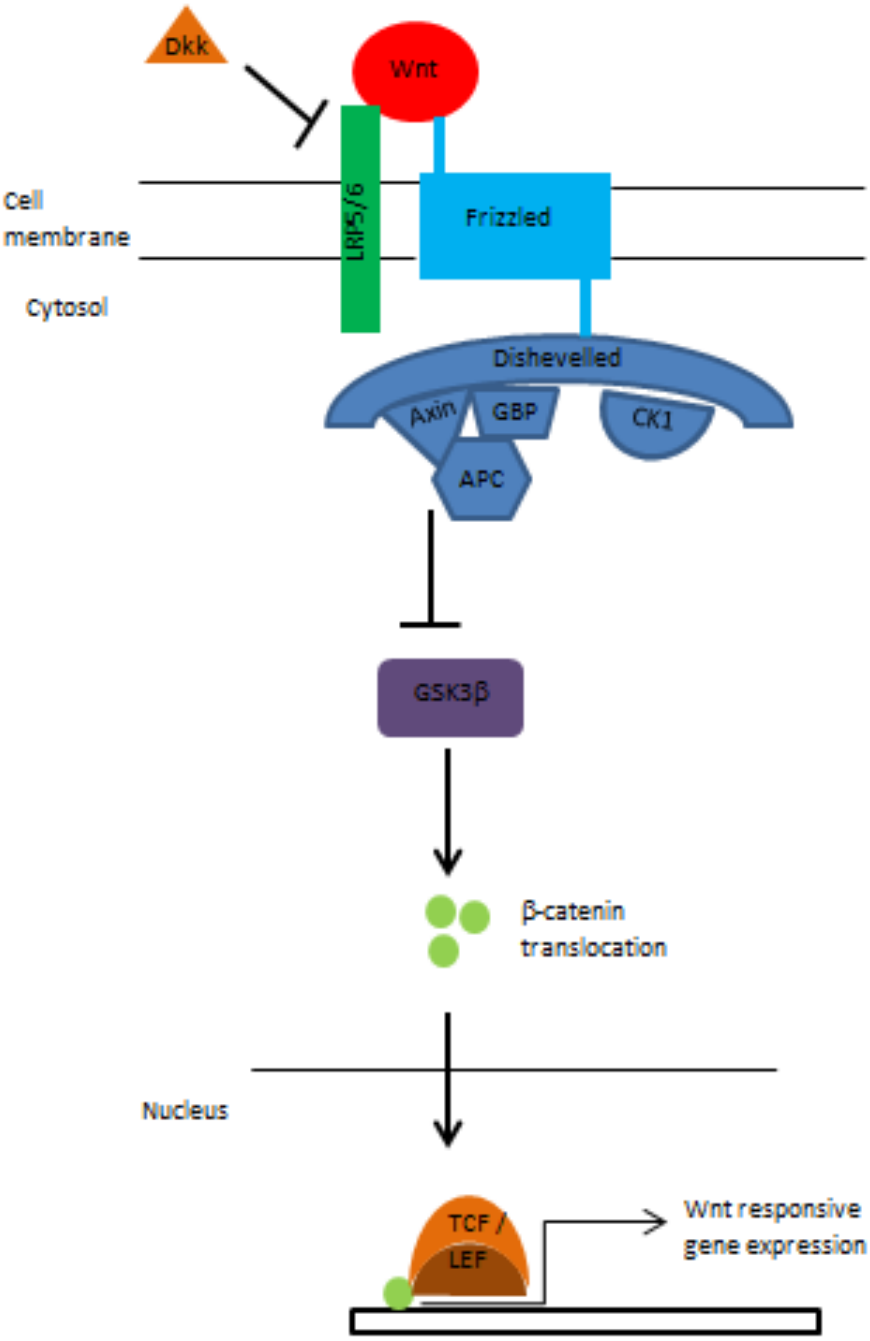

Figure 1.7. Diagram of the canonical Wnt signalling pathway.
Reception of Wnt proteins occurs at the cell membrane and involves binding to Frizzled and LRP5/6 co-receptors. In the cytosol this causes recruitment of Dishevelled to the activated receptor complex. This leads to inactivation of the destruction complex which consists of Axin, GBP, APC, CK1 and GSK-3β. Consequently, this leads to stabilisation and nuclear translocation of β-catenin and transcription of TCF/LEF responsive genes.

1.5.5 Wnt target gene transcription

The activation complex regulates the transcription and expression of a multitude of Wnt target genes with TCF/LEF binding sites (Logan and Nusse, 2004), (Schuijers et al., 2014), (Nusse, 1999) and is involved in the regulation of many cell processes. Some of the genes regulated by Wnt signalling include genes regulating the cell cycle, cell proliferation and oncogene expression. Examples here include c-Myc, Cyclin D1 (He et al., 1998), (Shtutman et al., 1999), (Rohrs et al., 2009), (Herbst et al., 2014) and COX2 (Nuñez et al., 2011), (Howe et al., 1999). Other Wnt responsive genes include regulatory proteins in the Wnt pathway such as LEF1 (Filali et al., 2002), TCF7 (Roose et al., 1999) and Wnt signalling inhibitors such as Dickkopf (Dkk1) (Rao and Kuhl, 2010). Feedback loops such as this help to provide a further level of control over Wnt pathway activity (Logan and Nusse, 2004).

1.5.6 Non-canonical Wnt signalling

Non-canonical Wnt signalling is a collective term for the Wnt signalling pathways that do not signal through β-catenin. There are multiple non-canonical Wnt pathways that use different intracellular messengers and result in a multitude of cellular effects including changes to the cell cytoskeleton, cell polarity and differentiation. The effects of non-canonical signalling vary depending on the cell type and species (Rao and Kuhl, 2010). The non-canonical pathways are characterised according to their intracellular mediators. The Wnt/JNK pathway proceeds through intracellular mediators such the Ras homolog (Rho) family of small GTPases and Jun N-terminal kinase (JNK) proteins whilst the Calcium pathway involves activation of calcium dependent enzymes and release of intracellular calcium.

1.5.6.1 Wnt/JNK pathway

The Wnt/JNK pathway strongly overlaps with the planar cell polarity pathway observed in *Drosophila*. JNK pathway activation occurs through Frizzled receptors in conjunction with Dishevelled. This pathway activates small GTPases e.g. Rho and other downstream kinases e.g. JNK and results in changes to protein localisation and cell polarity. In *Drosophila* the planar cell polarity pathway regulates cellular functions involved with polarised cell movements. e.g. gastrulation (Rao and Kuhl, 2010). The JNK pathway is also involved in ciliogenesis (Ross et al., 2005).

1.5.6.2 Calcium pathway

Wnt proteins can also activate calcium signalling, the evidence of this pathway was first observed in *Zebrafish* and *Xenopus* (Slusarski et al., 1997a), (Slusarski et al., 1997b). Wnt 5A has been shown to activate the calcium pathway in a number of cell types. This branch of Wnt signalling is dependent on small heterotrimeric G-proteins to propagate the signal and activate calcium dependant enzymes e.g. CAMK2, Protein kinase C (PKC), Calcineurin (Kremenevskaja et al., 2005), (Dejmek et al., 2006), (Ma and Wang, 2006), (Safholm et al., 2006), (Kuhl et al., 2000a), (Kuhl et al., 2000b). Non-canonical signalling in this manner (i.e. through CAMKII) can lead to inhibition of β-catenin signalling (Ishitani et al., 2003), (Ishitani et al., 1999). Furthermore, the type of calcium dependant enzyme activated determines which downstream transcription factors are activated. The Calcium/Calcineurin pathway, which acts through Nuclear factor of activated T-cells (NFAT) transcription factors, has important roles to play in cardiac development and has been associated with cardiac hypertrophy (Rao and Kuhl, 2010), (Dejmek et al., 2006), (Belema Bedada et al., 2005), (Heineke and Molkentin, 2006).

1.5.7 Wnt pathway antagonists

1.5.7.1 Dkk

The most widely studied Wnt pathway inhibitors are the Dickkopf WNT Signalling Pathway Inhibitor (Dkk) proteins. There are four known Dkk genes expressed in humans of which Dkk1 is the most widely studied (Krupnik et al., 1999), (Monaghan et al., 1999). Dkk is postulated to inhibit Wnt pathway activation through two mechanisms, both of which involve binding to and inhibition of Wnt co-receptors LRP5/6 and/or Kremen. This process is mediated through the cysteine rich domains harboured within Dkk. One proposed mechanism behind Dkk mediated Wnt pathway inhibition involves disruption of the Wnt induced LRP and Frizzled complex formation which prevents downstream pathway activation. The second mechanism involves internalisation of LRP into the cell cytosol, which therefore reduces the availability of LRP receptors for Wnt binding at the cell membrane. As these mechanisms involve LRP co-receptor inhibition, Dkk proteins are therefore able to specifically antagonise the canonical β-catenin pathway due to the requirement for LRP co-receptors in canonical pathway activation (Mao et al., 2002), (Bafico et al., 2001), (Mao et al., 2001), (Mao and Niehrs, 2003), (Krupnik et al., 1999), (Semenov et al., 2001). However, it should be noted that Dkk mediated LRP6 internalisation and degradation may not be the main mechanism of action in mammalian cells with endogenous LRP6 expression. In this scenario disruption of the Wnt-Frizzled-LRP complex may be the main effect of Dkk (Semenov et al., 2008).

Interestingly, Dkk2 has been shown to act as an agonist or antagonist of Wnt signalling depending on the cell type. For instance, agonistic activity of Dkk2 on LRP6 activity and Wnt pathway activation was observed in 293 fibroblasts. However this was only the case

in the absence of Kremen 2 expression, co-expression of Kremen 2 re-introduced the antagonistic effects of Dkk2 (Mao and Niehrs, 2003).

1.5.7.2 Other notable antagonists

Other major antagonistic proteins that regulate Wnt signalling include the secreted frizzled related proteins (sFRP) and Wnt inhibitory factors (WIF). Both of these classes of proteins act by binding to Wnt proteins and sequester the Wnt protein away from the cell surface receptors. This suggests that sFRP and WIF regulate Wnt stability and control extracellular distribution (MacDonald et al., 2009). It has also been reported that sFRP is capable of binding to Frizzled receptors. As canonical and non-canonical Wnt signalling both signal through Frizzled receptors, this renders sFRP capable of inhibiting both canonical and non-canonical pathways (Bovolenta et al., 2008). Five sFRP genes have currently been identified in mammals and they all share structural similarities to the extracellular domain of Frizzled receptors, including the presence of a cysteine rich domain (Chang et al., 1999), (Leimeister et al., 1998), (Rattner et al., 1997). Knock-out studies of sFRP have demonstrated that there is also functional redundancy amongst the sFRP family much like the Frizzled family of receptors (Satoh et al., 2008).

Another Wnt pathway modulator is known as Wise, which is a secreted protein that interacts with LRP6 and can act as a Wnt pathway inhibitor or activator. Wise has been shown to be involved in posterior neuron formation (Itasaki et al., 2003). Sclerostin is another LRP5/6 antagonist. Similar to Dkks, Sclerostin prevents Fz-LRP6 complex formation by binding to the extracellular domains of LRP5/6 thereby preventing formation of the receptor complex that is ordinarily formed as part of Wnt / β-catenin signalling (Semenov et al., 2005). Shisa proteins are also a distinct family of Wnt

antagonists. Shisa proteins act by trapping Frizzled receptors in the Endoplasmic Reticulum and by doing so prevents them from being transported and expressed at the cell membrane. This therefore prevents Wnt pathway activation by ablating Wnt signal reception at the cell membrane (Yamamoto et al., 2005).

1.5.7.3 Pharmacological antagonists of Wnt Pathways

Excessive or unrestricted Wnt pathway activation is involved in a wide array of diseases especially cancers (Herr et al., 2012). As a response there is great interest in developing pharmacological inhibitors of Wnt signalling. Currently, most antagonists of Wnt pathways act by promoting β-catenin degradation. This can be achieved using molecules that increase Axin expression which stabilises the destruction complex and promotes β-catenin degradation. One example of this type of compound is endo-Inhibitors of Wnt response 1 (endo-IWR1) (Lu et al., 2009), (Chen et al., 2009). Alternative mechanisms of inhibition target downstream transcription of Wnt responsive genes, which can be blocked by interfering with β-catenin binding to TCF/LEF responsive elements. One example here are the inhibitors of catenin responsive transcription (iCRT) compounds e.g. iCRT-14 (Gonsalves et al., 2011).

1.5.8 Wnt pathway agonists

Besides Wnt protein, there are multiple other protein ligands which are known to have agonistic effects on Wnt pathways. Norrin and R-spondin (Rspo) proteins are two classes of canonical pathway agonists. Norrin is a specific ligand for Frizzled 4 and acts in accordance with LRP6; this complex has been observed during retinal vascularisation (Xu et al., 2004). Similarly, R-spondin also has synergistic relationships with Wnt, Frizzled and LRP6 (Kazanskaya et al., 2004), (Kim et al., 2005), (Nam et al., 2006), (Wei et al., 2007) and

is involved in development during embryogenesis (Bell et al., 2008). R-spondins are often co-expressed with and may in fact depend on Wnt for expression. This suggests that R-spondin may act as part of a positive feedback loop that serves to reinforce a Wnt signal (Kazanskaya et al., 2004). Having said this, the finer elements behind R-spondins mechanism of action remains poorly understood. An alternative model suggests that R-spondin binds to Kremen and in this way prevent Dkk/Krm controlled LRP6 internalisation (Binnerts et al., 2007).

1.5.8.1 Pharmacological agonists of Wnt pathways

There is a growing array of synthetic molecules that have been developed as agonists or antagonists of Wnt pathways. The most widely used class of agonists of canonical Wnt signalling are GSK-3β inhibitors of which Lithium Chloride (LiCl) is most well-known. LiCl is a long established treatment for bi-polar disorder but has also been associated with high bone mass conditions (Zamani et al., 2009). LiCl acts as an activator of Wnt signalling by inhibiting the action of GSK-3β which is required to phosphorylate β-catenin which is necessary for initiating proteasomal degradation. As a result active β-catenin is able to mobilise to the nucleus to activate Wnt responsive genes (Freland and Beaulieu, 2012). Another class of GSK-3β inhibitors is 6-bromoindirubin-3'-oxime (BIO), which is a potent and selective inhibitor of GSK-3β. BIOs mode of action involves binding the Adenosine triphosphate (ATP) binding pocket of GSK-3β. It has also been shown to inhibit the phosphorylation of tyrosine residues in the GSK-3β active site. Like LiCl, the inactivation of GSK-3β allows the nuclear accumulation of β-catenin and activation of Wnt responsive genes. *In vivo* studies have shown that BIO can mirror the effects of Wnt signalling in *Xenopus* embryos (Meijer et al., 2003).

1.5.9 Peptide mediated modulation of Wnt pathways

There is a growing interest in developing upstream modulators of Wnt pathways that act on Wnt receptors at the cell membrane. One such peptide that has been shown to interact with Frizzled receptors is known as UM206 and was developed by Blankesteijn et al. (Blankesteijn Wessel Matthijs, 2010). The amino acid sequence of UM206 is based on a fragment of Wnt3A and Wnt 5A proteins (amino acids 296 - 307 and 324 - 335 respectively). The peptide sequence of UM206 is shown below:

Ac-Cys-Asn-Lys-Thr-Ser-Glu-Gly-Met-Asp-Gly-Cys-Glu-Leu-NH2

UM206 is a high affinity ligand for Frizzled 2 receptors and, to a lesser extent, Frizzled 1. The peptide has been shown to initiate activation of canonical Wnt signalling as demonstrated by increased Wnt reporter activity when the peptide is present in a cyclical conformation (EC_{50} 2.10-^{8}M). The cyclic conformation of UM206 can be formed by inducing a disulphide bridge between the two cysteine residues in the peptide. In contrast, when the peptide is presented in its linear conformation it has been shown to act as an inhibitor of Wnt pathway activity (IC_{50} 10^{-10} M). Restriction of Wnt signalling using UM206 in its linear conformation has been shown to be beneficial in preventing infarct expansion and heart failure after myocardial infarction (Blankesteijn Wessel Matthijs, 2010), (Laeremans et al., 2011).

1.6 Role of Wnt signalling in bone

Wnt signalling pathways play vital roles in regulating bone formation at all stages of development, from limb formation during embryogenesis, to bone remodelling and

fracture repair in adult bone (Regard et al., 2012). The important roles of Wnt signalling in bone are highlighted by the bone pathologies arising from mutations in the genes involved in Wnt signal transduction. For example, some patients displaying a high bone mass phenotype have been shown to harbour a mutation in the gene for the Wnt co-receptor LRP5 known as G171V. This mutation prevents the Wnt inhibitor Dkk1 from blocking Wnt pathway activation (Little et al., 2002), (Boyden et al., 2002). Another inactivating mutation of the SOST gene which encodes the LRP5/6 inhibitor Sclerostin is a cause of Sclerosteosis, which is also characterised by a high bone mass phenotype (Balemans et al., 2001). This suggests that increased Wnt pathway activity is a driver behind bone formation. In contrast loss of function mutations of LRP5 (e.g. frameshift and nonsense causing mutations) have been shown to cause low bone mass. This is observed in Osteoporosis Pseudoglioma syndrome which results in low trabecular bone volume (Gong et al., 2001). At the cellular level Wnt signalling has been shown to either promote or restrict osteoblast differentiation depending on the stage of cell differentiation. For instance, stimulation of Wnt signalling in early stage osteoblasts has been reported to enhance differentiation at later stages, whilst in mature osteoblasts mineralisation was inhibited (Eijken et al., 2008). Active Wnt signalling is also known to be prevalent in osteoblast precursor cells where β-catenin has been shown to be prevalent in the nucleus, an indication of Wnt pathway activity (Day et al., 2005). Wnt activity is also present during bone repair. For example, inducing a transcortical Tibial defect in transgenic mouse models expressing the TOPgal Wnt reporter was shown to induce reporter activity. This indicates that Wnt signalling is a response to injury and is required for bone repair (Kim et al., 2007). Conversely, impaired Wnt signalling has been

implicated in a range of diseases such as osteoporosis and osteopenia (Dimitriou et al., 2011), (Hoeppner et al., 2009).

1.6.1.1 Roles of Wnt signalling in regulating MSC fate

Wnt signalling is an important signalling pathway in development and in particular Stem cell proliferation and differentiation. This had made the Wnt signalling pathways a therapeutically relevant target not only in cancer but in the field of tissue engineering and regenerative medicine in which MSC are playing an important role. Fine tuning of Wnt signalling activity is also an important factor in the regulation of the developmental niche, including the MSC niche. One way of controlling Wnt activity is by establishing and presenting cells with Wnt gradients (Heller and Fuchs, 2015), (Kim et al., 2015). MSC are known to express a number of Wnt ligands including Wnt 2, 4, 5a, 11 and 16. Expression of a number of Frizzled receptors (Frizzled 2-6), co-receptors and pathway inhibitors has also been observed (Etheridge et al., 2004). This suggests that Wnt signalling has roles to play in MSC fate and lineage specificity. Wnt signalling has been shown to elicit different outcomes depending on the cell type and Wnt concentration, this is also evident in the context of osteogenesis (Quarto et al., 2010), (De Boer et al., 2004b). Activation of canonical Wnt signalling by Lithium or Wnt3A in hMSC has been shown to inhibit differentiation, decrease mineralisation and ALP activity but increase other bone-related markers whilst promoting proliferation and maintaining MSC multi-potency (de Boer et al., 2004a), (Boland et al., 2004), (Cho et al., 2006). These observations are presumably linked to the activation of Wnt responsive genes involved in cell cycle and proliferation like Cyclin D1 and c-Myc (Baek et al., 2003). One advantage of the proliferative effects of Wnt signalling is that this could allow the scale-up and banking of huge numbers of stem cells that are required for cell-based therapies, whilst maintaining stem cell multi-

potency. A dose response effect of Wnt signalling has also been observed. For instance, low levels of canonical Wnt signalling have been reported to promote cell proliferation (including in hMSC), whilst higher doses were shown to have suppressive effects (Gong et al., 2001), (De Boer et al., 2004b), (Qiu et al., 2007). Previous work has also demonstrated a differential expression pattern of Wnt related genes during hMSC osteogenesis. For instance, upregulation of the genes encoding Frizzled 6, ROR2, sFRP2/3 and Wnt 11 whilst down-regulation of the Wnt 9a and Frizzled 7 genes have been observed (Boland et al., 2004). Activated canonical Wnt signalling has been shown to promote osteogenesis in certain cellular contexts. For example canonical Wnt3A has been shown to promote osteogenesis in calvarial osteoblasts (Quarto et al., 2010) whilst LiCl has been shown to induce ALP activity in hMSC (De Boer et al., 2004b). In murine MSC and osteo-progenitor cells canonical Wnt signalling has been shown to promote osteoblastogenesis via up-regulation of RUNX2, DLx5 and SP7 (Bennett et al., 2005), (Gaur, 2005). Furthermore, the induction of relatively high activity of canonical Wnt signalling through addition of exogenous Wnt3a, overexpression of LRP6 or stabilised β-catenin has been shown to enhance hMSC osteogenesis (Gong et al., 2001), (De Boer et al., 2004b), (Qiu et al., 2007). It is also apparent that the stage of the target cell is also important when determining the cellular response to Wnt signalling. MSC committed to osteogenesis have been shown to exhibit enhanced osteogenesis in response to canonical Wnt signalling whilst this also inhibits their terminal differentiation in to osteoblasts (Kahler and Westendorf, 2003), (Kahler et al., 2006), (Eijken et al., 2008), (Kahler et al., 2008). The non-canonical pathway has also been associated with MSC osteogenic differentiation. The non-canonical pathway associated Wnt5a has been shown to promote osteogenic differentiation whilst at the same time blocking the effects of Wnt3a (Baksh et al., 2007), (Boland et al., 2004).

Furthermore, non-canonical associated Wnt11 has been shown to be up-regulated during osteogenic and chondrogenic differentiation (Lako et al., 1998). Evidently, there is a clear role for both canonical and non-canonical Wnt signalling pathways in controlling MSC differentiation. A comprehensive review detailing the roles of Wnt signalling on MSC proliferation and differentiation is provided by Ling et al. and is summarised in Table 1.1 (Ling et al., 2009).

	Wnt pathway			
MSC fate	**Canonical**		**Non-canonical**	
Self-renewal	*Stimulatory*	*Inhibitory*	*Inhibitory*	
	Low Wnt activity	High Wnt activity		
	(Subject to cellular context)		(Subject to cellular context)	
Osteogenic Differentiation	*Stimulatory*	*Inhibitory*	*Stimulatory*	
	High Wnt activity: Lineage commitment	Lineage commitment		
	Early differentiation	Terminal differentiation		
	Mouse MSC			
Chondrogenic differentiation	*Stimulatory*	*Inhibitory*	*Stimulatory*	*Inhibitory*
	Lineage commitment	Chondrocyte differentiation	Chondrocyte differentiation	Lineage commitment
	Maturation			Maturation
Adipogenic differentiation	*Inhibitory*		N/A	
Myogenic differentiation	*Stimulatory*		*Stimulatory*	

Table. 1.1. The effects of Wnt signalling on MSC fate.
Wnt signalling has both stimulatory and inhibitory effects on MSC self-renewal and differentiation. The outcome on cell fate is dependent on the Wnt dosage and the cellular context. Adapted from Ling et al. 2009 (Ling et al. 2009).

1.6.1.2 Use of Wnt in bone tissue engineering

The use of Wnt proteins *in vivo* for tissue engineering and regenerative medicine has been extremely limited to date. This is due to many factors including the multiplicity of Wnt ligands and their contextual effects which hinder the implementation of standardised dosing. These problems are also compounded by the difficulties in purifying substantial amounts of active Wnt protein with the appropriate post-translational modifications and hydrophobicity which are required for bio-activity (Willert et al., 2003), (Kikuchi et al., 2007), (MacDonald et al., 2009), (Logan and Nusse, 2004). Despite these issues there are some studies which have demonstrated the efficacy of Wnt delivery for *in vivo* bone repair. For example, direct delivery of Wnt protein or liposome encapsulated Wnt protein has been shown to increase bone volume and enhance bone repair in mouse models (Zhou et al., 2009), (Minear et al., 2010). Other groups have utilised transduced or transfected cells which over-express Wnt, these cells can then be delivered to sites of repair *in vivo*. This approach has also been shown to cause increases in bone density and formation in Severe combined immunodeficiency (SCID) mice models (Nalesso et al., 2011), (Qiang et al., 2008), (Liu et al., 2009), (Chang et al., 2007). Clearly new treatments that regulate Wnt signalling could be beneficial for bone regeneration. However one important aspect to consider is that potential treatments would have to be carefully controlled due to the role of Wnt pathways in tumourgenesis (Dimitriou et al., 2011), (Wagner et al., 2011).

1.7 Mechanotransduction

Mechanotransduction is the process of converting a physical force into a biological signal. This process is instrumental in development and governs many processes in embryogenesis and tissue patterning. Mechanotransduction at the cell occurs through so called mechano-sensitive proteins and receptors. Examples of mechanosensitive proteins include Integrins, ion channels and growth factor receptors. The central premise behind mechanotransduction is that applied forces induce conformational changes in these mechano-sensitive receptors. This leads to changes in their activation state and subsequent signalling to downstream intracellular signalling pathways (Kirkham et al., 2010), (Ingber, 2006), (Farge, 2003). Many cell types express mechano-sensitive receptors including bone cells, and mechanotransduction is a critical signalling mechanism controlling bone development. Activation of mechanosensors leads to downstream activation of many second messenger systems and signal transduction pathways such as Nitric oxide (NO) and Calcium signalling as well a host of growth factor signalling pathways (Liedert et al., 2006), (Ingber, 2006). Activation of these signalling pathways ultimately leads to transcription of mechano-sensitive genes and changes in gene expression that alter cell proliferation, migration, differentiation and the production of signalling molecules such as BMPs and cytokines (Mammoto et al., 2012), (Santos et al., 2011).

1.7.1 Mechanosensors

Mechanical forces are detected by the cell through mechanosensitive molecules. An overview of the molecules involved in Mechanotransduction is shown in Figure 1.8. Many mechanosensitive proteins are activated as a result of changes in their conformation and activity in response to external forces. A principle site for sensing mechanical forces is the

cell membrane where forces are detected by proteins such as primary cilia, growth factor receptors, ion channels, integrins and cadherins amongst others. Mechanical forces are also sensed via intracellular mediators such as the cell cytoskeleton and chromatin (Ingber, 2006). Mechanotransduction elicits different effects on cell behaviour depending on where the force is targeted. Some mechanosensitive molecules such as stress sensitive ion channels cause fluxes in ion transport across the cell in response to force. This occurs as a result of changes in their conformation which causes opening and closing of the channels and subsequent activation of downstream signalling that leads to changes in gene expression (Sukharev and Corey, 2004), (Itano et al., 2003). Other proteins such as integrins are linked to the cell cytoskeleton. When forces are applied to these structures this leads to cytoskeletal and organelle rearrangements and activation of signalling pathways such as nuclear factor kappa-light-chain-enhancer of activated B cells (NF-κβ) pathway (Wang et al., 1993), (Matthews et al., 2006), (Ralphs et al., 2002), (Maniotis et al., 1997), (Tzima et al., 2005). Alternatively, when forces are directly applied to transmembrane molecules that are not directly linked to the cell cytoskeleton, such as growth factor receptors, this results in localised effects on cell signalling (Ingber, 2006). For example, shear stress has been shown to activate the vascular endothelial growth factor receptor 2 (VEGFR2) which led to downstream activation of Akt and Mitogen Activated Protein kinases (MAPK) (Jin et al., 2003), (Shay-Salit et al., 2002). G-protein coupled receptors (GPCRs) have also been implicated in mechanotransduction. For instance, application of fluid shear stress to endothelial cells has been shown to cause changes in the activity of the GPCRs bradykinin B_2 and Gαq/11 (Chachisvilis et al., 2006), (dela Paz et al., 2015). Furthermore, membrane stretch has been shown to cause activation of transient receptor potential (TRP) ion channels and was shown to be

mediated through Gq/11 –coupled receptors in vascular smooth muscle cells (Mederos y Schnitzler et al., 2008).

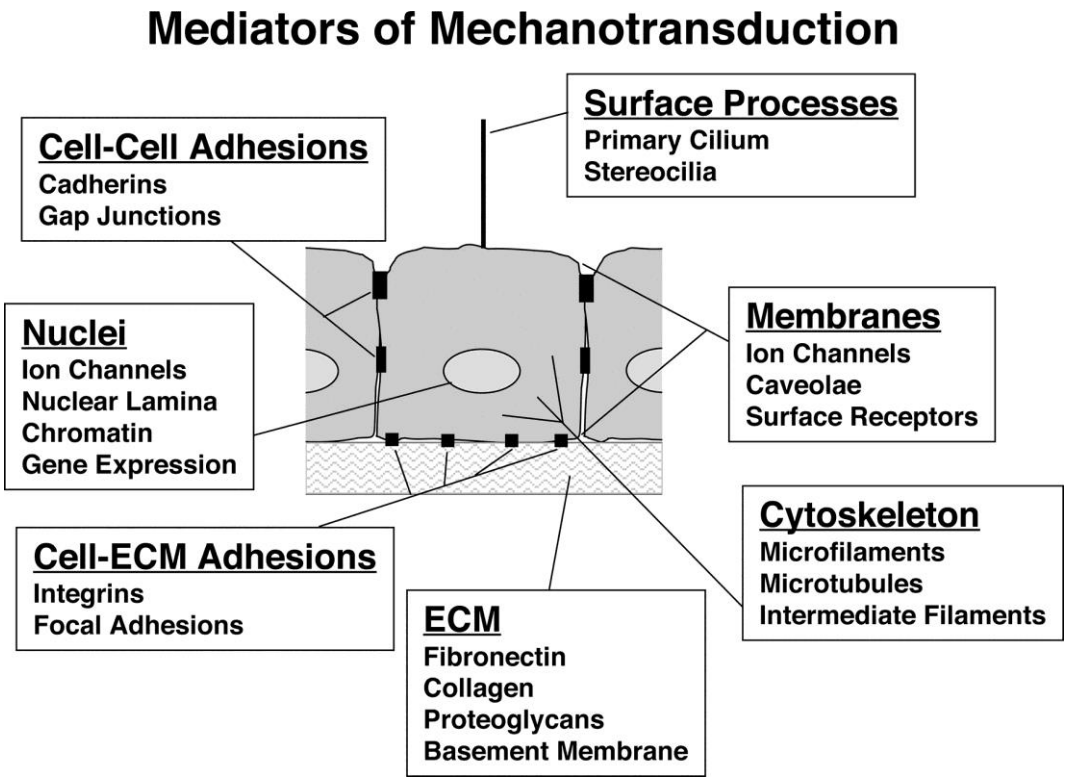

Figure 1.8. Mechanosensors.
Overview of mechanosensors. Mechanical forces are detected by many mechanosensitive proteins and receptors such as primary cilia, surface receptors, ion channels, Integrins, Cadherins, cell cytoskeleton etc. Image reproduced with permission from Ingber 2006 (Ingber, 2006).

1.7.1.1 Integrins

Integrins are a family of cell surface receptors that consist of two subunits known simply as α and β. Together, the α and β subunits form a functional dimer complex. Integrins link the extracellular matrix (ECM) to the cell cytoskeleton via focal adhesions and are involved in cell adhesion. The integrin complex facilitates mechanotransduction of external mechanical forces to the nucleus via the cell cytoskeleton (Hynes, 2002). This results in focal adhesion assembly via Rho signalling and actin polymerisation (Riveline et

al., 2001) as well as causing changes in mechanosensitive pathways mediated through c-fos, c-myc and MAPK (Benaud and Dickson, 2001), (Schwartz, 1997). Integrin mediated signalling has been implicated in the determination of cell fate, polarity, proliferation and differentiation through multiple intracellular pathways including Rho, Rho-associated protein kinase (ROCK), extracellular-signal-regulated kinases (ERK) and Akt signalling amongst others (Hynes, 2002).

1.7.1.2 Ion Channels

Mechanotransduction is also mediated through stretch activated ion channels. Mechanical perturbation of the cell membrane causes conformational changes in ion channels, which control ion flow across the cell membrane. Subsequently, these conformational changes cause opening and closing of the ion channels. This results in ion flux across the cell that results in changes to cell activity (Ingber, 2006). One such example is the MscCa channel which regulates cation flux across the cell membrane and is involved in the regulation of cell volume and movement. The gating of this channel has been shown to be regulated by changes in membrane tension (Maroto et al., 2005). Another example is the Twik-related potassium channel 1 (TREK1), an outwardly rectifying potassium channel that regulates the resting membrane potential of the cell (Lesage and Lazdunski, 2000), (Patel and Honore, 2001), (Fink et al., 1996). TREK1 is expressed in most tissues and is particularly prevalent in tissues of the nervous system, lung, heart and smooth muscle (Fink et al., 1996), (Medhurst et al., 2001), (Aimond et al., 2000), (Koh et al., 2001). TREK1 is known to be sensitive to a number of stimuli including heat, lipids and pH. TREK1 channels are also known to be mechanoresponsive and forces such as stretch can cause opening and closing of the channels. This results in movement of potassium

ions across the cell membrane that leads polarisation of the cell (Hughes et al., 2006), (Patel et al., 1998).

1.7.1.3 Growth factors

Growth factors and their receptors have also been implicated in mechanotransduction. The activity of the signalling pathways involved is known to be altered by mechanical forces. For example members of the Wnt pathway, insulin-like growth factor (IGF), Transforming growth factor-β (TGF-β) and BMP have all been shown to be induced in osteoblasts in response to loading (Liedert et al., 2006). A diagram illustrating the cell signalling pathways involved in mechanotransduction is shown in Figure 1.9.

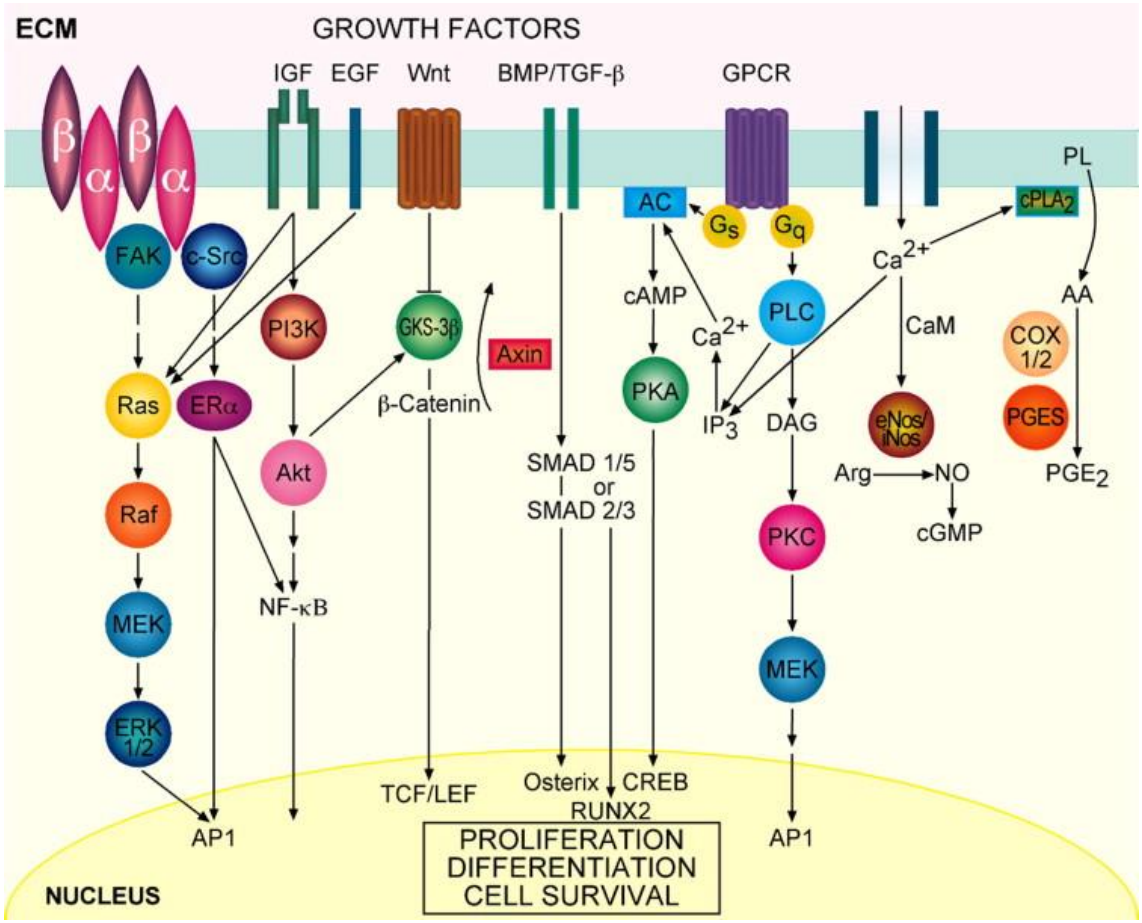

Figure 1.9. Mechanotransduction associated signalling pathways.
Mechanotransduction is mediated through multiple signalling pathways including integrins, growth factor receptors; G-protein coupled receptors (GPCRs) and ion channels. This leads to changes in gene expression that determines cell fate. Image reproduced with permission from Liedert et al. 2006 (Liedert et al., 2006).

1.7.2 Biological responses to mechanical force in bone

Mechanical loading is a key factor that regulates many physiological processes and is required for tissue morphogenesis and, at the cellular level, regulates cell behaviour and fate. This review will focus on the effects of forces in bone and bone cells; comprehensive reviews of the role of mechanical forces in development have been previously discussed (Heisenberg and Bellaiche, 2013), (Patwari and Lee, 2008). At the cellular level, bone cells have been shown to be sensitive to various mechanical stimuli. Fluid flow has been demonstrated to cause release of NO and PGE_2 from bone cells (Mullender et al., 2004).

Furthermore, direct stimulation of integrin receptors using magnetic nanoparticles has been shown to elucidate a number of responses in bone cells including changes to the cytoskeleton, MAPK activity, intracellular pH changes, and generation of calcium fluxes (Hughes et al., 2005). As well as causing activation of bone cells, mechanical stresses are known to influence the differentiation, proliferation and matrix production of progenitor and stem cells too. For instance, cyclic strain applied to MSC via substrate deformation has been shown to stimulate ERK1/2 signalling. This strain led to decreased cell proliferation and enhanced matrix mineralisation (Simmons et al., 2003). Fluid shear stress has also been reported to activate MAPK and calcium signalling in hMSC which also led to increased cell proliferation (Riddle et al., 2006). It has been shown that relatively small magnitudes of force are required to illicit a biological response at the cell and tissue level. For instance, stimulation of polyurethane based scaffolds seeded with hMSC was shown to promote cell proliferation and increase type 1 procollagen production. These effects were observed in response to perfusion applied at a rate of 10ml/min or compression strain applied at 10% strain (Liu et al., 2012). Furthermore, when 7-8 day old neonatal mouse tibia were stimulated with cyclic compression using forces in the magnitude of 500-7000 microstrain, DNA and protein synthesis were found to increase with peak effects observed at 1000 microstrain at a frequency of 1Hz (Kunnel et al., 2002). Low magnitude high frequency strains have also been shown to increase bone formation and density and inhibit osteopenia in various animal models (Rubin et al., 2001)

1.7.3 Mechanical stimulation systems in bone tissue engineering

Many bioreactor systems have been developed in recent years and used to apply loading regimes in order to mechanically condition cells and cell seeded constructs. This strategy is used as a means of optimising cell differentiation and tissue formation and is

particularly relevant in a bone tissue engineering context. Mechanical forces can be applied to cells or tissues in a passive and non-specific manner to cause generic membrane shear stresses to activate mechanotransduction pathways (Thompson et al., 2012). One type of generic stimulation system is compressive systems which can be used to apply generic compressive forces to a whole construct. This type of system has been used to investigate the osteogenic response of chick tibiotarsi in response to intermittent compressive loading provided by a simple piston system attached to a cam and weights. In this system ALP expression was maintained in comparison to the control and Collagen 1 expression was found to be increased (Zaman et al., 1992). Mechanical forces in the form of strain and stretching applied to osteoblast cells have also been shown to cause activation of the RUNX2 transcription factor through MAPK and ERK1/2 pathways resulting in upregulation in the expression of other osteogenic and bone related genes including ALP, Osteocalcin and Osterix (Kanno et al., 2007). The application of substrate strain to cells or cell seeded scaffolds has been shown to enhance the osteogenesis of hMSC by many groups (Haasper et al., 2008), (Friedl et al., 2007), (Ward et al., 2007). Perfusion based systems that utilise fluid-flow to induce shear stress are particularly common mechanical stimulation systems. This type of system has been shown to be beneficial for conditioning induced pluripotent stem cell (iPS)-derived mesenchymal progenitors cultured on osteo-conductive scaffolds. These cells showed a decrease in proliferation and an increase in lineage specific genes. This subsequently enabled the production of a functional bone substitute (de Peppo et al., 2013). Many groups have investigated the effect of shear stresses on the osteogenic differentiation of MSC. Perfusion systems that impart shear stresses on cell monolayers and cell seeded scaffolds have been found to increase bone marker gene expression and calcium deposition by

MSC (Kreke et al., 2008), (Bancroft et al., 2002), (Stiehler et al., 2009). A comprehensive review of the role of mechanics in directing MSC differentiation is provided by Potier et al. (Potier et al., 2010). One important aspect concerning the application of mechanical force is the relationship between cyclical and static strains. Studies have shown that cyclical force is the most important factor determining the scale of the biological response and that cyclical force appears to have a greater effect on the anabolism of tissue than static loading of higher magnitudes (Hsieh and Turner, 2001), (Liu et al., 2012). Cyclic forces have been shown to promote new bone deposition and tissue remodelling in conjunction with implanted scaffolds *in vivo* (Roshan-Ghias et al., 2011). Many hydrostatic force based stimulation systems have also been used to impart mechanical loads to cells and tissues. This approach has been shown to mimic fracture repair and upregulate osteogenic and angiogenic genes in a stress fracture rat model (Mosley and Lanyon, 1998), (Holtorf et al., 2005), (Wohl et al., 2009). Hydrostatic conditioning of chick femurs cultured *ex vivo* and cell seeded hydrogels has also been shown to be beneficial in driving new bone formation (Henstock et al., 2013). As an alternative to generically applied forces, controlled forces can be directionally applied to cells and target proteins using tools such as magnetic nanoparticles. This strategy has been shown to stimulate cell signalling pathways and promote the osteogenic differentiation of hMSC (Kanczler et al., 2010), (Hughes et al., 2008). This approach is discussed in more detail in section 1.8.

1.7.4 Mechano-activation of Wnt signalling

There is a clear link between mechanical forces, Wnt signalling and bone formation. There is growing evidence that the Wnt signalling pathway is activated in response to mechanical forces and that this is an important mechanism regulating bone remodelling (Huang and Ogawa, 2010), (Tu et al., 2012), (Crockett et al., 2011). As discussed

previously, the Wnt co-receptor LRP5 has long been associated with bone mass. For example, LRP knockout mice show significantly lower bone strength and mineral density and their osteogenic response to mechanical loading of the Ulna was found to be reduced. *In vitro* experiments also showed an inability of LRP5 knockout osteoblasts to synthesize Osteopontin after mechanical strain. This suggests that LRP5 is an important mediator of osteoblast activity in response to loading (Sawakami et al., 2006). Other *In vitro* experiments have investigated the link between Wnt pathway activity and mechanical loading. The application of fluid shear stress and mechanical strain by 4-point bending has been shown to initiate nuclear translocation of β-catenin and activation of a TCF reporter gene in Mouse MC3T3-E1 osteoblasts, ROS 17/2.8 cells and primary osteoblasts (Norvell et al., 2004), (Armstrong et al., 2007). Other *in vivo* models have demonstrated that mechanical loading of mouse tibias results in increased expression of Wnt pathway and Wnt target genes. Furthermore, there was a concomitant increase in this response from mice displaying the high bone mass phenotype LRP5 G171V. These results were corroborated *in vitro* where mechanical loading of MC3T3-E1 osteoblasts which were subjected to 5h of loading showed similar increases in Wnt gene activation including up-regulation of Frizzled 2 (Robinson et al., 2006). These studies suggest that the application of mechanical strain to influence Wnt signalling may be of benefit to bone formation for tissue engineering.

1.8 Magnetic Nanoparticles

The development of nano-scale technologies has opened up new fields of discovery in science and technology, and subsequently, new avenues of treatment in medicine

(Chakraborty et al., 2011). One particularly versatile set of tools in nanotechnology are magnetic nanoparticles (MNP). Broadly speaking, MNP are magnetic particles with dimensions in the nanometre scale. One type of MNP, known as superparamagnetic iron oxide nanoparticles (SPIONs), have proven to be useful in a wide range of biomedical fields such as imaging, diagnostics and biotechnology (Riehemann et al., 2009). There are also emerging applications for MNPs in tissue engineering and regenerative medicine; these applications will be discussed in section 1.8.6.

1.8.1 Composition of MNP

MNP typically consist of a magnetic core material, which is commonly iron oxide in the form of magnetite or maghemite (Mahmoudi et al., 2011). The magnetic core is often surrounded by a protective layer or biocompatible polymer e.g. dextran. This helps to prevent degradation of the core and reduce the cytotoxic effects of iron oxide based nanoparticles which has previously been observed in both *in vitro* (Hoskins *et al*) and *in vivo* studies (Hanini *et al*). The biocompatible MNP coating can then be functionalised with reactive groups such as carboxyl, hydroxyl or biotin. These reactive groups can then be used for attachment of biomolecules such as antibodies, therapeutic drugs and genes (Mahmoudi et al., 2011), (Fouriki et al., 2014), (Hoskins et al., 2012), (Hanini et al., 2011).

1.8.2 Magnetic properties of MNP

MNP are particularly useful as engineering tools because of their magnetic properties. The materials that make up the magnetic core of MNP can be varied to produce particles with different magnetic susceptibilities. Magnetic susceptibility occurs in materials with unpaired electrons and is defined as the ratio between the induced magnetisation and the applied magnetic field. Magnetite is a common core material used in MNP. When

magnetite based MNP are produced in the nano-scale dimension, this may cause the formation of single magnetic domains. Under these parameters magnetite based MNP may display superparamagnetic properties. Superparamagnetic materials only display magnetic susceptibility in the presence of an external magnetic field. In the absence of a magnetic field Brownian motion randomises the magnetic dipoles of the material and the particles retain no net magnetism. Superparamagnetic materials are particularly useful in medical applications where their colloidal stability and magnetic susceptibility need to be carefully controlled (Levy, 2012), (M. Hofmann-Amtenbrink, 2009), (Meng Lin et al., 2010), (Kumar, 2009).

1.8.3 MNP surface coatings

After synthesis of MNP, it is necessary to apply organic or inorganic coatings to the surface in order to stabilise the particle and help prevent particle aggregation. The surface coating can be modified to vary the physical properties of the MNP like surface charge, topography and protein binding capacity. For *in vivo* applications it also becomes necessary to coat the MNP with biocompatible substances such as Bovine Serum Albumin (BSA), Dextran or pullulan to reduce toxicity in the host (Gupta and Gupta, 2005), (Mehvar, 2000), (Hughes et al., 2005).

1.8.4 Particle Internalisation

Most cells (including MSC) will internalise micro- or nano- sized particles through endocytotic mechanisms such as caveolin and clathrin mediated endocytosis as well as by phagocytosis. The rate and method of internalisation is dependent on many factors such as the cell type, particle size, surface functionality etc. (Hughes et al., 2005), (Farrell et al., 2008). With respect to particle size, nanometre sized MNP in the range of 50-500nm have

been observed to be internalised more efficiently whilst larger particles above 1µm take longer to be internalised (Prabha et al., 2002), (Desai et al., 1997), (Foster et al., 2001). Surface functionality also affects the degree of MNP internalisation. For example, cationic functionalised gold nanoparticles have been shown to be more readily internalised than particles with anionic functionality (Jiang et al., 2015), (Jambhrunkar et al., 2014). The immediate fate of particles is dependent on the size and method of particle internalisation. MNP may be retained in the endosome or lysosome, or may be released and dispersed throughout the cytosol (Panyam et al., 2002).

1.8.5 Functionalisation of MNP

One of the attractive properties of MNP is their magnetic versatility and their capability to be functionalised with ligands. Ligands can be attached to MNP via functional groups located on the surface coating of the MNP (Lin et al., 2008). One common mechanism involves the covalent conjugation of the amine groups of proteins or peptides to carboxyl groups presented by MNP. This can be achieved using 1-Ethyl-3-(3-dimethylaminopropyl)-carbodiimide (EDAC) as a cross-linking agent which reacts with carboxyl groups to form a reactive O-acylisourea intermediate. This reactive intermediate can be stabilised using sulfo-N-hydroxy succinimide (NHS) to convert the O-acylisourea to a sulfo-NHS ester. The sulfo-NHS ester intermediate then reacts with primary amines to form a stable peptide bond between the particle and the ligand (Grabarek and Gergely, 1990), (Conde et al., 2014). A schematic depicting the conjugation process through carbodiimide activation is shown in Figure 1.10.

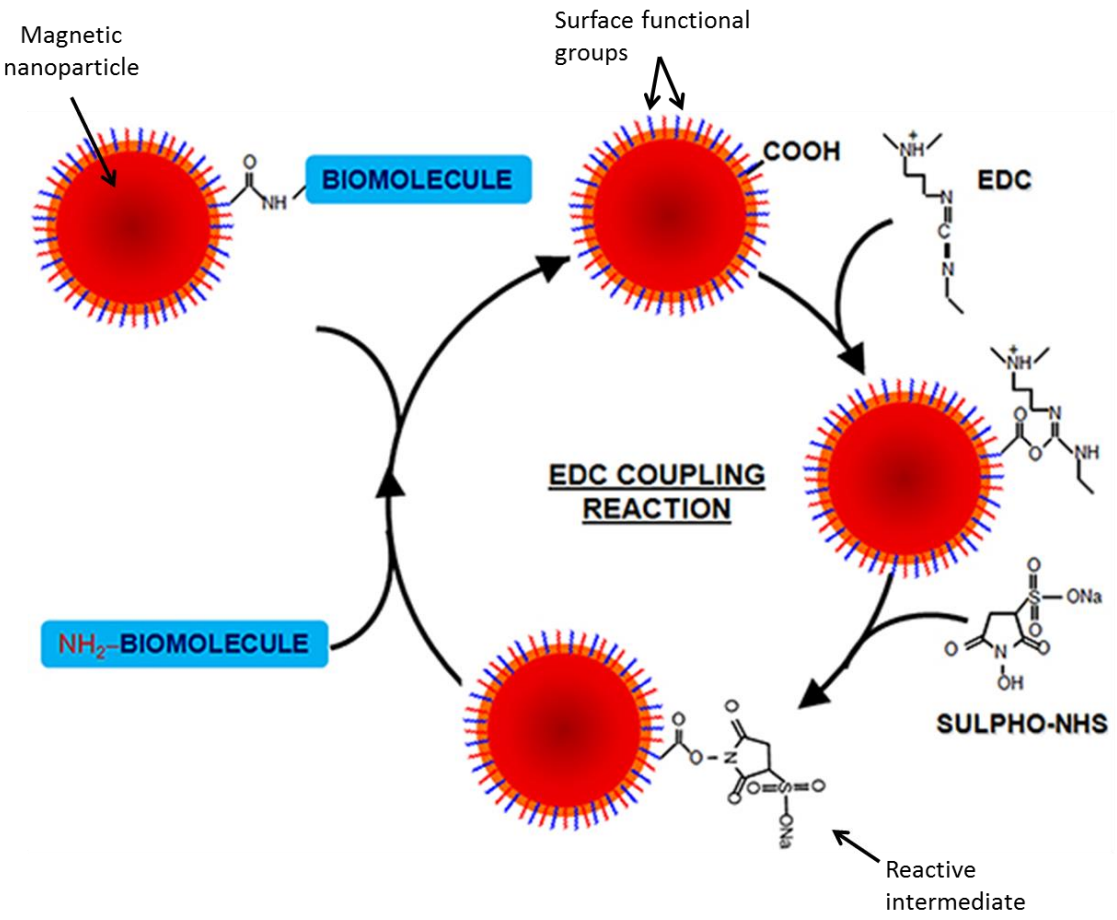

Figure 1.10. Carbodiimide cross-linking of carboxy-MNP with biomolecules. Reaction schematic illustrating cross-linking of Biomolecules to MNP. Reaction of carboxy-functionalised MNP with EDC and Sulpho-NHS results in a formation of a reactive sulpho-NHS intermediate. This intermediate reacts with amine groups present in biomolecules to form a peptide bond linking the biomolecule to the MNP. Image reproduced from Conde et al. 2014 (Conde et al. 2014), (Originally publsihed by Frontiers in Chemistry).

Other conjugation mechanisms include maleimide coupling. This involves the use of maleimide which reacts with sulfhydryl groups to form a thioether link and is used to conjugate primary amines to thiol groups (Brinkley, 1992), (Conde et al., 2014). Click chemistry based reactions such as the copper-catalysed azide-alkyne cycloaddition (CuAAC) reaction can also be used for bio-conjugation. These reactions rely on the reactivity of the Azide and alkyne functional groups for conjugation and have been used to conjugate various proteins to gold nanoparticles (Zhu et al., 2012). Alternatively, non-covalent methods can be used for MNP-ligand conjugation, these methods are discussed further by Conde et al. (Conde et al., 2014).

1.8.6 Biomedical applications of MNP

The physical properties of MNP such as size, composition, surface functionality and biocompatibility can be easily tailored to the intended purpose during production (Akbarzadeh et al., 2012). MNP can also be functionalised with a wide range of biological ligands such as small peptides or antibodies which allows targeting of MNP to specific tissues or cell populations via surface proteins (Conde et al., 2014) as shown in Figure 1.11. The versatility of these tools means that MNP can be applied to an enormous range of biomedical applications. In the field of nano-medicine MNP have been utilised for applications such as targeted gene or drug delivery, hyperthermia treatment of tumours and stem cell tracking by magnetic resonance imaging (MRI) (Lin et al., 2008).

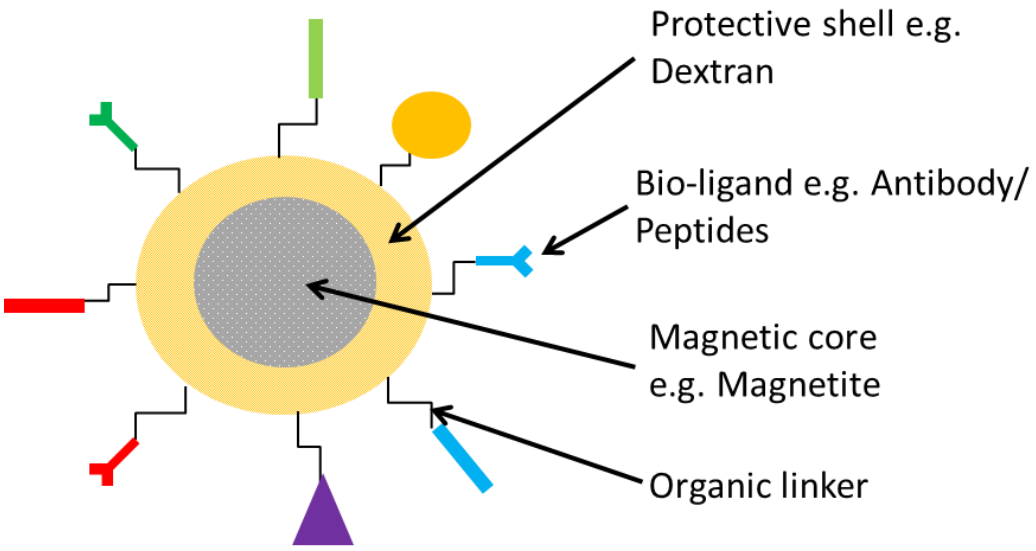

Figure 1.11. Schematic of MNP and surface coatings.
MNP typically consist of a magnetic core material surrounded by a protective matrix of biocompatible substrate such as Dextran. The MNP surface can be functionalised with various biomolecules including peptides, antibodies via surface functional groups or organic linkers.

1.8.6.1 Tracking and Tagging

MNP are particularly useful as tracking agents. For instance, MNP tagged cells that have been injected into the body can be easily located by magnetic resonance imaging (MRI). When cells are labelled with MNP, the MNP are eventually internalised by the cell. By doing so the magnetic properties of the MNP are effectively transferred to the cell. This makes it possible to track the cells by MRI (Ramaswamy et al., 2009). This strategy is useful in areas such as tissue engineering where the monitoring of the location and distribution of injected cells for cell therapies is important (Markides et al., 2012). Furthermore, MNP have been shown to be useful MRI contrast agents due to their high relaxation times and slow renal clearance. This is especially true for MNP sized <50nm in diameter (Talelli et al., 2009), (Mahmoudi et al., 2011). The use of SPION also tends to enable imaging of deeper tissues and often give superior image resolution when

compared to gadolinium based contrast agents (Talelli et al., 2009), (Jin et al., 2010). Examples of MNP that have made it to clinical use as contrast agents include Feridex and Endorem (Meng et al., 2009), (Martin et al., 2012). The tagging of cells with MNP also enables cells to be remotely guided and retained at the desired location. This can all be achieved using an external magnet. The applications of this strategy are clear in regenerative medicine where stem cells can be guided to damaged or hypertrophic tissue where they can then orchestrate repair of the tissue (Kyrtatos et al., 2009), (Arbab et al., 2004).

1.8.6.2 Cancer

Tumours have been shown to be particularly susceptible to heating compared to healthy tissue. Most cancer cells undergo cell death when heated to temperatures of 45^{o}C. The application of high temperatures causes many kinds of cell stress and results in protein denaturation, cytoskeleton and membrane damage and alters the activity of the enzymes involved in DNA replication and repair. In combination, these factors can lead to irreparable damage and cause apoptosis (Thanh, 2012). One way of generating localised heat at tumour sites is by using MNP. When tumours are loaded with MNP and exposed to an alternating magnetic field, the electromagnetic energy is converted to heat (Gneveckow et al., 2004). This results in controlled, localised heating of the tumour and subsequent tumour necrosis. Improved targeting of tumours can be achieved by combining antibody therapy with Hyperthermia treatment (Ito et al., 2004). Hyperthermia treatment of tumours is showing great promise in *in vivo* mouse models for a number of cancers (Hilger et al., 2005).

1.8.6.3 Drug delivery

MNP have also found applications as drug delivery vehicles. In this instance a high gradient external magnetic field can be used to guide and concentrate a drug loaded MNP that is intravenously or intra arterially injected to the desired location. At this point the drug or gene is then delivered using mechanisms such as enzymatic cleavage or changes in physiological condition e.g. pH, temperature (Shubayev et al., 2009), (Fouriki et al., 2014), (Lemke et al., 2004). This strategy has obvious benefits for reducing the doses required for chemotherapy where currently the administration of systemic (and often high) doses of a therapeutic agent are required for therapeutic efficacy but which can also induce side-effects. Targeted delivery systems that use MNP can help to maximise drug efficacy whilst minimising side effects, lowering the required dosage and therefore the cost of treatment (Alexiou et al., 2003). Drug delivery using this system has been assessed in rabbits with squamous cell carcinoma where it was demonstrated that Ferro-fluids loaded with Mitoxantrone could be manipulated to deliver the drug to the desired site using an external magnet (Alexiou et al., 2000).

1.8.6.4 Magnetofection

It is also possible to efficiently deliver therapeutic genes using MNP as a gene vector. This strategy has many applications in medicine e.g. treatment of genetic defects, cancer etc. The aim of gene therapy is to replace or introduce missing or faulty genes by the insertion of DNA. However, achieving successful and efficient transfection is notoriously difficult and current viral and non-viral methods frequently suffer from poor transfection efficiency (Dobson, 2006). Magnetic transfection has an advantage over other transfection systems that often impact cell viability or suffer from poor transfection efficiency (Durán et al., 2011). Furthermore, magnetic transfection requires shorter

incubation times, offers improved transfection of non-permissive cells and the potential for in vivo transfections (Dobson, 2006), (Scherer et al., 2002). For example, *in vitro* experiments have demonstrated improved transfection efficiency of MG63 cells without reducing cell viability (Fouriki et al., 2014). Also it has been shown that it is possible to transfect human umbilical vein endothelial cells (HUVECs) with VEGF in order to improve cell viability, this offers a novel method of treating heart ischemia (Cho et al., 2012).

1.8.7 MNP for cell activation

Another exciting application of MNP is remote activation of cell signalling pathways using MNP targeted to specific cell receptors. MNP can be functionalised with biomolecules and used to target specific cell receptors and signalling pathways. Signalling activity can then be modulated by applying external magnetic fields to the MNP. Under these conditions high gradient magnetic fields can be used to pull down, drag or oscillate the MNP in a given direction as illustrated in Figure 1.12. The magnetic field induces a translational force on the MNP which results in tension and deformation of the cell membrane or mechanosensitive receptor to which the MNP is attached or clustering of multiple receptors.

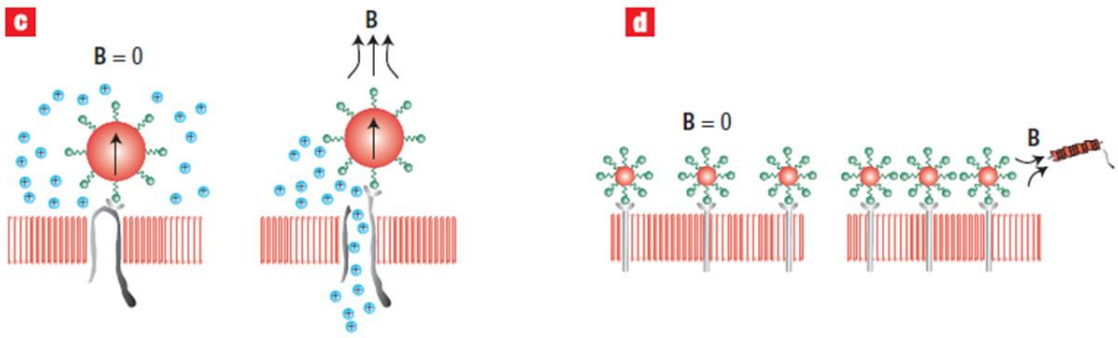

Figure 1.12. Magnetic activation of ion channels and receptor clustering. Illustration of magnetic particle mediated ion channel activation and receptor clustering after application of magnetic fields. Magnetic nanoparticles can be targeted to ion channels (c) or surface receptors (d) using antibodies. Application of magnetic fields causes opening of the channel and flux of ions across the cell membrane (C) or clustering of surface receptors that can activate signalling pathways. Image adapted with permission from Dobson, 2008 (Dobson, 2008).

1.8.7.1 Forces exerted by MNP

The force exerted by MNP can be estimated by mathematical modelling by taking into account to the particles size and magnetic field gradient. It has been shown that relatively low magnitude forces, in the order of piconewtons (pN), are required to induce magnetic activation. For instance, 250nm ferric-based MNP exerting forces ranging from 0.2pN-2pN have been shown to activate TREK1 channels and PDGF receptors respectively whilst ferro-based microparticles exerting 6pN forces have been shown to cause activation of BK channels in MSC (Dobson et al., 2006), (Hughes et al., 2008), (Kirkham et al., 2010) (Hu et al., 2014). One benefit of this strategy is that the force transduced by the MNP can be regulated by controlling parameters such as magnetic field strength, size and the number of attached particles (Hughes et al., 2005).

1.8.7.2 Magnetic force bioreactor

MNP can be controlled using external magnetic fields, which can be provided by permanent magnets or electromagnetic fields (Marcos-Campos et al., 2011), (Polyak et

al., 2008). The magnetic force bioreactor used in this work, provided by MICA Biosystems, consists of arrays of permanent magnets. The magnets can be remotely positioned to move the arrays toward and away from culture plates in a vertical plane to impart magnetic field gradients. The system can be housed inside a standard tissue culture incubator maintained at physiological conditions. The apparatus is controlled by software which regulates parameters such as the speed, frequency and number of loops of the arrays. When used in conjunction with MNP this system can be used to stimulate MNP labelled cells and tissues. An illustration showing an overview and principle behind the magnetic force bioreactor system is shown in Figure 1.13. The applications of this strategy are discussed in the following sections.

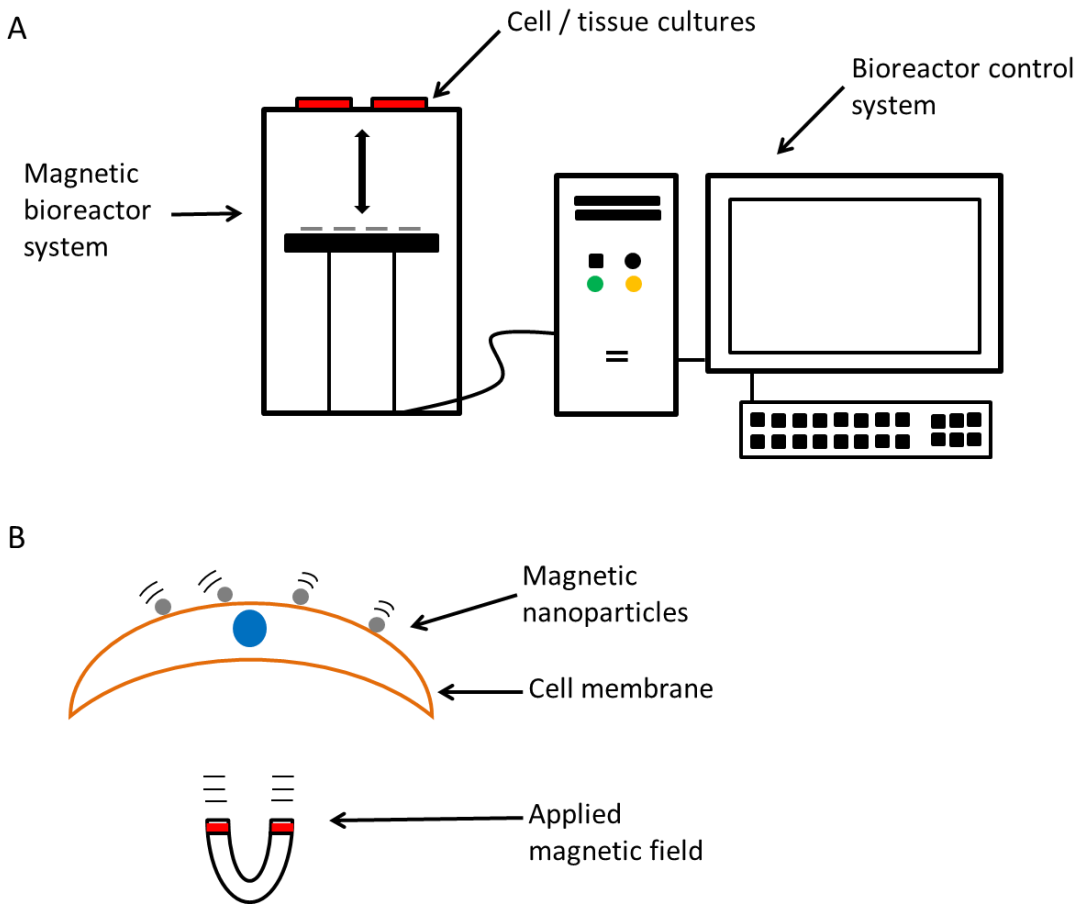

Figure 1.13. Schematic of the Magnetic force bioreactor system.
Tissue culture plates sit on place holders over the top of the magnetic arrays. The arrays move in the vertical plane underneath the culture plates. The apparatus is connected to a computer system operating software which controls the travelling speed, distance and cycling parameters of the arrays (A). Cells and tissues can then be remotely stimulated by magnetic particles using magnetic fields provided by the permanent magnetic arrays (B)

1.8.7.3 Magnetic stimulation of Integrin receptors

The RGD binding domain is prominently expressed by most integrin receptors. This enables proteins or peptides containing the RGD motif to bind Integrins at an interface between the α and β subunits (Ruoslahti, 1996), (Humphries et al., 2006). MNP can be easily functionalised with RGD peptides to allow attachment of MNP to Integrin receptors thereby enabling directed magnetic stimulation of Integrins. This approach has been shown to enhance proteoglycan and extracellular matrix protein synthesis by hMSC

(Kanczler et al., 2010) and increase endothelin-1 expression in endothelial cells (Chen et al., 2001). Furthermore, stimulation of Integrins using MNP functionalised with antibodies raised against α2 or β1 subunits has been shown to instigate changes in the actin cytoskeleton, formation of adhesion complexes, increased MAPK activity and generation of calcium fluxes in U-2 OS cells (Schmidt et al., 1998), (Pommerenke et al., 1996).

1.8.7.4 Magnetic activation of TREK1 channels

Twik-related potassium channel 1 (TREK1) is another target which has been shown to be mechanosensitive. TREK channels belong to the two pore domain potassium channel family (Ketchum et al., 1995), (Goldstein et al., 2001). As discussed previously, TREK channels are involved in the regulation of potassium transport across the cell membrane. In doing so they regulate the resting membrane potential of the cell (Lesage and Lazdunski, 2000), (Patel and Honore, 2001). Proof of concept studies have previously demonstrated that TREK channels are amenable to stimulation with magnetic nanoparticles. In these studies stimulation of discrete regions of TREK1 using MNP targeted to an extracellular loop region were able to cause membrane depolarisation consistent with ion channel activation. In contrast, this response was not seen when control particles or magnetic field stimulation were applied alone (Hughes et al., 2008).

1.8.7.5 Magnetic activation of Platelet Derived Growth Factor receptors

Platelet Derived Growth Factor receptors (PDGFR) belong to the receptor tyrosine kinase (RTK) family and play crucial roles in embryonic development. The PDGF growth factor is involved in the regulation of many cell processes including migration and proliferation. PDGF ligands signal through homo or hetero dimers of PDGF receptors alpha (PDGFRα) and beta (PDGFRβ) (Tallquist and Kazlauskas, 2004), (Lemmon and Schlessinger, 2010).

Previous work has demonstrated that PDGF receptors are mechanoresponsive (Hu et al., 1998), (Tanabe et al., 2000). The feasibility of using MNP to target PDGFRα has recently been demonstrated where receptor stimulation with antibody-functionalised MNP resulted in phosphorylation of PDGFRα and enhanced SMA expression in hMSC (Hu et al., 2014). Furthermore, this approach was also shown to enhance osteogenic marker expression and increased the mineral to matrix ratio when hMSC were subjected to three weeks of magnetic stimulation *in vitro* (Hu et al., 2013).

1.8.8 MNP and bone tissue engineering

Magnetic activation strategies using MNP have been extensively studied both *in vitro* and *in vivo,* particularly in a bone tissue engineering context. I*n vitro* studies have investigated labelling of human osteoblasts with RGD tri-peptide coated MNP which bind to integrin receptors. When this was coupled with magnetic stimulation over 7-21 days an increase in mineralized bone matrix and up-regulation of osteopontin and osteocalcin was observed. Furthermore, it was shown that cells with attached particles were proliferative and viable at 21 days (Cartmell et al., 2002), (Dobson et al., 2006), (Hughes et al., 2005). Also, hMSC have been shown to be load responsive when targeting the mechano-responsive ion channel TREK1 and integrin receptors using MNP functionalised with anti-TREK1 antibodies or RGD tri-peptide respectively. In this scenario, after 7 days of TREK1 stimulation it was shown that expression of chondrogenic and osteogenic related genes Sox9, core binding factor alpha1 (Cbfa1), and osteopontin were up-regulated. After 21 days expression of type 1 collagen and proteoglycan matrix was also increased (Kanczler et al., 2010). Remote activation of TREK channels has been shown to have beneficial effects on bone formation in an *ex vivo* foetal chick femur model of bone development. In this work, magnetic activation of TREK channels on hMSC that were injected into the

epiphyseal regions of the femurs was shown to cause an increase in bone production and induce areas of secondary mineralisation at the injection sites (Henstock et al., 2014). This strategy has also been translated *In vivo.* Studies in rats have shown that mechanical stimulation of TREK1 ion channels on hMSC increased proteoglycan matrix, expression of core binding factor alpha1 (Cbfa1), extracellular matrix production and led to elevated expression of type 1 and type 2 Collagen after 21 days. Additionally, the magnetic stimulation of hMSC labelled with RGD tri-peptide MNP enhanced proteoglycan and collagen synthesis, extracellular matrix production and elevated the expression of Collagen type 1 and type 2 both *in vitro* and *in vivo*. Importantly, hMSC labelled with MNP were also shown to be viable in these experiments (Kanczler et al., 2010). These studies highlight the potential benefits of MNP and magnetic activation strategies in bone tissue engineering.

1.9 Research Hypothesis and Objectives

The main hypothesis underpinning this work is that targeting Frizzled receptors with MNP may have an effect on Frizzled signalling activity. Therefore the primary objective of this research is to investigate the targeting and activating capabilities of functionalised MNP in conjunction with magnetic fields on Wnt signalling pathway activity in hMSC. As Wnt signalling is involved in the regulation of stem cell behaviour and is important in bone formation it is also hypothesized that magnetic activation of Frizzled receptors and Wnt signalling may have an effect on stem cell behaviour. Therefore the next objective is to assess the magnetic activation strategy in directing MSC osteogenic differentiation. Another objective is to characterise the MNP functionalisation process and to assess the

effects of functionalised MNP on stem cell toxicity. The role of directional signalling gradients is known to be important for regulating stem cell maintenance and differentiation. It is therefore possible that directional presentation of signalling cues to stem cells may provide a more contextually relevant environment for tissue formation. Therefore the final objective of this research is to explore the role of spatial and directionally presented Wnt cues on hMSC migration and osteogenic differentiation.

Chapter 2: Nanoparticle and magnetic field characterisation

2.1 Introduction

Magnetic Nanoparticles (MNP) have gathered much attention in recent years and have now become useful and popular tools in various fields of biomedical research and medicine (Q A Pankhurst, 2003). A major advantage pertaining the use of MNP is their adaptability for different applications. MNP can be positioned and bound to different cellular targets or surface proteins by functionalising their surface with biomolecules such as peptides and antibodies (Conde et al., 2014). The superparamagnetic properties of nano-scale MNP, which confers magnetic susceptibility only in the presence of magnetic field gradients, also presents unique opportunities for their spatial control and precise positioning. This particular feature of superparamagnetic nanoparticles is especially useful in medical applications that demand precise control of magnetic particles *in vivo* (Akbarzadeh et al., 2012), (Kumar, 2009).

Before MNP based treatments can be translated to the clinic however, the safety of these materials must first be demonstrated. In particular, the toxicity of MNP must be determined and the biocompatibility of MNP based treatments must be proven with clinically relevant cell types. One way of aiding MNP biocompatibility is by coating the magnetic core with a biocompatible substrate such as dextran. The safety of dextran based iron oxide MNP has previously been demonstrated by a number of groups, particularly in the context of MRI studies for tracking of MNP labelled cells (Huang et al., 2009), (Lalande et al., 2011), (Loebinger et al., 2009). A comprehensive review of MNP based toxicity in the broader context of regenerative medicine is discussed by (Markides et al., 2012).

One specific application of magnetic nanoparticles is the selective application of mechanical forces to mechanosensitive receptors. This has an added benefit of being able to exercise a level of control over the activation of mechanosensitive receptors and cell signalling pathways. Previous work has demonstrated that imparting comparatively low magnitude force in the order of 0.2-6pN using MNP is capable of altering the activation state of mechanosensitive proteins. Specifically, remotely torqueing MNP attached to TREK1 ion channels, Integrins and Platelet Derived Growth Factor receptors (PDGFR) using the same magnetic force bioreactor system introduced in chapter 1 has been shown to induce activation of signalling pathways associated with these targets (Dobson et al., 2006), (Kirkham et al., 2010), (Hughes et al., 2007), (Hughes et al., 2008), (Cartmell et al., 2002), (Hu et al., 2014). However, to date MNP mediated mechanical stimulation of the Wnt signalling pathway through direct application of mechanical forces to Frizzled receptors is still lacking.

The aims of the experiments presented in this chapter were to firstly characterise the biological ligand (i.e. peptides and antibodies) and MNP functionalisation process which was used to target Frizzled receptors. This is required in order to determine the efficacy of MNP functionalisation with these particular Frizzled targeting modalities. The next aim was to characterise the magnetic field profiles of the bioreactor system used to apply oscillating magnetic fields, in order to determine the magnitude of the magnetic fields applied. The third aim was to examine the toxicity profiles of the MNP and associated magnetic field treatments used in these experiments in a clinically relevant stem cell type, hMSC. These effects were examined in order to assess the safety and biocompatibility of these treatments. The fourth aim was to attempt tracking of the MNP, to determine the

longevity of hMSC-MNP labelling *in vitro*. The final aim was to provide an estimation of the forces transduced by the MNP onto the cells using mathematical modelling.

2.2 Methods

2.2.1 Cell culture

Fresh human bone marrow (Lonza, cat. no. 1M-125) was sourced from healthy volunteers with written, informed consent obtained by Lonza. No ethical approval was required for this project as the human tissue (bone marrow aspirate) was acquired from a commercially available source. The donor program is approved annually by a commercial institutional review board and Lonza Walkersville Inc. is a licensed tissue bank. The adherent cell population was selected from fresh bone marrow by culturing aliquots of aspirate for 2 weeks in Low glucose DMEM with 5% FBS, 1% L-glutamine and 1% Penicillin and Streptomycin with Media changes performed once per week. MSC were routinely characterised for expression of surface markers (CD73+, CD90+, CD105+ and CD45-, CD34-, CD14-, CD19- and HLA-DR-) and histological staining for osteogenic (Alizarin red), chondrogenic (Alcian blue) and adipogenic differentiation (Oil red O) (see appendix A). For cell expansion MSC were cultured in High glucose DMEM supplemented with 10% FBS, 1% L-glutamine and 1% Penicillin / Streptomycin (All reagents Lonza). Cells were passaged once per week and cells between passage 2 and 5 were used in all experiments.

2.2.2 MNP coating

250nm SPIO carboxyl functionalised magnetic nanoparticles (Micromod) were covalently coated with anti-Frizzled 2 (Abcam), TREK1 (Alomone labs), UM206 peptide (Pepceuticals, UK) or IgG-FITC antibodies by carbodiimide activation as described previously (Hu et al.,

2014). Briefly, 1mg of particles (for each ligand) were activated using EDAC and NHS dissolved in 0.5M MES buffer pH6.3 (All Sigma) for 60 mins. at room temperature with constant mixing. The particle suspension was washed and re-suspended in 0.1M MES buffer containing 20μg of anti-rabbit secondary antibody (Abcam) or 10μg of either L-UM206 or C-C-UM206 peptide. The particle suspensions were continuously mixed overnight at 4^{o}C then the antibody coated suspensions were washed and re-suspended in 0.1mL MES buffer containing 10μg of either anti-Frizzled 2 antibody (Abcam) or Anti-TREK1 antibody (Alomone labs). Particle suspensions were mixed for a further 3h at room temperature then all suspensions were blocked with 25mM Glycine (Sigma) for 30mins before final washing and re-suspension in 0.1% BSA (Fisher) in PBS (Sigma). In order to test the coating efficiency of MNP, samples of the coating solutions containing the antibodies or peptides described above were taken before and after incubation with MNP. The total protein content of each sample was determined using a BCA assay (Fisher). The amount of protein taken up by the MNP was determined according to the difference in protein concentrations between samples. As a control to determine the level of protein adhesion to reaction tubes, a 0.5mg/mL solution of BSA in 0.1M MES buffer was prepared, with samples taken before incubation in a 1.5mL eppendorf tube and after 3h incubation.

2.2.3 Total protein assay

Total protein was assessed using a BCA assay kit (Fisher). Samples were diluted 2x with d.H_2O and 25μL of each sample was aliquoted into 96 well plates. A working solution of BCA assay reagent was prepared using 10mL of reagent A and 200μL of reagent B. 200μL of working reagent was added to each sample and incubated for 30mins at 37^{o}C. The absorbance of the resulting solutions was measured at a wavelength of 562nm using a

Synergy 2 plate reader. The total protein concentration of the samples was determined by comparison to a standard curve of BSA dissolved in 0.1M MES buffer (see appendix B).

2.2.4 Zeta sizing and Zeta potential

Functionalised nanoparticles were analysed for surface charge and size by dynamic light scattering using a Zetasizer 3000 HSa (Malvern Instruments). Particles were diluted 500x in dH_20 and measurements performed at 25^oC. The size and surface charge of coated nanoparticles was compared to uncoated activated nanoparticles.

2.2.5 Magnetic Field Mapping

The magnetic fields for each magnetic array were mapped using Magscan 300 instrument (Redcliffe) at a resolution of 0.2 x 0.2 mm. The field maps and polarities at varying distances were determined by altering the distance between the magnetic arrays and the detector up to a maximum distance of 84mm from the array.

2.2.6 Cell labelling with MNP

Media was aspirated and cells washed with PBS. All cells were cultured in basal serum-free MSC expansion media for 3h before addition of MNP. Particles were added to appropriate groups at approximately 3μg MNP/cm^2 of culture surface area, and incubated for a further 1.5h with intermittent agitation. Media was aspirated, cells were washed with PBS to remove unbound particles before addition of fresh media (0% FBS for western blotting experiments, 2.5% FBS for luciferase experiments, 10% FBS for gene expression experiments).

2.2.7 Magnetic stimulation

Magnetically stimulated groups were placed in a vertically oscillating magnetic force bioreactor (MICA Biosystems) which was situated inside an incubator maintained at 37^oC,

5% CO_2. Non-stimulated control groups were kept in identical conditions (without magnetic field). Magnetically stimulated groups were exposed to a magnetic field of 25-120mT from an array of permanent magnets (NdFeB) situated beneath the culture plates at a frequency of approximately 1Hz. Magnetic field treatment was applied in 3x 1hr weekly sessions on alternate days. An image showing the magnetic bioreactor apparatus is shown in Figure 2.1.

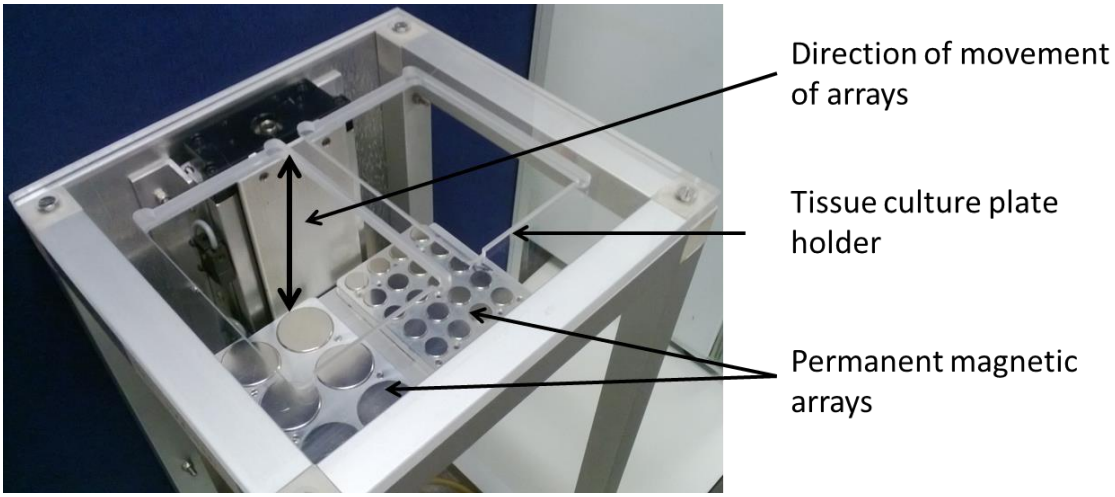

Figure 2.1. Magnetic force bioreactor apparatus.
Photograph showing the key components of the magnetic bioreactor system. Tissue culture plates are situated over the permanent magnetic arrays (6-well and 24-well arrays shown). The magnetic arrays are driven in a cyclic motion underneath the culture plates plane using a motorised drive-shaft. The apparatus is connected to software which controls the movement of the arrays (not shown).

2.2.8 Cell viability staining

Cells were labelled with MNP and treated with magnetic field stimulation as described above. After each time point, cells were washed with PBS then stained with a Live/dead assay solution (Sigma) consisting of Calcein AM (diluted 1:500) and Propidium iodide (diluted 1:1000) in PBS. Samples were stained for 15mins at 37^{o}C. Samples were then imaged on an Olympus IX83 confocal microscope operating Flourview 10 software.

2.2.9 MTT assay

Cells were labelled with MNP and treated with magnetic field stimulation as described above. After each time point, cells were washed with PBS then incubated with fresh media containing 0.5mg/mL Thiazolyl Blue Tetrazolium Bromide (MTT) (Sigma). Cells were incubated for 3h at 37^{o}C. After which media was aspirated and the purple formazan salt produced by the cells was extracted by adding 0.5mL DMSO (Sigma), samples were placed on an orbital shaker for 15mins during dye extraction. 100µL of extracted dye was aliquoted into a 96 well plate and the absorbance at wavelength 570nm was read, readings were corrected by measuring absorbance at 690nm. Readings were obtained using a Biotek Synergy 2 plate reader.

2.2.10 Prussian blue staining

Cells were labelled with MNP as described above. After which media was aspirated, cells washed with PBS then fixed using 90% methanol (Fisher) for 10mins. Samples were washed with PBS before staining for Iron deposits using a solution of 20% Conc. HCl (sigma) with 10% Potassium Ferrocyanide (Sigma). Samples were stained for 20mins then washed 3x with distilled H_2O. Samples were imaged on a Leica DMIL microscope operating LAS software.

2.2.11 Immunocytochemistry

For MNP staining, cells were fixed with 4% PFA in PBS (Sigma) for 10mins before blocking with 2% BSA/PBS for 1h. Cells were incubated with anti-Dextran (Stem cell technologies) diluted 1:1000 in 1% BSA / PBS overnight at 4^{o}C. Cells were washed with PBS then incubated with anti-Mouse-FITC secondary antibody (Sigma) diluted 1:1000 in 1% BSA / PBS for 1h at room temp. Cells were washed in PBS, and F-actin stained with Phalloidin-

Atto 565 (Sigma). Cells were washed with PBS before counterstaining with DAPI. Fluorescence microscopy was performed on a Nikon Eclipse Ti-S microscope operating NIS elements software.

2.2.12 Microscopy

Samples of MNP coated with IgG-FITC antibodies or uncoated MNP were aliquoted into wells of a 96-well plate (100µL of each particle type). Samples were diluted with 100µL PBS then imaged using Nikon Eclipse Ti-S microscope operating NIS elements software.

2.2.13 Forces exerted by MNP

The forces exerted by individual MNP in response to magnetic fields were estimated according to a mathematical model as previously described by (Dobson et al., 2006).

2.2.14 Statistical analysis

All data is presented as means +/- SEM or standard deviation as indicated. Statistical significance at 95% confidence level was determined using 1-way ANOVA with post-hoc Tukey tests using Mini-tab (v16) software.

2.3 Results

2.3.1 MNP functionalisation

The size and surface charge of peptide and antibody coated nanoparticles were analysed by zeta-sizing and zeta-potential and compared to uncoated MNP (Table 2.1). The size of uncoated MNP was measured as approximately 300nm whereas the size of functionalised MNP increased by at least 10% after conjugation with protein ligands. The surface charge (zeta potential) of uncoated-MNP was measured as approximately -19mV whereas the

charge of the protein functionalised MNP increased to between -16 to -7.2 mV after conjugation.

Particle surface coating	Size (nm)	Zeta Potential (mV)
Uncoated	299.7 ±4.9	-18.9 ±1.6
L-UM206	332.7 ±0.9	-15.8 ±1.5
C-C-UM206	345.7 ±4.7	-8.0 ±0.7
Fz2-IgG	337.3 ±3.8	-7.3 ±0.4
Trek-IgG	335.0 ±14.5	-7.4 ±2.9

Table 2.1. MNP size and surface charge after functionalisation.
Uncoated particles had a measured diameter of approximately 300nm and surface charge (Zeta Potential) of approximately 19mV. Functionalisation of MNP with UM206 peptides (L-UM206 or C-C-UM206), anti-Fz2 antibodies (Fz2-IgG) or anti-TREK1 antibodies (Trek-IgG) all increased the diameter of the MNP to between 333-346nm. Peptide or antibody Functionalisation also increased the Zeta potential to between -15.8 and -7.3mV. Samples read in triplicate, error represents standard deviation.

2.3.2 MNP coating efficiency

The amount of protein conjugated to MNP was indirectly determined by measuring the protein content of the respective MNP coating solutions before and after incubation with activated MNP (Table 2.2). The protein concentration of the coating solutions for each MNP coating type (peptides or antibodies) was found to decrease by between 5% and 25% after incubation with the activated MNP. The protein content of a control solution of BSA in MES buffer incubated for 3h in an eppendorf tube showed no difference in protein concentration (1.87±0.02 Abs) compared to the starting concentration (1.86±0.01 Abs).

Particle surface coating	Supernatant Protein conc. Pre coating (µg/mL)	Supernatant Protein conc. post coating MNP (µg/mL)	Difference (% protein coated on MNP)
L-UM206	259 ±21	190 ±5	27%
C-C-UM206	186 ±4	177 ±9	5%
Fz2-IgG	2512 ±30	2368 ±30	6%
Trek-IgG	1605 ±48	1379 ±54	14%
Rabbit-IgG	369 ±38	307±4	17%

Table 2.2. MNP coating efficiency.
Functionalisation of MNP with L-UM206, C-C-UM206, Anti-Fz 2 antibodies (Fz2-IgG), anti-TREK1 antibodies (Trek-IgG) or anti-Rabbit-IgG (Rabbit-IgG) all led to decreases in the total protein content of the coating solution supernatant of between 5-27%. Samples read in triplicate, error represents standard deviation.

2.3.3 MNP coating with IgG-FITC

In order to confirm that the MNP bio-functionalisation process resulted in the presence of protein on the MNP, model fluorescently tagged antibodies were coated onto MNP (IgG-FITC-MNP) and analysed by fluorescent microscopy (Figure 2.2). MNP coated with the IgG-FITC antibodies displayed a clear fluorescent signal after coating; in contrast no fluorescent signal was detected from uncoated MNP.

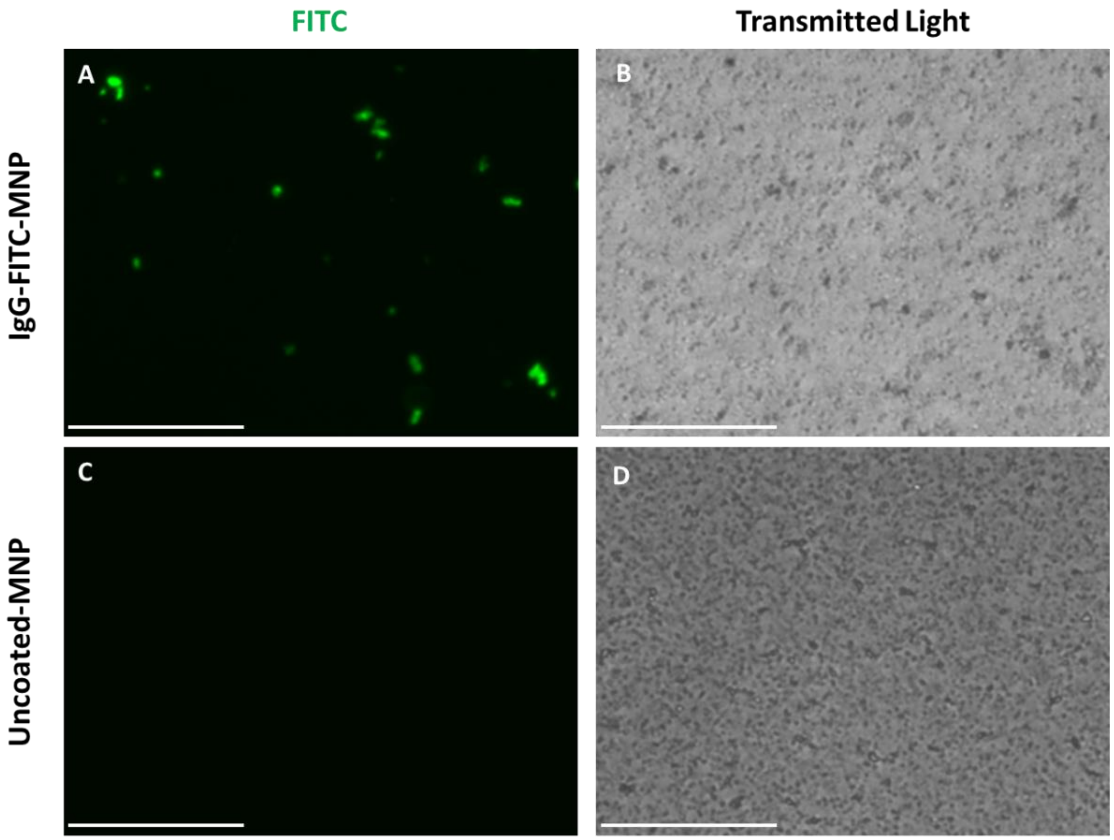

Figure 2.2. MNP coating with IgG-FITC.
Immunofluorescence and light microscopy images for antibody-FITC coated and un-coated-MNP. MNP functionalised with IgG-FITC antibodies displayed clear fluorescence after coating (A). No Fluorescence signal was observed for uncoated-MNP (C). Light microscopy images are shown in (B) and (D). Representative images of n=3 shown, scale bar represents 50µm.

2.3.4 Characterisation of permanent magnetic arrays

Next, the magnetic field strengths, polarities and gradients produced by the permanent magnetic arrays were mapped and modelled using a Magscan 300 instrument (Redcliffe). This allowed estimations of the magnetic field gradients that were applied to the MNP to be calculated.

2.3.4.1 6-well array field map

Using the 6-well magnetic arrays (Figure 2.3), at the level of the sample, the magnetic field profiles appeared to be regular and well defined as shown by cross-sections of the magnetic field array. The peak field strength was estimated to be 75mT. In contrast, when the magnetic array was moved away from the sample, the magnetic field profile became irregular and the field strength was reduced to approximately 1.4mT.

2.3.4.2 24-well array field map

Using the 24-well magnetic arrays (Figure 2.4), at the level of the sample, the magnetic field profiles again appeared to be regular and well defined as shown by cross-sections of the magnetic field array. The peak field strength was estimated to be 108mT. But when the magnetic array was moved away from the sample the magnetic field profile became irregular and the field strength was reduced to approximately 0.7mT.

2.3.4.3 Magnetic array field gradients

The magnetic field strengths across a range of distances were measured for both magnetic array types in order to simulate the applied magnetic field gradients experienced by cells *in vitro* (Figure 2.5). The 6-well array displayed overall stronger magnetic field strengths that peaked at approximately 300mT, whilst the 24-well array displayed weaker magnetic field strengths that peaked at approximately 120mT. The magnetic fields for both arrays decreased exponentially as a function of distance from the detector with minimum field strengths of approximately 1mT measured for each array.

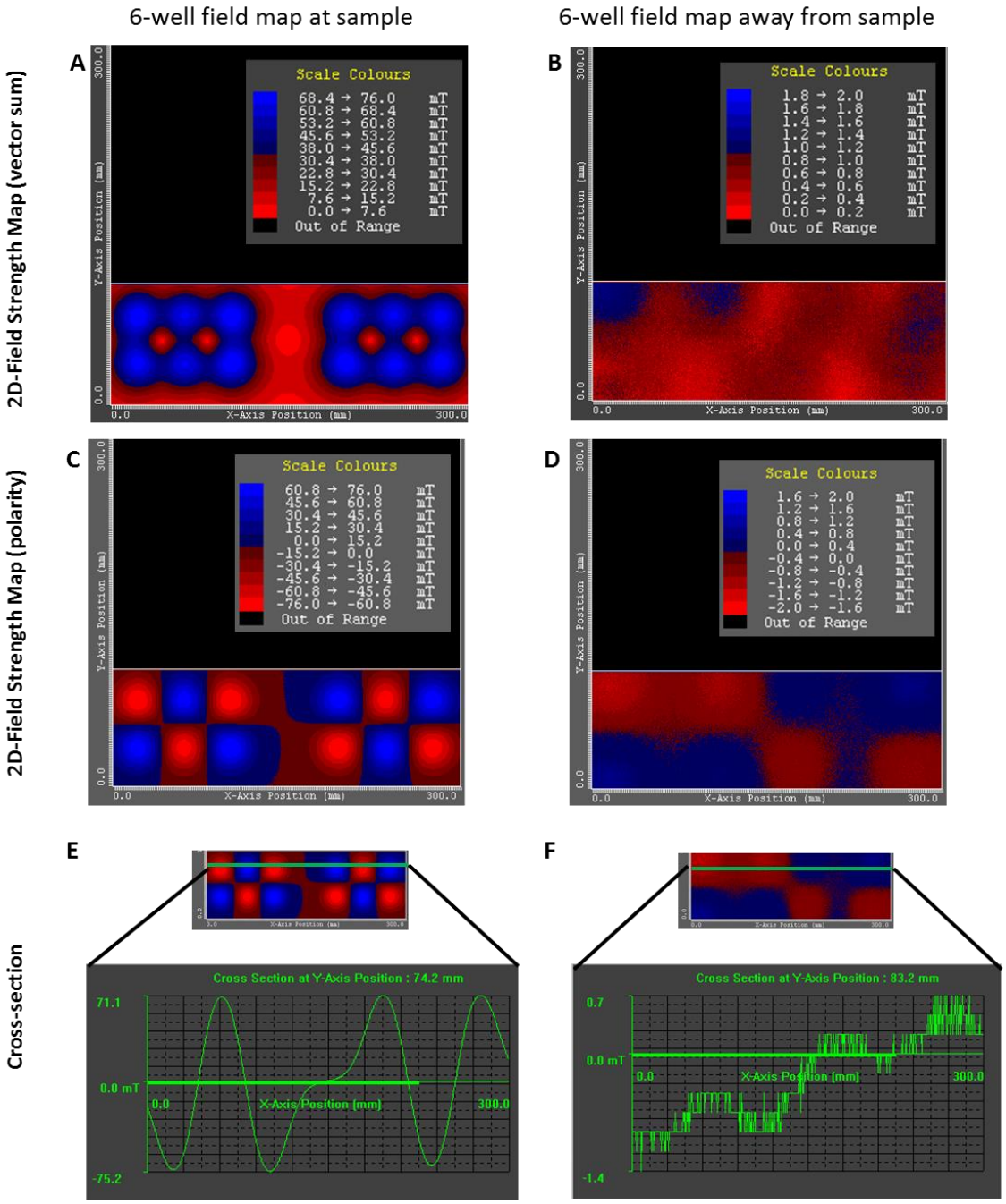

Figure 2.3. 6-well array magnetic field mapping.
2D model representations of magnetic field strength and polarity of 6-well permanent magnet arrays. When the magnetic array was closest to the samples (approx. 18mm) the peak magnetic field strength was ±75mT (A), the peak field strength and field polarity is shown in (C), A representative cross-section of the magnetic fields and polarity is shown in (E). When the magnetic array was the furthest (measurable) distance from the samples (approx. 84mm) the magnetic field strength was reduced to ±1.4mT (B), the field strength and field polarity is shown in (D), A representative cross-section of the magnetic fields and polarity is shown in (F).

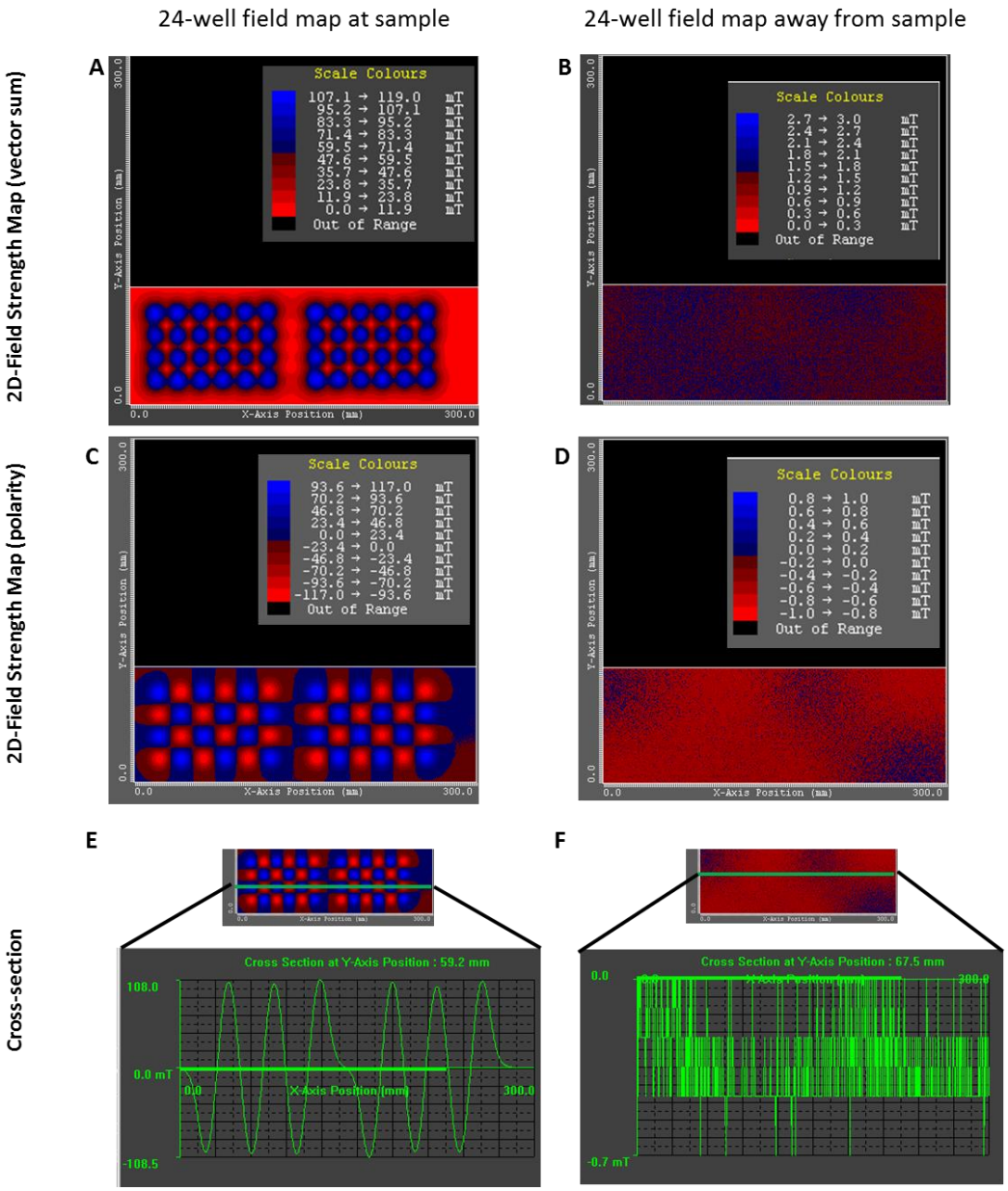

Figure 2.4. 24-well array magnetic field mapping.
2D model representations of magnetic field strength and polarity of 24-well permanent magnet array. When the magnetic array was closest to the samples (approx. 7mm) the peak magnetic field strength was ±109mT (A), the field strength and field polarity is shown in (C), A representative cross-section of the magnetic fields and polarity is shown in (E). When the magnetic array was the furthest (measurable) distance from the samples (approx. 84mm) the magnetic field strength was reduced to ±1.0mT (B), the field strength and field polarity is shown in (D), A representative cross-section of the magnetic fields and polarity is shown in (F).

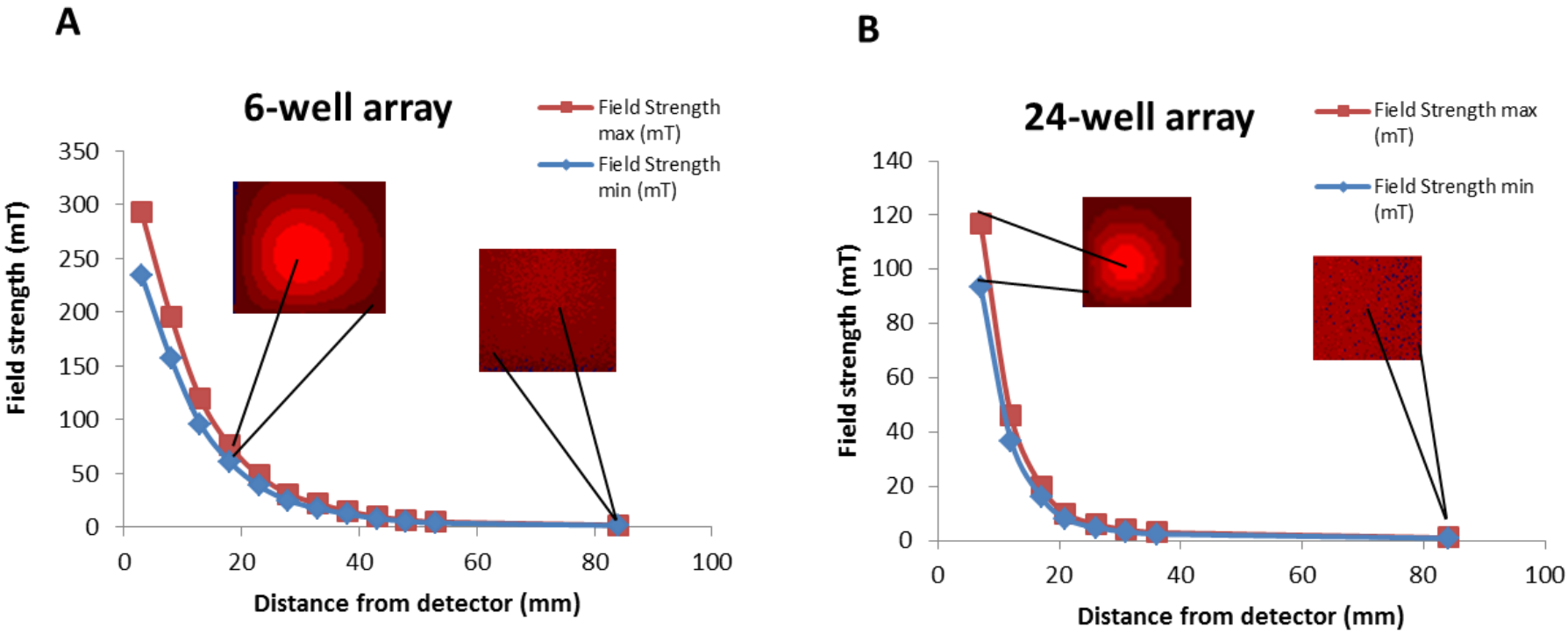

Figure 2.5. Magnetic field gradients.
Graphical representation of the magnetic field gradients of the 6-well and 24-well permanent arrays. For the 6-well array (A), when the array was positioned towards the samples (approx. 18mm distance) this resulted in a peak magnetic field range of 68-76mT. Away from the sample, at a distance of 84mm, the magnetic field strength was reduced to 1-2mT. For the 24-well array (B), when the array was positioned towards the samples (approx. 6mm distance) this resulted in a peak magnetic field range of 93-117mT. Away from the sample, at a distance of 84mm, the magnetic field strength was reduced to approximately 1mT.

2.3.5 Cytotoxic effects of MNP on hMSC

The cytotoxic effects of the MNP, their respective surface coatings and the effect of magnetic field stimulation were all assessed using two well established cytotoxicity assays measuring cell viability and metabolism.

2.3.5.1 Effects of MNP on hMSC viability

Changes to cell viability were assessed by Live/Dead staining to determine intracellular esterase activity and cell membrane integrity 24h (Figure 2.6) and 14 days (Figure 2.7) after MNP labelling and intermittent magnetic field stimulation. All MNP types with different surface coatings had no noticeable effect on hMSC viability 24h after labelling. Furthermore, application of magnetic field stimulation alone or in conjunction with all MNP had no noticeable effect on cell viability. After 14 days, a negligible degree of cell death was observed after treatment with MNP (regardless of MNP coating) with and without intermittent magnetic field stimulation. Treatment with magnetic fields alone had no observable effects on cell viability.

2.3.5.2 Effects of MNP on hMSC metabolism

The effects of MNP on cell metabolism 24h and 14 days after MNP labelling with intermittent magnetic field stimulation was also assessed by MTT assay (Figure 2.8). After 24h, no overall effect on cell metabolism was observed when cells were treated with magnetic field alone or when treated with either Fz-MNP or L-UM206-MNP with or without magnetic field stimulation. A marginal decrease in cell metabolism (not significant) was observed when cells were treated with C-C-UM206-MNP alone but no effect was observed in response to these MNP with magnetic field stimulation. After 14 days no overall effect on cell metabolism was observed when cells were treated with

either magnetic field alone or when treated with MNP of any types with or without magnetic field stimulation.

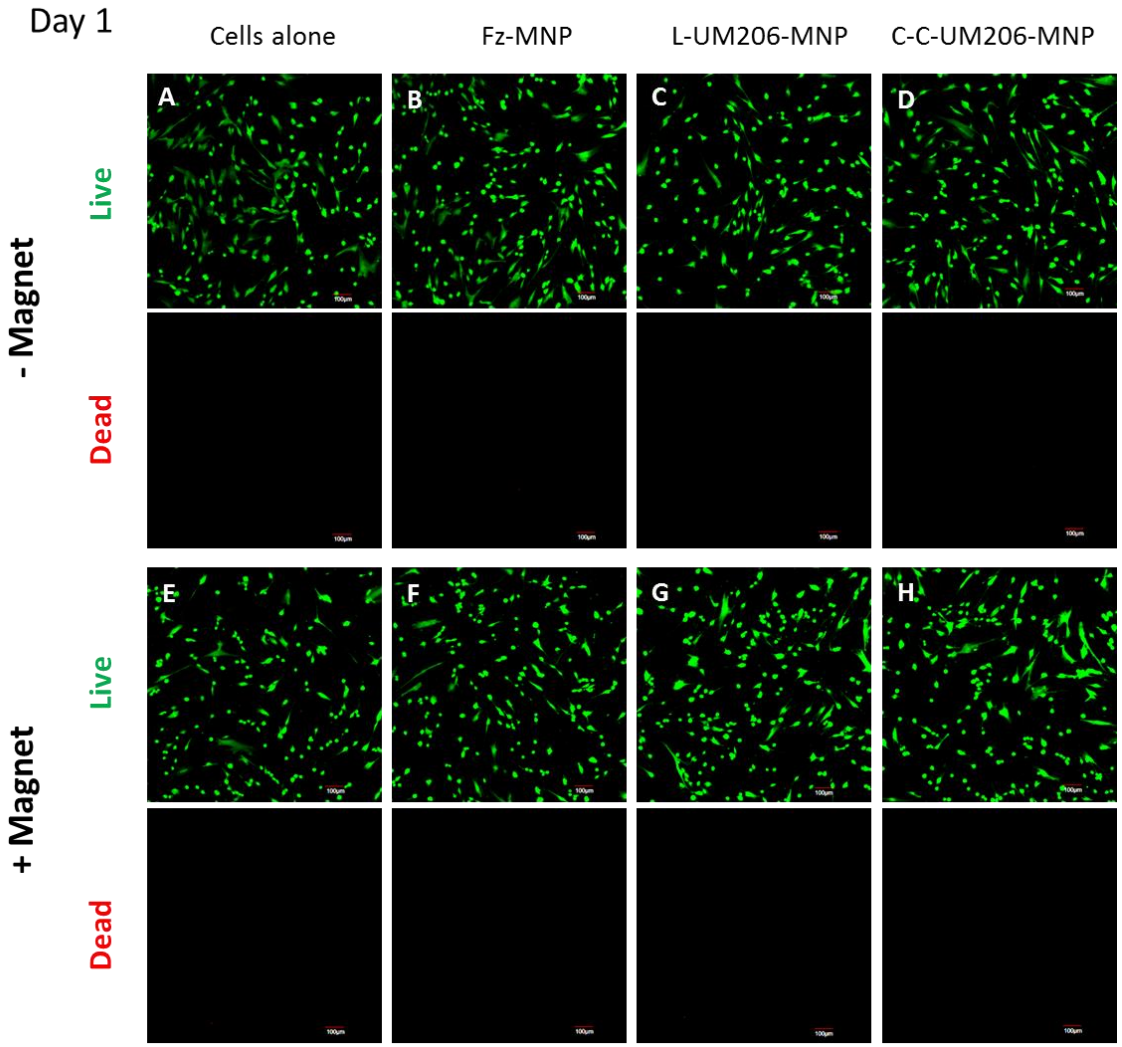

Figure 2.6. Effects of MNP and magnetic field on cell viability at 24h.
Immunofluorescence images showing Calcein-AM (Live) and Ethidium homodimer (Dead) staining after treatment with different MNP types with and without magnetic field after 24h. Cells treated with MNP alone with different surface coatings (B-D) or in conjunction with magnetic field (F-H) had no discernible effect on cell viability 24h post treatment compared to controls (A, E). Magnetic field treatment alone also had no discernible effect on cell viability after 24h (E). Representative images of n=3 shown, scale bar represents 100µm.

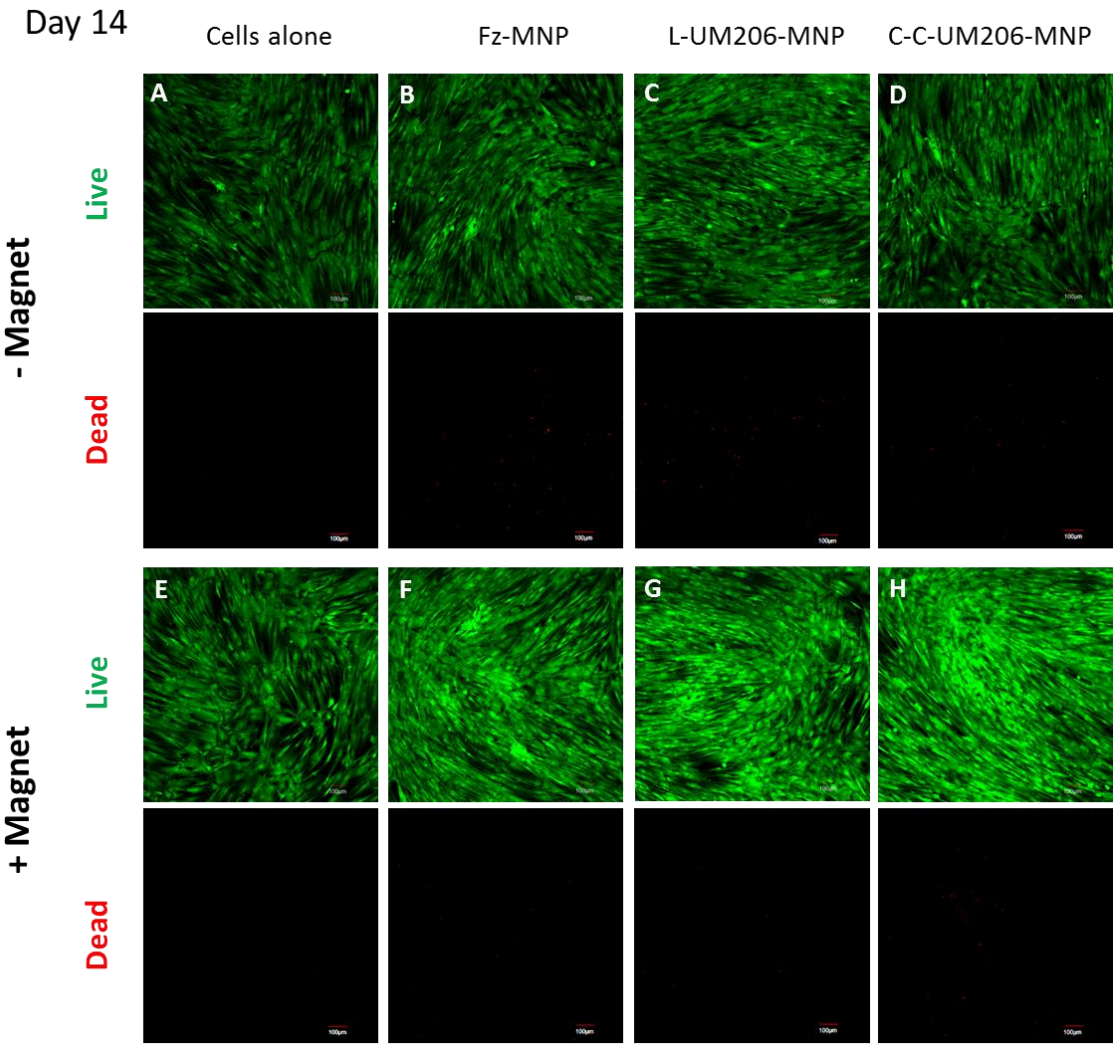

Figure 2.7. Effects of MNP and magnetic field on cell viability after 14 days. Immunofluorescence images showing Calcein-AM (Live) and Ethidium homodimer (Dead) staining after treatment with different MNP types with and without magnetic field after 14 days. Cells treated with MNP alone with different surface coatings caused negligible increases in cell death (B-D) compared to non-treated control cells (A). Addition of magnetic field stimulation also caused a negligible effect (F-H) compared to magnetic field treated cells (E). No observable effects were observed for cells treated with magnetic field alone after 14 days (E). Representative images of n=3 shown, scale bar represents 100µm.

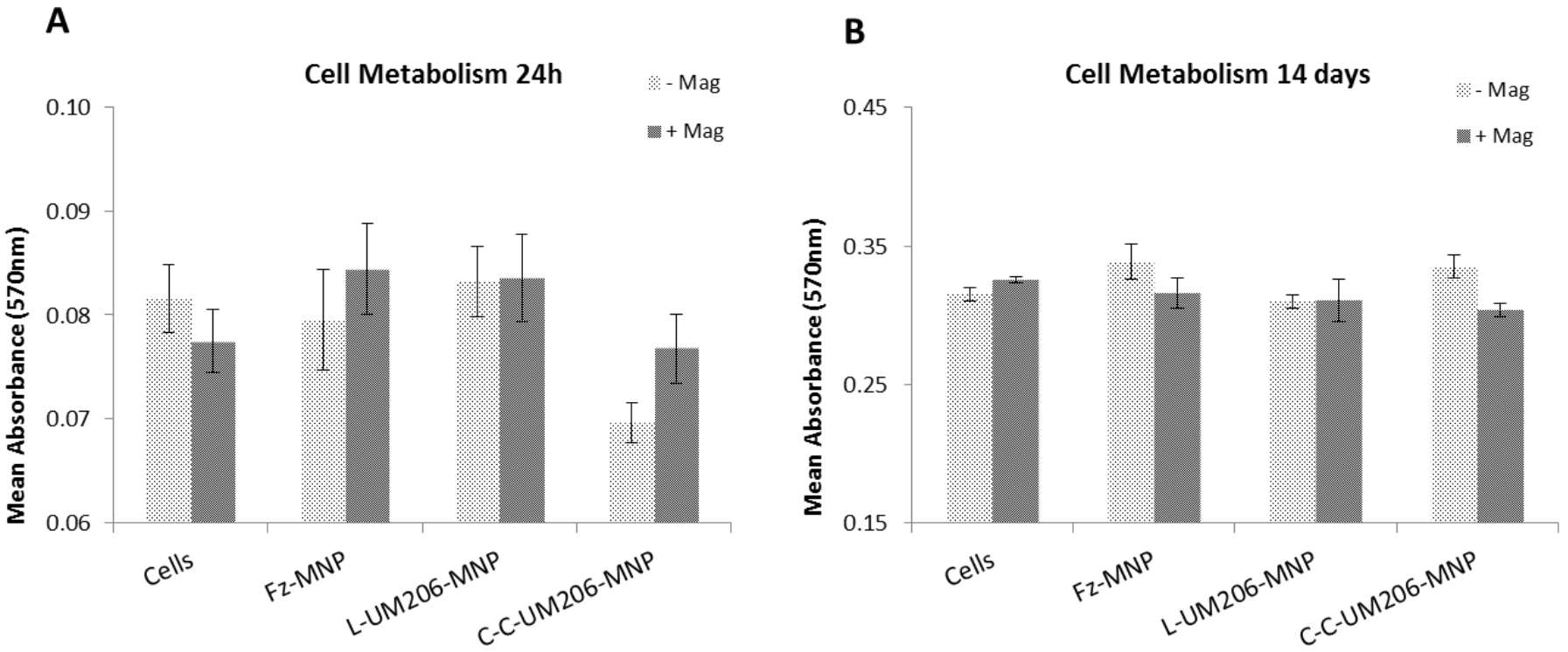

Figure 2.8. Effects of MNP and magnetic field on cell metabolism.
Graphs showing MTT metabolism in hMSC 24h and 14 days after treatment with MNP with or without magnetic field. No overall effect on cell metabolism over both time-points was observed for cells treated with Magnetic field alone, Fz-MNP (with or without magnetic field) or L-UM206-MNP (with or without magnetic field) (A, B). A minor decrease in cell metabolism (not significant) was observed in cells treated with C-C-UM206-MNP alone after 24h (A), but no effect was observed after 14 days. No overall effect was observed for cells treated with C-C-UM206-MNP with magnetic field after 24h and 14 days (B). Average absorbance values are shown, n=3, error bars represent SEM.

2.3.6 Tracking MNP distribution

MSC labelling with different MNP types was confirmed by biochemical staining to detect the iron oxide core of the MNP and by Immunofluorescence to detect the dextran shell coating. Cells were labelled with Fz-MNP, L-UM206-MNP or C-C-UM206-MNP then the iron oxide component of the MNP was visualised using Prussian blue staining. The reaction between Potassium Ferrocyanide with the iron oxide in the MNP causes formation of a blue precipitate (Ferric Ferrocyanide) which can be visualised. Figure 2.9 shows the presence of MNP and association of each MNP type with MSC after 1.5h incubation, the cell morphologies are shown in the polarised light images. MNP labelling of hMSC was also tracked over the course of 7 days using Immunofluorescence to identify the dextran component of the MNP, cells were counter-stained with Phalloidin and DAPI to locate the cell nuclei and cytoskeleton. A clear association between cells and MNP was observed for each MNP type. Cells labelled with Fz-MNP (Figure 2.10) showed clear labelling over 7 days with peak staining observed after 24h after which staining intensity decreased. Cells labelled with L-UM206-MNP (Figure 2.11) showed notable labelling over 7 days with peak staining observed after 3 days, staining intensity decreased after 7 days. Cells labelled with C-C-UM206-MNP (Figure 2.12) showed notable labelling up to 3 days after labelling with peak staining observed after 3 days, staining intensity decreased to negligible levels after 7 days.

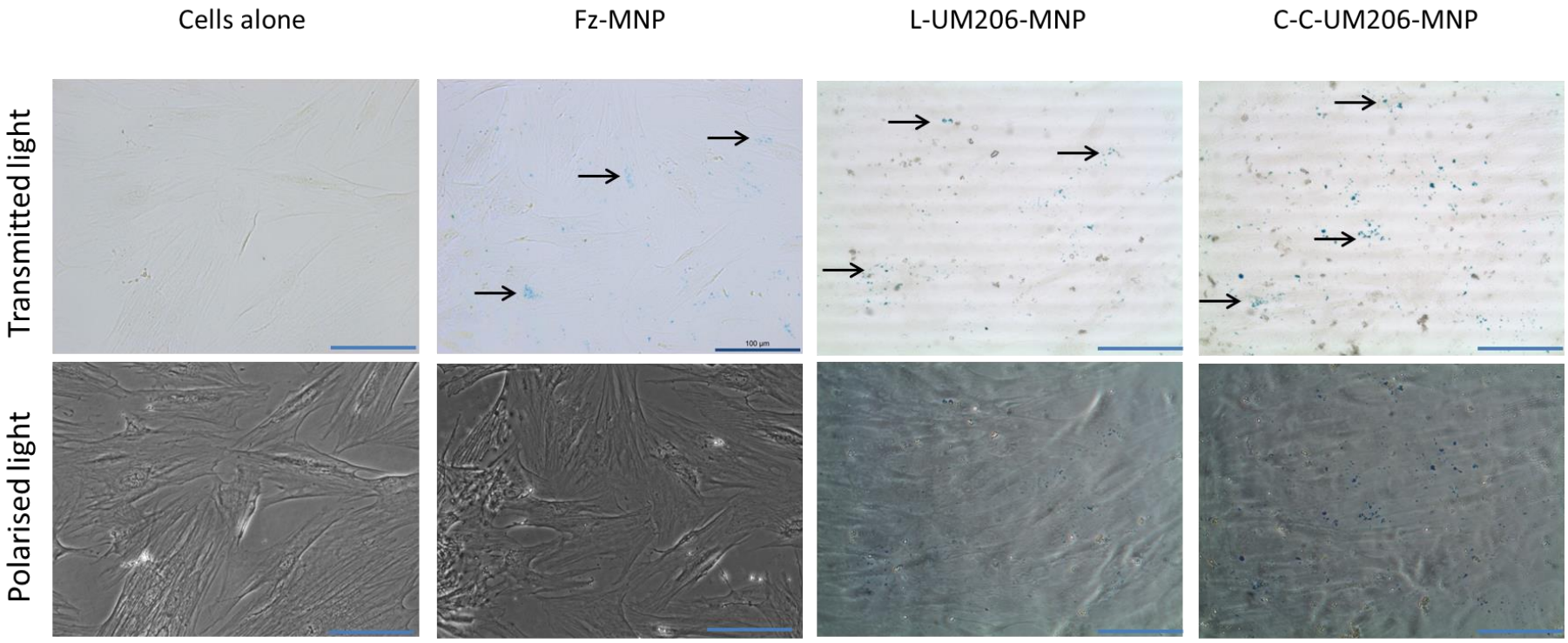

Figure 2.9. Prussian blue staining for MNP.
Transmitted and polarised light microscopy images showing presence of Iron (Prussian blue staining) localised with hMSC. Unlabelled cells were negative for Iron (A). Cells labelled with Fz-MNP (B), L-206-MNP (C) and C-C-206-MNP (D) were all positive for Iron post-labelling with MNP. Polarised light images showing cell morphology are shown E-H. Representative images of n=4 shown, scale bar represents 100µm.

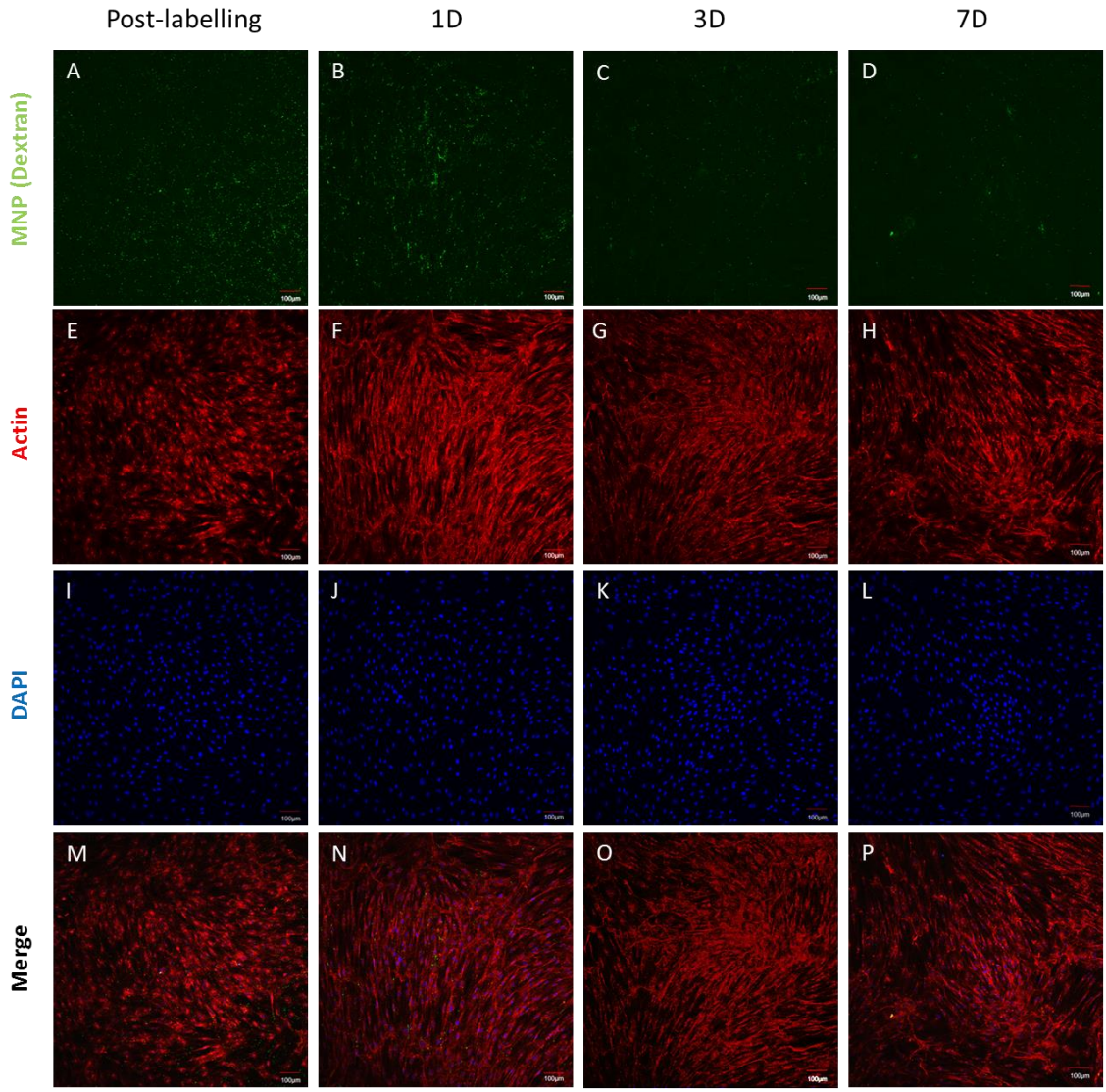

Figure 2.10. Fz-MNP tracking over 7 days.
Time-course of Immunofluorescence images showing presence of Fz-MNP over 7 days. Dextran staining (Green) for Fz-MNP was detectable over 7 days post-labelling (A-D). Peak Fz-MNP staining was observed after 24h (B), Fz-MNP staining decreased after 3 Days (C) and 7 days (D). Cell morphology is shown by Phalloidin staining (Red) for Actin (E-H), Nuclei (Blue) are shown by DAPI staining (I-L). Merge channel is shown (M-P). Representative images of n=3 shown, scale bar represents 100µm.

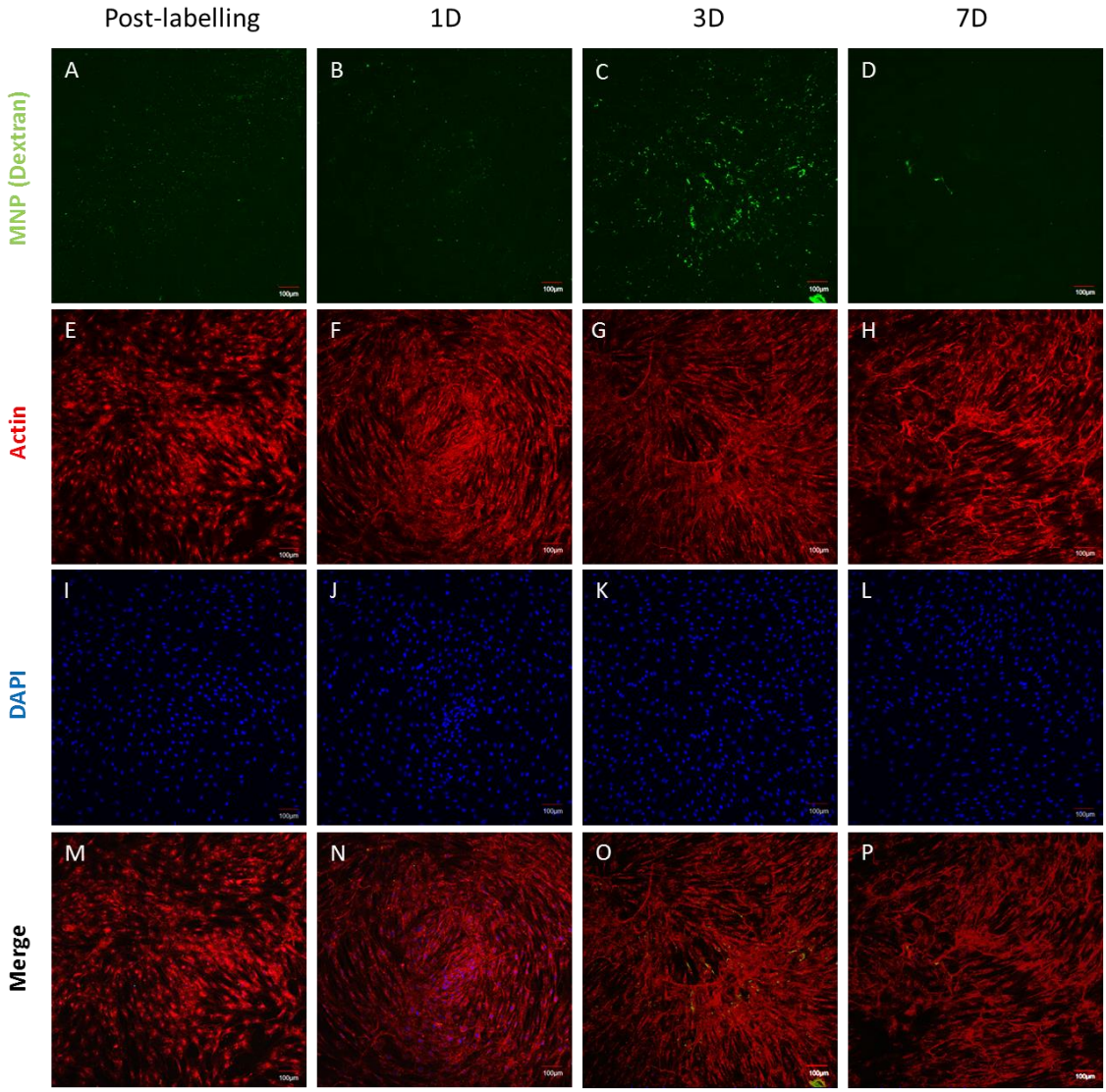

Figure 2.11. L-UM206-MNP tracking over 7 days.
Time-course of Immunofluorescence images showing presence of L-UM206-MNP over 7 days. Dextran staining (Green) for L-UM206-MNP was detectable over 7 days post-labelling (A-D). Peak L-UM206-MNP staining was observed after 3 days (C), L-UM206-MNP staining decreased after 7 days (D). Cell morphology is shown by Phalloidin staining (Red) for Actin (E-H), Nuclei (Blue) are shown by DAPI staining (I-L). Merge channel is shown (M-P). Representative images of n=3 shown, scale bar represents 100µm.

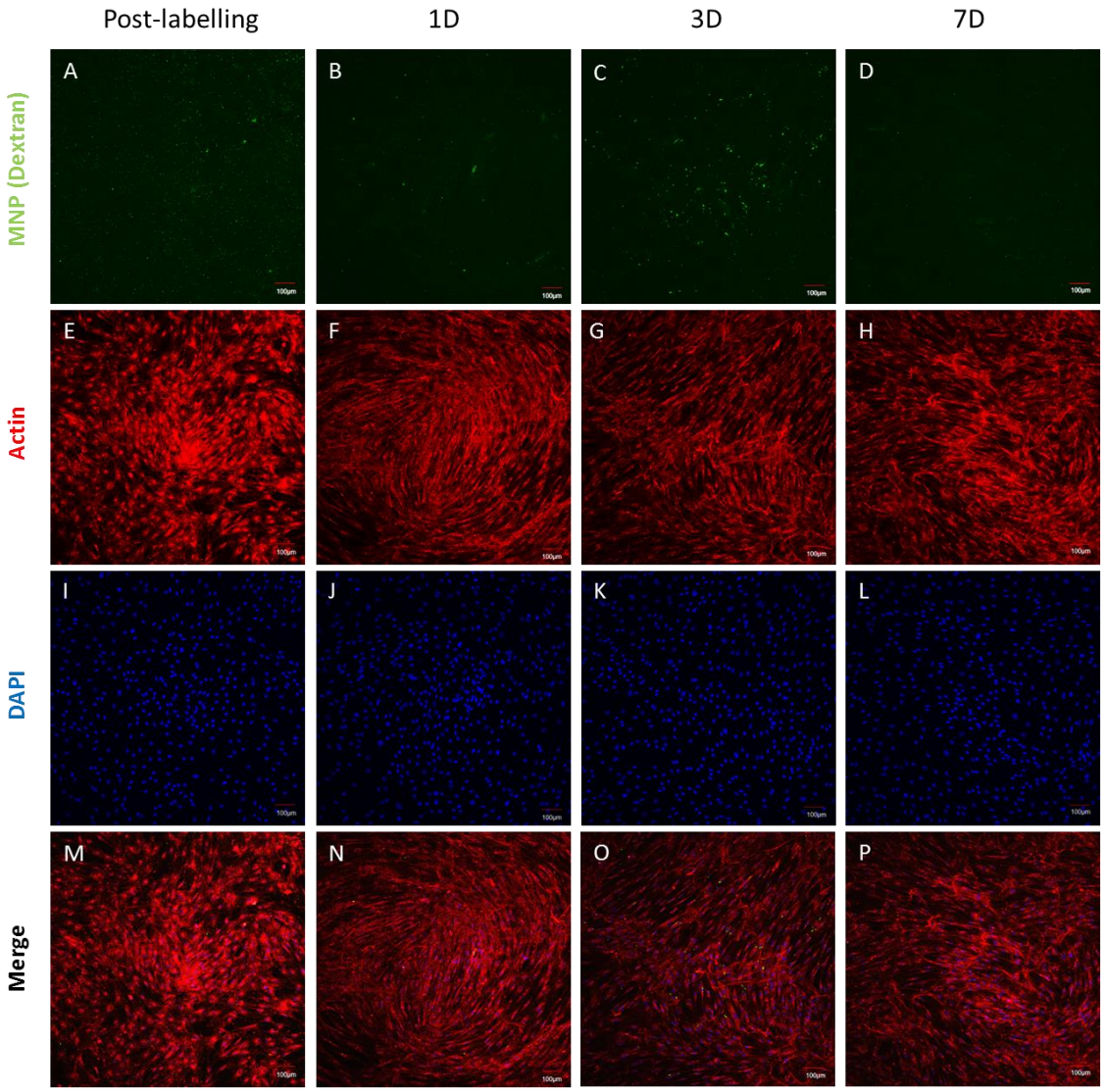

Figure 2.12. C-C-UM206-MNP tracking over 7 days.
Time-course of Immunofluorescence images showing presence of C-C-UM206-MNP over 7 days. Dextran staining (Green) for C-C-UM206-MNP was detectable up to 7 days post-labelling (A-D). Peak C-C-UM206-MNP staining was observed after 3 days (C), staining decreased after 3 days with negligible C-C-UM206-MNP staining observed after 7 days (D). Cell morphology is shown by Phalloidin staining (Red) for Actin (E-H), Nuclei (Blue) are shown by DAPI staining (I-L). Merge channel is shown (M-P). Representative images of n=3 shown, scale bar represents 100µm.

2.3.7 Force imparted by MNP

The force imparted by the MNP on to cells can be estimated using mathematical models. The model describing the force transduced (F_{mag}) is described in (Equation 2.1). This equation takes into account the size of the magnetic particle, the magnetic susceptibility of the magnetic core (in this case iron oxide), the relative magnetic susceptibility of the surrounding medium (effectively zero) and the magnitude and field gradient of the applied magnetic field. By this method the force imparted by the magnetic particles was estimated to be 0.1-1.7 pN per particle when particles were exposed to the magnetic field gradients originating from the 24 well magnetic array or the 6 well magnetic array respectively.

$$\mathbf{F}_{\mathrm{mag}} = (\chi_2 - \chi_1) V \frac{1}{\mu_o} \mathbf{B}(\nabla B)$$

F_{mag} = Force on the magnetic particle
χ_2 = Volume magnetic susceptibility of magnetic particle
χ_1 = Volume magnetic susceptibility of surrounding medium
V = Particle volume
μ_o= Permeability of free space
B = Magnetic flux density
∇B = Magnetic field gradient

Equation 2.1. Force estimation by MNP
The forces exerted by MNP can be estimated using an equation described by Dobson et al (2006).

2.4 Discussion

2.4.1 MNP functionalisation

The process of MNP functionalisation with bio-ligands (Peptides and Antibodies) was investigated by profiling the physical and biochemical changes in MNP properties before

and after coating. The protein-MNP conjugation process was shown to affect both the size and surface charge of MNP. This change in the physical properties of MNP after coating suggests the presence of protein on the MNP surface. Changes in the physical properties of MNP after functionalisation have previously been observed (Sader et al., 2015). Interestingly, although MNP size was increased after coating with either linear UM206 (L-UM206) or cyclic UM206 (C-C-UM206), coating with L-UM206 had a reduced effect on MNP zeta potential compared to coating with C-C-UM206. This may be an artefact of the change in conformational shape of UM206 induced by di-sulphide bond formation. Linear UM206 contains two cysteine residues harbouring negatively charged thiol groups, which may cause an overall decrease in zeta-potential. Conversely, in C-C-UM206 disulphide bond formation between the thiol groups would remove the net negative charge of these groups and may lead to an increase in the observed zeta-potential.

One particular advantage of using covalent attachment of bio-ligands to MNP is that the resulting peptide bond formed between the ligand and MNP is very stable (Radzicka and Wolfenden, 1996). Previous work has demonstrated the long-term stability bio-ligand functionalised MNP. For example Premaratne et al. showed that the peroxidase-like activity of Myoglobin which was coated onto MNP was detectable 4 months after coating (Premaratne et al., 2016) and Sui et al. showed that lipase functionalised-MNP retained 70% of its enzymatic activity 30 days after coating (Sui et al., 2012). The MNP-antibody conjugation process was also validated by conjugating fluorescently labelled secondary antibodies to the MNP. This resulted in a clear fluorescence signal from the FITC-IgG coated MNP. This provided a visual confirmation that the coating process results in

functionalisation of MNP with antibodies. Next, the amount of protein conjugated to MNP was estimated by measuring the changes in the supernatant protein concentration of the MNP coating solutions before and after incubation with carbodiimide activated MNP. It was found that the protein concentration of the coating solution decreased after incubation with activated MNP for all coating types. This difference may be expected and has been previously observed by many groups (Puertas et al., 2010), (Wang and Lee, 2003), (Kouassi and Irudayaraj, 2006b), (Kouassi and Irudayaraj, 2006a) and can be explained by increased conjugation of protein to the MNP surface thereby removing free protein from the coating solution. Interestingly, there was a clear difference in conjugation efficiency between L-UM206 and C-C-UM206. A reduction in conjugation efficiency was observed when MNP were coated with C-C-UM206, indicating that the peptide in this conformation binds less efficiently to the MNP. This could be due to steric hindrance effects caused by multiple cyclic peptides competing for the binding sites of the MNP. This would therefore result in lower levels of C-C-UM206 bound to the MNP surface.

2.4.2 Magnetic field characterisation

The magnetic field profiles of the magnetic arrays used in the experiments were also characterised by magnetic field mapping at different distances. As expected, the highest magnetic field strengths were observed closest to the magnetic array with the magnetic field gradient degrading exponentially as a function of distance. The field strengths applied in these experiments have been shown to be comparable to the field strengths applied in previous work for the activation of other cell surface receptors (Hu et al., 2013).

2.4.3 MSC labelling with MNP

The presence of MNP and association with cells was determined using biochemistry to detect the iron oxide core of the MNP and Immunocytochemistry to detect the dextran matrix. Both techniques confirmed that MNP were associated with MSC after labelling and MNP association with cells was shown to persist up to 7 days. This may be an indication that MNP internalisation has commenced and is consistent with previous work with other MNP which showed that endocytosis commences within days after labelling with complete internalisation of most adhered MNP after one week (Cartmell et al., 2005). Other work has identified the mechanism behind MNP internalisation to be clathrin and caveolae dependent endocytosis (Cores et al., 2015). However, the rate of MNP internalisation is dependent on numerous factors including the cell type, particle size, surface charge and particle coating (Hughes et al., 2005). The results from this work suggest that the MNP used here may be internalised after 3-7 days, although It is indeterminable whether these MNP are intact or to discern their intracellular or extracellular location using the methods shown here. Further work should investigate the intracellular location and fate of MNP which could be achieved high resolution or electron microscopy techniques. These results may suggest that a window of opportunity may exist for mechanical stimulation by MNP before internalisation of the MNP-target complex occurs. Having said this, some signalling pathways including the Wnt pathway require internalisation of surface receptors in order to propagate signalling. For example, caveolin and clathrin-mediated internalisation of Wnt and LRP6 initiated has been shown to be necessary for accumulation of β-catenin and Wnt pathway activation (Blitzer and Nusse, 2006), (Yamamoto et al., 2006). In this scenario internalisation of the MNP-

receptor complex may not preclude abrogation of signalling activity. Therefore the effect of MNP internalisation on signalling activity should be studied further.

2.4.4 Cytotoxic effects of MNP and Magnetic field

The effects of coated MNP on cell toxicity were investigated using two widely used methods. Firstly, the effect of MNP on short and medium term cell viability was determined using a Live/Dead assay. Fluorescent microscopy indicated that treatment of cells with coated MNP remained viable and metabolically active suggesting that there are no obvious adverse effects of functionalised MNP on cell membrane integrity or cell viability. This agrees with previous work which has shown that dextran-based MNP do not significantly affect MSC viability (Jasmin et al., 2011), (Moraes et al., 2012). Furthermore, the addition of magnetic field stimulation appeared to have no adverse effects on cell viability, this is unsurprising given that previous work has shown that both static and oscillating magnetic field gradients up to 600mT in magnitude have no deleterious effects on MSC viability (Schäfer et al., 2010), (Ross et al., 2015), (Fouriki and Dobson, 2013). Secondly, the effects of MNP on cell metabolism were assessed using an MTT assay. All MNP types regardless of surface functionality had no clear effect on cell metabolism indicating that they do not induce detrimental effects on cell metabolism and, once again, addition of magnetic field stimulation had no detrimental effects on cell metabolism. These findings also agree with previous work which has demonstrated that iron oxide-based MNP have negligible effects on MSC metabolism (Markides et al., 2013), (Sibov et al., 2012). Overall these results suggest that, at the doses used in these experiments, functionalised-MNP and applied magnetic fields are biocompatible and non-toxic to hMSC. Despite there being no clear effects of these MNP on cell viability at this dose and over this time-frame, a longitudinal study examining the toxicity of these MNP over a

broad dose range and using a greater variety of methods is needed. The toxicity of these MNP in other cell types both *In vitro* and *in vivo* should also be assessed.

2.4.5 Force transduced by MNP

Finally, the force exerted by the MNP used in these experiments was modelled according to an equation described by (Dobson et al., 2006) which estimated force transduction according to magnetic field strength, gradient and particle size. The force exerted by the MNP was estimated to be in the range of 0.1-1.7pN per particle. Although this may be considered to be a broad range for eliciting biological effects, previous work examining MNP mediated magnetic activation of cell surface receptors suggests that forces in this range do influence cell signalling behaviour. For example, Hughes et al demonstrated that 250nm ferric based MNP exerting forces of 0.2pN and targeted to the TREK1 ion channel caused changes to whole-cell currents in COS7 cells consistent with TREK channel activation (Hughes et al., 2008). Also, The application of 6pN forces using ferro-magnetic microparticles targeted to Integrin receptors was shown to cause hyperpolarisation of MSC which was mediated through BK channels (Kirkham et al., 2010).

The simplified mathematical model applied in this work may be appropriate for estimating the magnitude of force transduced by MNP in a vertical direction. However, this assumes that MNP act as single entities and does not take into account MNP aggregation which may inflate the applied forces. Furthermore, the orientation and angles at which MNP bind to target cells is also a factor when considering force transduction as these parameters will determine the direction of the applied force and may influence the magnitude of the force experienced by the cell. Further work should involve experimental validation of the forces applied by MNP to confirm this.

2.5 Conclusions

The use of MNP has revolutionised many areas of engineering and medicine. This is due, in part, to the adaptability of MNP which can be functionalised with biomolecules for specific applications. In these experiments it was shown that the bio-functionalisation process of MNP successfully resulted in conjugation of antibodies and peptides to the MNP surface. Functionalised MNP were also shown by a range of techniques to attach to human mesenchymal stem cells, a clinically relevant stem cell type that has already been adopted for cell therapies. The MNP used in these experiments were mechanically torqued using a magnetic force bioreactor that imparts magnetic field gradients on to the MNP. The magnitude and profile of the applied magnetic fields were elucidated and shown to be in the range of 60-120 mT. Further mathematical modelling, which takes into account the MNP used and magnetic field gradients, allowed the magnitude of the force transduced by the MNP to the cells to be estimated at approximately 0.1-1.7 pN/particle. The safety and biocompatibility of nano-materials is also an important consideration which must be proven before the translation of novel cell treatments to clinical practice. To this end, the biocompatibility and cytotoxic effects of MNP with different surface coatings was also investigated using well established methods. The MNP used in these experiments were shown to be non-toxic to hMSC at the applied doses over short and medium terms and the addition of magnetic field stimulation to MNP and cells also had no obvious effect on cell cytotoxicity. Finally, tracking of MNP *in vitro* using Immunocytochemistry suggested that MNP labelling of MSC persists up to 7 days.

Chapter 3: Remote activation of Wnt signalling pathways using magnetic nanoparticles

3.1 Introduction

Wnt signalling is a complex pathway involved in the regulation of a range of biological processes ranging from cell proliferation and differentiation to embryogenesis, tissue formation and regulation of stem cell niches (Nusse, 2008) (Clevers, 2006). The primary receptor for Wnt ligands are Frizzled receptors (Binnerts et al., 2007). Frizzleds have an extended N-terminal region harbouring a cysteine rich domain (CRD) which is required for Wnt reception (Logan and Nusse, 2004), (MacDonald et al., 2009), (Wang et al., 2006). In Canonical Wnt/β-catenin signalling, Wnt proteins interact with a receptor complex comprised of Frizzled (Fz) and Low density lipoprotein (LDL) receptor-related protein (LRP) located at the cell membrane (Cong et al., 2004), (Holmen et al., 2005), (Tolwinski et al., 2003). When activated by Wnt, LRP becomes phosphorylated at multiple sites. The activated Fz/LRP receptor complex recruits Axin to the cell membrane (Tamai et al., 2004), (Zeng et al., 2005), this causes the sequestration of several other intracellular proteins required for Wnt signalling modulation. In the absence of an external Wnt signal, GSK-3, Dvl and APC form a destruction complex that regulates the cytoplasmic pool of the transcriptional regulator β-catenin (Logan and Nusse, 2004). In the presence of a Wnt signal the destruction complex dissociates and is deactivated, as a result active β-catenin accumulates in the cytoplasm and nucleus. Nuclear β-catenin acts as a transcriptional regulator and interacts with the lymphoid enhancer-binding factor 1/T-cell specific transcription factor (LEF/TCF) family of transcription factors (Logan and Nusse, 2004) which bind to and activate Wnt responsive genes with TCF/LEF binding sites (Logan and Nusse, 2004).

Human Mesenchymal Stem Cells (hMSC) are multipotent stem cells involved in bone and cartilage formation during development and are of particular interest in tissue engineering (Oreffo et al., 2005), (Ling et al., 2009). Human MSC have been shown to exhibit Wnt pathway activity and are known to express a number of Wnt ligands and Frizzled receptors including Frizzled 2 and co-receptors such as LRP (Etheridge et al., 2004), (Kolben et al., 2012), (Okoye et al., 2008). There is also a clear role for mechanical forces in MSC and Wnt signalling. Previous work has shown that hMSC are responsive to mechanical loading both *in vitro* and *in vivo* (Kanczler et al., 2010), (Henstock et al., 2014). The Wnt signalling pathway has also been shown to be activated in response to fluid flow (Arnsdorf et al., 2009). This suggests that mechanical loading of MSC may be a viable and alternative way of targeting and modulating Wnt signalling pathways.

The main drawback of using recombinant Wnt protein for bioengineering applications is the limited ability to obtain large quantities of bio-active Wnt (Coudreuse and Korswagen, 2007), (Willert and Nusse, 2012). As a result there is now great interest in the development of modulators of Wnt receptors using small molecules such as peptides. This approach allows a more targeted method of regulating pathway activity compared to pharmacological modulators such as the GSK-3β inhibitor LiCl (Freland and Beaulieu, 2012). One such example of peptide mediated modulation of Wnt signalling is the synthetic peptide UM206 which is based on a conserved fragment of Wnt3A and Wnt 5A. UM206 is a high affinity ligand for Frizzled 2 receptors (and to a lesser extent Frizzled 1) with the capability of acting as an agonist of canonical Wnt signalling in HEK293 cells when present in a cyclical conformation (EC_{50} of 2.10^{-8}M). Alternatively UM206 has been shown to behave as a Wnt pathway antagonist when present in its linear conformation

(IC_{50} of 10^{-10} M). Conversion of linear UM206 to its cyclic conformation is possible with disulphide bond formation between its Cysteine residues. This therefore allows an element of control over peptide activity (Blankesteijn Wessel Matthijs, 2010). Representational models of the peptide sequence and conformations of UM206 are shown in Figure 3.1.

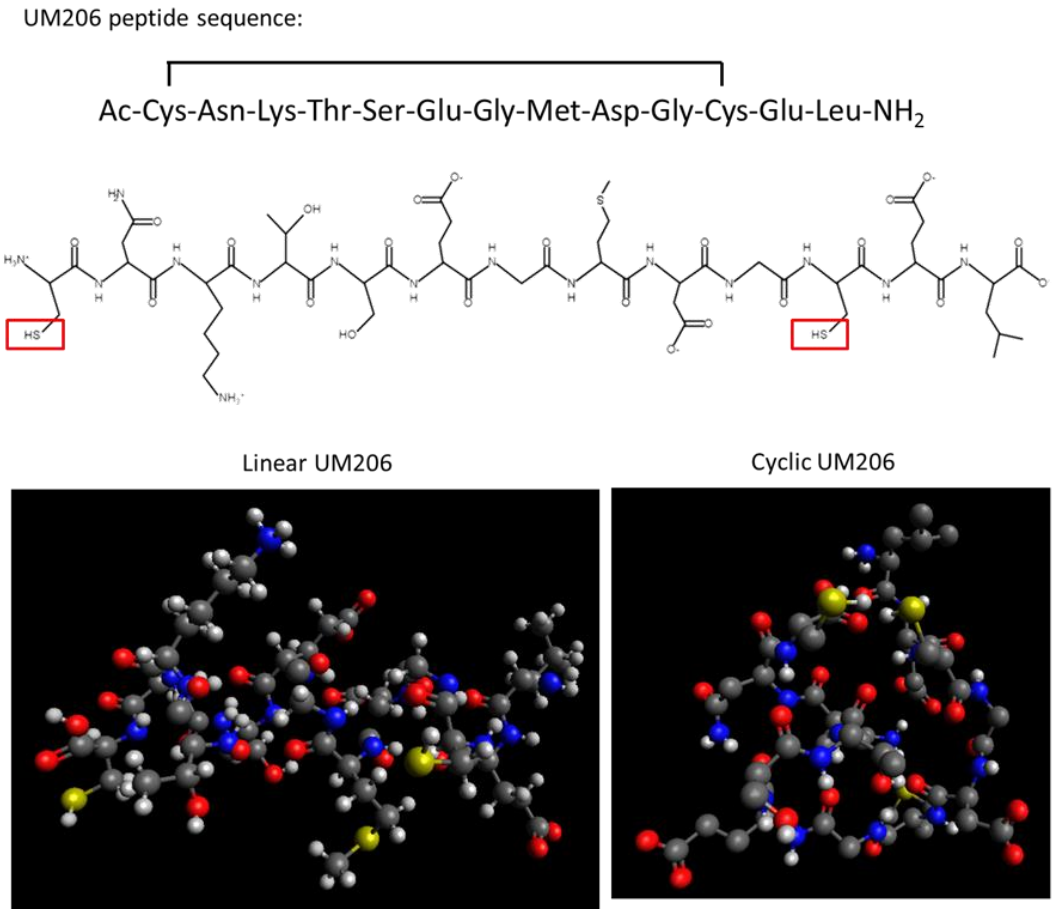

Figure 3.1. Representational models of UM206 peptide.
The amino acid sequence of UM206 is shown in the top diagram; the Cysteine residues involved in disulphide bond formation are indicated by lines and circled. Ball and stick models of the two conformation of UM206 are shown in the bottom panels. UM206 in the linear conformation is shown bottom left, the cyclic conformation is shown on the bottom tight image. Atoms are colour coded as follows, Grey = carbon, Red = Oxygen, Blue = Nitrogen, Yellow = Sulphur, White = Hydrogen atoms.

A further strategy for Wnt pathway modulation is to target Wnt receptors using MNP technology. When MNP are coupled with oscillating magnetic field gradients, this causes a translational torque on the MNP which results in changes in target receptor conformation. This strategy has previously been demonstrated for the activation of other mechanosensitive receptors (Hughes et al., 2005), (McBain et al., 2008), (Yiu, 2011). The main aim of the experiments presented in this chapter was to investigate the effects of Frizzled 2 targeting using antibodies and UM206 peptides bound to MNP, and to assess the effects of magnetic stimulation of these targeted MNP on canonical Wnt pathway activity in hMSC.

3.2 Methods

3.2.1 Cell culture

Bone marrow derived human MSC were sourced as described in chapter 2. For cell expansion MSC were cultured in high glucose DMEM supplemented with 10% FBS, 1% L-glutamine and 1% Penicillin & Streptomycin (All reagents Lonza). Cells were passaged once per week and cells between passage 2 and 5 were used in all experiments. For UM206 peptide treated groups, cells were cultured in basal media containing 1µg/mL of either L-UM206 or C-C UM206 peptide. For positive Wnt signalling control groups, either recombinant Wnt 3A (20ng/mL) (R&D systems) or diluted Wnt 3A conditioned media collected from Wnt 3A overexpressing L-M(TK-) cells (LGC standards) was used (see appendix C).

3.2.2 Transient transfections

For Wnt luciferase reporter studies, hMSC (P3-5) were transiently transfected with a Gaussia Luciferase reporter gene under control of an 8x TCF/LEF promoter (provided by Dr Hu Bin and Neil Farrow, Keele University). Cells were seeded at $1X10^4$ cells /well in 24-well plates and cultured in reduced serum opti-MEM media without the addition of antibiotics during transfection. Cells were transfected according to the manufacturer's instructions. Briefly, 100μL of transfection solution consisting of 0.5μg of TCF/LEF reporter plasmid, 2.25μL of Lipofectamine LTX and 0.5μL of Plus reagent (All Invitrogen) was added to each well. 4h after transfection media was aspirated and replaced with fresh antibiotic free media.

3.2.3 MNP coating

250nm SPIO carboxyl functionalised magnetic nanoparticles (Micromod) were covalently coated with anti-Frizzled 2 (Abcam), Trek1 (Alomone labs), Linear UM206 peptide or Cyclic UM206 peptide by carbodiimide activation as described in chapter 2. For IgG and RGD coated MNP, 1mg of MNP (per ligand) were activated for 1h as stated previously. After washing, the particle suspensions were re-suspended in 0.1M MES buffer containing either 20μg/mg of MNP of anti-rabbit IgG antibody (Abcam) or 50μg/mg of MNP of RGD tri-peptide (Sigma). The particle suspensions were continuously mixed overnight at 4^oC. Particle suspensions were then blocked, washed and re-suspended in 0.1% BSA (Fisher) in PBS (Sigma) as stated previously.

3.2.4 Cell labelling with MNP

Cells were labelled with MNP as described in chapter 2. Briefly, Cells were washed with PBS then cultured in basal serum-free media before addition of MNP at approximately

3μg MNP/cm^2 of culture surface area. Cells were incubated for a further 1.5h with intermittent agitation, then unbound particles were removed by washing with PBS before addition of fresh media. Serum free basal media was used in western blotting experiments, basal media with 2.5% FBS was used in luciferase experiments, basal media with 10% FBS was used for gene expression experiments.

3.2.5 Magnetic stimulation

Magnetic field stimulation was applied using the magnetic force bioreactor (MICA Biosystems) described in chapter 2. Magnetic field treatment was applied in 1hr and 3h sessions at a frequency of approximately 1Hz.

3.2.6 Total Protein assay

Total protein was assessed using a BCA assay kit (Fisher). Lysates were diluted 2x with d.H_2O and 25μL of each sample was aliquoted into 96 well plates. Samples were incubated with a working solution of BCA assay reagent as detailed in chapter 2. The total protein concentration of the samples was determined using a standard curve of BSA dissolved in Luciferase lysis buffer (for luciferase samples) or RIPA buffer (for Western blotting samples) (see appendix B).

3.2.7 Western blotting

Cells were lysed with RIPA buffer containing a mixture of protease and phosphatase inhibitors (Sigma) (See appendix C). Cell Lysates were clarified and the total protein of each sample using a BCA assay kit (Thermo). The total protein concentration of the samples was determined using a standard curve of BSA dissolved in RIPA buffer. For PAGE, 25-30μg of protein was mixed with LDS sample buffer with added β-mercaptoethanol (both Invitrogen). Samples were then heated for 10mins at 70^oC and

briefly centrifuged before being loaded onto a Tris-Glycine 4-20% gel in Tris-Gly running buffer (NuSep) and subjected to PAGE. Proteins were transferred to 0.4µm PVDF membrane (Thermo) which was then blocked with 5% milk powder (Co-operative) in TBST buffer (Sigma) (5% BSA in TBST used for GAPDH probe). Membranes were then incubated with anti-LRP6 (New England Biolabs) (1:1000), anti (Ser1490) phospho-LRP6 (New England Biolabs) (1:1000), anti-LRP5 (New England Biolabs) (1:1000), anti-phospho-LRP5 (Abnova) (1:1000), anti-Frizzled 2 (Santa Cruz) (1:500) or anti-GAPDH (Abcam) (1:1000, in 5% BSA/TBST). All antibodies were diluted in 5% Milk in TBST unless stated otherwise. All blots were incubated overnight at 4^{o}C with constant mixing. Membranes were washed with TBST 3x before incubation with anti-rabbit-HRP, anti-Mouse-HRP (Abcam) or anti-Goat-HRP (Santa Cruz) respectively. All secondary antibodies were diluted 1:1000 in 5% Milk/TBST and mixed for 1h at room temp. Membranes were washed 5x in TBST and chemiluminescence developed using a PicoWest chemiluminescent kit (Thermo Pierce) followed by image capture using a Protein Simple Flourchem M imaging system.

3.2.8 Immunocytochemistry

For β-catenin mobilisation experiments cells were seeded onto glass cover slips (SLS). At 24h post treatment media was aspirated, cells washed with PBS (Sigma), then fixed with ice cold (90%) methanol (Fisher) for 10mins. Cells were permeabilised with 0.1% triton-x in PBS (Sigma) for 10mins then then blocked in 2% BSA (Fisher) in PBS for 1h at room temp. Cells were then incubated with anti-active β-catenin antibody (Millipore) 1:1000 dilution in 0.1% BSA in PBS overnight at 4^{o}C. Afterwards, cells were washed 3X with PBS, then incubated with anti-mouse-FITC conjugated secondary antibody (Sigma) in 0.1% BSA in PBS for 1h at room temp. Cells were then washed 3X in PBS and counterstained with DAPI (Sigma). Fluorescence microscopy was performed on Nikon Eclipse Ti-S microscope

with NIS elements software. All images are representative of 3 replicate samples. Pixel intensity analysis to assess nuclear β-catenin staining was performed using ImageJ v1.48s

3.2.9 Luciferase reporter assays

Luciferase activity was assessed 48-72h post-transfection. Experiments were performed in 24-well plates with reduced serum (2.5%). For Wnt pathway blocking experiments cells were cultured in reduced serum (2.5%) media containing either 0.1μg/mL Dkk1 or 50μM iCRT14 (R&D Systems). At each time point, media samples were taken and analysed for secreted Gaussia luciferase activity using a luciferase flash assay kit (Thermo Pierce). 20μL of sample was aliquoted into opaque 96 well plates then 50μL of luciferase assay reagent consisting of Coelenterazine diluted 100x in luciferase assay buffer (Thermo Pierce) was injected into each well using an automatic injection system. Luminescence measurements were acquired immediately after addition of Coelenterazine using a Biotek Synergy 2 plate reader controlled by Gen5 software. Luciferase activity was normalised to the total protein content of the cell lysates taken at the experimental end-point. Cells were lysed in 100μL of Luciferase lysis buffer (Fisher) for 10mins. Fold changes for each treatment were calculated relative to the cells only control.

3.2.10 Reverse transcription PCR

At each time-point, total RNA was extracted using an RNAeasy extraction kit (Qiagen) according to the manufacturer's instructions (see appendix C). Reverse transcription was performed on 600ng RNA using a high capacity reverse transcription kit (Applied Biosystems) according to the manufacturer's instructions (see appendix C). RT-PCR reaction mixes were prepared using diluted cDNA mixed with PCR master mix (Applied Biosystems) and commercially available primers for Frizzled 2 (Hs_FZD2_1_SG) and

GAPDH (Hs_GAPDH_2_SG) (both Qiagen), (see appendix C). Thermocycling was performed on a Stratagene MX3000P. 10µL of PCR products were mixed with 2.5µL of loading buffer (Sigma), loaded and run on a 2% Agarose gel for 1h at 100v. Gels were imaged on a GelDoc-It2 imager system (UvP).

3.2.11 Quantitative reverse transcription PCR

At each time-point, media was aspirated, cells washed with PBS then lysed using TRI reagent (Sigma), total RNA was extracted using the chloroform / isopropanol extraction method according to the manufacturer's instructions (see appendix C). Reverse transcription was performed on 500ng total RNA (120ng for 1h samples) using a high capacity reverse transcription kit (Applied Biosystems). Quantitative PCR reaction mixes were prepared using 5µL of diluted sample mixed with 10µL of q-PCR master mix consisting of 7.5µL of SYBR-Green master mix (Applied Biosystems), 1.5µL of H_2O and 1µL of commercial primers for either COX2 (Hs_PTGS2_1_SG), c-Myc (Hs_MYC_1_SG), NF-κβ (Hs_NFKB1_1_SG) or GAPDH (Hs_GAPDH_2_SG) (all Qiagen) (see appendix C). Quantitative PCR was performed over 40 cycles using a Stratagene MX3000P system with MxPro software. Gene expression was normalised to GAPDH and fold change in gene expression was calculated using the delta-delta Ct method.

3.2.12 Statistical analysis

All data is presented as means ±SEM. Statistical significance at 95% confidence level was determined using 1-way ANOVA with post-hoc Tukey tests using Mini-tab (v16) software.

3.3 Results

3.3.1 Expression of Frizzled 2 in hMSC

Expression of Frizzled 2 in hMSC was determined at transcriptional and translational level using RT-PCR and Western blotting respectively (Figure 3.2). RT-PCR for the Frizzled 2 gene indicated that gene expression was stable over 21 days in basal or osteogenic media. Western blotting was used to assess the level of Frizzled 2 expression at the translational level. In basal media Frizzled 2 expression appeared to increase over time with peak expression at Day 14. In osteogenic media clear expression was observed at Day 3 but then reduced until Day 21 where maximum expression was observed.

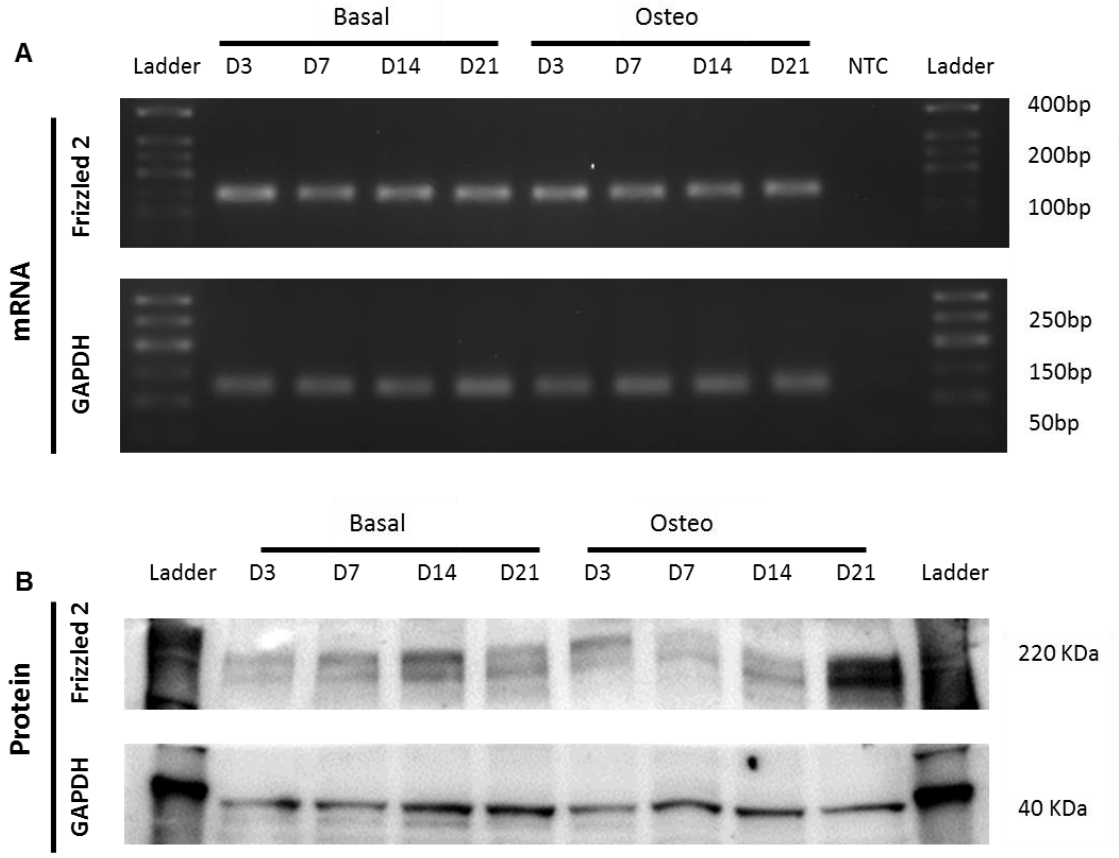

Figure 3.2. hMSC express Frizzled 2.
RT-PCR gels and Western blots showing Frizzled 2 expression in hMSC. RT-PCR for Frizzled 2 mRNA expression (A) indicated that Frizzled 2 is expressed in Basal and Osteogenic media over the course of 21 days. Western blotting for Frizzled 2 confirmed expression of Frizzled 2 at the protein level (B), GAPDH is used as a housekeeping gene.

3.3.2 β-catenin mobilisation studies

To determine if Frizzled 2 targeted MNP were causing Wnt signalling activation downstream of Frizzled, the mobilisation and nuclear localisation of the intracellular messenger β-catenin was investigated using immunocytochemistry.

3.3.2.1 β-catenin is mobilised in response to Fz-MNP and L-UM206-MNP

β-catenin localisation was studied in hMSC after treatment with anti-Frizzled-MNP (Fz-MNP), Linear UM206-MNP (L-UM206-MNP) or Cyclic UM206-MNP (C-C-UM206-MNP).

Samples were also treated with magnetic field stimulation to determine the effects of added mechanical stimulation on β-catenin mobilisation. Wnt3a conditioned media (Wnt-CM) was used as a positive control in these experiments (Figure 3.3). Non-treated cells displayed negligible β-catenin nuclear localisation after 24h. When cells were treated with anti-Fz MNP, L-UM206-MNP and to a lesser extent C-C-UM206-MNP (without magnetic field), clear nuclear localisation of β-catenin was observed and pixel intensity analysis of the cell nuclei confirmed a significant increase in nuclear localisation compared to non-treated control (non-significant increase for C-C-UM206-MNP). Magnetic field stimulation of Fz-MNP or L-UM206-MNP labelled cells caused a further increase in β-catenin mobilisation, whereas magnetic stimulation of C-C-UM206-MNP labelled cells resulted in a marginal increase in β-catenin mobilisation. Pixel intensity analysis also confirmed a significant increase in nuclear staining by Fz-MNP and L-UM206-MNP compared to cells with magnet control (Figure 3.4). Cells treated with Wnt-CM showed noticeable nuclear localisation after 24h which was again significant over the non-treated control according to pixel intensity analysis.

3.3.2.2 Control-MNP do not mobilise β-catenin

Control particles coated with IgG (IgG-MNP) or the RGD peptide (RGD-MNP) both caused overall minor increases in β-catenin activation (not significant) but no additive effect was observed when cells were treated with either control MNP with addition of magnetic field (Figure 3.5). Pixel intensity analysis confirmed that control-MNP had no overall effect on β-catenin mobilisation with or without magnetic field (Figure 3.6).

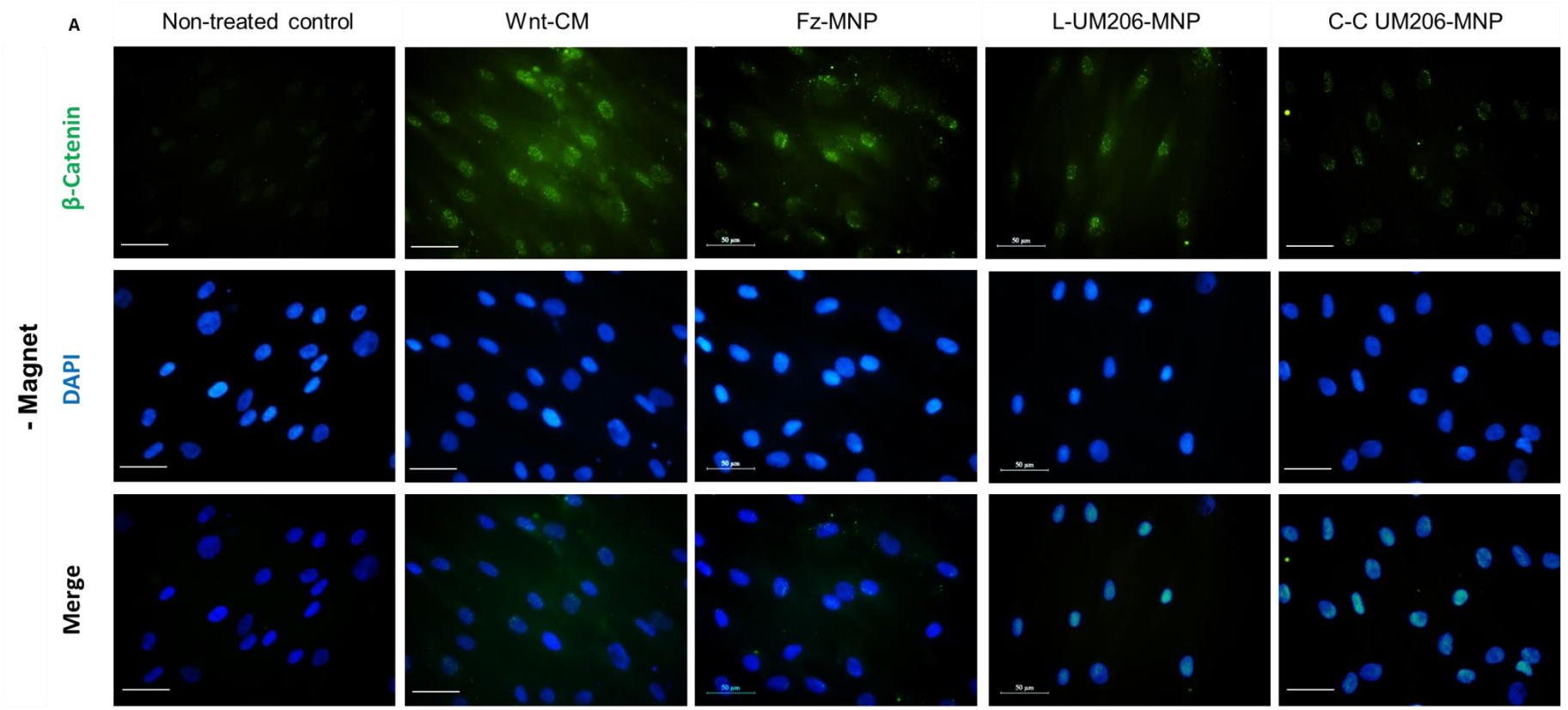
A
Non-treated control
Wnt-CM
Fz-MNP
L-UM206-MNP
C-C UM206-MNP
- Magnet
β-Catenin
DAPI
Merge

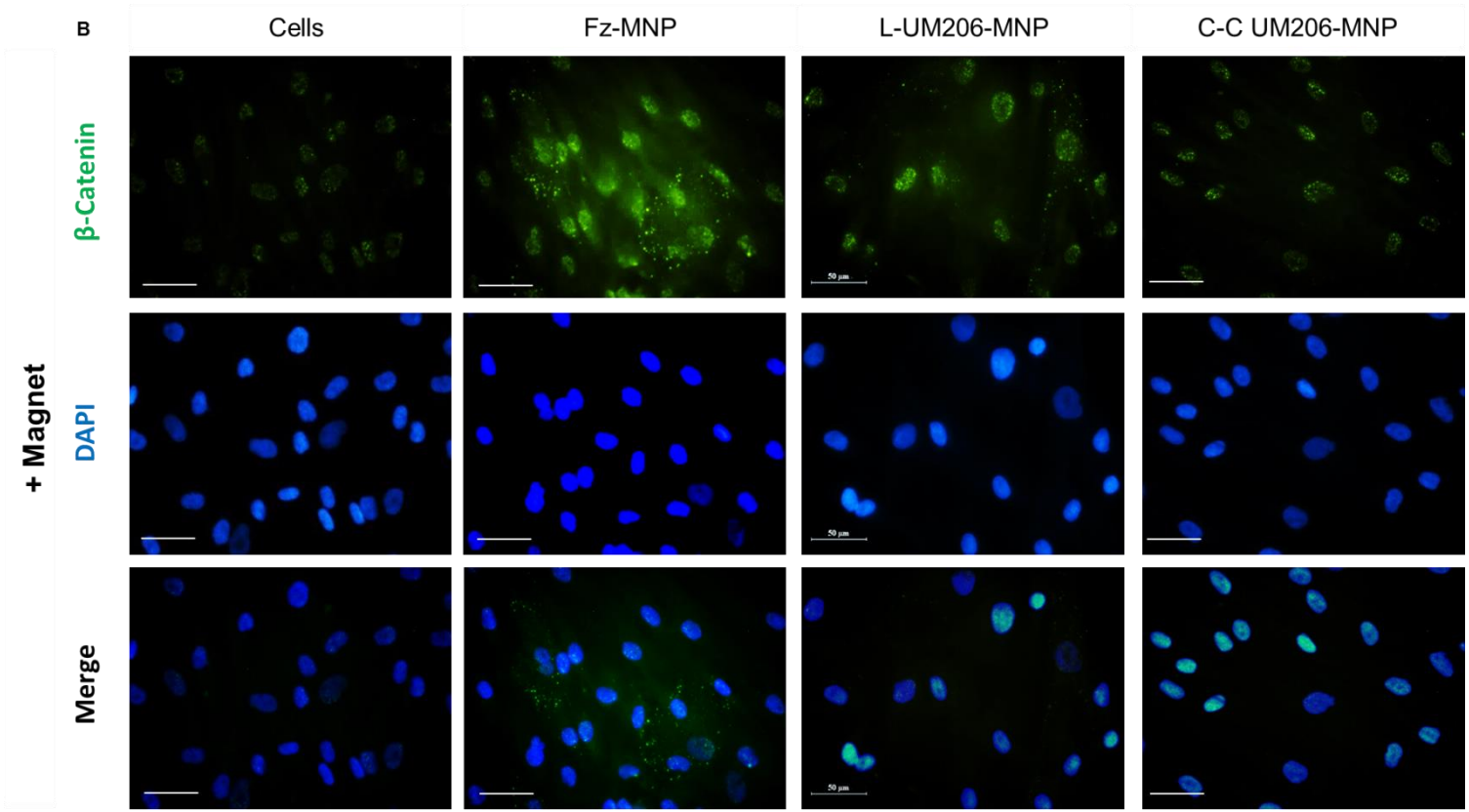

Figure 3.3. Frizzled-MNP and L-UM206-MNP promote β-catenin activation and mobilisation.
Fluorescent images showing localisation of active β-catenin (Green) after 24h, DAPI was used to visualise cell nuclei (Blue), Merged images show location of β-catenin in relation to cell nuclei. Non-treated cells (A) showed negligible β-catenin localisation. Treatment with anti-Frizzled magnetic nanoparticles (Fz-MNP) or L-UM206-MNP without magnet (A) showed notable nuclear localisation with an added effect when these particles were used in conjunction with magnetic field (B). Treatment with Wnt-conditioned media (A) also showed notable nuclear β-catenin after 24h. In contrast treatment with C-C-UM206 MNP resulted in a negligible increase in β-catenin localisation with and without magnetic field. Representative images, n=3, scale bar = 50µm.

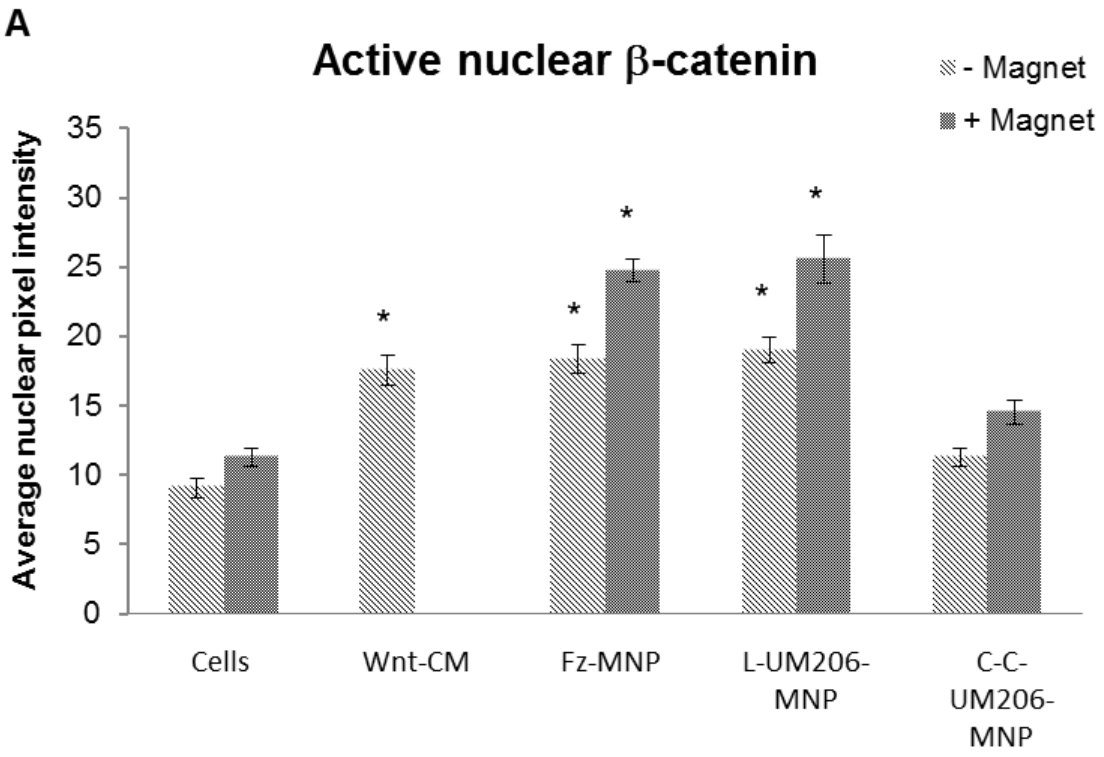

Figure 3.4. Quantification of Fz-MNP and L-UM206-MNP β-catenin mobilisation. Quantification of nuclear pixel intensity (A) indicated levels of nuclear (active) β-catenin. Treatment with magnetic field alone or C-C-UM206-MNP (with or without magnetic field) caused negligible increases in levels of nuclear β-catenin whereas treatment with Fz-MNP, L-UM206-MNP or Wnt-CM all increased β-catenin mobilisation to similar levels. An added effect was observed when Fz-MNP or L-UM206-MNP were used in conjunction with magnetic field. Average pixel intensities shown, n=3, error bars represent SEM, * denotes $p<0.05$

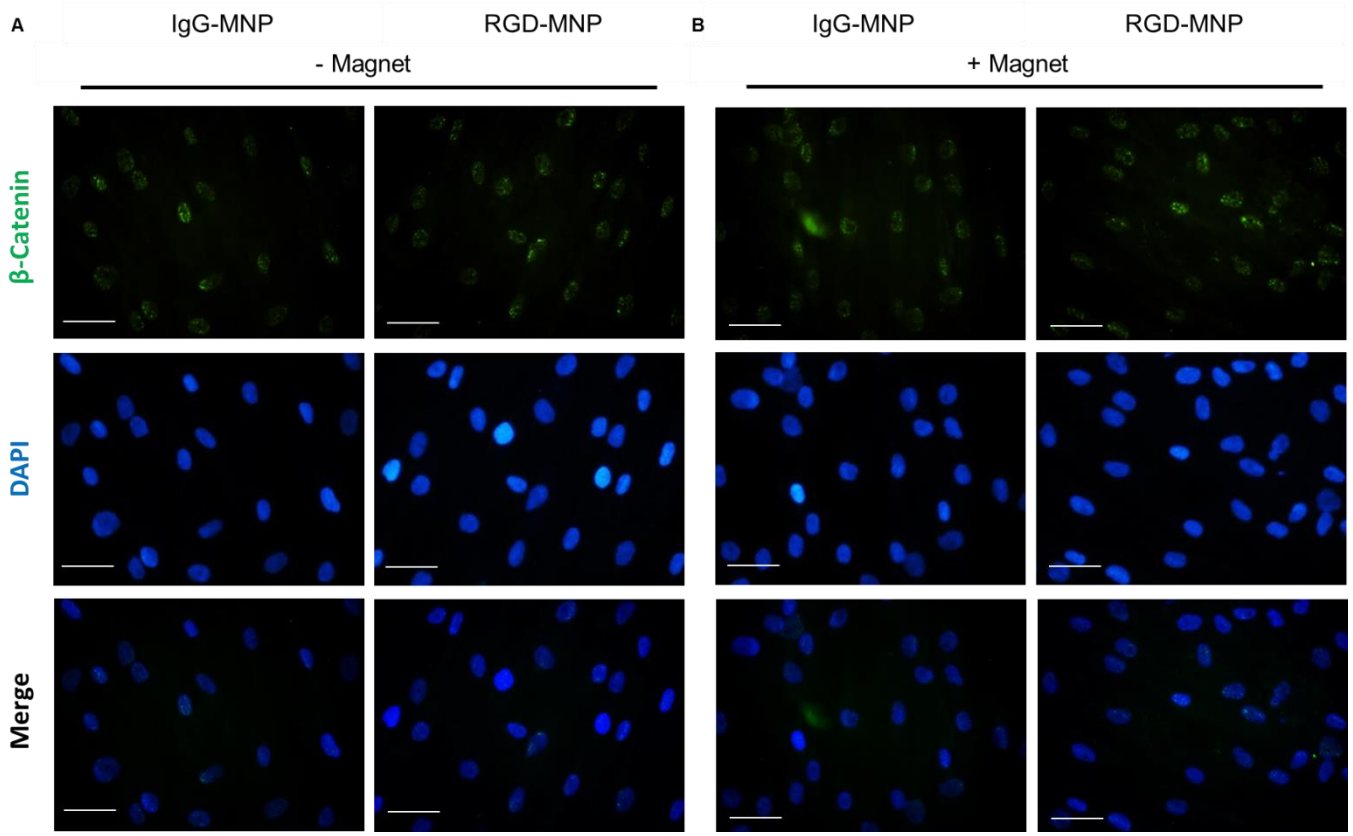

Figure 3.5. Control MNP do not mobilise β-catenin.
Fluorescent images showing localisation of active β-catenin (Green) after 24h, DAPI was used to visualise cell nuclei (Blue), Merged images show location of β-catenin in relation to cell nuclei. Cells treated with IgG-MNP or RGD-MNP (A) resulted in minor increases in nuclear localisation, and addition of magnetic field (B) had no overall effect. Representative images, n=3, scale bar = 50µm.

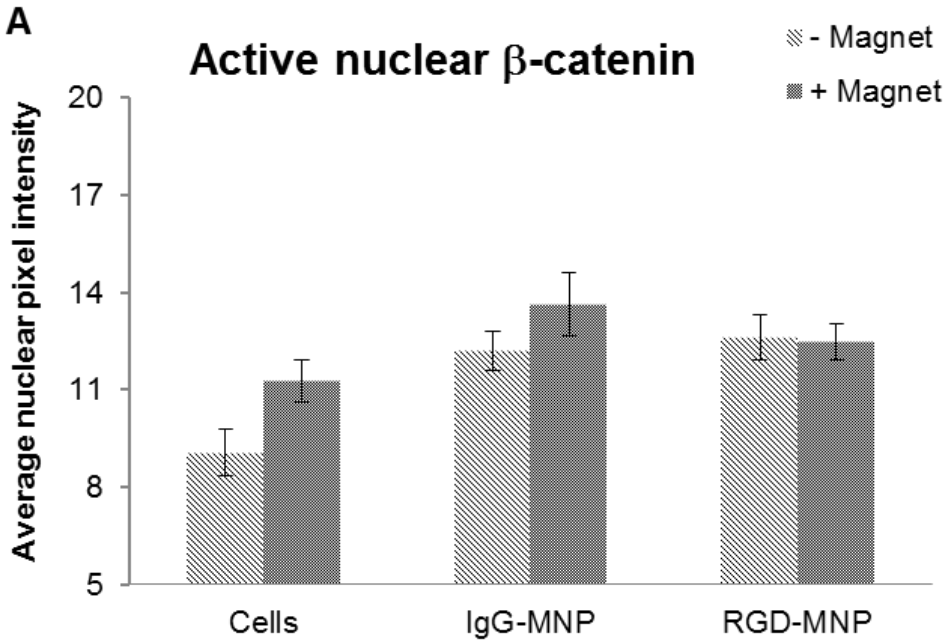

Figure 3.6. Quantification of control-MNP β-catenin mobilisation.
Quantification of nuclear pixel intensity indicated levels of (active) β-catenin. Treatment with magnetic field alone, IgG-MNP or RGD-MNP (with or without magnetic field) all caused similar (non-significant) increases in the levels of active nuclear β-catenin. Average pixel intensities shown, n=3, error bars represent SEM.

3.3.3 TCF/LEF reporter studies

A Gaussia luciferase reporter under control of a TCF/LEF promoter was then used to directly asses the transcriptional activity of Wnt target genes over 24 hours in response to UM206 peptides and antibody/UM206 functionalised MNP. Wnt3a-conditioned media was used as a positive control. Samples were also treated with magnetic field stimulation for 3 hours to determine the effects of added mechanical stimulation on TCF/LEF reporter activity. The activation mechanisms of the treatments were also probed using different Wnt pathway blockers to determine through which control nodes pathway activity was signalling through.

3.3.3.1 Wnt3a activates TCF/LEF signalling

Transfected hMSC showed a 3-fold increase in Wnt reporter activity 6h after treatment with Wnt-conditioned media (Wnt-CM) with maximal reporter activity observed after 24h (Figure 3.7). Wnt-CM mediated pathway activation was successfully blocked at both time-points using Dkk1 which inhibits LRP co-receptor activation at the cell membrane. Pathway activation was also successfully blocked with iCRT14 which blocks downstream Wnt pathway activation by inhibiting β-catenin interaction with TCF/LEF transcription factors and subsequent Wnt target gene expression.

3.3.3.2 UM206 peptides alone do not activate TCF/LEF signalling

Treatment of transfected hMSC with 1µg/mL of UM206 in the linear conformation (L-UM206-peptide) had no overall effect on reporter activity at 6h or 24h after treatment (Figure 3.8). However, treatment with 1µg/mL UM206 in the cyclic conformation (C-C UM206-peptide) decreased reporter activity after 6h but after 24h reporter activity remained similar to the control.

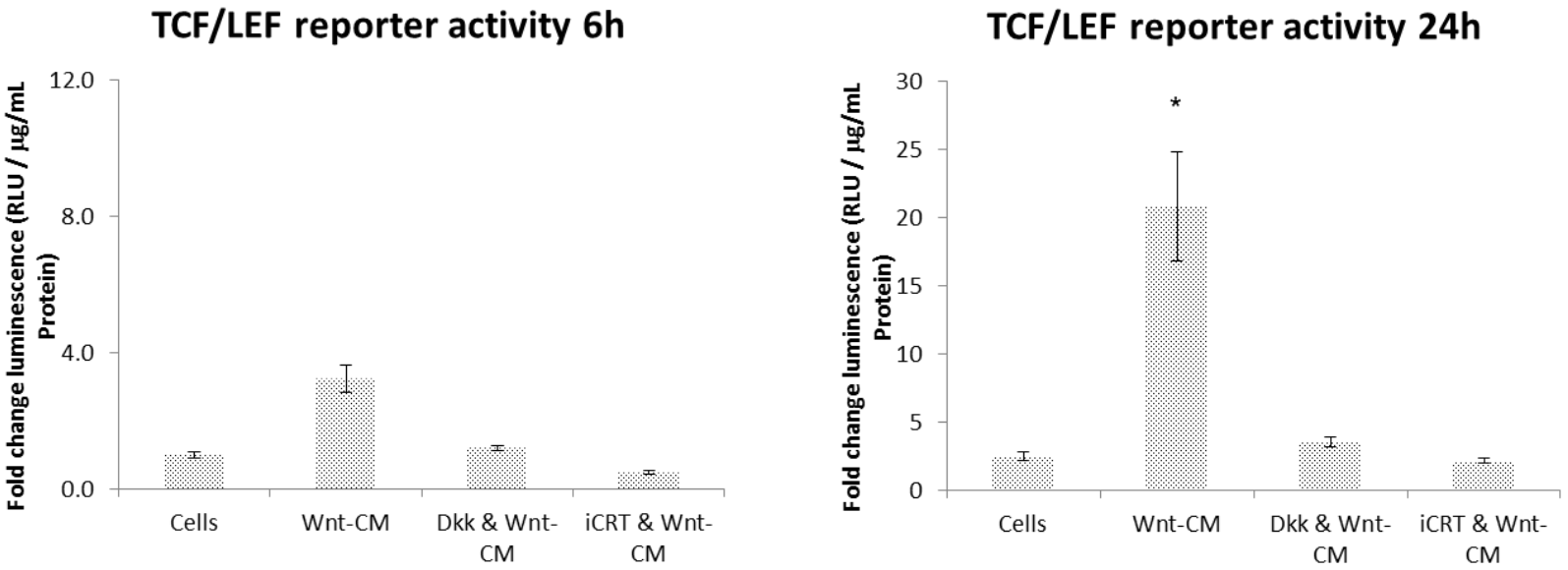

Figure 3.7. Wnt3a-CM activates a TCF/LEF reporter.
TCF/LEF reporter activity from transiently transfected hMSC 6h and 24h after treatment. Treatment of hMSC with Wnt3a-conditioned media (Wnt-CM) resulted in a 3 fold increase in luciferase reporter activity after 6h (A) which significantly increased to approximately 20 fold after 24h (B). Treatment with the Wnt blocker Dkk1, which blocks LRP co-receptor activation by Wnt, restricted reporter activity to basal levels over both time-points. Treatment with the Wnt blocker iCRT14, which blocks end-point Wnt activation by disrupting TCF/LEF binding, also restricted reporter activity to basal levels over both time-points. Values represent mean fold change in luciferase activity relative to cells only with luciferase activity normalised to total protein. Error bars represent SEM, n=4, * denotes $p<0.05$

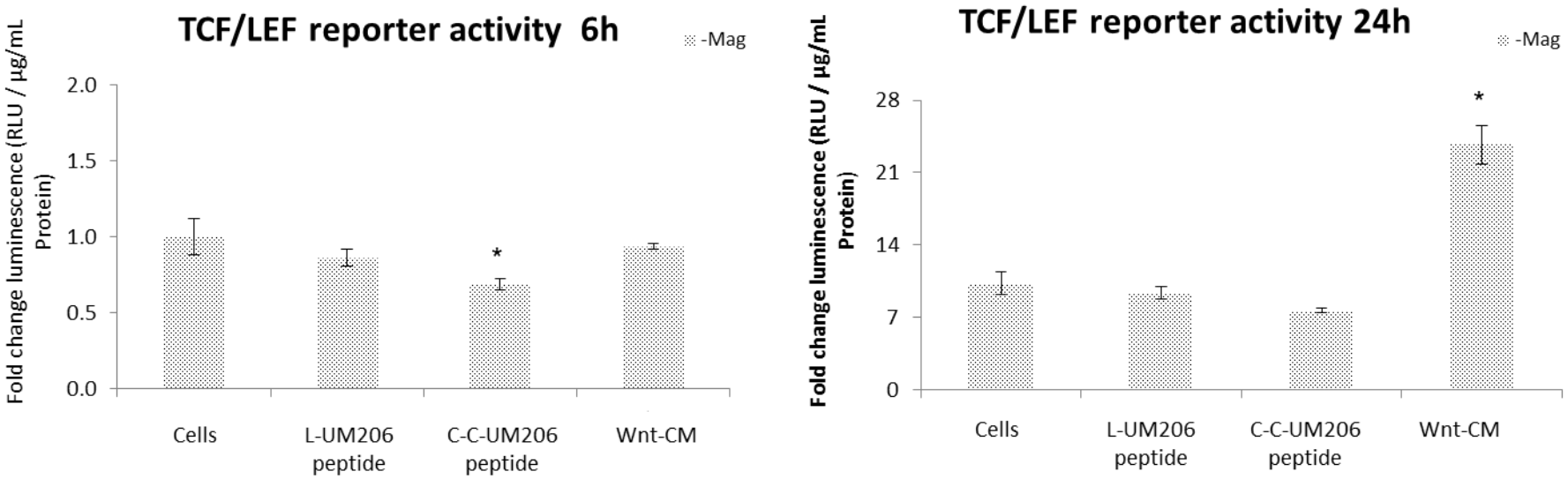

Figure 3.8. UM206 peptides alone do not activate a TCF/LEF reporter.
TCF/LEF reporter activity from transiently transfected hMSC 6h and 24h after treatment. Treatment with 1µg/mL L-UM206 peptide had no effect on reporter activity after 6h (A) or 24h (B). Treatment with 1µg/mL C-C-UM206 peptide reduced reporter activity after 6h (A) but no overall effect was observed after 24h (B). Treatment with Wnt-CM had no effect on reporter activity after 6h (A) but increased reporter activity after 24h (B). Values represent mean fold change in luciferase activity relative to cells only. Luciferase activity normalised to total protein. Error bars represent SEM, n=4, * denotes $p<0.05$.

3.3.3.3 Fz-MNP activate TCF/LEF signalling

Transfected hMSC showed a notable 3-fold increase (not statistically significant) in luciferase reporter activity 6h after treatment with MNP coated with antibodies targeted to Frizzled 2 (Fz-MNP) (Figure 3.9). A similar level of activity was observed when cells were treated with Wnt-conditioned media. An added 6-fold increase in reporter activity was observed when cells were treated with Fz-MNP with magnetic field. The increase in reporter activity by Fz-MNP (with or without magnetic field) was unaffected by the LRP co-receptor blocker Dkk1 but was reduced to basal levels when cells were treated with downstream Wnt blocker iCRT14 that disrupts TCF/LEF activity. After 24h, Fz-MNP treated cells showed a moderate increase in reporter activity (not significant) but a 17 fold increase in reporter activity (significant) was observed when magnetic field stimulation was applied in conjunction with Fz-MNP. A similar level of reporter activity was observed in the Wnt-CM control group after 24h. Treatment with Dkk1 again had no effect on Fz-MNP induced reporter activity which remained elevated but reporter activation was again successfully blocked using the downstream inhibitor iCRT-14 after 24h. Magnetic field treatment alone caused non-significant changes in reporter activity at both time-points.

3.3.3.4 L-UM206-MNP activate TCF/LEF signalling

Transfected hMSC showed a significant 4-fold increase in luciferase reporter activity at 6h after treatment with MNP coated with Linear UM206 peptides alone (L-UM206-MNP) (Figure 3.10). A similar level of activity was observed when cells were treated with Wnt-conditioned media. An added 8-fold increase in reporter activity was observed when cells were treated with L-UM206-MNP with magnetic field stimulation. The increase in reporter activity by L-UM206-MNP (with or without magnetic field) was unaffected by the LRP co-receptor blocker Dkk1 but was reduced to basal levels when cells were treated

with downstream Wnt blocker iCRT14 that disrupts TCF/LEF activity. At 24h, L-UM206-MNP treated groups showed a moderate increase in reporter activity (not statistically significant) but an added 20-fold increase in reporter activity (significant) was observed when magnetic field stimulation was also applied with L-UM206-MNP. A similar level of reporter activity was also observed in the Wnt-CM control group at 24h. Treatment with Dkk1 again had no effect on reporter activity at 24h when used in conjunction with L-UM206-MNP which remained elevated but reporter activation was again successfully blocked using the downstream inhibitor iCRT-14 after 24h. Magnetic field treatment alone caused minor increases in reporter activity (not significant).

3.3.3.5 C-C UM206-MNP do not activate TCF/LEF signalling

Treatment of transfected hMSC with MNP coated with the Cyclic UM206 peptide (C-C-UM206-MNP) had no effect on reporter activity after 6h and no effect was observed when cells were treated in conjunction with magnetic field stimulation (Figure 3.11). After 24h, C-C-UM206-MNP marginally increased reporter activity (not significant) but again no effect was observed when used in conjunction with magnetic field treatment. In contrast Wnt-CM significantly increased reporter activity after 24h treatment.

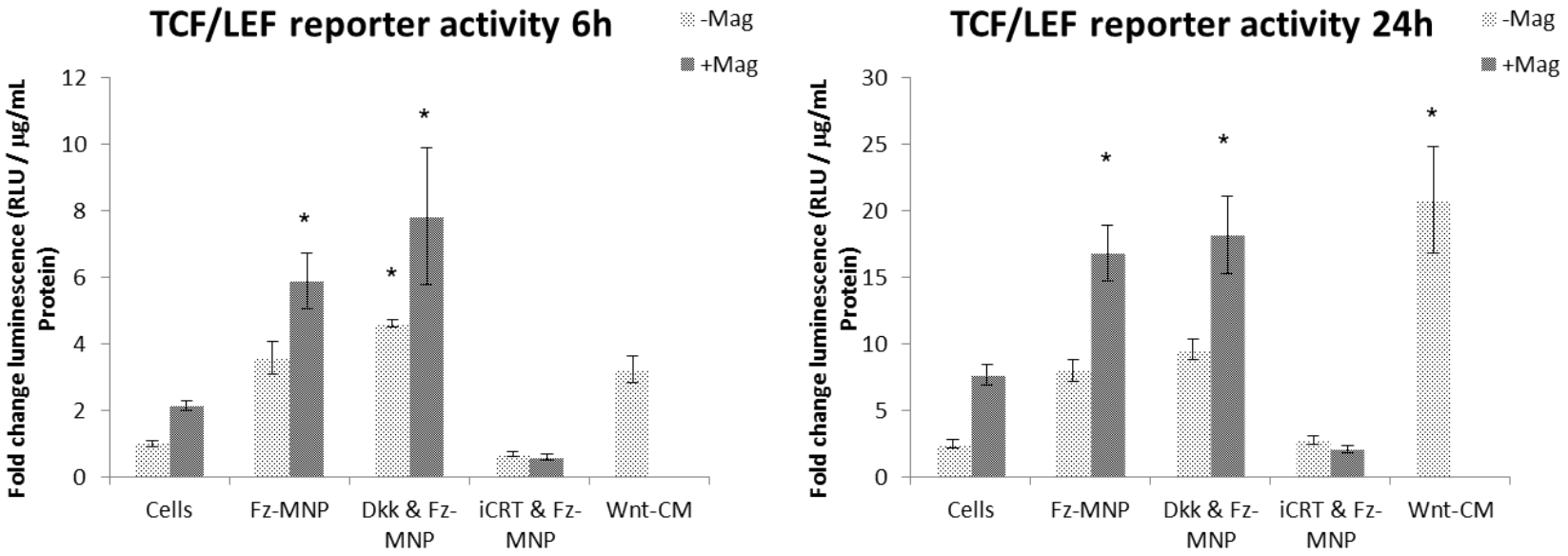

Figure 3.9. Anti-Fz MNP activate a Wnt TCF/LEF reporter.

TCF/LEF reporter activity from transiently transfected hMSC 6h and 24h after treatment. Magnetic field alone (Cells + Mag) increased reporter activity at both time points (not significant) (A,B). Treatment with anti-Frizzled MNP (Fz-MNP) alone caused a 3 fold increase in reporter activity after 6h (A) and remained elevated after 24h (B) (not statistically significant). An added significant 6 fold increase in reporter activity was observed after 6h when magnetic field with Fz-MNP treatment was applied (A) with reporter activity remaining high after 24h (B). Addition of the Wnt signalling blocker Dkk1 which inhibits LRP5/6 activation failed to prevent reporter activation by Fz-MNP. However activation was successfully blocked using iCRT14, a downstream inhibitor which blocks TCF/LEF activity. Treatment with Wnt-Conditioned Media (Wnt-CM) increased reporter activity to a similar level as Fz-MNP alone after 6h (A), with maximum activity observed after 24h (B). This effect was successfully blocked using Dkk1 or iCRT14 with reporter activity being reduced to basal levels. Values represent mean fold change in luciferase activity relative to cells only. Luciferase activity was normalised to total protein. Error bars represent SEM, n=4 , * denotes $p<0.05$

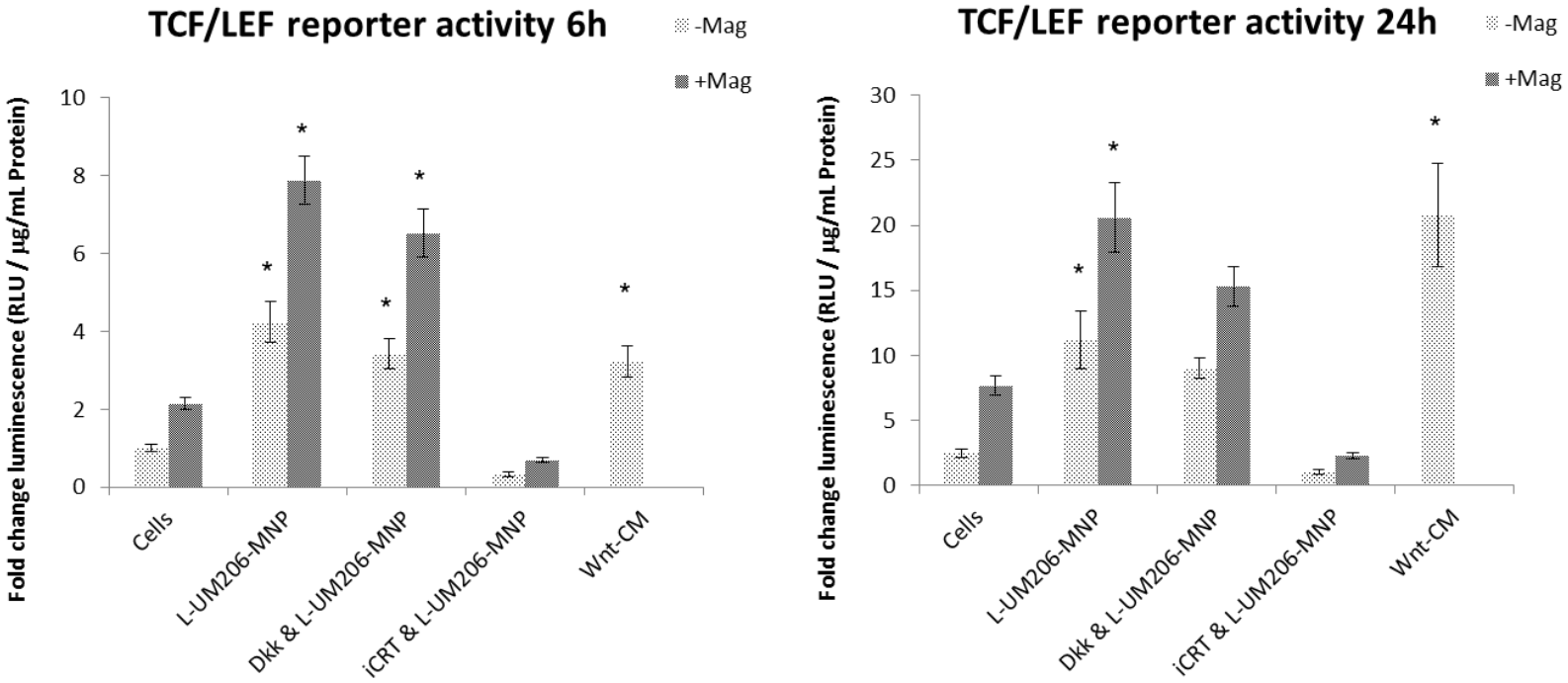

Figure 3.10. L-UM206-MNP activate a TCF/LEF reporter.

TCF/LEF reporter activity from transiently transfected hMSC 6h and 24h after treatment. Treatment with L-UM206-MNP alone significantly increased reporter activity by 4 fold after 6h (A) and remained elevated after 24h (B). An added significant 8 fold increase in reporter activity was observed after 6h when magnetic field with L-UM206-MNP was applied (A) with reporter activity remaining elevated after 24h (B). L-UM206-MNP mediated reporter activation was unaffected by the LRP5/6 blocker Dkk1 but was successfully blocked using the downstream Wnt pathway inhibitor iCRT14 at both time-points. Treatment with Wnt-conditioned media (Wnt-CM) increased reporter activity to similar levels as L-UM206-MNP alone at 6h(A) with maximum activity observed after 24h (B). Treatment with magnetic field alone marginally increased Wnt reporter activity at both time-points (not significant). Values represent mean fold change in luciferase activity relative to cells only. Luciferase activity normalised to total protein. Error bars represent SEM, n=4, * denotes $p<0.05$.

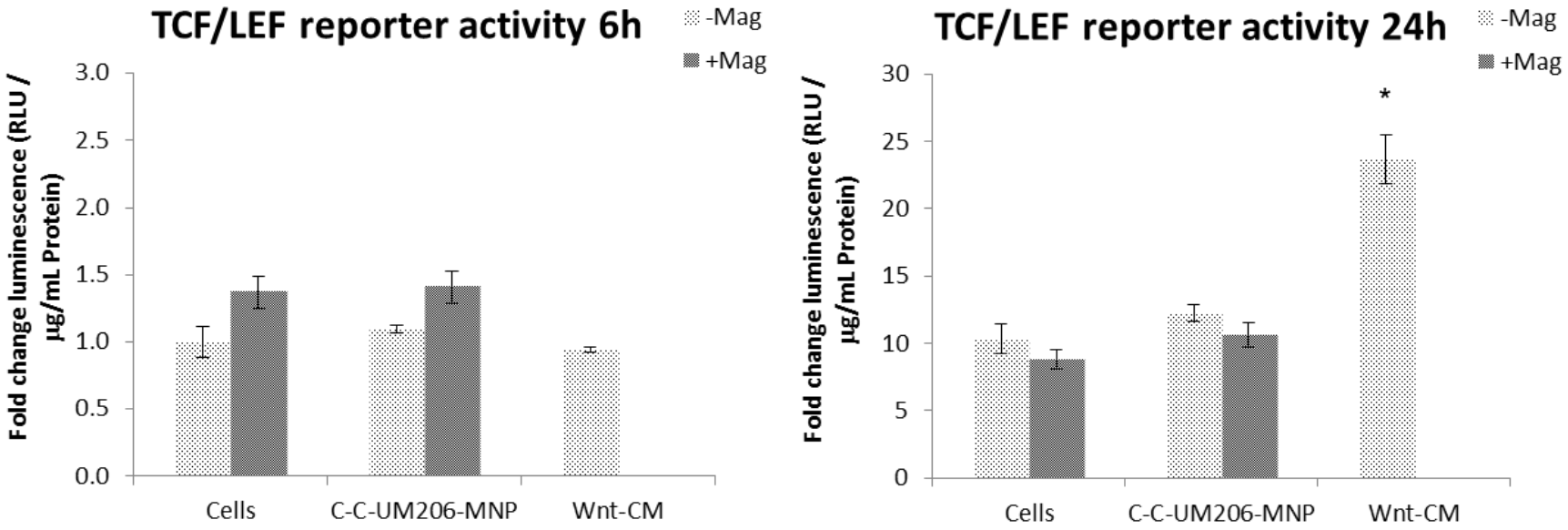

Figure 3.11. C-C-UM206-MNP do not activate a TCF/LEF reporter

TCF/LEF reporter activity from transiently transfected hMSC 6h and 24h after treatment .Treatment with C-C-UM206 MNP had no overall effect on reporter activity compared to controls over both-time-points and no overall effects on were observed with magnetic field treatment. Values represent mean fold change in luciferase activity relative to cells only with luciferase activity normalised to total protein. Error bars represent SEM, n=4, * denotes $p<0.05$

3.3.3.6 Control MNP have no effects on TCF/LEF reporter activity

Treatment of transfected hMSC with control MNP which were coated with generic IgG antibodies (IgG-MNP) or RGD tri-peptide (RGD-MNP) had no overall effect on reporter activity 6h or 24h after treatment (Figure 3.12). Furthermore no added effects on reporter activity were observed when cells were treated with either of the control MNP with the addition of magnetic field stimulation 6h or 24h after treatment.

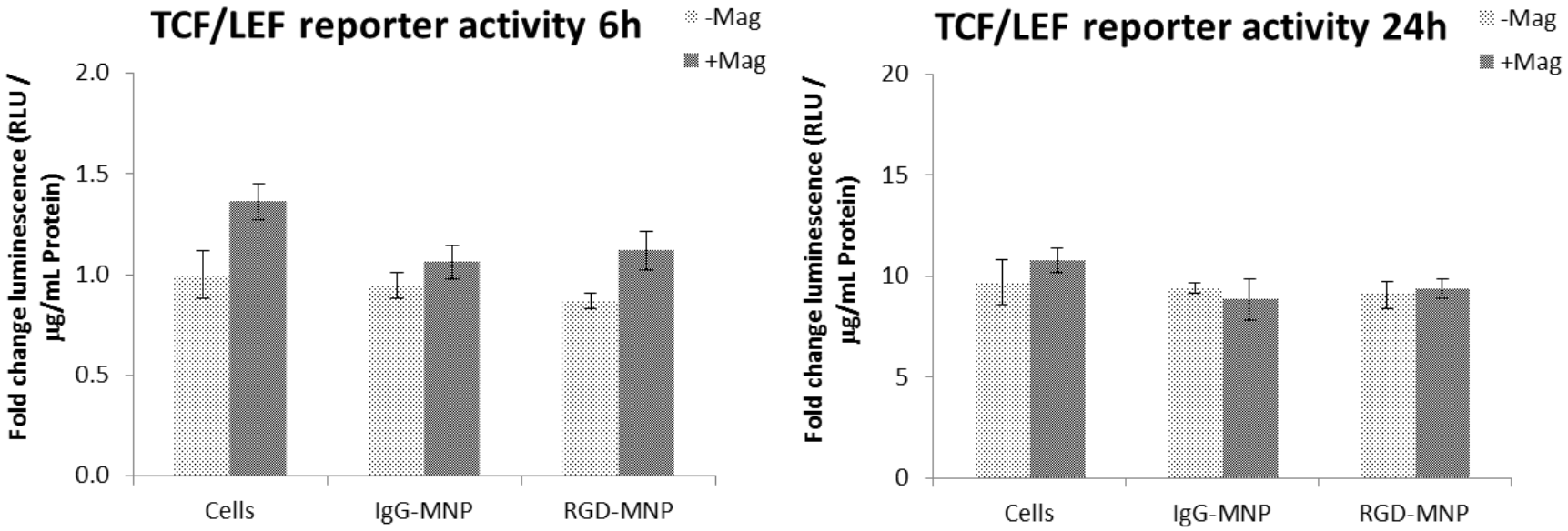

Figure 3.12. Control MNP have no effect on TCF/LEF reporter activity.
TCF/LEF reporter activity from transiently transfected hMSC 6h and 24h after treatment. Magnetic field alone caused minor increases in reporter activity at both time points (not significant) (A,B). Treatment with Control particles coated with either anti-Rabbit-IgG (IgG-MNP) or RGD peptide (RGD-MNP) caused no increase in reporter activity at 6h (C) or 24h (D) and no added effects were observed when with the addition of magnetic field stimulation. Values represent mean fold change in luciferase activity relative to cells only. Luciferase activity was normalised to total protein. Error bars represent SEM, n=4.

3.3.4 Fz-MNP and L-UM206-MNP signal through an LRP5/6 independent mechanism

Western blotting was used to elucidate the mechanism of Wnt signalling activation by Fz-MNP and L-UM206-MNP. This was assessed by probing for the active (phosphorylated) forms of the Wnt co-receptor Low density lipoprotein (LDL) receptor-related protein 5 and 6 (LRP5/6) which is an indicator of co-receptor activation (Figure 3.13). Untreated cells showed a low basal level of LRP6 phosphorylation as did treatment with Fz-MNP or L-UM206-MNP. Whereas treatment with Wnt conditioned media resulted in a clear increase in LRP6 phosphorylation which was mostly blocked with the addition of the LRP6 inhibitor Dickkopf 1 (Dkk1). In the case of LRP5, non-treated cells displayed a clear basal level of phosphorylation and this was shown to be unaffected by either Fz-MNP, L-UM206-MNP or Wnt-CM. Treatment with Dkk with Wnt-CM did result in a marginal decrease in LRP5 phosphorylation. GAPDH was used as a loading control.

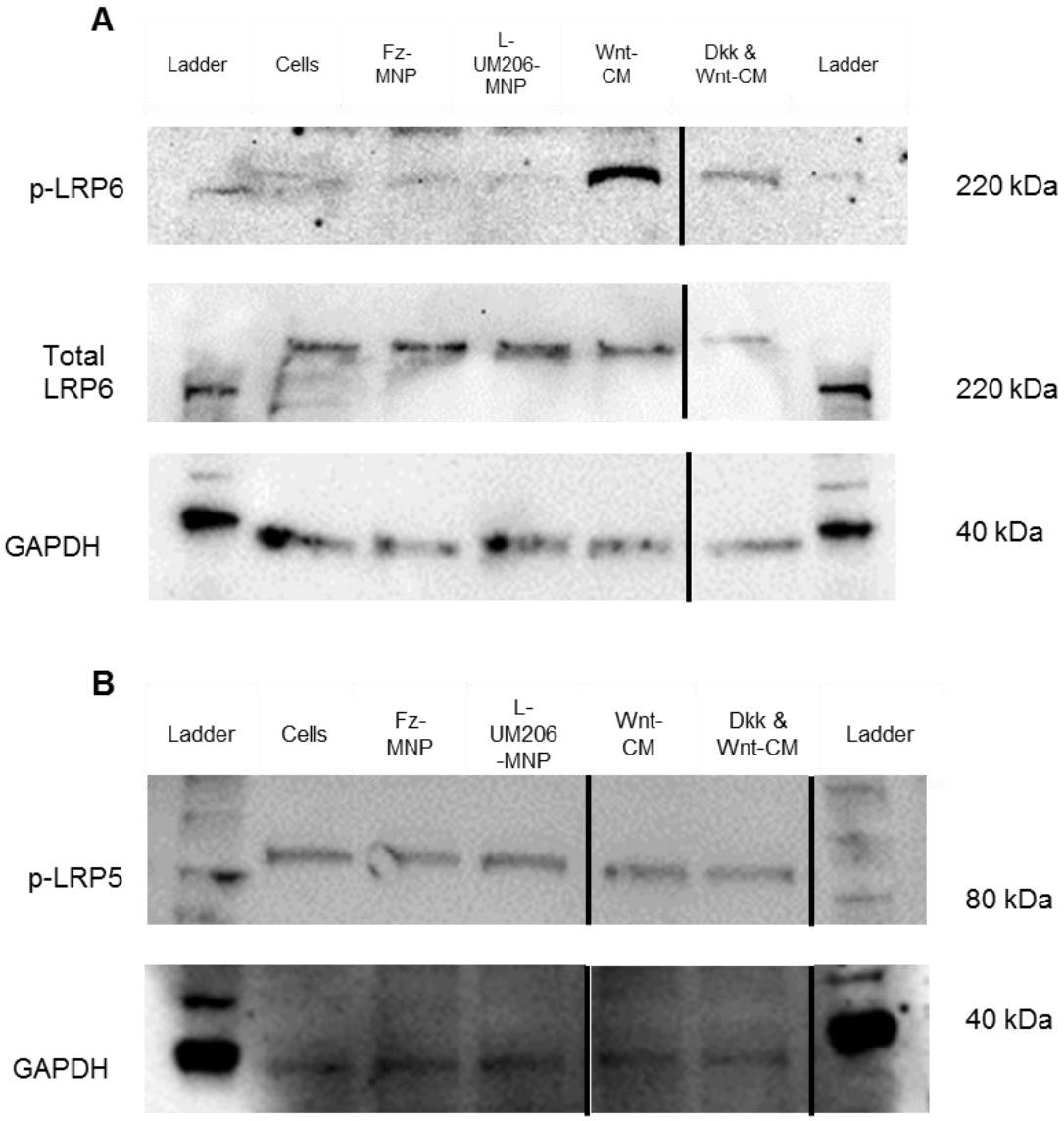

Figure 3.13. MNP signal through an LRP-independent mechanism.
(A) Non-treated cells displayed negligible LRP6 phosphorylation. Treatment of hMSC with anti-Frizzled-MNP (Fz-MNP) or L-UM206-MNP had no effect on LRP6 co-receptor phosphorylation. In contrast Wnt conditioned media (Wnt-CM) caused clear LRP6 phosphorylation which was blocked using the Wnt inhibitor Dkk 1. (B) Non-treated cells displayed a basal level of Wnt co-receptor LRP5 phosphorylation (B). Treatment of hMSC with Fz-MNP, L-UM206-MNP or Wnt conditioned media (Wnt-CM) all had no overall effect LRP5 phosphorylation levels. Treatment with Dkk and Wnt-CM marginally decreased LRP5 phosphorylation. Black lines denote none adjacent lanes. GAPDH and total LRP6 are shown as loading controls.

3.3.5 Fz-MNP alter stress response gene expression

Gene expression analysis for stress response genes c-Myc, Cox2 and NF-κβ was also examined over early time-points. These investigations were performed to determine the levels of mechano-stimulatory response of cells to Fz-MNP and Wnt-3a. The stress gene response to Fz-MNP was compared to control particles anti-TREK1-MNP (Trek-MNP) which are known to induce a cellular mechanical stress response (Figure 3.14). As predicted, treatment with control particles Trek-MNP caused a significant up-regulation in NF-κβ expression after 1h followed by a down-regulation in expression after 3h when compared to cells + magnet control groups. All other groups showed small but not significant levels of elevation at 1 and 3 hours compared to the TREK labelled response to magnetic field.

Investigations of responses in two other early response genes c-Myc and Cox2 showed low level variations in expression but none to the same extent as the NF-κβ response observed to TREK coated particles with oscillating magnetic field. Small elevations in c-Myc expression was observed in all groups at 1 hour which fell by 3 hours with the most significant again observed in the TREK activated magnetic particle group. Similar levels of elevation were observed in Wnt3A activation as with particles alone, particles with magnetic field and magnetic field alone.

A similar low level pattern of response was observed in the expression of Cox2. Again small elevations in Cox2 were observed in all groups after 1 hour which fell after 3 hours with the greatest variation seen to magnetic field alone and magnetic field with Fz-MNP. No significant difference was observed between experimental groups at one hour after treatment.

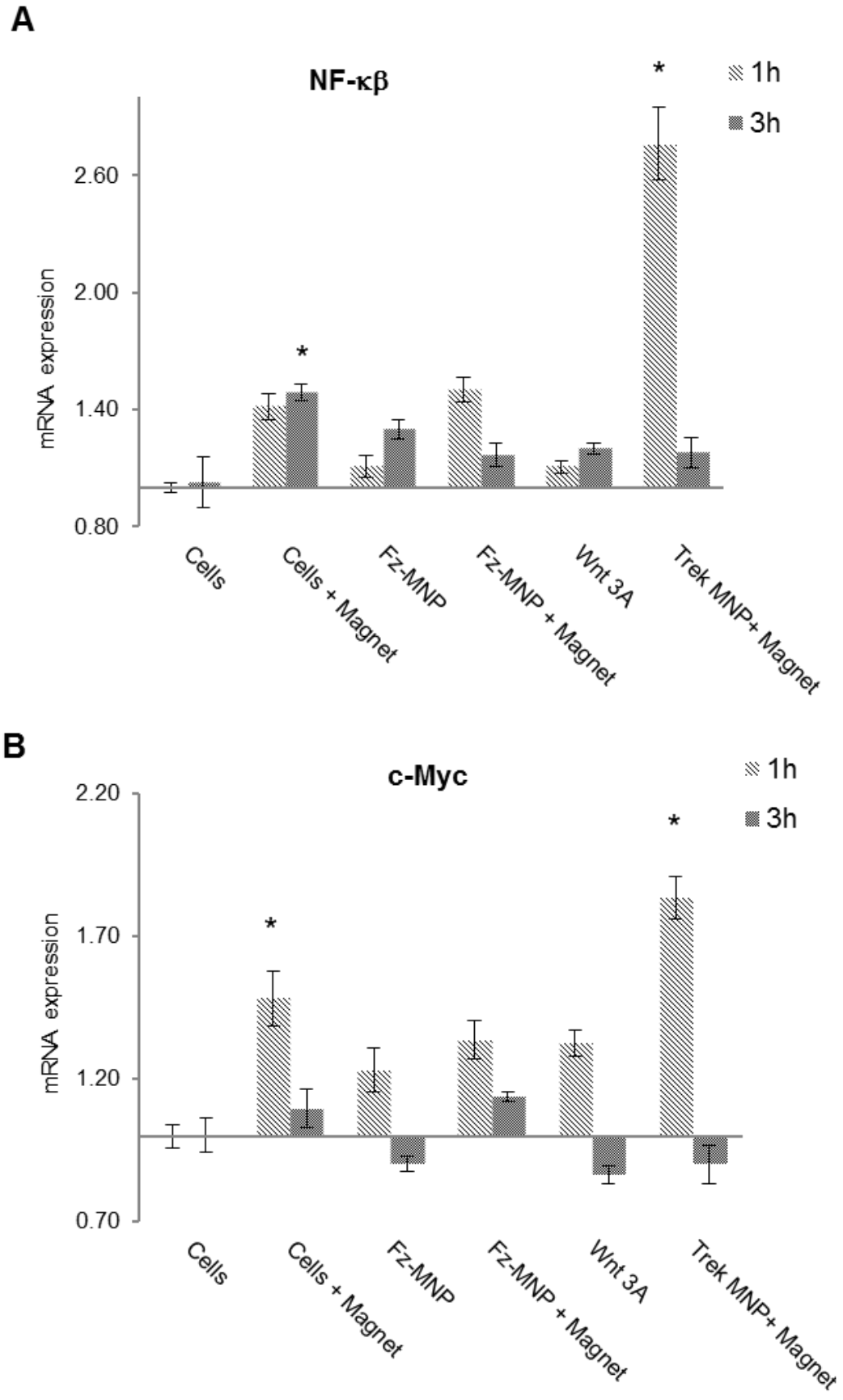
A
NF-κβ
1h
3h
mRNA expression
2.60
2.00
1.40
0.80
*
*
Cells
Cells + Magnet
Fz-MNP
Fz-MNP + Magnet
Wnt 3A
Trek MNP+ Magnet
B
c-Myc
1h
3h
mRNA expression
2.20
1.70
1.20
0.70
*
*
Cells
Cells + Magnet
Fz-MNP
Fz-MNP + Magnet
Wnt 3A
Trek MNP+ Magnet

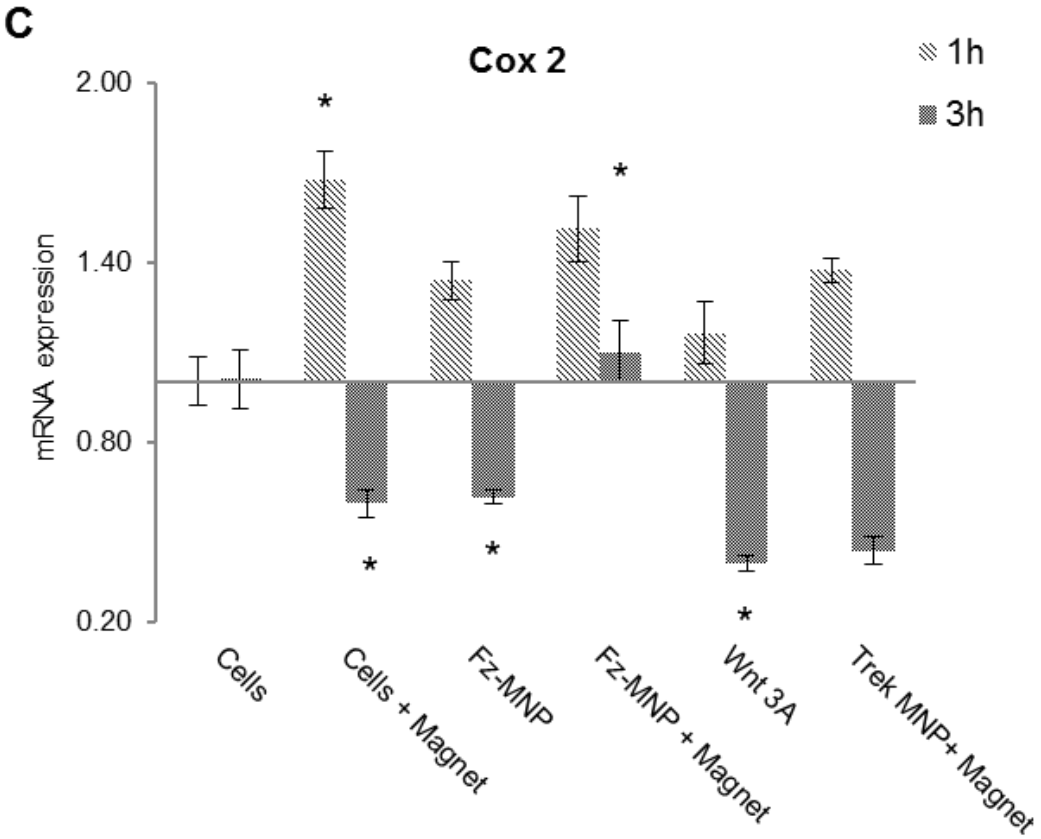

Figure 3.14. Fz-MNP alter expression of mechanosensitive genes.
Gene expression analysis of mechano responsive genes (Nf-κβ, c-Myc, Cox 2) in response to anti-frizzled particles (Fz-MNP) or control particles (Trek-MNP) and magnetic field stimulation was evaluated using quantitative real-time PCR after 1h and 3h treatment. NF-κβ gene expression (A) was increased by Trek-MNP (compared to cells + magnet control) after 1h. Magnetic field treatment alone also increased Nf-κβ expression (compared to cells only control) after 3h. Treatment with Fz-MNP or Wnt 3A both showed similar but minor shifts in Nf-κβ gene expression. Expression of c-Myc (B) was increased after 1h treatment with magnetic field alone (cells + magnet) with an added increase when used in conjunction with Trek-MNP. Treatment with Fz-MNP or Wnt 3A again both showed similar but negligible shifts in c-Myc expression. Expression of COX 2 (C) was shown to be significantly increased after 1hr by magnetic field treatment alone but a decrease in expression was observed after 3h. Treatment with Fz-MNP (without magnet) or Wnt 3A both caused significant decreases in COX 2 expression after 3h treatment. Treatment with Fz-MNP (with magnet) was shown to significantly increase COX 2 expression when compared to Cells + magnet control after 3h. Figures show mean fold change in gene expression normalised to GAPDH, Error bars represent SEM, n=4, ANOVA $p < 0.05$ for all genes, * denotes $p < 0.05$

3.4 Discussion

Wnt signalling is a crucial pathway controlling stem cell behaviour and has become an attractive target for modulation with potential applications in stem cell therapies. The results in this chapter have demonstrated the feasibility of using antibody and small peptide functionalised magnetic nanoparticles to specifically target and stimulate Frizzled 2 receptors expressed by hMSC for the activation of Wnt / β-catenin signalling pathways.

3.4.1 Frizzled 2 expression in hMSC

Expression of Frizzled 2 in hMSC was confirmed at the gene and protein level by RT-PCR and Western blotting respectively. Frizzled 2 was shown to be stably expressed over 21 days in either basal or osteogenic media. This agrees with previous work which has also shown that Frizzled 2 is expressed in hMSC (Etheridge et al., 2004), (Okoye et al., 2008).

3.4.2 Effects of MNP on β-catenin mobilisation

To determine if magnetic oscillation of Fz-MNP, L-UM206-MNP or C-C-UM206 were capable of causing downstream Wnt signalling activation, β-catenin mobilisation in response to MNP treatment was studied. It was shown that Fz-MNP and L-UM206-MNP but not C-C-UM206-MNP were capable of activating β-catenin mobilisation to the nucleus. Furthermore, oscillation of Fz-MNP or L-UM206-MNP in magnetic fields also led to increased β-catenin nuclear mobilisation. β-catenin mobilisation to the nucleus is a hallmark of active Wnt β-catenin signalling and a precursor to transcription of Wnt responsive genes. This phenomenon is frequently used as a qualitative indicator of active Wnt signalling (Ehrlich et al., 2010) (Cong et al., 2003). These results suggest that the binding action of Fz-MNP or L-UM206-MNP to Frizzled receptors is enough to initialise Wnt signalling and cause mobilisation of β-catenin. Furthermore, magnetic field

stimulation of MNP labelled cells caused a further increase in β-catenin mobilisation and nuclear localisation. This suggests that there is an enhanced mechanoactivation of Frizzled receptors caused by torque of the functionalised MNP in the magnetic field. Cells treated with Wnt-CM also showed noticeable nuclear localisation after 24h which was again significant over the non-treated control according to pixel intensity analysis of the nuclear β-catenin staining. These observations agree with the findings of other groups who have showed that treatment with Wnt causes β-catenin mobilisation after 24h (Carthy et al., 2011), (Staal et al., 2002). A low level of background mobilisation of β-catenin was also observed in control groups suggesting basal levels of Wnt signalling are present in MSC, this is in agreement with Liu et al 2009 who also showed MSC express endogenous Wnt signalling activity (Liu et al., 2009).

3.4.3 Effects of MNP on TCF/LEF reporter activity

The critical downstream pathway of Wnt signalling has been shown to be transcriptional activation of TCF/LEF responsive genes (Schuijers et al., 2014, Nusse, 1999). In this work it was shown that treatment with Wnt-CM results in an elevation of the TCF/LEF reporter constructs in transiently transfected hMSC. Furthermore it was demonstrated that mechanical activation via Fz-MNP or L-UM206-MNP (but not C-C-UM206-MNP) resulted in similar levels of activation of the downstream reporter. This observation confirms that Fz-MNP and L-UM206-MNP activate Wnt-responsive elements after a short time period and have similar effects as Wnt-CM on pathway activity. The increase in Wnt luciferase reporter activity by Wnt-CM was potently blocked using the Wnt LRP5/6 co-receptor blocker Dkk1; this can be expected as signalling activation by Wnt protein requires LRP co-activation. However, in these experiments Dkk1 had no effect on the blocking of reporter activity (at both time-points) when cells were activated through the oscillating

Fz-MNP or L-UM206-MNP. This suggests that functionalised MNP are signalling through an LRP independent mechanism. This result is in agreement with the Western blotting data which showed no noticeable increase in LRP5/6 phosphorylation after treatment with Fz-MNP or L-UM206-MNP which would indicate receptor activation. This again suggests an alternative mode of Wnt/β-catenin activation by functionalised MNP which warrants further investigation. At 24h Fz-MNP and L-UM206-MNP treated groups remained elevated. This is further evidence of a level of mechanoactivation of Wnt signalling and demonstrates that functionalised MNP are capable of causing sustained Wnt pathway activation. Treatment with Wnt-CM also significantly activated reporter activity to comparable levels as the functionalised MNP (with magnet). Taken together, this would suggest that a lag phase or threshold exists after stimulation with Wnt-CM that must be overcome before Wnt signalling activity peaks. This observation is again in agreement with results from Carthy *et al* who showed activation of a Wnt TCF reporter after 24h treatment with recombinant Wnt 3A (Carthy et al., 2011). Although Dkk1 was unable to block Wnt pathway activation by functionalised MNP, reporter activation by Fz-MNP, L-UM206-MNP and Wnt-CM was successfully blocked using a downstream Wnt signalling blocker- iCRT-14, which acts by disrupting β-catenin's association and interaction with TCF transcription factors which is required for the expression of Wnt target genes.

3.4.4 Contrasting effects of Linear and Cyclic UM206

Interestingly, in these experiments MNP coated with C-C-UM206 peptides had no effect on reporter activity. These data also agree with the β-catenin mobilisation data which indicated a negligible effect of C-C-UM206-MNP on β-catenin mobilisation. These observations suggest that C-C-UM206-MNP may not bind to Frizzled 2 receptors with

sufficient affinity to activate downstream signalling. Also, L-UM206 or C-C UM206 peptides alone were found to have no activating effects on reporter activity despite a comparatively high peptide dose of 1µg/mL. In fact cyclic UM206 (C-C-UM206) was actually found to have a mild but significant inhibitory effect on reporter activity after 6h treatment. These findings are in contrast with Blankesteijn *et al* who observed clear agonistic and antagonistic activities of C-C UM206 and L-UM206 respectively at a dose of 1µg/mL in HEK293 cells (Blankesteijn Wessel Matthijs, 2010). In that study HEK293 cells were engineered to over-express Frizzled 2. It is therefore possible that the stoichiometry of the interaction between UM206 peptide binding and frizzled receptors is different between these systems which may alter pathway responsiveness to peptide stimulation. Another possibility is that the signalling kinetics between MSC and HEK293 or HEK293 over-expressing Frizzled 2 are inherently different which may result in different outcomes in Wnt pathway activation between these cell types.

3.4.5 Control MNP do not activate Wnt/β-catenin signalling

Finally, Control MNP coated with IgG antibodies or the tri-peptide RGD were also used to assess the effects of generic and integrin mediated membrane stimulation on Wnt pathway activation. In these experiments both control MNP types were found to have no activating effects on either β-catenin mobilisation or Wnt reporter activity over 24h. This indicates that generic or Integrin mediated mechano-stimulation is not enough to activate Wnt signalling in hMSC at the magnitude of forces applied in these experiments.

3.4.6 Effects of MNP on LRP co-receptor activation

The mechanism of Wnt signalling by MNP was also investigated. Treatment of hMSC with the Wnt pathway activating particles (Fz-MNP or L-UM206-MNP) resulted in no

noticeable changes in LRP5/6 phosphorylation. This indicates that these MNP are not activating and signalling through LRP co-receptors. The canonical Wnt signalling co-receptor Low density lipoprotein (LDL) receptor-related protein 5/6 (LRP5/6) forms an active signalling complex with Frizzled and a Wnt ligand (Brown et al., 1998). Upon receptor activation, LRP is successively phosphorylated at multiple sites by kinases such as GSK. This process is part of downstream Wnt signal transduction which occurs through Axin (Zeng et al., 2005). Phosphorylation of LRP in response to Wnt 3A has been shown previously (Grumolato et al., 2010). In contrast Wnt conditioned media resulted in clear phosphorylation of LRP6 after 3h which was partially blocked with the addition of the LRP6 inhibitor Dickkopf 1 (Dkk1). In the case of LRP5 co-receptor signalling, a basal level of LRP5 phosphorylation in untreated cells was observed which was not altered by Fz-MNP, L-UM206-MNP or indeed Wnt-CM. This suggests that LRP5 is not the main co-receptor for transduction of Wnt signals in hMSC. This is in agreement with Perobner et al. who showed that LRP6 is indispensable for canonical Wnt signalling in hMSC and not LRP5 (Perobner et al., 2012). Altogether, this suggests that Fz-MNP and L-UM206-MNP are activating Wnt signalling via a different mechanism to Wnt protein. One explanation for this observation could be receptor clustering and dimerization of Frizzled receptors caused by functionalised MNP which results in pathway activation. This mechanism has been shown to be an alternative route for Frizzled receptor activation by Carron *et al*. who showed that dimerization of Frizzled receptors is enough to activate Wnt/β-catenin signalling (Carron et al., 2003). LRP independent signalling has also been shown to be involved with increased murine osteoblast proliferation in response to strain *in vitro* (Javaheri et al., 2012). Further work could involve the investigation of the

phosphorylation and activation status of LRP6 after targeting and stimulation with anti-LRP6 functionalised MNP to determine if this also leads to Wnt signalling activation.

3.4.7 Effects of MNP on Stress response gene expression

Finally, gene expression analysis for stress response genes previously shown to respond to generic mechano-stimulation at early time-points were investigated. C-Myc is an oncogene associated with stress response; it has also been identified as a Wnt responsive gene (He et al., 1998). Overall low levels of up-regulation in all groups were observed after one hour of treatment and both Fz-MNP treatment (with or without magnetic field) and Wnt 3a treatment all up-regulate c-Myc expression after 1h to similar levels. This is comparable to results from Gujral *et al* who showed that c-Myc expression increases in the first 3h after Wnt stimulation in HEK293 cells (Gujral and MacBeath, 2010). Furthermore, in this experiment the expression profile of Fz-MNP matches the expression profile produced by Wnt 3a closely, whereas treatment with control particles targeted to the Trek-1 ion channel (Trek-MNP) produced a broadly different expression profile to Wnt3A and Fz-MNP with Magnet (at 1h time-points). This is an indication that the Fz-MNP and Wnt 3a are having a similar effect on c-Myc gene expression. COX2 expression has also been shown to increase in response to cytotoxic stress e.g. cytokines, endotoxins, γ-radiation (Feng et al., 1995) (Steinauer et al., 2000). Recent evidence has also shown that the COX-2 promoter harbours TCF/LEF response elements and that activation of canonical Wnt signalling by lithium or Wnt 3A results in increased COX2 mRNA expression (Nuñez et al., 2011). The results again showed low levels of expression elevation at 1 hour in all experimental groups without a clear expression pattern emerging. However, once again Fz-MNP alone and Wnt3a both induced a similar expression pattern whilst Fz-MNP with magnet and Trek induced different levels of Cox2 expression, particularly after 3h. In

contrast, investigation of the levels of NF-κβ show a clear elevation in response to the control group labelled with TREK particles. NF-κβ is a stress response gene activated when cells are subjected to physiological stresses e.g. mechanical stimulation (Mercurio and Manning, 1999), (Kumar and Boriek, 2003). The expression profile of NF-κβ is similar when cells are treated with either Wnt 3A or Fz-MNP without magnet with these treatments causing slight increases in NF-κβ expression (trend only). In contrast, treatment with control particles (Trek-MNP) caused a significant up-regulation in NF-κβ expression after 1h when compared to cells plus magnet control group. This again demonstrates the differing outcomes when cells are treated with either Fz-MNP or Trek-MNP. Although Fz-MNP had no clear effects on stress-response gene expression over the early time-points studied here, expression of other stress response genes in response to other MNP types should be investigated over later time-points in order to reveal any longer term effects of MNP stimulation on gene expression.

3.5 Conclusions

Wnt signalling pathways are important for the regulation of cell behaviour and there is increasing interest in the development of modulators of Wnt signalling. These modulation tools may have therapeutic potential in fields such as stem cell science, development, cell and tissue engineering and cancer. One way of controlling cell signalling is by using bio-functionalised MNP. To date no one has attempted to locally target and stimulate Wnt receptors in order to modulate Wnt signalling. The work presented in this chapter has shown that it is possible to tag Frizzled receptors expressed by hMSC with antibody or peptide-functionalised nanoparticles and use an oscillating magnetic field to impart

focused mechanical stimulation onto the receptors to enhance receptor signalling. This strategy has enabled unconventional, co-receptor independent activation of Wnt signalling pathways in hMSC. By initialising Wnt-Frizzled signalling in a co-receptor independent manner, functionalised-MNP can override many of the top-level inhibitors of Wnt signalling. Furthermore, it has been shown that the magnetic activation process can be enhanced or reduced by operating an external magnetic switch, which affords a degree of external control and temporal regulation of Wnt pathway activation. In these experiments Immunofluorescence showed clear mobilisation of the Wnt signalling messenger β-catenin and activation of a Wnt signalling reporter construct was also observed in response to Fz-MNP and L-UM206-MNP. Gene expression analysis also showed different expression of stress response genes in response to Fz-MNP and Wnt compared to treatment with control MNP. Taken together, these results suggest that Fz-MNP and L-UM206-MNP are acting via different mechanisms to Wnt protein to activate Wnt β-catenin signalling. The mechanism behind Wnt signalling activation by functionalised MNP may include receptor clustering or alternative co-receptor recruitment and requires further investigation. Furthermore, the effects on hMSC fate and applications in tissue engineering should also be studied. Finally, the remote stimulation of other Frizzled receptors and co-receptors for the modulation of Wnt pathways using MNP technology should be investigated. The development of this technology raises the possibility of remotely controlling Wnt signalling and consequently the control of stem cell behaviour for therapeutic purposes.

Chapter 4: Remote control of hMSC differentiation using MNP

4.1 Introduction

Human mesenchymal stem cells (hMSC) are a promising cell source for autologous cellular therapies, particularly for orthopaedic tissue engineering (Oreffo et al., 2005), (Ling et al., 2009). The differentiation of hMSC into osteoblasts results from an array of signalling cascades which are triggered by growth factors including Wnts and Bone Morphogenetic Proteins (BMPs, as well as environmental conditions such as physical stimuli. These signalling networks interact with each other and form feedback loops to regulate cell differentiation (Augello and De Bari, 2010), (James, 2013). The Wnt pathway is known to be a pivotal regulator of hMSC fate and hMSC have been shown to express a range of Wnt proteins and receptors (Etheridge et al., 2004). Some researchers have suggested that Wnt signalling acts as a master regulator of osteoblast differentiation (Milat and Ng, 2009). The modulation of the Wnt pathway in hMSC could therefore be beneficial in bone tissue engineering.

Wnt signalling pathways have a multitude of effects on cell behaviour including changes to polarity, proliferation and differentiation. These effects are shown to be highly dependent on cell type and Wnt protein concentration (Rao and Kuhl, 2010), (Quarto et al., 2010), (de Boer et al., 2004a). Activation of canonical signalling by Wnt3A has been shown to promote hMSC proliferation, preserve multipotency and inhibit differentiation (De Boer et al., 2004b), (Boland et al., 2004), (Cho et al., 2006). However, in calvarial osteoblasts Wnt3A has been shown to promote bone formation (Quarto et al., 2010). *In vitro*, both overexpression of the canonical Wnt co-receptor LRP6 and stabilised active β-catenin have been shown to promote osteogenic differentiation of hMSC (De Boer et al., 2004b), (Gong et al., 2001), (Qiu et al., 2007). *In vivo*, Wnt 3A has been shown to enhance

the proliferation and differentiation of skeletal progenitor cells causing accelerated bone repair in sensitised (Axin2 knockout) mice (Minear et al., 2010).

Despite the significant role of Wnt in directing tissue formation, its *in vivo* use for bone repair has so far been limited as a consequence of the complicated and costly production methods required to produce pharmacological quantities of bioactive protein (Gothard et al., 2014), (Coudreuse and Korswagen, 2007). In addition, the multiple Wnt ligands have varying biological potencies which complicate standardised dosing. Therefore, there is considerable interest in developing synthetic Wnt analogues in order to pharmacologically regulate Wnt signalling pathways in hMSC for therapeutic use. The synthetic peptide UM206, introduced in chapter 3, is a specific ligand for Frizzled 2 receptors whose signalling activity is conformational dependent (Blankesteijn Wessel Matthijs, 2010). In chapter 3 the efficacy of remotely activating Wnt signalling using anti-Frizzled 2 antibodies (Fz-MNP) or linear UM206 (L-UM206) peptide coated MNP targeted against Frizzled receptors was demonstrated. Due to supplier issues that limited availability of the anti-Frizzled 2 antibody, UM206 was taken forward and used as the Frizzled 2 targeting strategy for MNP in these experiments.

The aims of this chapter were to investigate the potential of the UM206-mediated magnetic Wnt pathway activation approach for the regulation of osteogenesis and bone formation. This approach was first assessed *in vitro* by investigating the osteogenic response of hMSC in monolayer to both Linear and Cyclic UM206-MNP respectively. Secondly, the potential *in vivo* aspects of this magnetic activation approach were evaluated using an *ex vivo* foetal chick femur model of bone development adopted by Smith et al. (Smith et al., 2013), (Smith et al., 2014a), (Smith et al., 2014b). Using this

model, microinjection of hMSCs pre-labelled with UM206-MNP into organotypically cultured chick femurs was demonstrated.

4.2 Methods

4.2.1 Cell culture

hMSC were sourced and processed as detailed in chapter 2. Cells were expanded in basal media (high glucose DMEM, 10% FBS, 1% L-glutamine and 1% penicillin/streptomycin) (Lonza) with media changes performed twice per week. Osteogenic media consisted of basal media supplemented with 0.2mM Ascorbic acid, 10mM sodium β-glycerophosphate and 0.1µM Dexamethasone. Cells were cultured for up to 28 days with two media changes per week. For Wnt-treated control groups diluted Wnt3A conditioned media collected from Wnt3A overexpressing L-M (TK-) cells (LGC standards) was used. Cells between passage 1 and 5 were used in all experiments.

4.2.2 Magnetic nanoparticle coating and cell labelling.

250nm SPIO carboxyl functionalised magnetic nanoparticles (Micromod) were covalently coated with UM206 peptide by carbodiimide activation and cells were labelled as described in chapter 2.

4.2.3 Magnetic stimulation.

Magnetically stimulated groups were treated using the magnetic force bioreactor as described in chapter 2. Treatment was performed in 3x 3h weekly sessions for *in vitro* studies. For chick femur cultures all femurs were stimulated with 5x 1h sessions per week for 2 weeks. Stimulations were performed at a frequency of approximately 1Hz. Non-

stimulated control groups were kept in identical conditions (without magnetic field stimulation).

4.2.4 Biochemical assays

At each time-point cells were washed with PBS then lysed for 10 mins in 0.1% Triton-X 100 in dH_2O containing 10µM Pepstatin A, 1mM Phenylmethanesulfonyl fluoride (PMSF) and a protease inhibitor cocktail (All Sigma) diluted 10x in RIPA buffer. The ALP activity of cell lysates was assessed using a 4-MUP assay (Sigma). 50µL of lysate was mixed with 50µL of 1M DEA buffer containing 0.5mM MgCl. Reactions were started with the addition of 50µL of 4-MUP substrate and incubated at 37^{o}C for 30mins. Reactions were stopped using 50µL of 1M NaOH. The fluorescence of each sample was measured on a Biotek synergy 2 plate reader using an excitation wavelength of 360nm and emission wavelength of 440nm. The amount of 4-MU produced was determined using a standard curve of 4-MU dissolved in DEA buffer (see appendix B). The total protein concentration of cell lysates was determined using a BCA assay kit (Thermo Fisher) according to the protocol described in chapter 2. Protein concentration was determined using a standard curve of BSA dissolved in $d.H_20$. The DNA content of cell lysate samples was also determined using a PicoGreen assay kit (Invitrogen). 20µL of lysate was mixed with 100µL of PicoGreen reagent dissolved 200x in 1x Tris-EDTA (TE) buffer. Samples were mixed for 10mins. and fluorescence was determined on a Biotek synergy 2 plate reader using an excitation wavelength of 480nm and emission wavelength of 520nm. DNA concentrations were determined using a standard curve of DNA dissolved in 1x TE buffer (see appendix B).

4.2.5 Immunocytochemistry.

After 28 days of culture cells were fixed with 90% Methanol and blocked as above before incubation with anti-Osteocalcin or anti-Osteopontin (R & D systems) diluted 1:2000 in 1% BSA / PBS overnight at 4^{o}C. Cells were washed 3x with PBS and incubated with anti-Mouse-FITC secondary antibody (Sigma) diluted 1:1000 in 1% BSA / PBS for 1h at room temp. Cells were washed 3x in PBS, and counterstained with DAPI. Fluorescence microscopy was performed on an Olympus IX83 confocal microscope operating Flourview 10 software. All images are representative of n=3.

4.2.6 Chick foetal femur culture.

Foetal chick femur extraction was performed by Dr J. Henstock (Keele University). Intact femurs were removed from freshly-killed Dekalb white chick foetuses after 11 days incubation and carefully cleaned of all muscle tissue by rolling on sterile tissue paper. Femurs were cultured *ex vivo* on porous polycarbonate membrane inserts (Millipore) in cell culture plates as described by (Kanczler et al., 2012). Femurs were cultured in osteogenic media consisting of alpha-MEM containing 1% penicillin-streptomycin and 150 µg/ml ascorbic acid, 2mM sodium β-glycerophosphate and 10^{-8}M dexamethasone (Sigma) for 14 days at 37°C in a 5% CO_2 humidified incubator. Media changes were performed every 24h.

4.2.7 Micro-injection.

Micro-injection of hMSC was performed with the assistance of Dr J. Henstock (Keele University). Cells were first fluorescently tagged with a DiO membrane tracker before labelling with magnetic nanoparticles at a concentration of 25µg MNP/2x10^5 cells. Cells were introduced into three sites in the femur; both cartilaginous epiphyses and the mid-

point of the diaphyseal bone collar using a 1ml syringe microinjection system (Linton Instrumentation, UK) and a glass capillary needle with a ~70µm tip diameter. 20nl of solution was injected into each site, equating to approximately 10^3 cells per injection. Co-injections of cells and BMP2 microparticles consisted of a suspension of cells mixed with microspheres. Microinjections were performed under sterile conditions with the aid of a Leica MZ10F dissecting microscope.

4.2.8 BMP2 microparticle encapsulation.

BMP2 microparticles were prepared and provided by Dr O. Qutachi (University of Nottingham). Poly vinyl alcohol (PVA, molecular weight: 13000 – 23000 Da, 87-89% hydrolysed), human serum albumin (HSA), Poly (DL-lactide-co-glycolide), (PLGA) polymers with lactide: glycolide ratios of 50:50 (DLG 4.5A 59 kDa) were all purchased from Surmodics (Birmingham, USA). Recombinant human BMP-2 (BMP-2) was purchased from Professor Walter Sebald (University of Wurzburg, Germany). Poly (DL-lactide-co-glycolide) microparticles were formed using a water-in-oil-in-water (w/o/w) emulsion method as previously described by (Kirby *et al*, 2011). Briefly, triblock copolymer was added to PLGA to provide weight percentages of 30% (w/w) of the 1g total mass in 5 ml dichloromethane. BMP-2 and HSA (human serum albumin) solution were prepared at a ratio of 1:9 for a 1% w/w loading in the microparticles. In order to manufacture microparticles, the aqueous solution of HSA and BMP-2 was added to a solution of PLGA-tri block copolymer. These phases were homogenised for two minutes at 4,000 rpm in a Silverson L5M homogeniser (Silverson Machines, UK) to form the water-in-oil emulsion. This primary emulsion was transferred to 200 ml 0.3% (w/v) PVA solution and was homogenised for a second time at 9,000 rpm. The resultant double emulsion was stirred at 300 rpm on a Variomag 15-way magnetic stirrer for a minimum of 4h to facilitate DCM

evaporation. Microparticles were then washed and lyophilized until dry (Edwards Modulyo, IMA Edwards, UK).

4.2.9 X-ray microtomography.

X-ray microtomography analysis of chick femurs was performed by Dr J. Henstock (Keele University). End-point femur density and volume were assessed by X-ray microtomography (µCT) using a Scanco µCT40 (beam energy: 55 kVp, beam intensity: 145µA, 200ms integration time, spatial resolution: 10µm). Femurs were analysed at two density thresholds (50/1000 and 120/1000), firstly to determine the total size, volume and average density of each femur following treatment and secondly at a higher threshold to determine the mineralised portion of the femur in the diaphysis (bone collar) and its average density. These thresholds were conserved throughout the experiments, allowing for comparison of bone formation across the investigation. All analysis on the reconstructions was performed using Scanco software tools.

4.2.10 Histological staining.

Cells were washed and fixed as described above then stained with 1% (w/v) Alizarin red in d.H_2O or 1% (w/v) for 10mins followed by 3x washes with d.H_2O or Sirius red dissolved in 1.3% Picric acid solution (Sigma) for 45mins followed by 3x washes with d.H_20. Samples were imaged on a Leica DMIL microscope with LAS software. After imaging, Alizarin red dye was extracted by incubating samples with 10% (w/v) CPC solution for 10mins on an orbital shaker. Samples of extracted dye were quantified by measuring absorbance at 562nm. Sirius red staining was extracted by incubating samples with 1M NaOH solution for 15mins on an orbital shaker. Samples of extracted dye were quantified by measuring absorbance at 540nm. For chick femur experiments, femurs were fixed, stained with

Alizarin Red and imaged. This was performed by Dr J. Henstock (Keele University). Femurs were fixed in 4% paraformaldehyde for 48h and washed in PBS. Whole mount histological staining for calcium deposition was performed by immersing the femurs in 1% Alizarin red for 1h followed by washing in PBS. Femurs were imaged using a Leica S6D dissection microscope fitted with a Nikon D500 digital camera. For sectioning, samples were first dehydrated in increasing concentrations of Industrial methylated spirits (IMS), followed by clearing in xylene. Samples were embedded in wax overnight then 7µm sections of femurs were obtained using a Microtome (Thermo-Shandon AS325). Tissue sections were re-hydrated by immersing in xylene for 2mins followed by decreasing concentrations of IMS (2mins each) and rinsed in water for 2mins. Sections were then stained for Calcium or Collagen using Alizarin Red or Sirius red respectively as described above. sGAG were stained for 10mins using 1% (w/v) Alcian blue dissolved in Acetic acid for 10mins followed by 3x d.H_20 washes.

4.2.11 Immunohistochemistry

Femurs were processed for histological staining as above. Antigen retrieval on re-hydrated sections was first performed by incubating samples with Proteinase K solution (20µg/mL) dissolved in TE/Triton buffer for 20mins at 37^{o}C (Sigma). Sections were then blocked with 1%BSA / TBS for 1h and incubated with anti-Osteocalcin (Abcam) diluted 1:200 in 1%BSA / TBS-Triton overnight at 4^{o}C. Sections were washed 2x with TBS-Triton. Endogenous peroxidase activity was then blocked with 0.3% H_2O_2 in TBS for 15mins at room temperature. Secondary antibody incubation and DAB staining was then performed using ABC staining system (Santa Cruz). Stained sections were dehydrated, cleared and mounted using DPX (Sigma). Sections were imaged using an Olympus CKX41 microscope operating with Image Pro Insight software.

4.2.12 Statistical analysis

All data is presented as means +/- SEM. Statistical significance at 95% Confidence level was determined using 1-way ANOVA with post-hoc Tukey tests using Mini-tab. µCT data was analysed by 1-way ANOVA with post-hoc Dunnett's test, all groups were compared to the Sham injection control group.

4.3 Results

The effects of UM206-MNP stimulation on the osteogenic differentiation of hMSC cultured in monolayer and in an *ex vivo* foetal chick femur model were investigated. For monolayer experiments cells were labelled with L-UM206-MNP or C-C-UM206-MNP and cultured for up to 28 days in osteogenic media with intermittent sessions of magnetic stimulation and studied for indicators of differentiation.

4.3.1 Biochemical analysis

Cell lysates were obtained from cells treated with MNP with and without magnetic field at three time-points (day 7, 14, 21) and samples were assayed for ALP activity, total protein and DNA content.

4.3.1.1 ALP activity

ALP activity was unaffected by magnetic field treatment alone at each time-point (Figure 4.1) whilst treatment with L-UM206-MNP or C-C-UM206-MNP alone marginally increased ALP activity at each time-point (not significant). Treatment with L-UM206-MNP in conjunction with magnetic field stimulation led to an added increase in ALP activity at all time-points with the most prominent effects observed after 7 and 21 days respectively (significant). Treatment with C-C-UM206-MNP and magnetic field also significantly

increased ALP activity after at all time points. Treatment with Wnt-CM caused increases in ALP activity at day 7 (Not significant) and day 14 (Significant) to similar levels as L-UM206-MNP and C-C-UM206-MNP, whilst a significant decrease in ALP activity was observed after 21 days.

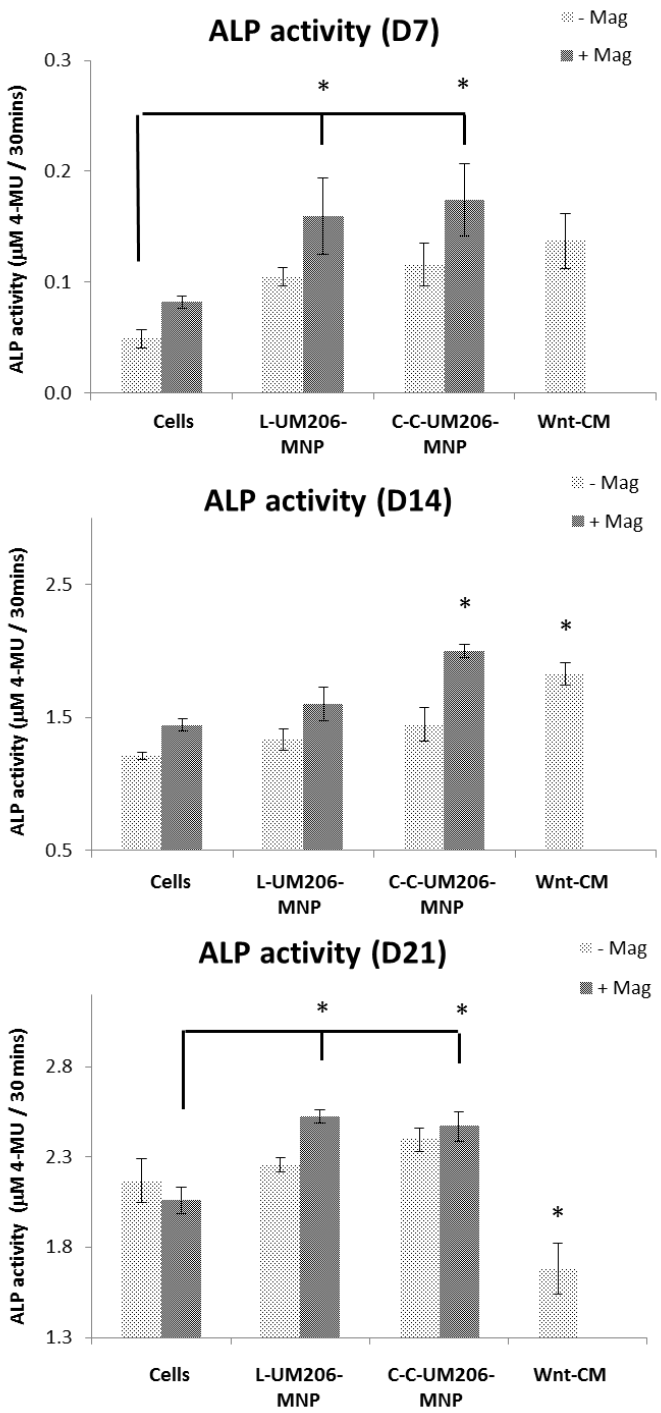

Figure 4.1. UM206-MNP increase ALP activity.
Magnetic field alone had negligible effects on ALP activity at all time points (not significant). Treatment with L-UM206-MNP or C-C-UM206-MNP (without magnetic field) marginally increased ALP activity at all time-points (not significant). Treatment with L-UM206-MNP (with magnetic field) increased ALP activity at day 7 and day 21 (significant) and treatment with C-C-UM206-MNP with magnetic field increased ALP activity at all time-points (significant). Treatment with Wnt-Conditioned media (Wnt-CM) increased ALP activity at day 7 (not-significant) and day 14 (significant), but significantly reduced ALP activity at day 21. n=4, values represent average ALP activity, error bars represent SEM, * represents $p<0.05$.

4.3.1.2 Total protein production

Total protein production was marginally raised by magnetic field treatment after 7 days (not significant) and remained similar to the non-treated control group after 14 days and 21 days respectively (Figure 4.2). Treatment with L-UM206-MNP or C-C-UM206-MNP alone also resulted in elevated total protein at day 7 (not significant) and remained similar to the non-treated control group at day 14 and day 21 respectively. Treatment with L-UM206-MNP with magnetic field resulted in marginal increases in total protein production after 7 and 21 days respectively (not significant), but no overall effect was observed after 14 days treatment. Treatment with C-C-UM206-MNP with magnetic field stimulation significantly raised total protein production at all time-points with most notable increase at later time-points. Treatment with Wnt-conditioned media (Wnt-CM) also significantly increased total protein production at all time-points.

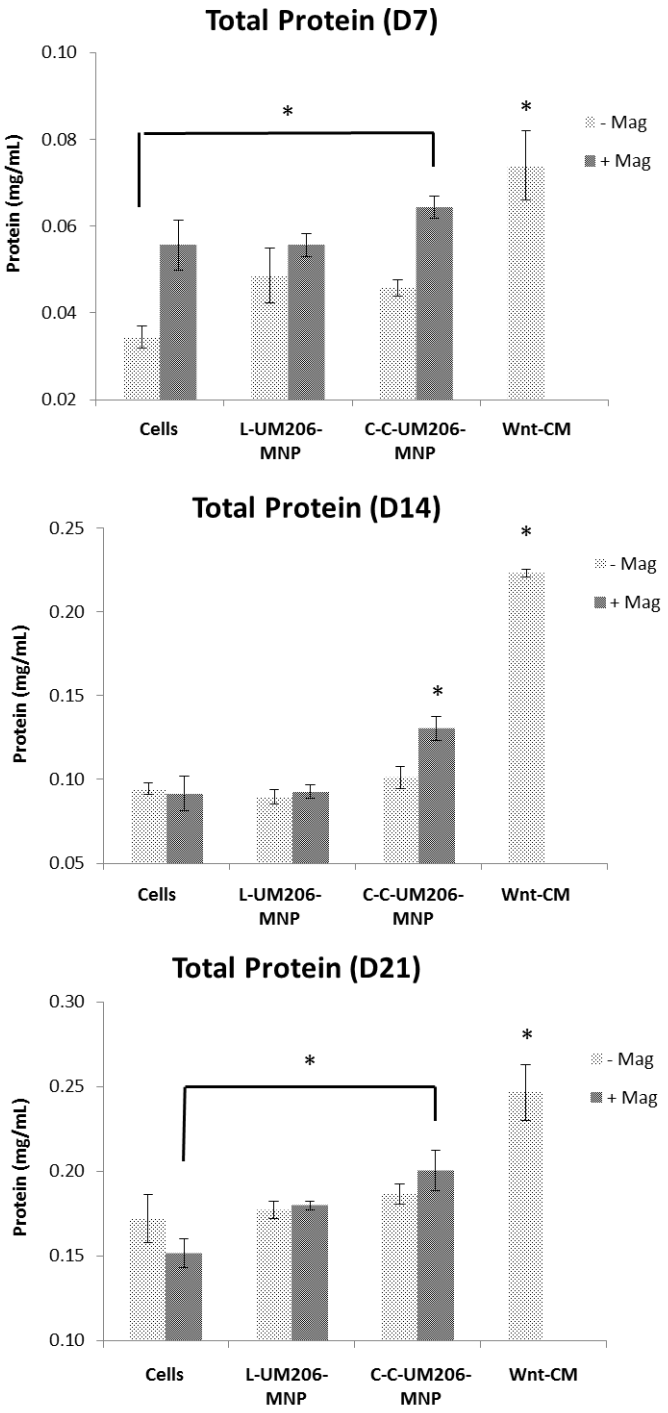

Figure 4.2. Effects of UM206-MNP on Total Protein content.
Magnetic field alone caused an increase in Total protein content at day 7 (not significant) and was not affected at day 14 or day 21. Treatment with L-UM206-MNP or C-C-UM206-MNP (without magnetic field) increased ALP activity at day 7 (not significant) and had no effect at day 14 or day 21. Treatment with L-UM206-MNP (with magnetic field) marginally increased Total protein at day 7 and day 21 compared to the non-treated control (not significant) and no effect was observed after 14 days. Treatment with C-C-UM206-MNP and magnetic field significantly increased Total protein content at all time-points, with most notable increases at day 14 and day 21. Treatment with Wnt-Conditioned media (Wnt-CM) significantly increased Total protein content at all time-points. n=4, values represent average total protein content of cell lysates, error bars represent SEM, * represents $p<0.05$.

4.3.1.3 DNA content

The DNA content of cell lysates was also assessed. Magnetic field treatment alone was found to have no effect on DNA content at each time-point (Figure 4.3). Treatment with L-UM206-MNP or C-C-UM206-MNP alone had no effect on DNA content at day 7 and day 14, whilst a minor increase in DNA content was observed after 21 days treatment compared to the non-treated control group (not significant). Treatment with L-UM206-MNP in conjunction with magnetic field resulted in a significant increase in DNA content after 7 days only but no effect was observed after 14 and 21 days respectively. Treatment with C-C-UM206-MNP resulted in a significant increase in DNA content after 7 and 21 days with a marginal increase in DNA content observed after 14 days (not significant). Treatment with Wnt-conditioned media (Wnt-CM) elevated the DNA content of cell lysates at all time-points with a significant increase observed after 14 days only.

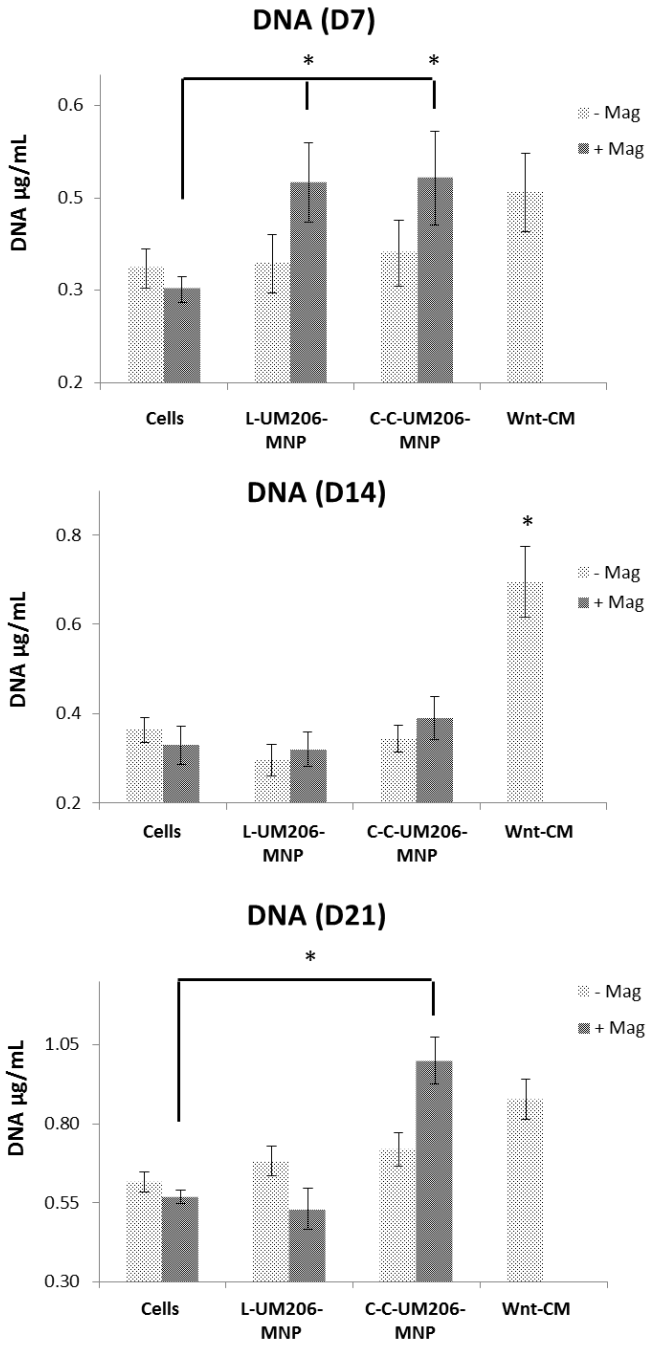

Figure 4.3. Effects of UM206-MNP on DNA content.
Treatment with magnetic field alone had no overall effect on DNA content at each time-point studied. Treatment with L-UM206-MNP or C-C-UM206-MNP had no effect of DNA content at day 7 and day 14, a marginal increase in DNA content was observed after 21 days (not significant). Treatment with L-UM206-MNP with magnetic field stimulation caused a significant increase in DNA content at day 7, no effect was observed at day 14 or day 21. Treatment with C-C-UM206-MNP and magnetic field stimulation caused a significant increase in DNA content at day 7 and day 21, no effect was observed after 14 days. Treatment with Wnt-conditioned media (Wnt-CM) increased DNA content at each time-point (significant at day 14 only). n=4, values represent average DNA content of cell lysates, error bars represent SEM,* represents $p<0.05$.

4.3.1.4 ALP/DNA ratio

The ALP activity of cell lysates was also normalised to the DNA content of the respective lysates to account for changes in cell numbers between groups (Figure 4.4). Treatment with magnetic field alone caused minor non-significant increases in the ALP/DNA ratio at day 7 and day 14, whilst no effect was observed at day 21. Treatment with either L-UM206-MNP or C-C-UM206-MNP alone caused relative increases in the ALP/DNA ratio at day 7 and 14 respectively (not significant) whilst no effect observed at day 21. An additive, but non-significant increase in ALP/DNA was observed when cells were treated with L-UM206-MNP with magnetic field stimulation at all time-points. Treatment with C-C-UM206-MNP with magnetic field stimulation also caused minor, non-significant increases in the ALP/DNA ratio at day 7 and day 14, whilst a decrease was observed at day 21 (not significant). Treatment with Wnt-conditioned media (Wnt-CM) transiently increased ALP/DNA at Day 7 (not significant), but a reduction was observed after 14 days (not significant) with a significant reduction in ALP/DNA observed after 21 days treatment.

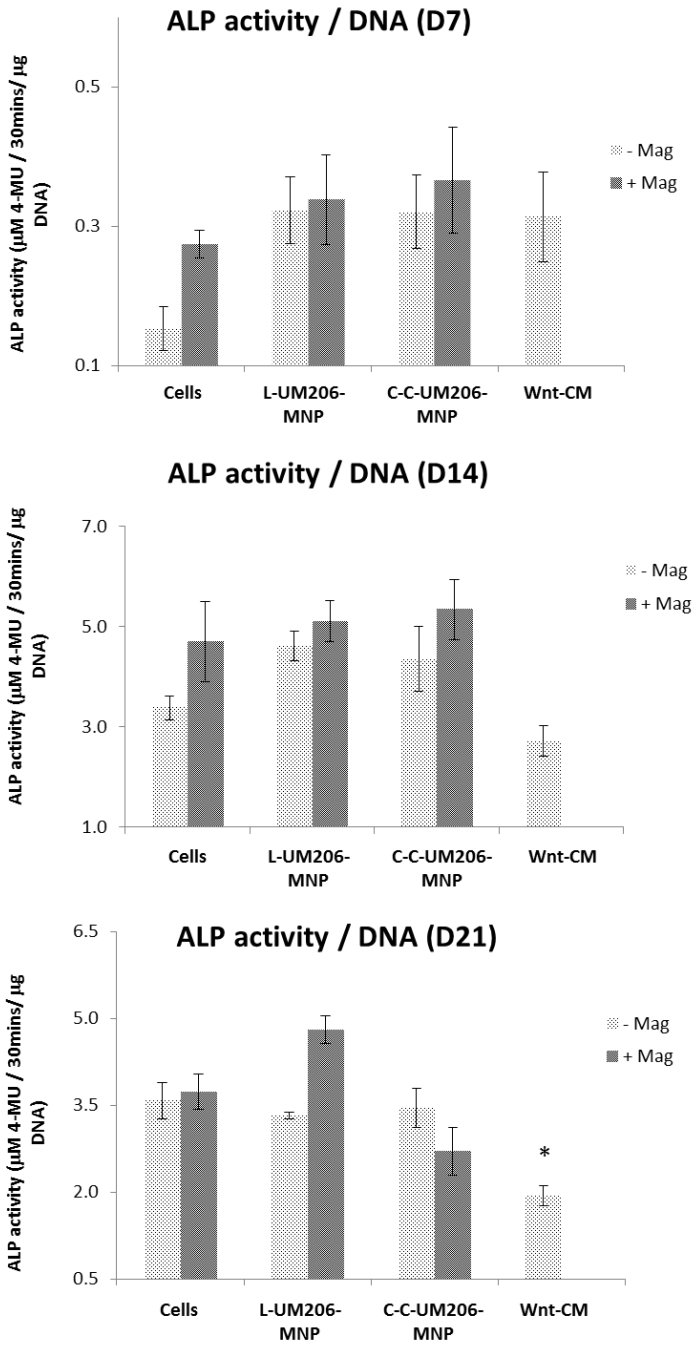

Figure 4.4. Effects of UM206-MNP on ALP/DNA ratio.
Treatment with magnetic field alone caused minor increases in the ALP/DNA ratio at day 7 and day 14 (not significant), no effect was observed after 21 days. Treatment with L-UM206-MNP or C-C-UM206-MNP alone caused increases in ALP/DNA at day 7 and day 14 (not significant) with no effect observed at day 21. Treatment with L-UM206-MNP with magnetic field stimulation increased ALP/DNA at all time-points (not significant). Treatment with C-C-UM206-MNP and magnetic field increased ALP/DNA at day 7 and day 14 (not significant) and a decrease in ALP/DNA was observed at day 21 (not significant). Treatment with Wnt-conditioned media (Wnt-CM) increased ALP/DNA at day 7 (not significant), whilst decreases in ALP/DNA were observed after 14 days (not significant) and 21 days (significant). n=4, values represent averages of ALP activity normalised to DNA content of cell lysates. Error bars represent SEM,* represents $p<0.05$.

4.3.2 *In vitro* histological analysis

4.3.2.1 Collagen deposition

Treatment with magnetic field, L-UM206-MNP or C-C-UM206-MNP alone all caused marginal changes in collagen production as shown by Picro-Sirius red staining for collagen (Figure 4.5). Whilst treatment with either type of UM206-MNP in conjunction with magnetic field appeared, by microscopic analysis, to increase localised collagen production. However quantification of the total collagen production after dye extraction with NaOH indicated that collagen content remained similar to the non-treated control for each treatment (Figure 4.6). In contrast, treatment with Wnt-CM clearly increased collagen production which was confirmed after quantification.

4.3.2.2 Calcium deposition

Treatment with magnetic field or L-UM206-MNP alone appeared to cause marginal increases in calcium deposition as shown by Alizarin red staining for calcium (Figure 4.7), whilst C-C-UM206-MNP alone had no overall effect on calcium deposition. Treatment with either L-UM206-MNP or C-C-UM206-MNP in conjunction with magnetic field appeared to increase localised calcium deposition by microscopic analysis. Although again quantification of the total calcium production after dye extraction with CPC indicated that the calcium content of the samples remained similar to the non-treated control for each treatment (Figure 4.8). In contrast, treatment with Wnt-CM caused a noticeable decrease in calcium deposition. This effect was also shown after quantification although was found not to be statistically significant.

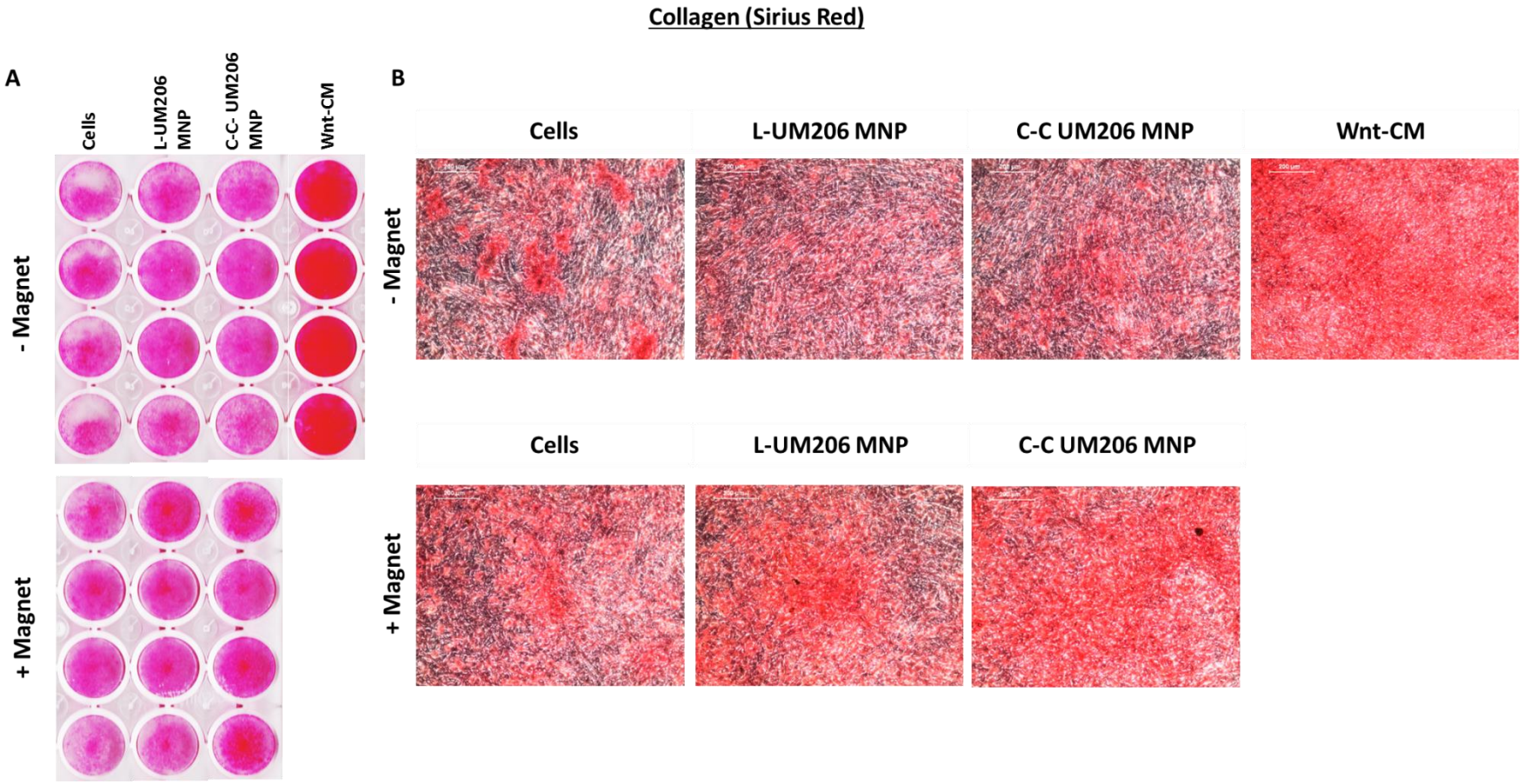

Figure 4.5. UM206-MNP enhance localised Collagen production.
Treatment with Magnetic field alone or L-UM206-MNP (without magnetic field) had a negligible effect on collagen deposition compared to the non-treated control (A). Whereas an increase in localised local collagen deposition was observed after treatment with L-UM206 with magnetic field compared to the magnetic field only control group. Treatment with Wnt-CM caused a clear increase in collagen deposition after 28 days. High magnification images are shown in (B) Images representative of n=4. Scale bar represents 200µm.

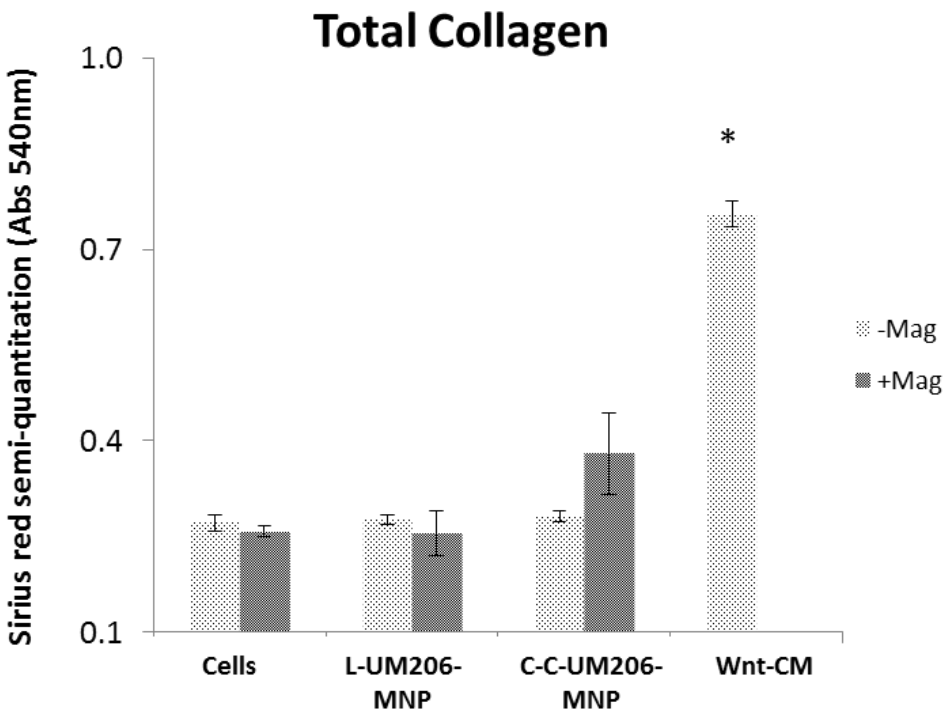

Figure 4.6. UM206-MNP do not affect total Collagen production. Quantification of total Collagen deposition after dye extraction with NaOH indicated that Collagen deposition across the wells was broadly similar across all groups apart from the Wnt-CM treated group which displayed a significant increase in total Collagen deposition after 28 days. Error bars represent SEM, n=4, * represents $p<0.05$

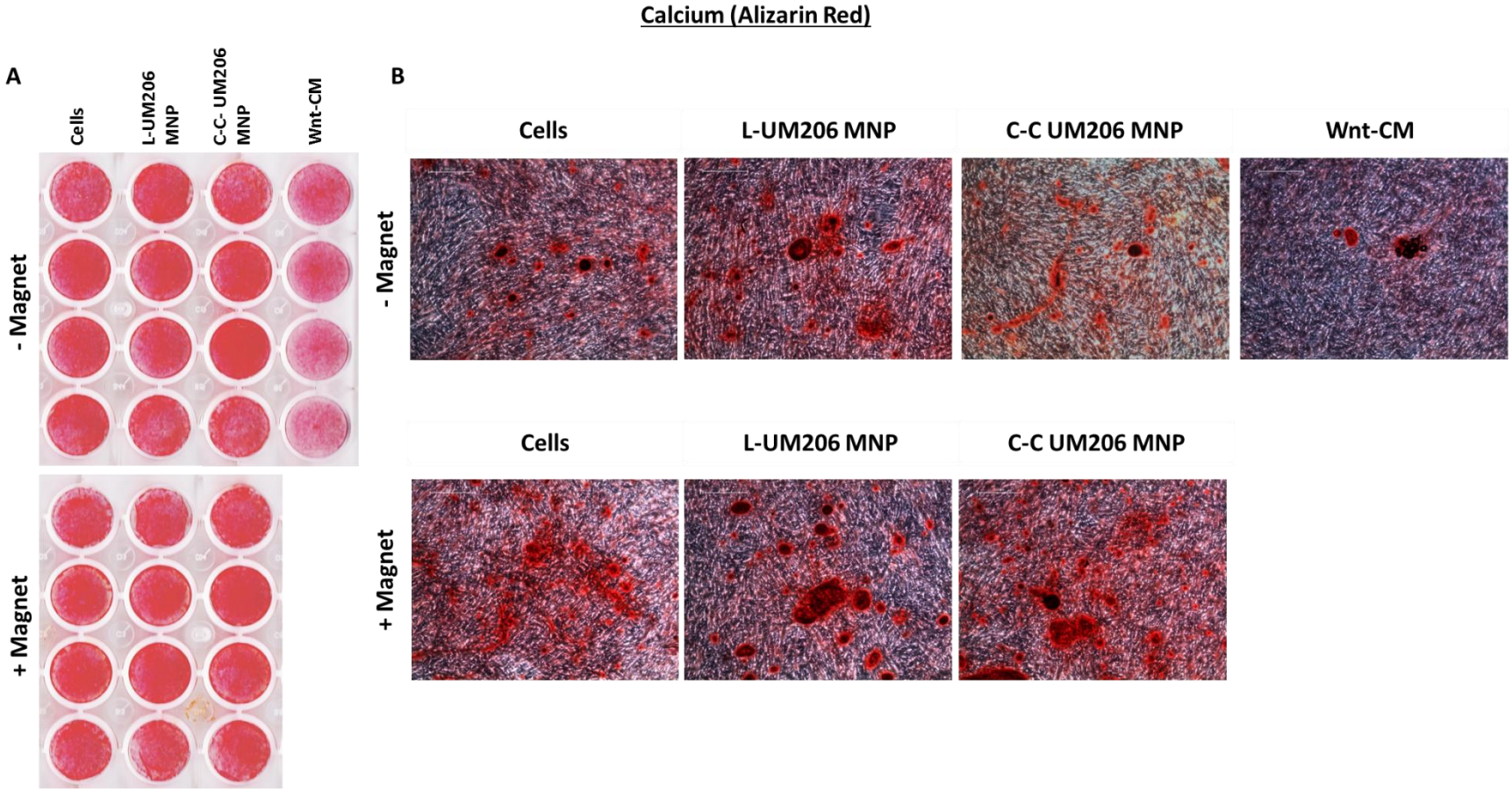

Figure 4.7. UM206-MNP enhance local mineralisation.

Treatment with Magnetic field alone or UM206-MNP (without magnetic field) resulted in minor increases of localised bone nodule formation compared to the non-treated control (A). Treatment with L-UM206-MNP (with magnetic field) caused a noticeable increase in localised nodule numbers compared to the magnetic field alone control group. In contrast treatment with Wnt-CM for 28 days caused a clear decrease in nodule formation. High magnification images are shown in (B) Images representative of n=4. Scale bar represents 200µm.

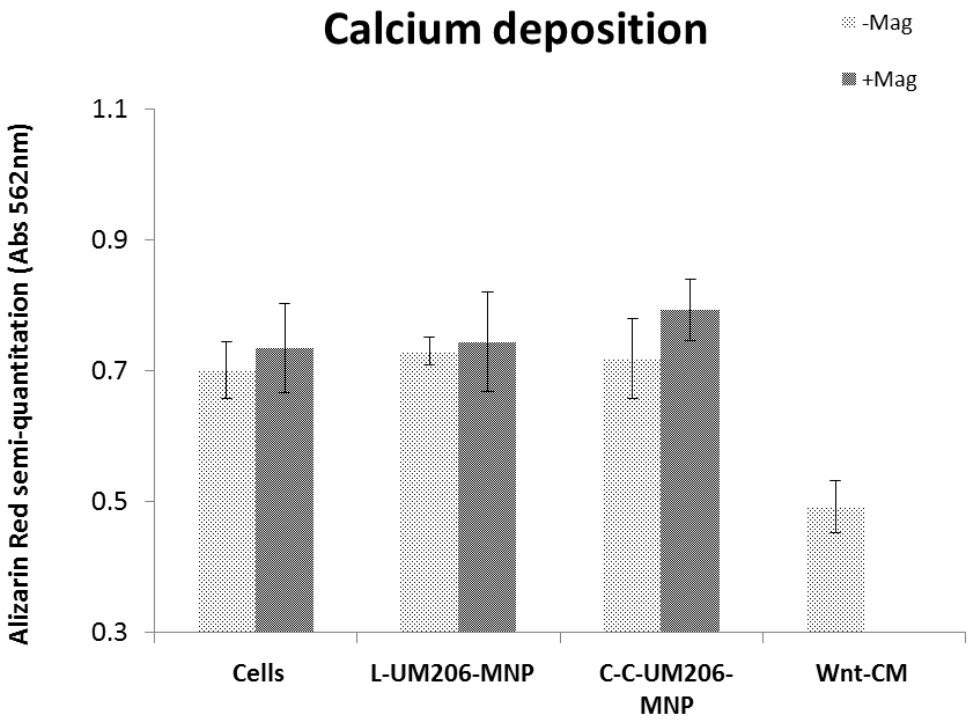

Figure 4.8. UM206-MNP do not affect total mineralisation.
Quantification of total calcium deposition after CPC extraction indicated that calcium deposition across the wells was broadly similar across all groups apart from the Wnt-CM treated group which displayed a significant decrease in total calcium deposition after 28 days. Error bars represent SEM, n=4.

4.3.3 *In vitro* matrix marker expression

Matrix production was assessed by immunostaining for bone markers Osteocalcin and Osteopontin.

4.3.3.1 Osteocalcin

Treatment with magnetic field or either L-UM206-MNP or C-C-UM206-MNP alone appeared to increase overall Osteocalcin production after 28 days (Figure 4.9). An added increase was observed when cells were treated with either C-C-UM206-MNP or in particular L-UM206-MNP when subjected to magnetic field stimulation. Treatment with Wnt-CM also marginally increased Osteocalcin production after 28 days.

4.3.3.2 Osteopontin

Treatment with magnetic field or either L-UM206-MNP or C-C-UM206-MNP alone appeared to have no overall effect on Osteopontin production after 28 days (Figure 4.10). Whilst a marginal increase in Osteopontin production was observed after treatment with L-UM206-MNP or C-C-UM206-MNP in conjunction with magnetic field stimulation. Treatment with Wnt-CM also marginally increased Osteopontin production after 28 days.

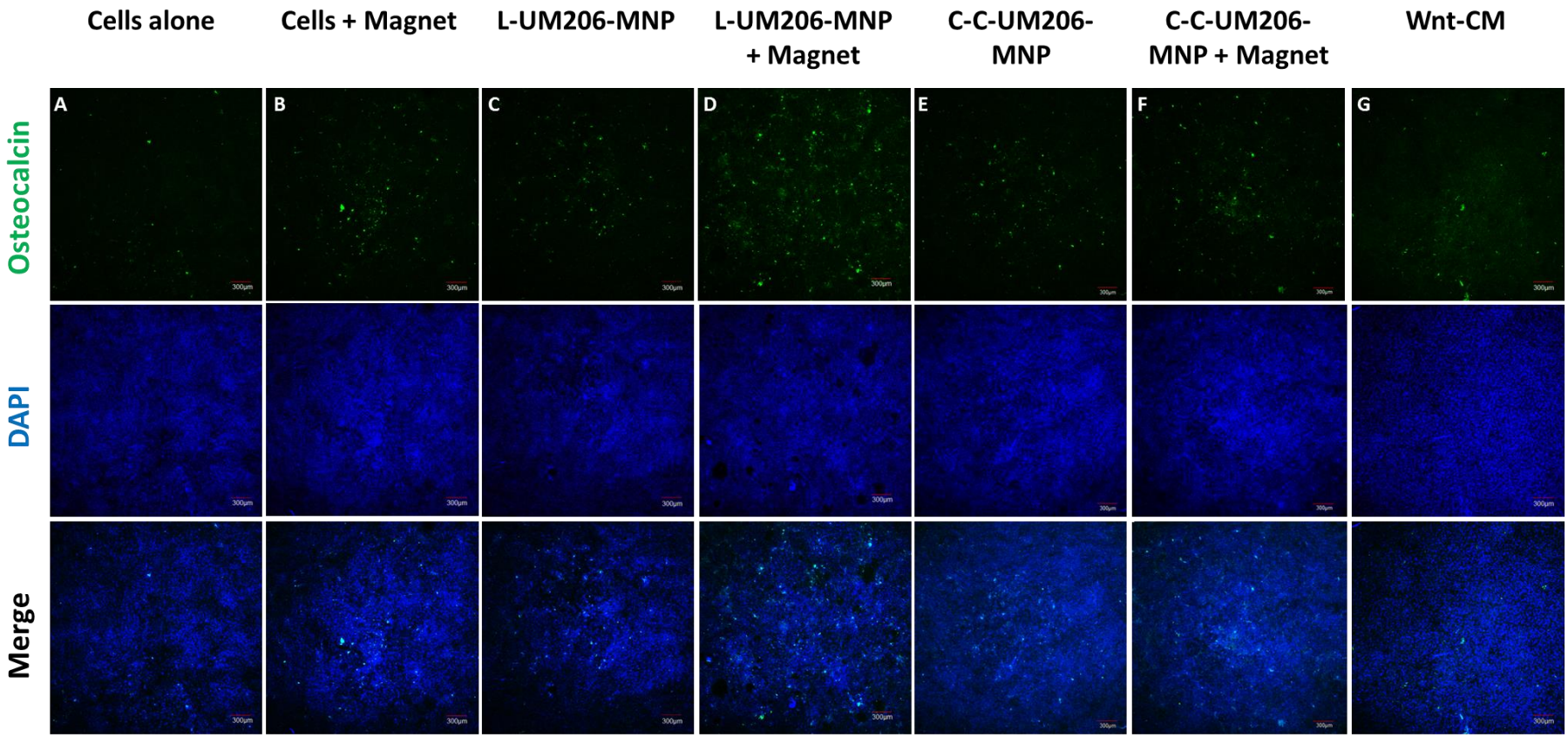

Figure 4.9. UM206-MNP enhance Osteocalcin production.
Treatment with Magnetic field alone (B) or either L-or C-C-UM206-MNP without magnetic field (C,E) caused increases in Osteocalcin expression relative to the non-treated control group (A). Treatment with L-UM206-MNP with magnetic field (D) caused a notable increase in Osteocalcin expression after 28 days. Treatment with C-C-UM206-MNP with magnetic field (F) or Wnt-CM (G) caused minor increases in Osteocalcin expression. Images representative of n=3. Scale bar represents 200µm.

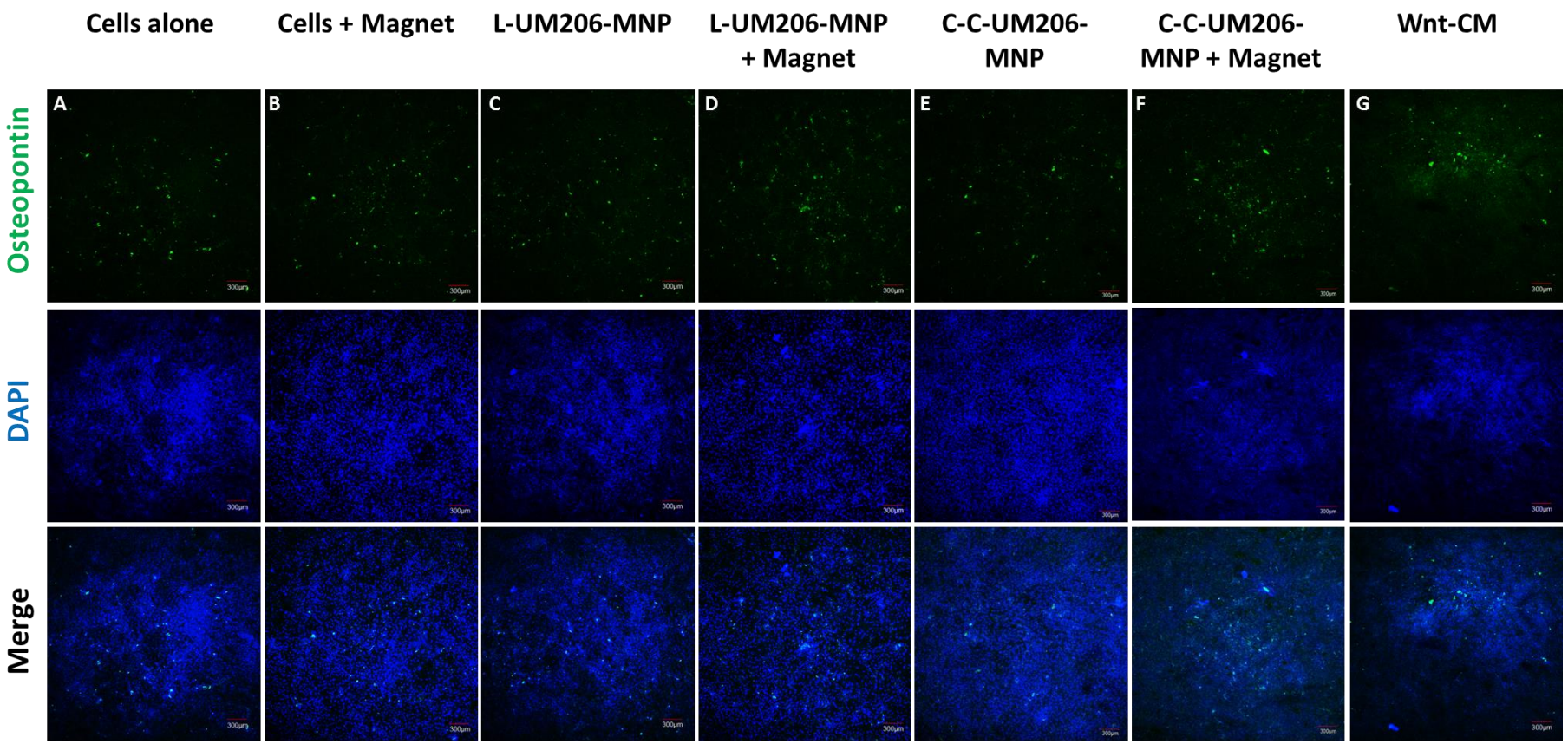

Figure 4.10. UM206-MNP do not affect Osteopontin production.
Treatment with Magnetic field alone (B) or with either L-UM206 or C-C-UM206-MNP without magnetic field (C, E) had a negligible effect on Osteopontin expression compared to the non-treated control (A). Treatment with L-UM206-MNP or C-C-UM206 MNP with magnetic field (D, F) caused negligible increases in Osteopontin expression. Treatment with Wnt-CM (G) had no overall effect on Osteopontin production. Images representative of n=3. Scale bar represents 200µm.

4.3.4 Effects of L-UM206-MNP on *ex vivo* bone production

The effects of L-UM206-MNP, magnetic field treatment and synergistic effects of BMP2 on bone formation were investigated in an *ex vivo* foetal chick femur model. Delivery of cells to femurs was confirmed by fluorescent microscopy which showed fluorescence of tagged-cells in the epiphyseal regions 24h after injection, sham injected femurs displayed background auto-fluorescence only (Figure 4.11). Injection of hMSC alone or hMSC pre-labelled with L-UM206-MNP into the foetal femur resulted in the formation of secondary mineralisation sites in the injected epiphysis and evidence of extension of the bone collar was also observed after 14 days (Figure 4.12). This effect was also observed when hMSC with or without labelling with L-UM206-MNP were co injected with BMP2-releasing microspheres which provided controlled release of BMP2.

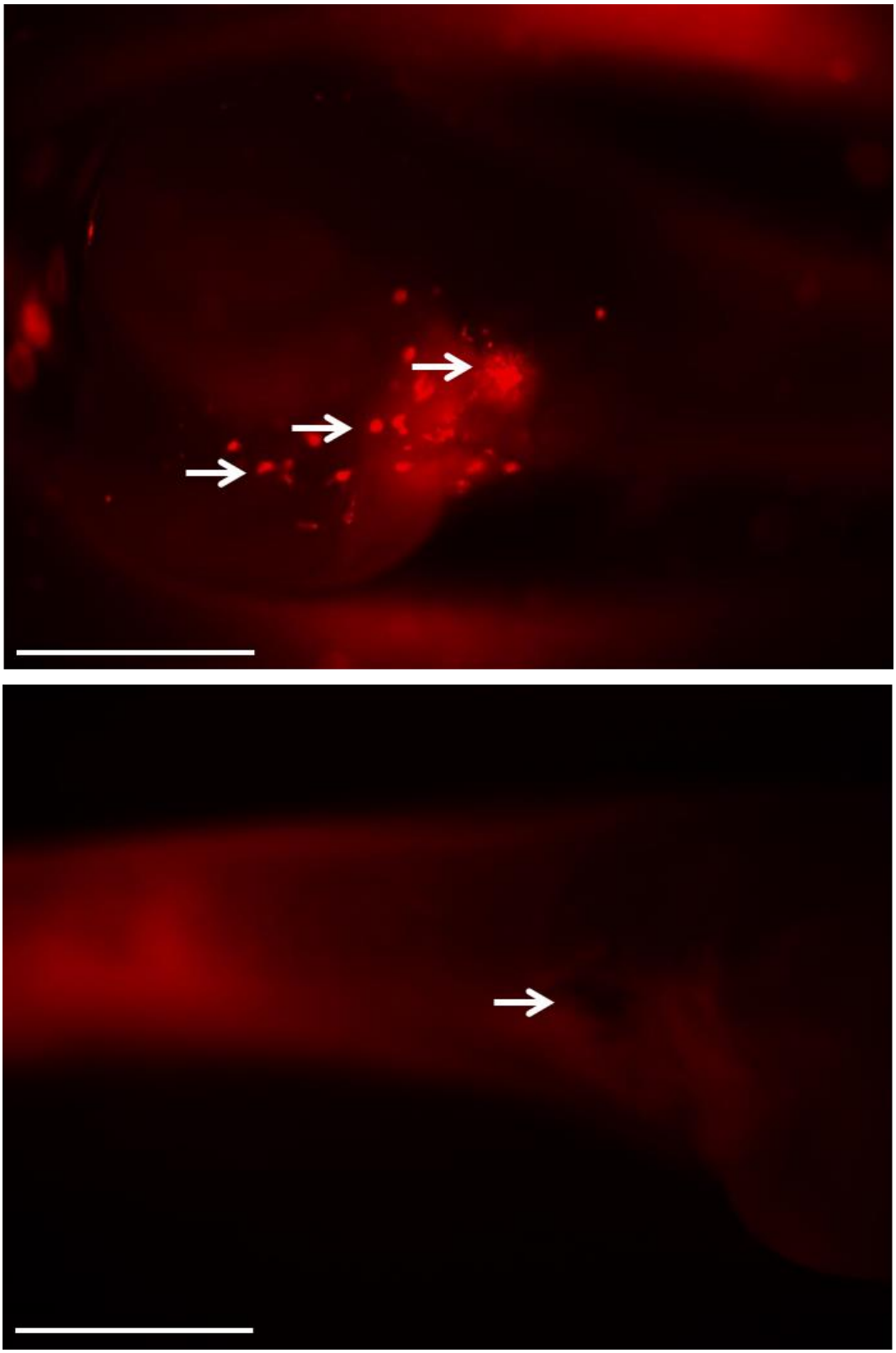

Figure 4.11. Microinjection of MSC into foetal femurs.
Fluorescence dissection microscopy images showing delivery of injected hMSC into foetal chick femurs 24h post-injection (Top). Auto-fluorescence of sham injected femur is shown in the bottom image. Arrows indicate injection sites. Representative images from MSC injection and Sham injection groups are shown. N=8, scale bar represents 1mm.

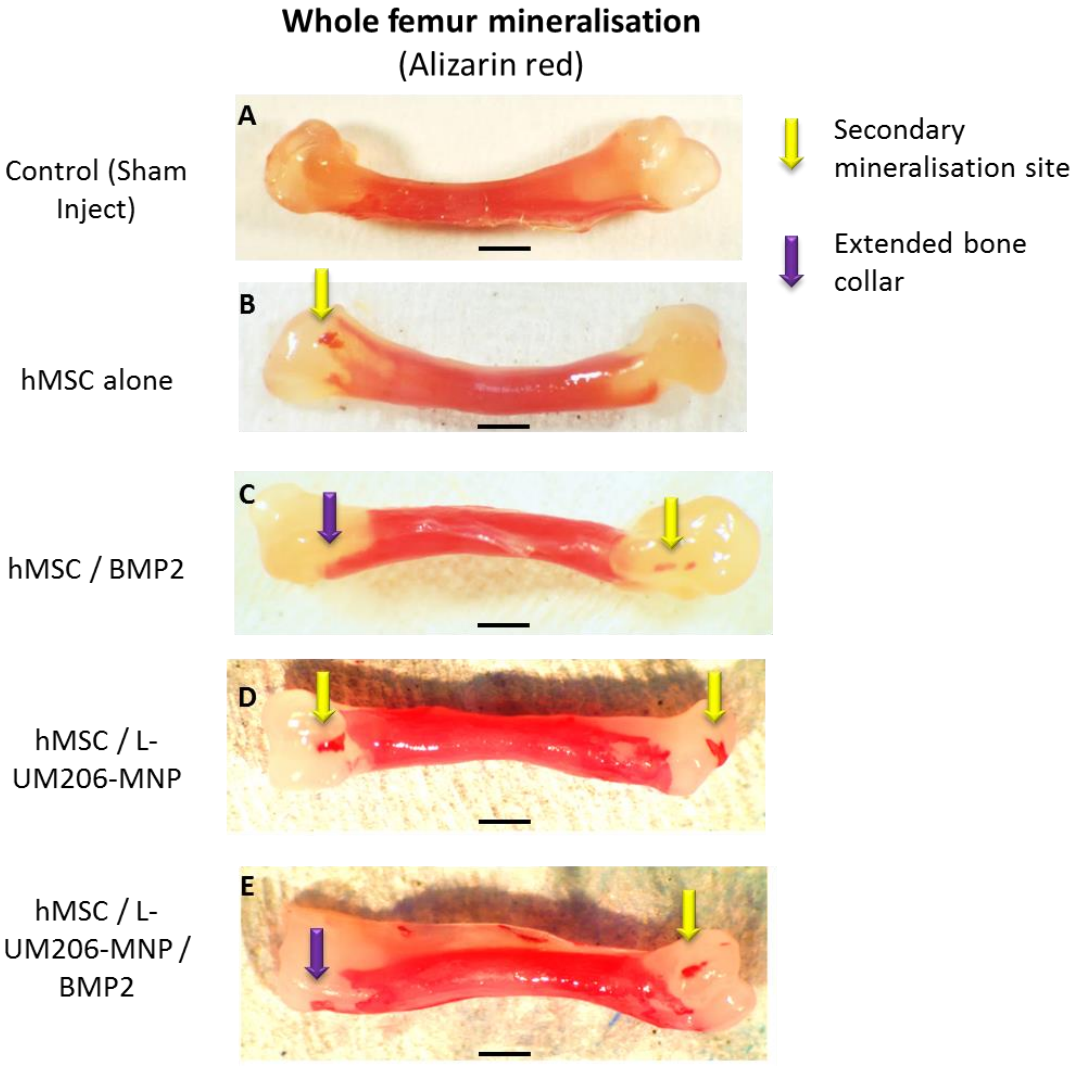

Figure 4.12. UM206-MNP and BMP releasing microparticles increase bone formation in foetal femurs.
Whole mount dissection microscopy images showing calcium deposition (Alizarin red staining) primarily in the bone collar in all groups including the control sham injection group (A). In treated groups secondary mineralisation sites were observed at the microinjected regions in epiphyses injected with hMSC alone (B) , hMSC with BMP2-releasing microparticles (C) hMSC labelled with L-UM206 and (D) and L-UM206-labelled hMSC with BMP2 microparticles (E). Images representative of n=8. Scale bar represents 1mm.

4.3.5 Micro-computed tomography analysis

4.3.5.1 Total Bone density and volume

The bone density and volume of foetal femurs was determined by µCT analysis (Figure 4.13). Injection of hMSC alone caused a minor decrease in total femur volume whilst total femur density was marginally increased (not significant). In contrast, injection of hMSC with BMP2 microparticles resulted in a significant increase in total bone volume, mainly as a result of increased mineralisation at the diaphyseal bone collar but overall a minor decrease in total bone density was observed (not significant). Injection with L-UM206-MNP labelled MSC with and without BMP2 releasing microparticles had no overall effect on the total bone volume or density of femurs.

4.3.5.2 Bone Collar density and volume

The density and volume of the diaphyseal bone collars were also analysed (Figure 4.14). Injection of hMSC alone or hMSC pre-labelled with L-UM206-MNP (with or without BMP2) all caused minor decreases in bone collar volume whilst bone collar density was marginally increased in these groups (not significant). Injection of hMSC with BMP2 releasing microparticles resulted in a minor increase in bone collar volume (not significant) but no effect was observed on bone collar density. The highest collar density was observed in femurs co-injected with hMSC with L-UM206-MNP and BMP2 although this was not found to be statistically significant.

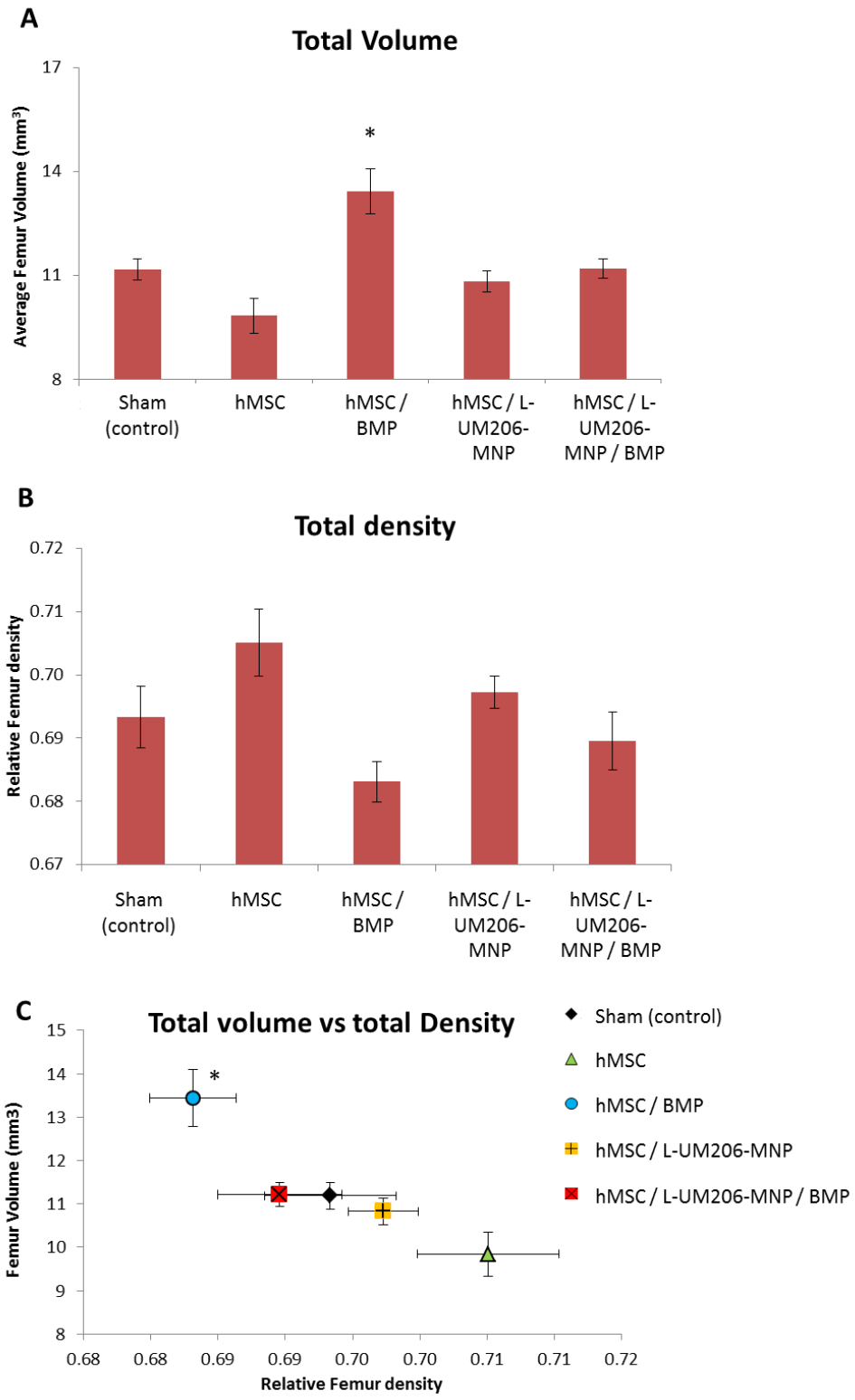

Figure 4.13. UM206-MNP do not affect total bone volume or density.
Microinjection of hMSC, hMSC labelled with UM206-MNP or UM206-MNP with BMP2 had no overall effect on Total bone volume (A) or total density (B). In contrast micro-injection of hMSC with BMP2 releasing micro-particles caused an overall increase in the total volume of bone formed (**A**) but did not affect the total bone density (B). A scatter plot of bone volume and bone density is shown in (C). N=8, error bars represent SEM, * represents $p<0.05$.

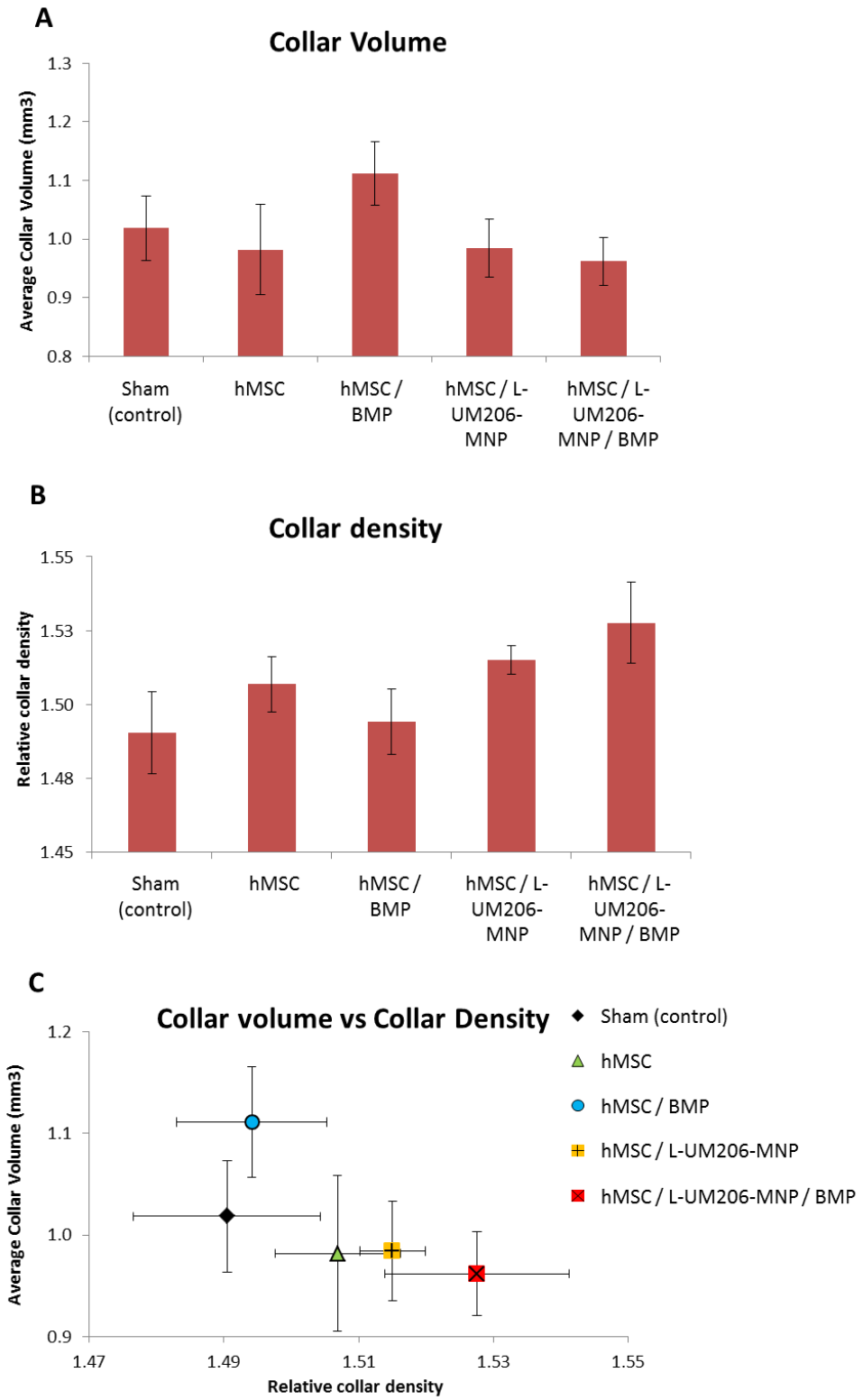

Figure 4.14. UM206-MNP increase Bone collar density in foetal femurs.
Microinjection of hMSC, hMSC labelled with UM206-MNP or UM206-MNP with BMP2 had no overall effect on Bone collar volume (A) but did increase bone collar density (trend only) with highest collar density observed in UM2060-MNP with BM2 injection group (B). Injection with BM2 caused a minor (not significant) increase in Collar volume (A) but had no effect on collar density (B). A scatter plot of bone collar volume and collar density is shown in (C). N=8, error bars represent SEM.

4.3.5.3 Relative Bone Collar density and volume

In order to control for differences between femurs, the bone collar volume and density of each femur was normalised to the total bone volume and density of each respective femur (Figure 4.15). Injection of hMSC alone appeared to increase relative collar volume (not significant) whilst no effect was observed on relative collar density. Injection of hMSC with BMP2 releasing microparticles with or without L-UM206-MNP caused a marginal decrease in relative collar volume (not significant) and no effect was observed on femurs injected with L-UM206-MNP labelled hMSC alone. However injection with hMSC and BMP2 microparticles, or L-UM206-MNP labelled MSC both resulted in increases in relative collar density with the highest relative collar density observed in L-UM206-MNP and BMP2 injected femurs (significant).

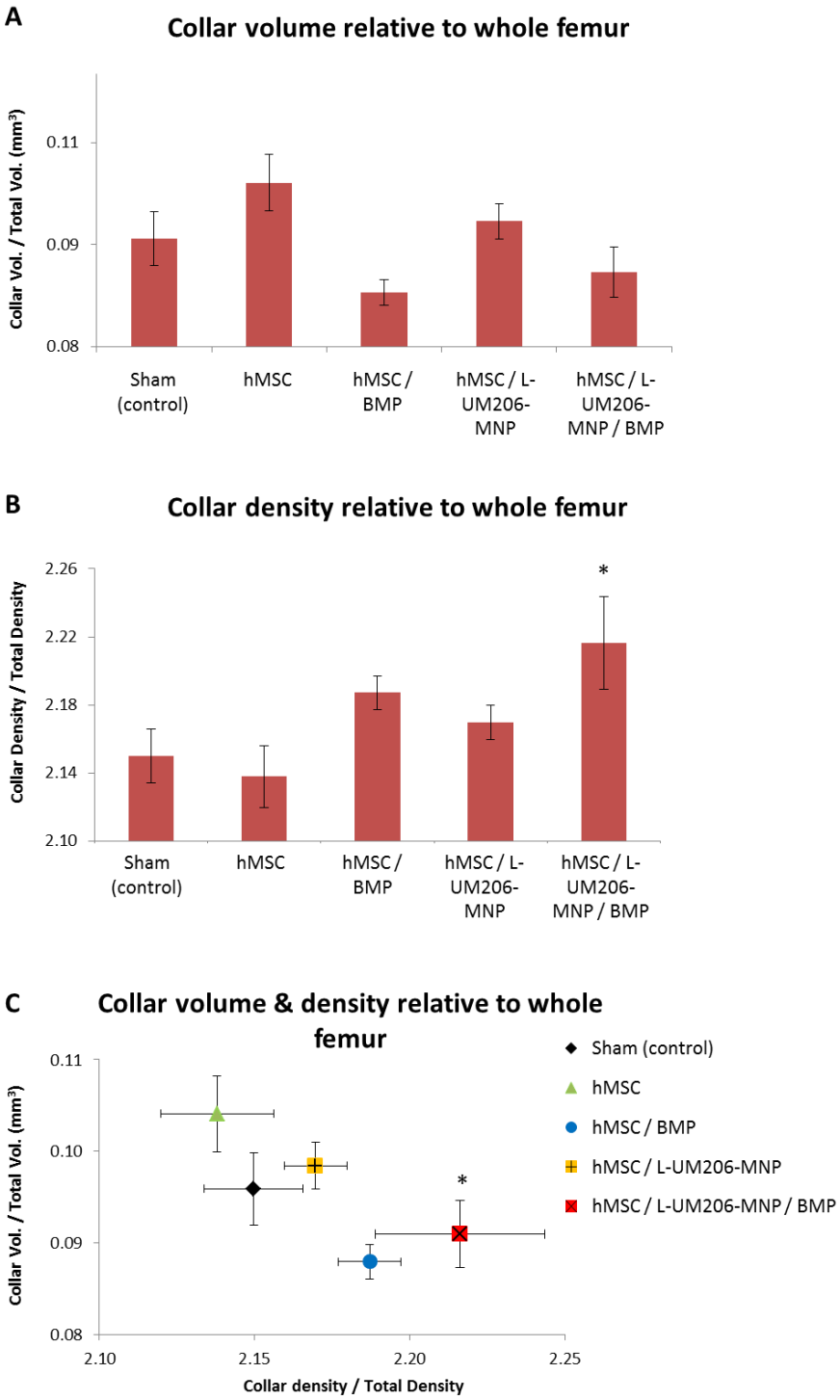

Figure 4.15. UM206-MNP increase relative Bone collar density in foetal femurs. Microinjection of hMSC alone caused a minor (not significant) increase in relative collar volume (A) but had no effect on relative collar density (B). Injection of BMP2 microparticles caused a minor decrease (not significant) in relative collar volume (A) but caused an increase (not significant) in relative collar density (B). Injection of L-UM206-MNP labelled MSC with or without BMP2 microparticles had no overall effect on relative collar volume but did increase relative collar density (Significant for L-UM206-MNP & BMP2). A scatter plot of relative bone collar volume and relative collar density is shown in (C). N=8, error bars represent SEM, * represents $p<0.05$.

4.3.6 *Ex vivo* histological analysis

Injected femurs were sectioned and subjected to histological analysis in order to investigate the observed secondary mineralisation sites after alizarin red staining. The degree of tissue remodelling at the injection site was also investigated using histological staining.

4.3.6.1 Calcium deposition

Femurs injected with hMSC (with or without BMP2 and UM206-MNP) all displayed evidence of secondary mineralisation at the injection sites as shown by Alizarin red staining for calcium indicating the presence of mineralised matrix (Figure 4.16). In contrast, negligible mineralisation apart from normal bone deposition at the bone collar was observed at the injection sites in the sham injected control femurs.

4.3.6.2 sGAG and collagen deposition

Femur sections were also stained with Alcian blue and Sirius red to reveal sGAG and collagen deposition respectively. This allows the degree of tissue remodelling at the injection sites of the femurs to be assessed. Femurs injected with hMSC (with or without BMP2 and UM206-MNP) all showed a degree of increased collagen or sGAG deposition at the injection sites (Figure 4.17) indicating a level of tissue remodelling after treatment. In contrast negligible tissue remodelling was observed in the sham injected control femurs.

4.3.6.3 Osteocalcin production

Immunocytochemistry was also performed on femur sections to probe for the presence of Osteocalcin which is an indicator of mature bone matrix (Figure 4.18). Once again femurs injected with hMSC (with or without BMP2 and UM206-MNP) all displayed evidence of Osteocalcin expression at the injection sites which was most noticeable at the

epiphyseal regions of the femurs. In contrast sham injected femurs were negative for epiphyseal osteocalcin expression.

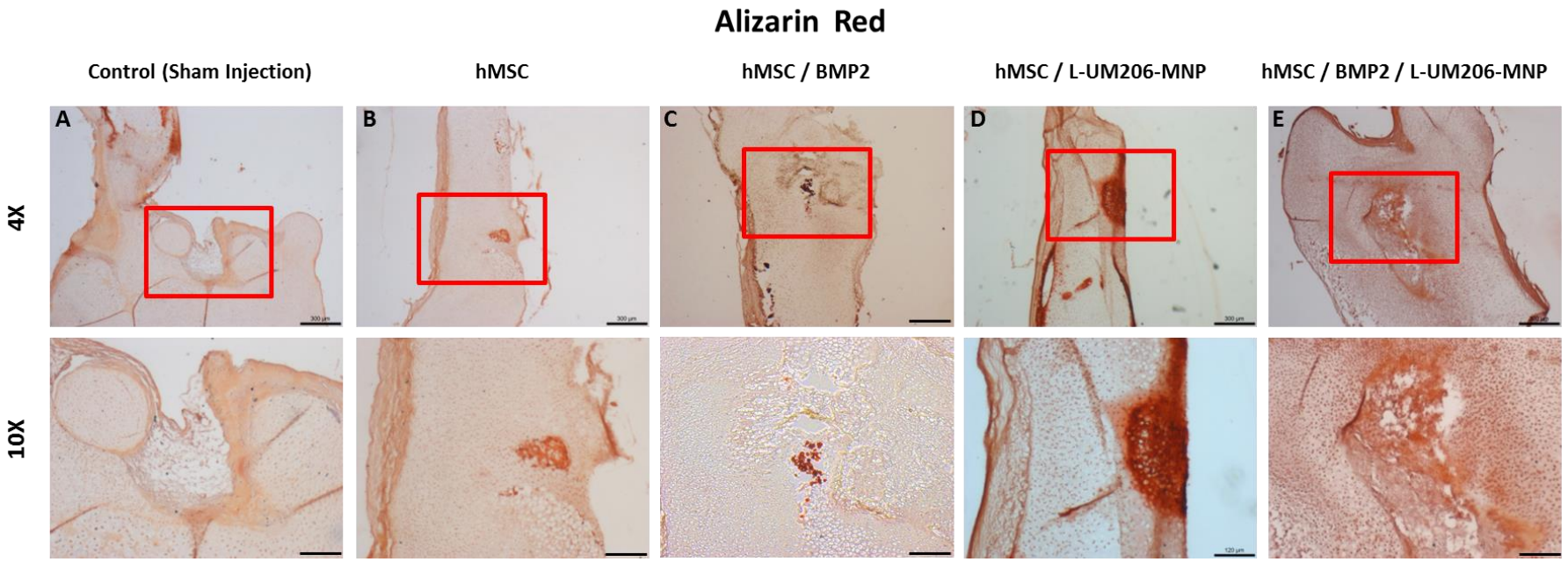

Figure 4.16. Secondary mineralisation sites after L-UM206-MNP injection.
Alizarin red staining showing calcium deposition in femur histology sections. Sham injected (control) femurs (A) showed little evidence of epiphyseal mineralisation at injection sites. In contrast Injection of hMSC alone (B), hMSC with BMP2 microparticles (C), hMSC labelled with L-UM206-MNP (D) and L-UM206-MNP co-injected with BMP2 microparticles (E) resulted in formation of secondary mineralisation sites. Higher magnification images are shown in the bottom row. Scale bars represent 300 µm (top row) and 120µm (bottom row) respectively, Images representative of n=8 shown.

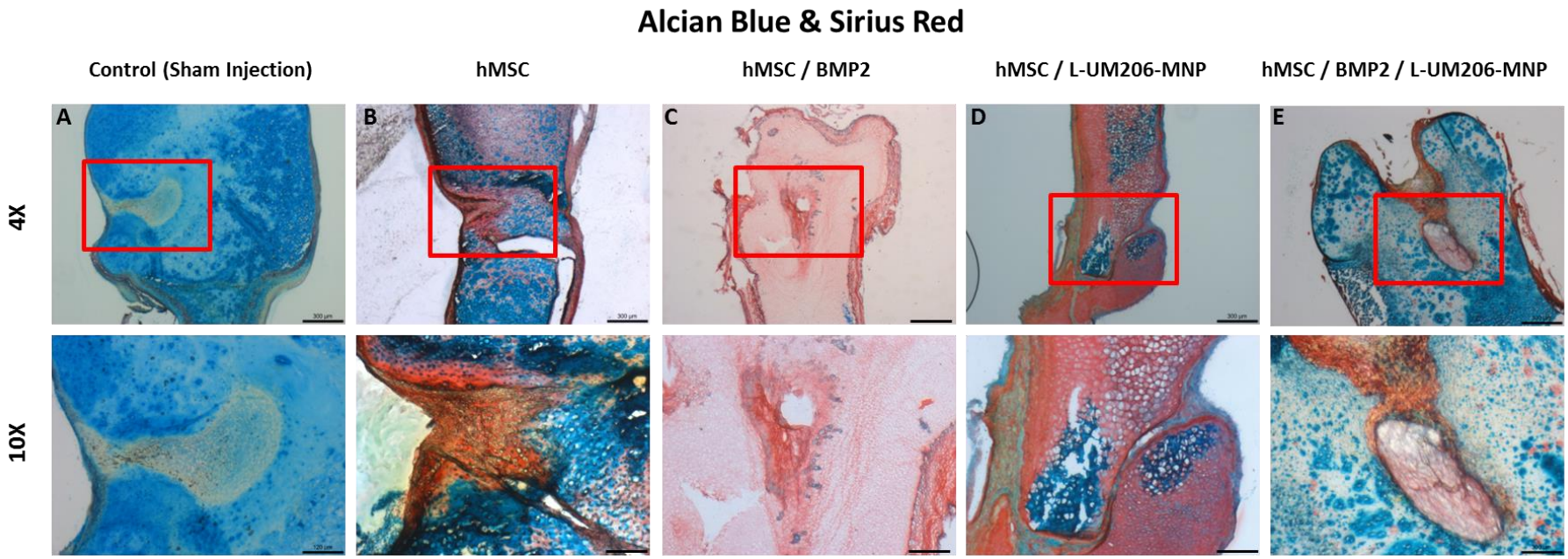

Figure 4.17. Tissue remodelling after L-UM206-MNP injection.
Alcian blue and Sirius red staining showing Glycosaminoglycan (GAG) and Collagen deposition in femur histology sections. Sham injected (control) femurs (A) showed little evidence of epiphyseal tissue remodelling after injection. In contrast Injection of hMSC alone (B), hMSC with BMP2 microparticles (C), hMSC labelled with L-UM206-MNP (D) and L-UM206-MNP co-injected with BMP2 microparticles (E) resulted in increased collagen deposition and tissue remodelling at the injection sites . Higher magnification images are shown in the bottom row. Scale bars represent 300 µm (top row) and 120µm (bottom row) respectively, Images representative of n=8 shown.

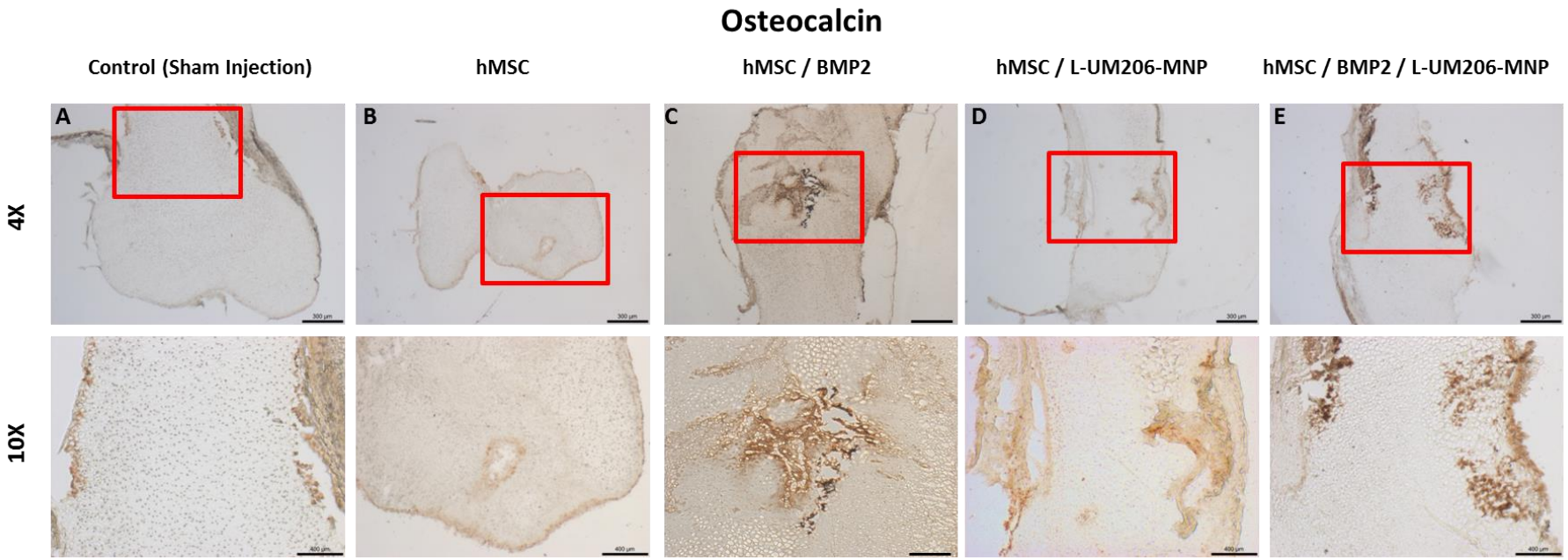

Figure 4.18. Matrix formation after L-UM206-MNP injection.
Immunohistochemistry staining for Osteocalcin in femur histology sections. Sham injected (control) femurs (A) showed little evidence of epiphyseal osteocalcin production after injection. In contrast Injection of hMSC alone (B), hMSC labelled with L-UM206-MNP (C) and L-UM206-MNP co-injected with BMP2 microparticles (D) resulted in increased Osteocalcin deposition at the injection sites . Higher magnification images are shown in the bottom row. Images representative of n=8 shown.

4.4 Discussion

4.4.1 Role of Wnt signalling in Osteogenesis

The complex role of Wnt signalling on the regulation of hMSC fate is well known. Wnt has been shown to have contradictory actions on MSC fate with both inhibitory and promoting effects on MSC osteogenesis. Previous work has shown that Wnt3a promotes MSC proliferation and maintains multipotency (Boland et al., 2004) whilst other groups have shown that high doses of exogenous Wnt3a can promote MSC osteogenesis, and for MSC which are already committed to the osteogenic lineage Wnt has also been shown to stimulate their differentiation (Ling et al., 2009), (De Boer et al., 2004b). In this chapter the effects of MNP mediated Wnt stimulation on hMSC osteogenesis was explored *in vitro* by examining expression of osteogenic and matrix associated markers. Finally, the effects of MNP stimulation coupled with BMP2 released from microspheres were investigated on bone formation in an *ex vivo* foetal femur model.

4.4.2 Effects of MNP on Alkaline phosphatase activity

Alkaline phosphatase (ALP) is an established marker of osteogenesis (Aubin, 2001) and is a widely used indicator of osteogenic differentiation and a predictor of the osteogenic potential of hMSC (Kulterer et al., 2007), (Birmingham et al., 2012). In these experiments treatment of cells with either Linear UM206-MNP (L-UM206-MNP) or Cyclic UM206-MNP (C-C UM206-MNP) alone resulted in minor elevations in ALP activity over 21 days. Whilst a further increase was observed when these MNP were applied in conjunction with magnetic field stimulation. This indicates a positive role of UM206-MNP on MSC osteogenesis and highlights the enhancing effects when magnetic field stimulation of MNP is used. Treatment with Wnt-conditioned media also elevated ALP activity at the earlier time-points but was reduced after 21 days. ALP activity is known to fluctuate

during hMSC osteogenesis (Jaiswal et al., 1997), particularly in the presence of mechanical forces (Yourek et al., 2010). The differences observed between UM206-MNP mediated ALP activity and the effects observed by Wnt-Conditioned media may be explained by the differing effects of mechanoactivation by UM206-MNP and the dose-response effects of Wnt signalling on MSC osteogenesis (Ling et al., 2009), (Janeczek et al., 2016). Continual Wnt pathway stimulation by Wnt-conditioned media may therefore be resulting in reduced end-point osteogenic differentiation of hMSC.

4.4.3 Changes in DNA and total protein content in response to MNP

The DNA and total protein content of cells are commonly used as indicators to assess changes in cell proliferation. In these experiments treatment of hMSC with L-UM206-MNP or C-C UM206-MNP both caused increases in DNA content at the early time-point when applied with magnetic field stimulation. Cyclic UM206-MNP (C-C-UM206-MNP) also increased DNA at the later time-point, whereas treatment with Wnt-CM consistently led to increases in DNA content over all time-points. Increased cell proliferation is a known to be both a response to Wnt signalling and part of the osteogenic induction process (Hoffman and Benoit, 2015), (Luu et al., 2009). Increased hMSC proliferation in response to UM206-MNP or Wnt may therefore be an indicator of increased hMSC osteogenesis. In the case of total protein, treatment with Linear UM206-MNP (L-UM206-MNP) caused minor changes on total protein production whilst Cyclic UM206-MNP (C-C-UM206 MNP) with magnetic field in particular led to increased protein production at all time-points. Total protein production was also increased by Wnt-Conditioned media (Wnt-CM) at each time-point. These trends may be linked to the increased cell numbers which were evident by the increased DNA content of the Cyclic UM206-MNP and Wnt-conditioned media groups. When ALP activity was normalised to DNA content, to account for changes in cell

proliferation, an enhancement of early ALP activity was observed in both UM206-MNP and Wnt conditioned media treated groups in particular. At later time-points L-UM206-MNP continued to elevate relative ALP activity whilst Wnt-conditioned media reduced relative ALP activity. These results suggest that MNP-mediated stimulation and Wnt stimulation of hMSC have different effects on the progression of hMSC osteogenesis. Overall these results suggests that MNP treatment is having a positive effect on cell proliferation and ALP activity in a manner that may be more beneficial than prolonged and constant treatment with Wnt3a alone.

4.4.4 Effects of MNP on *in vitro* monolayer MSC osteogenesis

The effects of UM206-MNP stimulation on matrix production and mineralisation were also investigated. It was found that intermittent stimulation of hMSC with L-UM206-MNP over 28 days resulted in some increases in collagen synthesis, matrix maturation as shown by Osteocalcin (and to a lesser extent Osteopontin) staining and matrix mineralisation. All of these markers are indicative of a differentiated osteoblast phenotype (Marom et al., 2005), (Birmingham et al., 2012), (Delaine-Smith et al., 2012). In contrast treatment with Wnt-CM over 28 days resulted in marked increase in collagen synthesis but a decrease matrix mineralisation. The discrepancy between the outcomes of L-UM206-mediated and Wnt-mediated pathway activation on hMSC osteogenesis could again be explained by the apparent differential dose-response effects of Wnt signalling which was also seen with ALP activity. The results from chapter 3 suggest that Wnt pathway activation through L-UM206-MNP is a transient stimulus which, in the context of MSC osteogenic differentiation, is initially beneficial for lineage commitment to osteogenesis but enables terminal differentiation after signal dissipation. This agrees with the findings of Ling et al. and Janeczek et al. who also showed that Wnt is beneficial for

hMSC commitment to the osteogenic lineage but Wnt withdrawal is ultimately required for terminal osteoblast differentiation and robust bone formation (Ling et al., 2009), (Janeczek et al., 2016)

4.4.5 Application of MNP in an *ex vivo* femur model

This chapter introduces the foetal chick femur which is an established model of endochondral bone development. Delivery of MSC was confirmed by fluorescent tracking of the tagged cells 24h after injection. The effects of combined stimulation of Wnt transduction *via* L-UM206-MNP and BMP2 release from polymer microparticles on bone formation were then investigated over 14 days. This combinatorial strategy utilising controlled release of growth factors is particularly relevant and has applications in tissue engineering approaches for regenerating bone defects (Kirby et al., 2011). In this model, injection of BMP2 releasing microparticles with MSC increased total bone volume across the whole femur. This can be expected due to the well-known anabolic properties of BMP2 on bone formation (Chen et al., 2007). Interestingly, no overall effect on total bone volume or density was seen when BMP2 was injected in conjunction with hMSC labelled with L-UM206-MNP but this treatment had the greatest effect on bone collar density. This highlights the complex nature of Wnt and BMP2 signalling cross-talk and suggests that tight regulation of pathway activity is required for optimal bone formation. When bone collar volume and density were compared relative to the total bone volume and density, bone formation at the bone collar was found to be increased by injection of BMP2 and L-UM206-MNP and resulted in increases in bone density. This indicates the presence of a more mature, functional bone matrix and suggests enhanced bone development in response to MNP mediated Wnt activation and BMP2 signalling. This was confirmed by histological staining for calcium which showed clear evidence of

mineralisation and IHC for osteocalcin production both of which were observed at the injection sites. Future work should interrogate other non-collagenous bone markers expressed in the foetal femur injection sites such as Alkaline phosphatase and Osteopontin. The differential effects of MNP and/or BMP2 on bone volume and density observed at the diaphysis or epiphyses suggest that the complex spatial and temporal signalling and the different cell types present across the femur may be impacting on the degree of hMSC and chick cell induced bone formation in these zones. Previous work from (Smith et al., 2013) have shown that different cell populations isolated from distinct zones of the chick femur have different morphologies and phenotypes; it is therefore plausible that injection of cells into different zones of the femur is resulting in different outcomes in terms of tissue generation.

4.4.6 Cross-talk between Wnt and BMP2 signalling in bone formation

The interactions between Wnt and other cell signalling pathways in stem cells are complex. Amongst these interactions, a clear relationship between Wnt and BMP2 signalling in the regulation of bone formation has been observed. For example Wnt and BMP2 have been shown to act reciprocally to regulate osteoblastic differentiation of both hMSC (Cook et al., 2014) and mouse C3H10T1/2 cells (Bain et al., 2003). There is also evidence to suggest that BMP induced osteoblast differentiation is dependent on Wnt pathway activity (Chen et al., 2007), (Rawadi et al., 2003). Other studies have found that BMP2 signalling resulted in the upregulation of Wnt antagonists Sfrp2 (secreted frizzled related protein 2) and Wif1 (Wnt inhibitory factor 1) in the late phase of MSC differentiation (Vaes et al., 2005). Evidence also exists for the activation of TCF/LEF response elements by both BMP/TGF and Wnt signalling during development (Letamendia et al., 2001). In the experiments presented here the ability of L-UM206-MNP

with BMP2 to trigger bone formation may be attributed to the reciprocal relationship between Wnt and BMP signalling where L-UM206-MNP act to initially trigger lineage commitment via Wnt signalling before promotion of terminal differentiation by BMP2. This may explain why the combination of L-UM206-MNP and BMP2 resulted in the greatest enhancement of relative bone formation in this model. In these experiments an enhancement of bone formation mediated by L-UM206-MNP was seen in the *ex vivo* femur model compared to *in vitro* bone formation by cells cultured in monolayer. This observation underlines how the complexity of relevant models which consist of multiple cell types and signalling gradients arranged in 3-dimentions are all needed to obtain optimum tissue engineered constructs.

4.5 Conclusions

The role of Wnt signalling in stem cell maintenance, differentiation and tissue development is well established. The results presented here indicate that the use of conjugated magnetic nanoparticle technology coupled with magnetic fields to activate Wnt signalling may be useful in modulating signal transduction with positive outcomes on cell differentiation and bone formation. This strategy has applications both as an *in vitro* research tool and potentially as a future clinical treatment in orthopaedics. Due to the expense and difficulty in preparing recombinant Wnt protein, easily synthesised ligands conjugated to magnetic nanoparticles present a viable method for activating Wnt pathways for the control of cell signalling and direction of stem cell differentiation. The results from this chapter show that UM206 peptide functionalised MNP can modulate Wnt pathway activation and that these MNP can modestly augment end-stage hMSC

osteogenesis with subsequent promotion of localised bone and matrix formation in an *ex vivo* foetal femur model. Importantly, this magnetic activation approach has also been shown to work in synergy with the controlled release of bone promoting growth factors such as BMP2, which already have proven relevance in the clinic. As such, the applications of this approach for the magnetic activation of stem cells for tissue engineering are apparent and indicate a positive step forward in the development of injectable cell therapies.

Chapter 5: Engineering the stem cell niche with Wnt

5.1 Introduction

The previous chapters of this thesis have focused on the use of magnetic nanoparticles for the remote modulation of Wnt signalling. The application of magnetic nanoparticles in this manner essentially allows remote control of signalling magnitude and duration. However the spatial and directional control of signalling at the cellular level using this approach is somewhat limited due to the fact that MNP must be applied in solution. One of the most important roles of Wnt signalling is the regulation of adult tissue homeostasis and the maintenance of the stem cell niche. Part of the mechanism behind this role involves maintaining the balance between promoting stem cell self-renewal and orchestrating lineage commitment (Clevers et al., 2014), (Baksh and Tuan, 2007). One particularly important aspect of Wnt mediated niche maintenance is the role of spatial Wnt gradients which have been shown to be critical for properly controlled and normal tissue development (Heller and Fuchs, 2015). There is now great interest in the application of Wnt proteins in stem cell research and tissue engineering. Current research utilising Wnt proteins revolves around the use of purified and soluble recombinant Wnt protein. Consequently, soluble Wnt often requires storage in detergents to preserve the bio-activity of the protein (Willert et al., 2003). The perceived benefit of this is that it allows the generalised and global application of Wnt protein to a cell population at relatively high concentrations. However application of Wnt in this manner excludes the spatial and directional presentation of Wnt gradients to target cells. This limitation is also a factor to consider in the current system for the magnetic activation approach introduced in the previous chapters. Recent work by Habib *et al*. has shown that spatial orientation of Wnt signalling using Wnt-3a immobilised on beads can initiate asymmetric

division of embryonic stem cells. In this system the daughter cell proximal to the Wnt signal retained a stem cell phenotype whilst the daughter cell distal to the Wnt signal expressed markers of differentiation (Habib et al., 2013). This highlights the crucial role of spatially presented and localised Wnt signalling on stem cell fate.

As discussed in the previous chapters there is a clear role for human mesenchymal stem cells (hMSC) in tissue engineering. Furthermore, there is a clear role for Wnt signalling as a critical regulatory pathway affecting MSC self-renewal and osteogenic lineage commitment (De Boer et al., 2004b). Wnt signalling also plays a role in regulating the migratory capacity of MSC. Wnt pathway activation using Wnt3a or LiCl has been shown to promote MSC migration through human ECM coated Transwell filters *in vitro* (Neth et al., 2006), (Kollar et al., 2009). Therefore, there is a demonstrable role for the modulation of Wnt signalling and, in particular, Wnt gradients for the control of MSC osteogenic differentiation for tissue engineering purposes.

The primary aim of this chapter was to introduce a novel tissue engineering platform which utilises Wnt protein immobilised on glass slide surfaces. These slides can be overlaid with cells and biocompatible scaffold materials such as Collagen 1 hydrogels. This system can then be used as a screening tool to develop putative tissue engineered constructs whilst allowing the investigation of the role of localised Wnt gradients in the maintenance of the stem cell niche and stem cell differentiation in a bone tissue engineering context.

5.2 Methods

5.2.1 Preparation of immobilised Wnt sides

Wnt3a immobilised slides were prepared and provided by Dr S. Habib (Kings College London). Recombinant Wnt-3A was acquired from Drosophila S2 cells expressing Wnt-3A. Wnt protein was purified by Blue sepharose affinity and gel filtration. Alternatively, commercially available Wnt 3A (R&D systems) was reconstituted in 0.1% BSA to 40ng/µL. This was diluted in PBS to a final volume of 40uL per drop and used to cover a working area of 64mm^2 on VSS25 Vantage Silylated Aldehyde Slides (CEL Associates) with a Wnt3A concentration range of 10-40ng. Wnt coated slides were incubated for 1h at room temperature. The biological activity of immobilised Wnt3a was confirmed using a SuperTOPFlash reporter system expressed in L cells using a luciferase reporter assay (data not shown). Control surfaces (consisting of inactivated Wnt3a) were prepared by incubating Wnt3a coated slides with 20mM DTT for 30mins at room temperature. All coated surfaces were washed 3x with PBS and incubated with basal media for 10mins before seeding with cells.

5.2.2 Cell culture

hMSC were sourced and processed as detailed in chapter 2. Cells were expanded in basal media (10% FBS, 1% L-glutamine and 1% penicillin/streptomycin) (Lonza) with two media changes performed per week. Cells were passaged once per week and cells between passage 2 and 5 were used in all experiments. Cells were seeded onto the Active Wnt 3a or DTT treated control substrates at 80000/cm^2 and cultured for 24h after which 100µL of 1mg/mL rat tail Collagen 1 (BD biosciences) pre-neutralised with 1M NaOH (25µL per mL of gel) and diluted in serum-free media was laid over the cell monolayer. Samples were

incubated overnight at 37^{o}C, 5% CO_2 to complete gelation. Media was then changed to Osteogenic inducing media consisting of basal media with the addition of Dexamethasone (0.1µM), β-Glycerophosphate (β-GP) 10mM, Ascorbic Acid (50µM) and non-essential amino acids (NEAA) 1x v/v. Samples were cultured for 7 days with 2 media changes performed. A diagram depicting the experimental setup is shown in Figure 5.1.

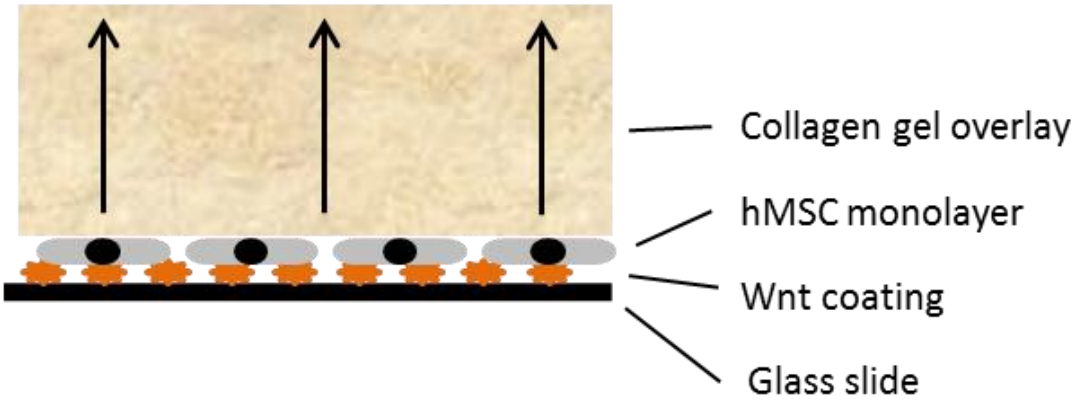

Figure 5.1. Schematic of Wnt slide.
Schematic representation of the Wnt slide. Wnt protein is immobilised onto glass slides. Cells are seeded onto the Wnt-coated surface then overlaid with collagen gel. Cell migration and phenotype can then be monitored throughout the system.

5.2.3 Immunocytochemistry

Media was aspirated and cells washed with PBS (Sigma), then fixed with 4% PFA (Sigma) in PBS for 10mins. Cells were permeabilised with 0.1% Triton-X in PBS (Sigma) for 10mins then then blocked with 2% BSA (Fisher) in PBS for 2h at room temp. Cells were then incubated with Anti-Human Stro1 (R&D systems) diluted 1:50 in 1% BSA in PBS overnight at 4^{o}C. Samples were washed 3x 5mins with PBS before incubation with Anti-Mouse-FITC (Sigma) 1:1000 in 1% BSA in PBS for 1hr at room temperature. Samples were washed 3x 5mins with PBS. This procedure was repeated for Osteocalcin staining where cells were re-blocked with 2% BSA in PBS for 2h before incubation with Anti-Human Osteocalcin

(R&D systems) diluted 1:1000 in 1% BSA in PBS overnight at 4^{o}C. Cells were washed 3x 5min with PBS before incubation with Alexa Flour Anti-Mouse-647 (Life Technologies) 1:2000 in 1% BSA in PBS for 1hr at room temperature. Samples were washed 3x 5mins with PBS and counterstained with DAPI (Sigma) diluted to 1µg/mL in PBS for 10mins at room temperature. DAPI solution was aspirated and samples stored in PBS at 4^{o}C before imaging.

5.2.4 Imaging

Imaging was performed on an inverted axio-imager fluorescence microscope (Zeiss) using Zen 2 (Bleu edition) software. Z-stacks were obtained with a step size of 1.5µm obtained from a total of 8 regions across two gels for each condition.

5.2.5 Image Analysis

The gels were separated into three layers in the z-dimension, a lower layer constituting the lower 46% (up to 72µm) from the gel base, a middle layer constituting up to 85% (up to 132µm) from the gel base and an upper layer constituting up to 100% (up to 156µm) from the gel base. The total number of migrating cells (cells across all migration layers) was determined from 8 regions across the gels along with the average cell number per gel layer to assess differences in migration patterns. To overcome the variation in cell number across the gel and high levels of fluorescence intensity in the base where cells were most confluent, the background corrected average Stro1 and Osteocalcin staining intensity per cell for the base layer and the three identified migration layers was determined using ImageJ (v1.48s).

5.2.6 Histological staining

Samples were stained with 1% w/v Alizarin Red S solution (in d.H_2O) for 10mins at room temperature then washed 5x 5mins with d.H_2O. Samples were imaged using a Leica S6D dissection microscope fitted with a Nikon D500 digital camera.

5.2.7 Statistical analysis

The cell migration per gel layer was assessed using 1-way ANOVA with post-hoc Tukey tests with statistical significance at 95% confidence level determined using Mini-tab (v16). Stro1 and Osteocalcin staining intensity was assessed using Kruskal-Wallis with statistical significance at 95% confidence level. Post-hoc Mann-Whitney tests were used to determine statistically significant differences between groups.

5.3 Results

5.3.1 Wnt 3A increases hMSC migration

The effects of immobilised Wnt on hMSC migration through collagen gel were monitored using immunocytochemistry. MSC were seeded onto immobilised Wnt surfaces at confluent density, overlaid with collagen gel and cultured in osteogenic media for 7 days. Confocal microscopy of the DAPI stained cells revealed a clear increase in the migratory capacity of the cells in response to the active Wnt3a surface (Figure 5.2). In contrast, cells cultured on the control surface consisting of inactivated Wnt 3a displayed a basal level of cell migration. Quantification of the total numbers of cell migration after 7 days confirmed the migratory capacity of cells cultured on the Wnt surface (151 migrated cells) compared to the control surface where a total of 13 migrated cells were observed across 8 regions. This increase in the migratory capacity of MSC was also reflected in the spatial

location of cells in the gels where a significant 4 fold increase in average cell numbers were observed in the lower section of the gels when cells were cultured on the Wnt surface compared to the inactive Wnt control surface (Figure 5.3). This trend continued in the middle section and even in to the upper section of the gel (up to 156 μm from the Wnt3a surface) where increased cell migration was observed in response to the active Wnt surface. Whilst on the control surface lower cell numbers were observed in the middle section and no migrated cells were observed in the upper section of the gels.

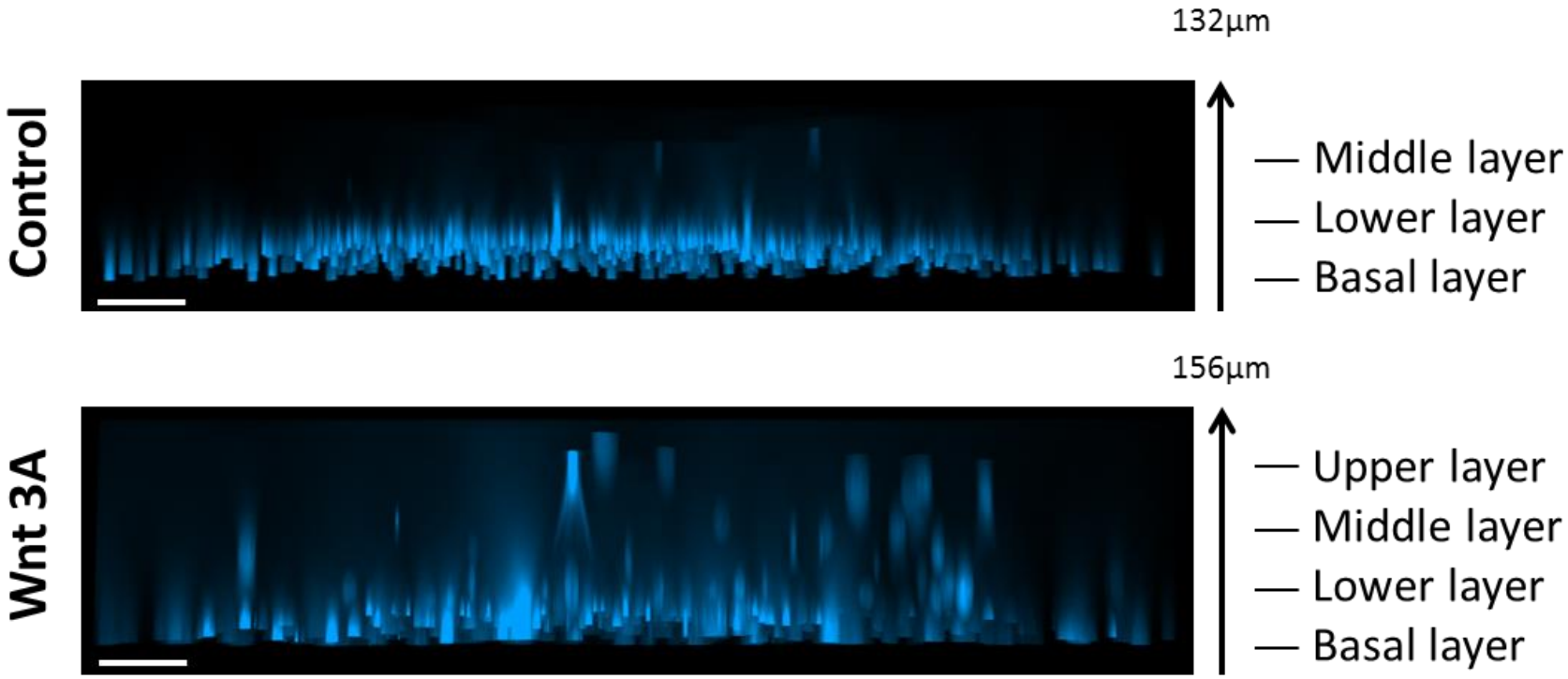

Figure 5.2. Wnt3a increases MSC migration in Collagen gel.
Confocal images of DAPI stained cells (Blue) 7 days after treatment. Fluorescent imaging was used to locate migrated cells through collagen gels. MSC cultured on Inactive Wnt 3A surfaces (Control) showed basal levels of cell migration. When MSC were cultured on active Wnt 3A surfaces (Bottom image) cell migration was noticeably increased with cells migrating further upwards through the gels. Representative images of 8 regions for each condition are shown. Scale bar represents 100µm.

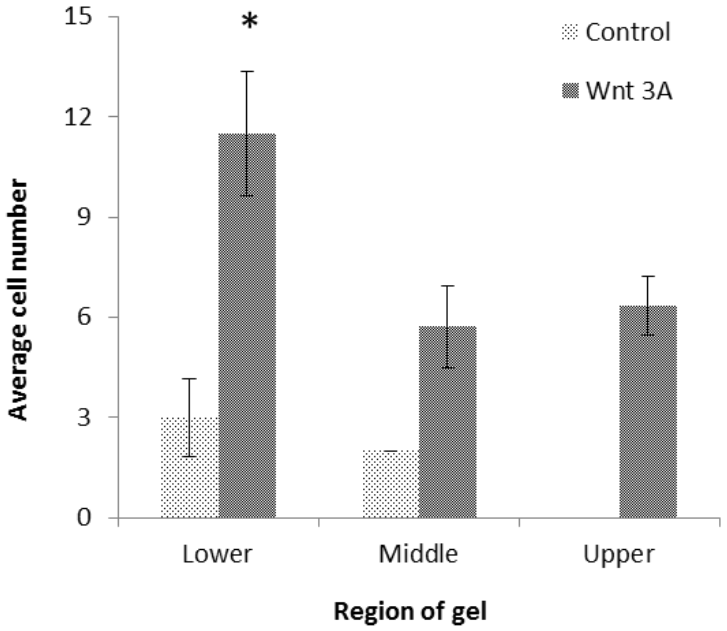

Figure 5.3. Quantification of hMSC migration in collagen gels.
Quantification of hMSC migration through Collagen gels after 7 days. The average number of cells per layer of the gels was determined. Cells cultured on the active Wnt3A substrate resulted in increased cell migration into the lower (up to 72µm / 46% gel), middle (up to 132µm, 85% gel) and upper layers (up to 156µm, 100% gel) of the gel . No cells were observed in the upper gel layers of the control groups. Values represent average cell counts counted across 8 regions from 2 gels, error bars represent SEM, * denotes $p<0.05$.

5.3.1 Wnt3a gradient influences MSC stemness and differentiation

Immunostaining of MSC was then performed for Stro1, a stemness marker for MSC and Osteocalcin, a mature marker of the osteogenic lineage in order to ascertain if the immobilized Wnt surface recapitulated the inversely correlated gradient of Stro1 and OCN which is seen *in vivo*. In this system Osteocalcin expression was found to increase as the cells migrated upward with peak Osteocalcin expression observed in cells located in the upper gel layer. This was in contrast to Stro1, which was mainly expressed in the base and lower migration layer nearest to the Wnt signal and then decreased as the cells migration upward (Figure 5.4). This effect was reduced on control surfaces where Osteocalcin and Stro1 expression both remained at basal levels. Quantification of the staining intensity of each marker was also performed and confirmed that Osteocalcin expression increased as cells migrated upwards with significant increases in Osteocalcin expression observed in the Middle and Upper gel layers (Figure 5.5). In contrast significant Stro1 expression was observed in the base and lower gel layers and decreased to approximately basal levels in the middle and upper gel layers. In the control groups both Osteocalcin and Stro1 expression remained around basal levels in each region of the gel.

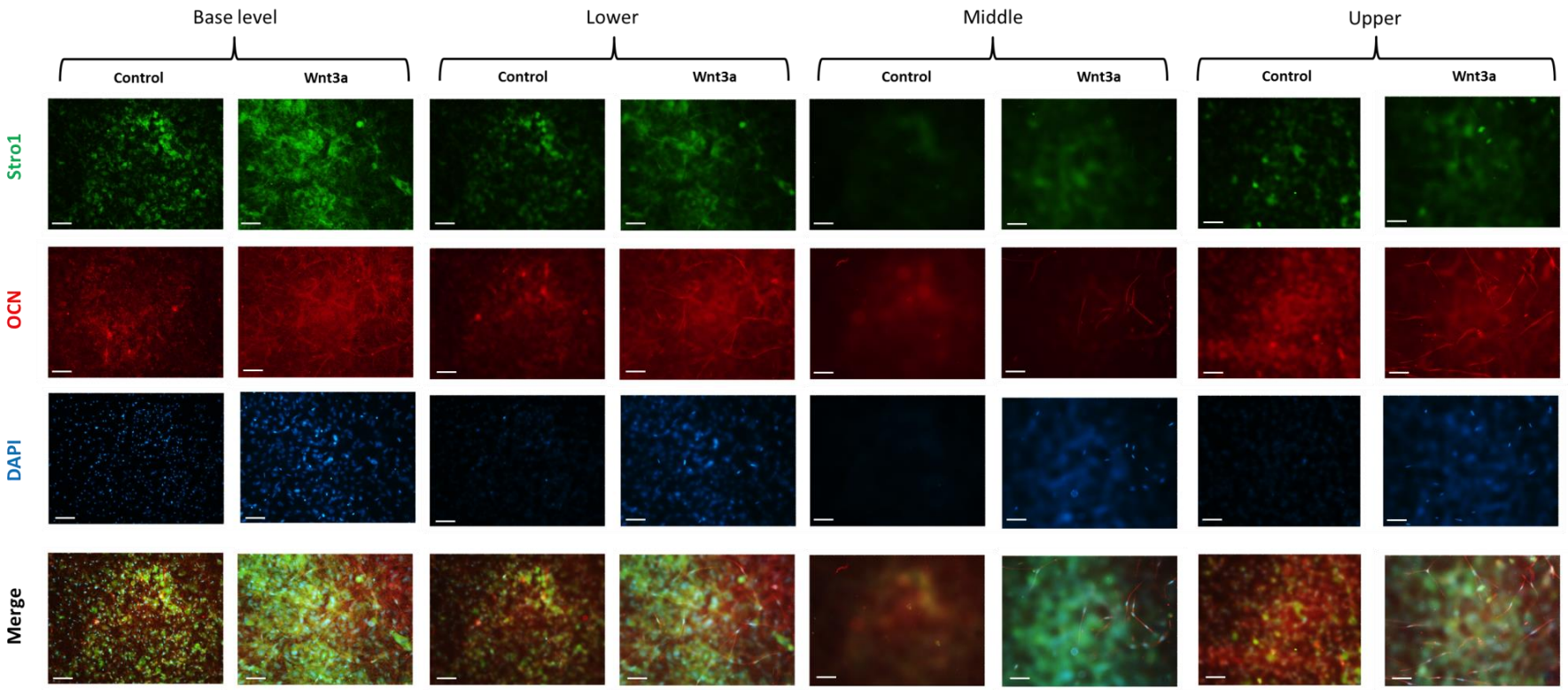

Figure 5.4. Wnt3a modulates Osteocalcin and Stro1 expression in migrating cells.
Fluorescent immunostaining for Stro1 (green), and osteocalcin (red) expression in hMSC in collagen gels after 7 days in culture on active Wnt 3A and inactive wnt3A (control) substrates. Merged images show spatial pattern of staining in relation to cell nuclei (blue) (a). Levels of osteocalcin expression were higher in upper levels of the gel (up to 156µm, 100% gel), whilst cells cultured on the inactive Wnt3a (control) substrate showed basal levels of expression. Cells cultured on the active Wnt3a substrate showed a progressive decrease in Stro1 expression through the gel with peak expression observed in the base and lower gel layers (up to 72µm / 46% gel) closest to the Wnt source, whilst cells cultured on the inactive Wnt3a (control) substrate showed overall reduced levels of Stro1 expression. Representative images shown from 8 regions of interest from two gels, scale bar represents 100µm.

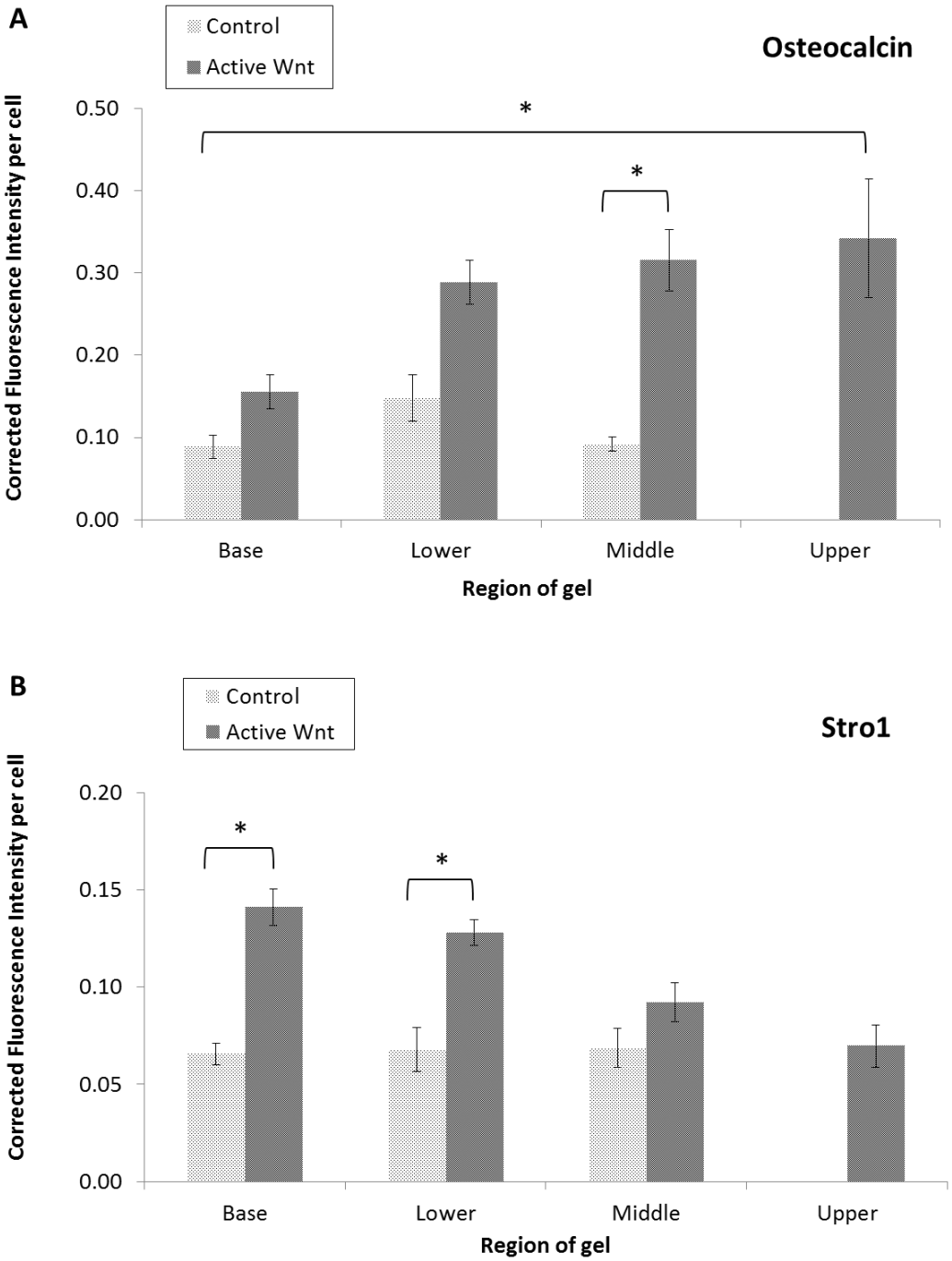

Figure 5.5. Quantification of Osteocalcin and Stro1 expression in migrating cells. Quantitation of image pixel intensity relative to cell number for osteocalcin (A) and Stro1 (B). Levels of osteocalcin expression were significantly increased in middle and upper layers of the gels (up to 156µm, 100% gel), whilst cells cultured on the inactive Wnt3a (control) substrate showed basal levels of expression (A). In contrast, cells cultured on the active Wnt3a substrate showed maximum Stro1 expression in the Base level and lower gel layer (up to 72µm / 46% gel) closest to the Wnt signal with a progressive decrease in Stro1 expression in the middle and upper gel layers, whilst cells cultured on the inactive Wnt3a (control) substrate showed overall reduced levels of Stro1 expression (B). Values represent average fluorescence intensities per cell, error bars represent SEM, * denotes $p<0.05$.

5.3.2 Wnt3a promotes early bone nodule formation

Assessment of mineralised nodule formation was also determined histologically using Alizarin red to visualise early stage calcium deposits. Cells cultured on the Wnt3a surface were shown to form putative mineralised nodules after 7 days of treatment in two out four of the gels whilst no evidence of nodule formation was observed in the gels of control surfaces (Figure 5.6).

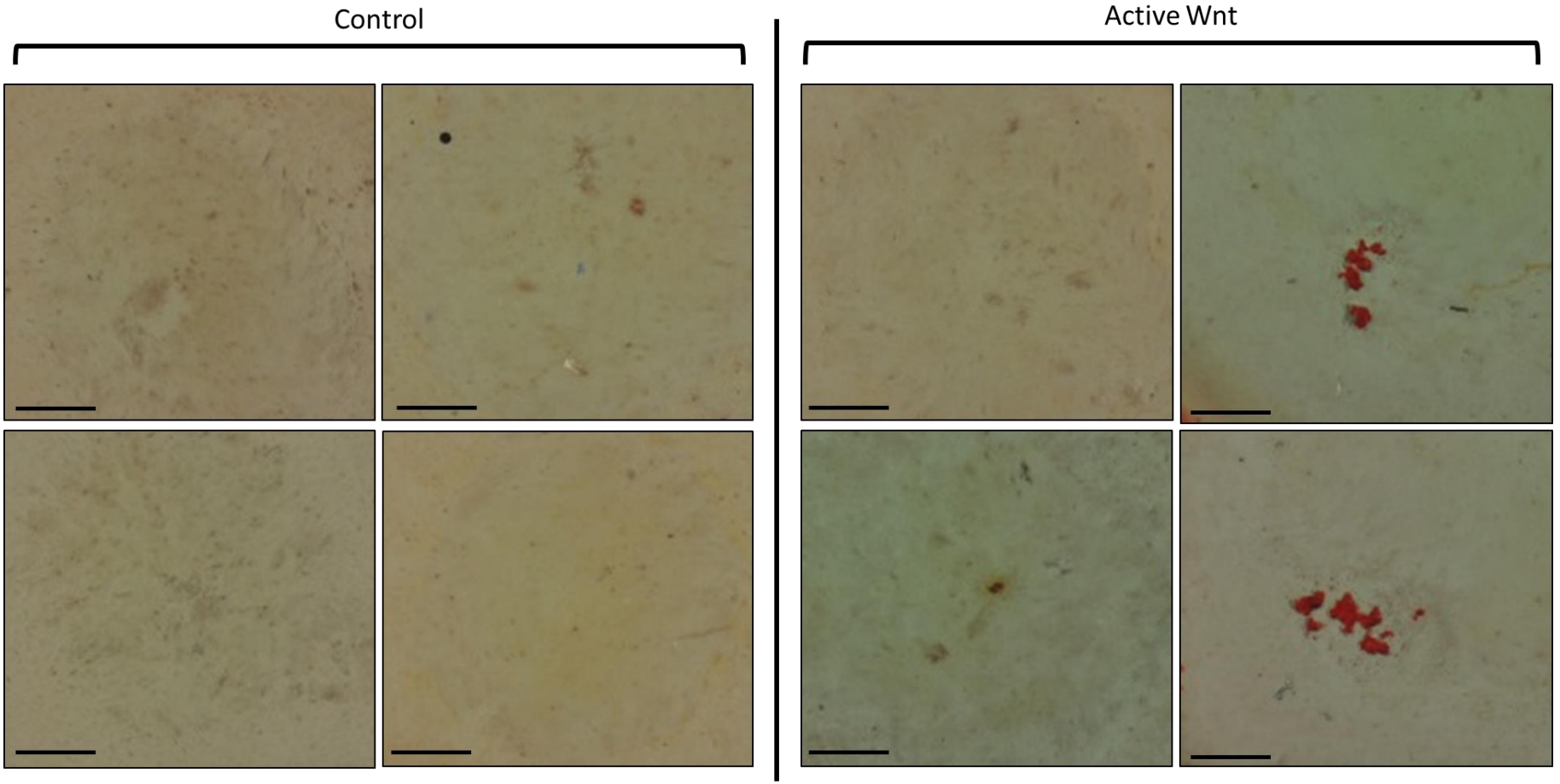

Figure 5.6. Wnt3a induces early mineralised nodule formation.
Histological staining for calcified nodule formation after 7 days of culture. Alizarin red staining indicated early formation of mineralised nodules in 2/4 gels in response to Active Wnt 3A substrates (right panels) whilst no mineralised nodules were observed in the control group (Left panels). n=4, Scale bar = 100µm.

5.4 Discussion

5.4.1 Migration inducing effects of Wnt

The results presented in this chapter indicate that there is a clear role of Wnt signalling in stimulating hMSC migration. There was a clear increase in the number of migratory cells on the active Wnt surface compared to control surfaces, and these cells migrated further into collagen gels than cells cultured on the surfaces. The migration promoting effects of Wnt have been observed in previous work, for example Neth et al. observed that Wnt3A or LiCl prompted MSC to migrate through Transwell filters coated with human ECM (Neth et al., 2006). The MSC in this system were seeded on top of a surface functionalised with Immobilised Wnt protein, this means that only the basal surface of the cells would be presented with an exogenous Wnt stimulus. Previous work has shown that localised Wnt stimuli asymmetrically imparted onto embryonic stem cells using Wnt coated beads results in asymmetric cell division. In this scenario the daughter cell proximal to the Wnt signal displayed pluripotency markers and the distal daughter cell expressed markers of differentiation (Habib et al., 2013). Therefore an asymmetric cell division response to localised Wnt stimuli may be a contributing factor behind the increased MSC migration that was seen in these experiments. It should also be noted that a basal level of migration was also seen on the control surfaces. This phenomenon could be expected due to the unsorted, heterogeneous population of MSC which was used in these experiments. Previous work has shown that subpopulations of hMSC that exhibit high endogenous Wnt pathway activity are present in heterogeneous, unsorted populations of MSC. Therefore the limited migration of cells in the control group may be a reflection of the high Wnt signalling capacity of these MSC sub-populations.

5.4.2 Role of Wnt gradients in MSC osteogenic differentiation

The role of Wnt gradients in maintaining adult tissue homeostasis is well-known, and these signalling gradients are known to play a role in regulating the MSC niche (Kim et al., 2015). As discussed in the previous chapter, Wnt signalling plays a pivotal role in maintaining the self-renewal of MSC whilst withdrawal of Wnt signals is known to allow progression of MSC differentiation down the osteogenic lineage. A dose-response relationship between Wnt pathway activity and MSC differentiation has previously been observed whereby a reduction of Wnt signalling is required to enable MSC differentiation *in vitro* (Ling et al., 2009), (Janeczek et al., 2016). In the work presented here, a clear increase in Stro1 expression was observed at the basal layer closest to the Wnt signal indicating maintenance of the stem cell population. Whilst the inverse relationship was observed in Osteocalcin expression, a mature bone cell marker. Here, Osteocalcin expression increased as cells migrated away from the Wnt signal, which indicates a more differentiated phenotype of these cells. This inverse expression pattern of stem cell markers such as Stro1 and mature bone markers as cells progress from a stem cell phenotype to a differentiated bone cell phenotype has been observed before. Previous work has demonstrated that human osteoblast-like cells extracted from trabecular bone and human bone marrow stromal cells have different bone marker expression and capacities for bone generation depending on the expression of their surface markers. Cells that were expressing Stro1 were shown to have a limited bone forming capacity and expressed lower levels of bone markers whilst ALP+ cells displayed higher expression of bone markers and had a higher bone forming capacity (Gronthos et al., 1999), (Stewart et al., 1999). Another factor to consider is the mitogenic effects of Wnt stimulation on osteo-progenitor cell proliferation. Previous work has suggested that Wnt enhances

osteo-progenitor proliferation. This suggests that Wnt activity is an important driver of bone formation (Baksh et al., 2004), (Kato et al., 2002). The work presented in this chapter also supports this hypothesis. An increase in migratory cell numbers were observed in response to Wnt 3A, this may be explained by enhanced migration followed by proliferation of these osteo-progenitors before dissipation of the Wnt signal which allowed differentiation of the migrated cells. This hypothesis requires further investigation.

Finally, the collagen gel constructs were stained for calcium to determine if the Wnt surfaces could affect osteogenic differentiation and end-stage mineralised nodule formation, which is an indicator of terminally differentiated osteoblasts. In this experiment, clear evidence of early stage mineralised nodule formation was observed in 2/4 of the Wnt3a gels whilst no nodules were observed in the control gels. This indicates a clear role of Wnt signalling gradients in MSC osteogenesis and formation of mineralised nodules. As discussed previously, the effects of Wnt signalling on MSC differentiation *in vitro* are often contradictory depending on the experimental conditions and cell lines used but it is clear that regulated Wnt signalling is required for bone development. Overall, these results suggest that the immobilised Wnt system presented here is potentially capable of maintaining and recapitulating the stem cell niche whilst promoting migration and then differentiation of stem cells further away from the Wnt signal. Further work is needed to fully dissect the phenotype of both basal layer cells and migrated cells. The level of Wnt pathway activity in these populations should also be determined in order to confirm the effects of Wnt gradients on MSC maintenance and differentiation. In the broader context of this thesis, it could also be postulated that Wnt gradients and

asymmetric cell division may be contributing factors governing hMSC osteogenesis mediated through MNP induced Wnt pathway activation described in chapter 4. The role of asymmetric cell division in MNP-mediated direction of MSC fate should be investigated to assess this.

5.5 Conclusions

The role of Wnt in maintaining the stem cell niche is well-known. One important aspect of niche regulation is the formation of spatial signalling gradients which regulates cell fate depending on the presentation and directionality of signalling proteins to cells. The results presented here demonstrate the importance of spatial presentation of Wnt in the regulation of the MSC niche which has been shown to be important for MSC migration and subsequent commitment to the osteogenic lineage. The immobilised Wnt platform may be able to improve the sustainability of the Wnt signal compared to the use of soluble Wnt whilst providing a localized basal Wnt stimulus to cells. This strategy has clear implications for the control of growth factor delivery that should inform the development of tissue engineered solutions for regenerative medicine.

Chapter 6: General Discussion

6.1 The importance of Wnt signalling: from stem cells to bone

The role of Wnt signalling in the regulation of stem cell maintenance and differentiation is well known. These pathways also play critical roles in regulating bone development from the limb bud to adult bone formation. The control of Wnt signalling for therapeutic purposes is therefore of particular relevance in a tissue engineering context. Manipulation of these pathways can be used to regulate stem cell fate in order to augment tissue development. It was hypothesised that magnetic activation of Wnt signalling could have beneficial effects on stem cell differentiation in a bone tissue engineering context. This thesis has introduced prototype engineering platforms which have been developed to explore the role of Wnt signalling as a regulator of the stem cell niche in bone development. Stimulation of hMSC using Wnt receptor targeting MNP was shown to activate Wnt/β-catenin signalling. Although signalling activation in this manner had modest effects on hMSC differentiation in vitro, combining this approach with BMP was subsequently shown to have a beneficial effect on bone formation in an *ex vivo* model of bone development. The results presented in earlier chapters suggest an important and beneficial role of Wnt signalling gradients in the control of stem cell migration and differentiation. This aspect of signalling regulation raises important implications for the development of future tissue engineering strategies.

6.2 Wnt signalling and regulation of the stem cell niche

Many studies utilising Wnt proteins for cell and tissue engineering purposes focus on the general application of different Wnt doses to a cell population. One often overlooked aspect in tissue engineering is the spatial role of signalling gradients which are required

for normal tissue development *in vivo* (Heller and Fuchs, 2015). This thesis has briefly highlighted the importance of Wnt gradients in the regulation of the MSC niche using an immobilised Wnt platform. This approach has been shown to be beneficial in maintaining a stem cell phenotype in cells proximal to the Wnt signal whilst promoting migration in a collagen gel and subsequent enhancement of differentiated markers in the cells distal to the Wnt signal. One mechanism behind this observation may be Wnt induced asymmetric cell division. This process has been shown to be an important factor regulating ES cell fate and results in maintained stemness in the daughter cell proximal to the Wnt signal whilst promoting differentiation markers in the cell distal to Wnt (Habib et al., 2013). In the hMSC system presented here, asymmetric cell division may be one of the mechanisms influencing cell migration and differentiation. Taken together, these results highlight the advantages of controlled and patterned delivery of growth factors in tissue engineering approaches allowing the development of functional tissues. This aspect of patterned growth factor delivery should inform future studies and be investigated further.

6.3 Remote modulation of Wnt signalling using MNP

The work presented in this thesis has demonstrated the possibility of remotely targeting and activating Wnt signalling pathways using MNP targeted to Frizzled receptors at the cell membrane. With the use of oscillating magnetic fields, this has allowed the application of targeted mechanical stimulation of Frizzled receptors for remote activation of Wnt signalling pathways. This level of control of cell signalling is a promising development that brings distinct advantages over traditional drug delivery techniques that apply systemic and generalised drug doses. This is particularly important in the

context of Wnt signalling where systemic delivery of therapeutic agents is complicated due to the critical roles this pathway plays in development and disease in many tissues. Therefore the control afforded by magnetic activation is particularly advantageous for avoiding unwanted side-effects of aberrant Wnt pathway activation.

6.3.1 Conformation dependent activities of UM206

The main MNP targeting strategy in this work involved the use of the Frizzled binding peptide UM206. This peptide is derived from a fragment of the amino acid sequence from Wnt3a and Wnt5a and exists in two conformations. In the linear conformation, UM206 has been shown to antagonise Wnt signalling in HEK293 cells. UM206 can also be induced into a cyclic conformation, which is formed by disulphide bond formation between two cysteine residues in the peptide. In the cyclic conformation UM206 has been shown to act as an agonist of Wnt signalling in HEK293 cells (Blankesteijn Wessel Matthijs, 2010). The experiments presented here suggest that the signalling ability of UM206 to act as an agonist or antagonist of Wnt signalling is different in hMSC compared to HEK293 cells. This may be due to many factors. One possible explanation is that the signalling dynamics may be different between HEK293 cells and MSC as a result of different expression patterns of Wnt receptors, inhibitors or intracellular mediators. Indeed the conformational dependent activity of UM206 was originally observed in HEK293 cells which were engineered to overexpress Frizzled 2 receptors, whilst the studies presented here used hMSC with endogenous Frizzled receptor expression. As a result this may alter the binding kinetics or affinity of UM206 to bind Frizzled receptors endogenously expressed in comparison to Frizzled overexpressing cells. A thorough study comparing the expression profile of Wnt components in hMSC and HEK293 cells would help to test this hypothesis. Interestingly linear-UM206 was found to activate signalling when bound to

MNP whereas cyclic-UM206-MNP did not. There are multiple possible reasons for this observation. Firstly, the cyclic peptide is known to have a lower affinity for Frizzled receptors and displays lower bio-activity. In HEK293 TCF/LEF reporter cells the EC50 value of the cyclic peptide was measured to be 2.10^{-8}M, in contrast the linear peptide displayed an IC50 value of 10^{-10}M (Blankesteijn Wessel Matthijs, 2010). These differences suggest that the linear peptide binds more efficiently to Frizzled receptors and so may be more potent in activating signalling. Secondly, the activating activity of Linear-UM206-MNP may be expected if the mechanism of pathway activation involves the simultaneous binding and formation of multiple Frizzled dimers which has been suggested previously (Carron et al., 2003). It is therefore plausible that the mechanical forces exerted by addition of magnetic field stimulation enhances peptide-receptor binding or causes further receptor clustering. This hypothesis could be investigated using Fluorescence Resonance Energy Transfer based assays. With respect to the inactivity of C-C-UM206-MNP, it is possible that the MNP and Cyclic-UM206 conjugation process may be inducing changes to the conformation of the cyclic peptide which could result in diminished Frizzled binding affinity. It is also possible that the Cyclic peptide-MNP conjugation process is not as efficient, which was suggested by the coating efficiency studies presented in chapter 2. Furthermore, the conjugation of multiple cyclic peptides to MNP may be inducing steric hindrance effects, which may also reduce the binding efficiency to Frizzled 2. This hypothesis could be explored further using binding assays to quantify the degree of MNP binding to cells when MNP are coated with Linear or Cyclic UM206. Another explanation could be related to the natural oxidising effects of the iron oxide core of MNP. This property of iron oxide could be inducing di-sulphide bond formation in Linear UM206.

Hypothetically, this could switch the linear peptide to the cyclic conformation and therefore alter its bioactivity.

6.4 Use of Magnetic Nanoparticles

Magnetic nanoparticles have emerged as extremely useful and adaptable tools in science, engineering and medicine. There is now a large scope for the application of nanoparticles of different sizes and functionality in many fields (Bao et al., 2015), (Salata, 2004). One particularly useful attribute of MNP is the ability to track them using various imaging modalities. For instance, the introduction of fluorescent tags to the matrix of MNP is easily achieved and enables convenient visual tracking of nanoparticles, which is a particular advantage in studies requiring MNP or cell tracking. There is also a clear role for different sized nanoparticles. Modifications to MNP size alters the rate of internalisation and changes the magnitude of the forces imparted by them (Hughes et al., 2005). In turn, this can have different effects on cell behaviour depending on the target and cell type. In the context of MNP-mediated mechanoactivation, the application of varied forces and stimulation regimes may result in differential signalling responses and changes in cell behaviour.

6.4.1 Forces applied by MNP

The forces imparted by MNP are measured in the order of piconewtons (pN). These are relatively low magnitude forces in comparison to other mechanical loading techniques. However, when considered that these forces are applied directly to proteins, it is not surprising that forces of this magnitude lead to changes in protein activity. This principle is shown by previous work utilising optical tweezers to impart load to cells and proteins. For instance, Cecconi *et al* discovered that application of 5.5pN forces is capable of

causing partial unfolding of RNase H in E-coli (Cecconi et al., 2005). Also, Walker *et al* demonstrated that 7pN loading of the cell bodies of individual bone cells resulted in changes in intracellular calcium signalling (Walker et al., 1999). In terms of magnetic particle mediated activation, both nano- and micro-sized MNP have been shown to be capable of initiating the same cellular signalling responses. This suggests that just the direct application of pN forces to protein targets is required to elicit a biological response (Hughes et al., 2008). In any case, the low magnitude forces imparted by MNP have distinct advantages in tissue engineering systems unable to accommodate larger magnitude and/or global loading profiles. One such application is the mechanical loading of cell seeded hydrogel scaffolds which have shown promise in tissue engineering. Hydrogel scaffolds have particular advantages over denser scaffold materials such as the capability to directly control cell seeding, scaffold shape / volume and mechanical properties (El-Sherbiny and Yacoub, 2013). The benefits of MNP mediated stimulation in hydrogels has been demonstrated by Henstock *et al* who showed that MNP-mediated stimulation of Trek and integrin receptors on hMSC encapsulated in Collagen hydrogel resulted in increased bone formation and hydrogel density (Henstock et al., 2014).

6.5 Magnetic Force Bioreactor

Conditioning of cells and tissues using Bioreactor systems has become mainstream practice in Biomedical engineering. This work has centred on the use of an oscillating magnetic force bioreactor to impart magnetic field stimulation to magnetic nanoparticles for remote and targeted mechanical stimulation of cells and tissues. The use of this type of system brings numerous advantages for stem cell conditioning. Firstly, this system

affords a high degree of control of treatment parameters, for example the magnetic field dose can be modified to suit the level of force required by altering the magnetic arrays used or the distance of the arrays from the samples. The technology is also scalable, for instance the number of magnets on the array can be modified depending on experimental conditions allowing the capability for high-throughput assays. The fact that the forces applied are remote allows is also advantageous in that it permits a unique way of controlling cell signalling and, in a tissue engineering context, it permits conditioning of cells and softer scaffolds in a sterile environment. As a result this system has demonstrated its value both as a high throughput screening tool and as a non-invasive cell and tissue conditioning bioreactor for tissue engineering.

6.6 Applications of magnetic stimulation in bone tissue engineering

The use of functionalised MNP and magnetic fields for the stimulation and activation of stem cells has emerged as a viable strategy for the promotion of bone formation both *in vitro* and *in vivo*. There are now numerous proof of concept studies demonstrating the potential of this strategy to modulate numerous mechanotransduction pathways for directing osteogenesis of stem cells for the enhancement of bone repair (Wimpenny et al., 2012), (Markides et al., 2015). This strategy has also been shown to be amenable and synergistic with a range of growth factors and biomaterials enabling mechanical conditioning of cell-seeded scaffolds for enhancement of bone formation (Hu et al., 2013), (Henstock et al., 2014), (Hughes et al., 2007). In the context of the array of signalling pathways that have been shown to be responsive to mechanical stimulation, the work presented here suggests that Wnt signalling pathway may be another mechano-

responsive target that can be modulated for the promotion of bone formation when combined with other anabolic growth factors. This is particularly relevant to patients suffering from osteoporosis and neurodegenerative disorders where a decrease in Wnt signalling has been associated with disease progression (Hoeppner et al., 2009), (Terstappen et al., 2006).

6.7 The foetal chick femur model

This thesis has introduced the foetal chick femur as a model of early bone development. In this work, chick femurs were extracted at 11 days of gestation (E11). This is a comparatively early model of bone formation at approximately half-way through gestation. At this stage the tissue is mainly cartilaginous with only a mineralised bone collar present and is absent of blood vessel invasion. With this in mind, it is quite possible that a different outcome, in terms of tissue generation, may be expected if the magnetic activation strategy were to be applied to *ex vivo* femurs at later stages of development. One way to investigate this is to use later stage chick femurs e.g. gestation day E13-E17. Although femurs at this later stage do not display extensive vasculature, they are significantly more developed compared to the E11 stage and have robustly formed bone matrix (Smith et al., 2012), (Kanczler et al., 2012), (Smith et al., 2015), (Nowlan et al., 2007). Vasculogenesis is an instrumental process in bone development and repair (Kanczler and Oreffo, 2008). In this respect, one avenue for exploring the effects of vasculogenesis on bone development is the Chorioallantoic membrane model (CAM), which has recently been utilised by Smith et al. (Smith et al., 2013). The CAM is a highly vascularised extraembryonic membrane surrounding chick embryos. In this model, tissue

engineering constructs can be cultured on a vascular bed which is accessible from a window excised from the egg shell. Culture of explants on the CAM allows vascular intrusion into the constructs; this model could allow the simultaneous evaluation of MNP stimulation and vasculogenesis on bone formation. However, one caveat is that this would require further development and modifications to the magnetic stimulation system before this study could take place.

Despite the numerous similarities in the bone developmental processes between chick and human, there are also developmental differences which should be considered (Smith et al., 2013). Embryonic avian bones have a single ossification centre during gestation compared to the secondary ossification centres observed in mammals. Cartilage vascularisation is also absent in the chick until mineralisation occurs which is in contrast with mammalian development (Nowlan et al., 2007). Also, the avian growth plate is not as ordered and substantially increases in thickness during development whilst the mammalian growth plate remains a constant thickness (Roach, 1997). These factors may influence the apparent efficacy of cell based tissue engineered strategies in chick models and therefore the translational potential of such treatments. Therefore, the efficacy of these novel cell and MNP therapies would need to be fully assessed in other animal models first.

6.8 Future work

6.8.1 Development of the Magnetic force bioreactor

Bioreactors have been demonstrated to be incredibly useful platforms for cell conditioning and engineering tissue constructs. This work has focused on mechanical

stimulation of cells and tissues using magnetic nanoparticles coupled with an innovative magnetic force bioreactor. There is scope for the future development of this system. The magnetic force bioreactor utilised in these experiments relied upon the magnetic field produced by permanent rare earth magnets on a platform driven by a drive shaft. This results in heavy apparatus which requires cooling during operation which raises potential safety problems if this technology is to be translated into the clinic. An improvement to this system could be the replacement of heavy permanent magnets with electromagnets. This would make the system lighter, more controllable and negate the need for constant cooling.

6.8.2 Improving MNP functionalisation

The MNP functionalisation process used in this work is based on carbodiimide activation of carboxyl groups on MNP. This reaction results in formation of a peptide bond between the MNP carboxyl group and amine groups present on the protein ligands. Although peptide bond formation results in very stable bonding between molecules (Montalbetti and Falque, 2005), (Radzicka and Wolfenden, 1996), non-specific cross-linking between MNP and ligands could lead to high density packing of biomolecules on the MNP surface. This may lead to steric hindrance and limit the targeting capabilities of the bio-ligands. One way of off-setting this potential issue is through the use of molecular spacers such as organic linkers. This would increase the molecular spacing between ligands potentially allowing the correct orientation of ligands to occur which in turn may improve targeting efficiency. One commonly used spacer is poly ethylene glycol (PEG), this has been shown to improve ligand/receptor interactions in a targeting therapy for tumour imaging (Varasteh et al., 2014) and for folate-receptor targeted liposomes for drug delivery in cancer models (Kawano and Maitani, 2011).

6.8.3 Investigating alternative nanoparticles

These experiments were underpinned by the application of one type of super paramagnetic nanoparticle. It is possible that other types of nanoparticle may influence the magnitude of the effects on cell signalling activation. MNP of different sizes have different magnetic properties and impart different mechanical loads which in turn may augment or reduce signalling activation. The application of other types of nanoparticles should therefore be investigated to study this possibility. Further to this, different magnetic stimulation regimes with different doses of MNP may be better suited to different targets or when stimulating different cell types. A thorough investigation into magnetic stimulation regimes and a dose-response study of MNP is also needed in order to fully optimise the protocol for controlling cell differentiation.

6.8.4 Exploring the mechanism behind magnetic activation of Wnt pathways

There are multiple mechanisms through which Wnt/β-catenin signalling can be induced. Wnt proteins act through Frizzled and co-receptors whilst pharmacological activation through small molecules such as LiCl acts on the intracellular mediator GSK-3β (Freland and Beaulieu, 2012). Mechano-activation of Wnt signalling has also been previously demonstrated. Norvell *et al*, showed that fluid shear stress is capable of mobilising cadherin associated β-catenin with the subsequent activation of Wnt signalling (Norvell et al., 2004). The results from chapter 3 suggest that magnetic activation of Wnt signalling also occurs through a different mechanism to Wnt protein in a way that is co-receptor independent. As MNP are known to torque and induce forces in response to magnetic fields it is therefore possible that this mechanical stimulation could induce a cadherin mobilising effect similar to the effects of shear stress when the MNP are bound to the cell surface. Frizzled clustering and dimerisation has also been shown as another mechanism

of Wnt pathway activation. This has been demonstrated both experimentally and by mathematical modelling (Carron et al., 2003), (Voronkov et al., 2008). When considering that MNP functionalised with peptides and antibodies will contain multiple ligands per particle, it is therefore feasible that these MNP are inducing receptor clustering that causes subsequent pathway activation. Both of these mechanisms should be investigated further to determine the precise mechanism of MNP mediated Wnt activation.

6.8.5 Targeting other Wnt pathway receptors

There are multiple receptors involved in Wnt signalling at the cell membrane. The targeting strategy used in this work has used antibodies and peptides that interact with one of the Frizzled receptors. There are nine other Frizzled receptors in humans along with a plethora of other co-receptors which control other aspects of Wnt signalling pathways. If targeting strategies can be developed for these other targets, the mechano-responsiveness of these receptors and downstream effects on Wnt signalling could be investigated and may even allow greater control of pathway activity which may influence the outcome on cell fate. This work has focused on the effects of functionalised MNP on canonical Wnt signalling. However there is growing evidence that the non-canonical Wnt signalling pathways are also involved in MSC fate including the promotion of osteogenic differentiation of MSC (Arnsdorf et al., 2009), (Chang et al., 2007), (Baksh and Tuan, 2007). Therefore the effects of targeted MNP on non-canonical pathway activity in MSC and effects on cell fate should also be investigated.

6.8.6 Interplay between growth factor and MNP-mediated signalling

Wnt signalling acts in concert with a wide array of other signalling pathways during development. The cross-talk between these signalling networks is crucial for properly

controlled bone development. This work has given a snapshot into the synergistic roles of Wnt and BMP signalling for bone generation using a foetal chick femur model. Future work should interrogate the cross-talk with other signalling pathways and the molecular mechanisms underpinning them (e.g. gene expression analysis) in order to elucidate the optimum signalling environments for bone generation. The effects of spatial gradients and the temporal nature of signalling pathways are also important considerations in bone development and require investigation.

6.8.7 Optimising cell targets for differentiation

It is clear that the effects of Wnt signalling on stem cell proliferation and differentiation are complex and tight regulation of this pathway is ultimately required to optimise stem cell differentiation and tissue development. This thesis has examined the role of intermittent Wnt signalling activation on the osteogenic differentiation of MSC for bone formation. However, Wnt signalling is known to play roles in most cells types of the osteogenic lineage ranging from osteoprogenitor cells to osteocytes and osteoblasts (Leucht et al., 2008) and has been shown to have different effects on cell function depending on the differentiation state of the target cells (Quarto et al., 2010). In this case, targeting other cells at other stages of differentiation should also be investigated to ascertain if bone formation can be driven more efficiently by targeting these cell types.

6.8.8 Re-creating the stem cell niche

The work presented in this thesis has also hinted at the advantages of developing localised Wnt signalling gradients to promote MSC migration and regulate MSC osteogenic differentiation in migrated cells. Future work should interrogate the phenotype of the cells at different levels of migration. This could be achieved by looking

at other MSC markers of stemness in basal cell layers closest to the Wnt signals such as CD73, CD90 and CD105 whilst examining other differentiation markers in migrated cells which are further from the Wnt signal such as RUNX2, Osteopontin and Collagen 1. The level of Wnt pathway activity in migrated MSC and the role of asymmetric cell division in these processes are other exciting avenues for future research.

6.9 Final conclusions

The work presented in this thesis has shown that it is possible to engineer magnetic nanoparticles to target cell surface receptors and activate the Wnt signalling pathway in hMSC, a clinically relevant stem cell type. It has also been demonstrated that this strategy can have beneficial effects on hMSC osteogenic differentiation in *ex vivo* bone formation models particularly when used in conjunction with other growth factors. Importantly, this strategy was shown to be complementary to BMP2 signalling in supporting bone development. A table summarising the effects of MNP and hMSC stimulation on Wnt signalling and osteogenesis is presented in tables 6.1, 6.2 and 6.3.

Assay / Treatment	β-catenin mobilisation	TCF/LEF response	Dkk blocking	iCRT blocking	LRP activation
Anti-Fz-IgG (Fz-MNP)	+++	+++	=	+++	=
Linear UM206 MNP (L-UM206-MNP)	+++	+++	=	+++	=
Cyclic UM206 MNP (C-C-UM206-MNP)	+	=	N/A	N/A	N/A
IgG-MNP	=	=	N/A	N/A	N/A
RGD-MNP	=	=	N/A	N/A	N/A

Table 6.1. Summary of the effects of MNP on Wnt pathway activation.
+ denotes increased effect, - denotes decreased effect, = denotes no change

Assay / Treatment	ALP activity	Total Protein	DNA	Collagen production	Mineralisation	Osteocalcin	Osteopontin
Linear UM206 MNP (L-UM206-MNP)	+	=	+	=	=	++	=
Cyclic UM206 MNP (C-C-UM206-MNP)	++	+	++	=	=	+	=

Table 6.3. Summary of the effects of MNP on *in vitro* MSC osteogenesis.
+ denotes increased effect, - denotes decreased effect, = denotes no change

Assay / Treatment	Ex vivo mineralisation	Total volume	Total density	Collar Volume	Collar Density	Alcian blue & Sirius Red	Osteocalcin
hMSC	+	-	+	=	+	+	+
hMSC & BMP	+	+	-	+	=	+	++
hMSC & L-UM206-MNP	+	=	=	=	=	+	+
hMSC & L-UM206-MNP & BMP	+	=	=	=	+	+	++

Table 6.2. Summary of the effects of MNP on *ex vivo* bone formation.
+ denotes increased effect, - denotes decreased effect, = denotes no change

This work also demonstrates the multiple advantages to using magnetic nanoparticles to apply forces to cells and tissues. The fact that MNP can be produced relatively easily at different sizes with different magnetic properties and functionality enables their use to be tailored and their dose to be scaled to the desired application. Furthermore, the fact that the mechanical forces provided by MNP are translated directly to cells allows a high degree of control over the magnitude of the forces applied which can be altered by changing the MNP dose or stimulation regime. This also means that cells can be mechanically conditioned on a wider array of scaffolds including softer scaffolds unable to accommodate direct mechanical loading. This work has also touched upon the benefits of creating directional Wnt signalling gradients which are important for the maintenance of the stem cell niche in bone. This approach has been shown to have beneficial effects on the regulation of MSC osteogenic differentiation.

In conclusion, this work has shown the benefits of remote stem cell activation and directional application of Wnt gradients for the regulation of stem cell differentiation and bone formation. One key advantage of this approach is that it is cell therapy based; this allows the possibility of developing a treatment that could be administered with a simple injection. Added to this, the use of nanoparticles targeted to specific cell receptors effectively allows for a controlled dose of cell activation which could be administered with the application of an externally controlled magnetic field. With further development, the techniques applied here could conceivably be adapted to produce a minimally invasive cell therapy which could be readily translated to the clinic.

References

AHITUV, N. 2012. *Gene Regulatory Sequences and Human Disease*, Springer New York. Pages 56-60

AHN, S. & JOYNER, A. L. 2004. Dynamic changes in the response of cells to positive hedgehog signaling during mouse limb patterning. *Cell,* 118**,** 505-16.

AIMOND, F., RAUZIER, J. M., BONY, C. & VASSORT, G. 2000. Simultaneous activation of p38 MAPK and p42/44 MAPK by ATP stimulates the K+ current ITREK in cardiomyocytes. *J Biol Chem,* 275**,** 39110-6.

AKBARZADEH, A., SAMIEI, M. & DAVARAN, S. 2012. Magnetic nanoparticles: preparation, physical properties, and applications in biomedicine. *Nanoscale Research Letters,* 7**,** 144-144.

ALEXIOU, C., ARNOLD, W., KLEIN, R. J., PARAK, F. G., HULIN, P., BERGEMANN, C., ERHARDT, W., WAGENPFEIL, S. & LUBBE, A. S. 2000. Locoregional cancer treatment with magnetic drug targeting. *Cancer Res,* 60**,** 6641-8.

ALEXIOU, C., JURGONS, R., SCHMID, R. J., BERGEMANN, C., HENKE, J., ERHARDT, W., HUENGES, E. & PARAK, F. 2003. Magnetic drug targeting--biodistribution of the magnetic carrier and the chemotherapeutic agent mitoxantrone after locoregional cancer treatment. *J Drug Target,* 11**,** 139-49.

ANDERSON, H. C. & REYNOLDS, J. J. 1973. Pyrophosphate stimulation of calcium uptake into cultured embryonic bones. Fine structure of matrix vesicles and their role in calcification. *Dev Biol,* 34**,** 211-27.

ARBAB, A. S., JORDAN, E. K., WILSON, L. B., YOCUM, G. T., LEWIS, B. K. & FRANK, J. A. 2004. In vivo trafficking and targeted delivery of magnetically labeled stem cells. *Hum Gene Ther,* 15**,** 351-60.

ARMSTRONG, V. J., MUZYLAK, M., SUNTERS, A., ZAMAN, G., SAXON, L. K., PRICE, J. S. & LANYON, L. E. 2007. Wnt/beta-catenin signaling is a component of osteoblastic bone cell early responses to load-bearing and requires estrogen receptor alpha. *J Biol Chem,* 282**,** 20715-27.

ARNSDORF, E. J., TUMMALA, P. & JACOBS, C. R. 2009. Non-canonical Wnt signaling and N-cadherin related beta-catenin signaling play a role in mechanically induced osteogenic cell fate. *PLoS One,* 4**,** e5388.

AUBIN, J. 2001. Regulation of Osteoblast Formation and Function. *Reviews in Endocrine and Metabolic Disorders,* 2**,** 81-94.

AUGELLO, A. & DE BARI, C. 2010. The regulation of differentiation in mesenchymal stem cells. *Hum Gene Ther,* 21**,** 1226-38.

BAEK, S. H., KIOUSSI, C., BRIATA, P., WANG, D., NGUYEN, H. D., OHGI, K. A., GLASS, C. K., WYNSHAW-BORIS, A., ROSE, D. W. & ROSENFELD, M. G. 2003. Regulated subset of G1 growth-control genes in response to derepression by the Wnt pathway. *Proc Natl Acad Sci U S A,* 100**,** 3245-50.

BAFICO, A., LIU, G., YANIV, A., GAZIT, A. & AARONSON, S. A. 2001. Novel mechanism of Wnt signalling inhibition mediated by Dickkopf-1 interaction with LRP6/Arrow. *Nat Cell Biol,* 3**,** 683-6.

BAGHABAN ESLAMINEJAD, M. & MALAKOOTY POOR, E. 2014. Mesenchymal stem cells as a potent cell source for articular cartilage regeneration. *World Journal of Stem Cells,* 6**,** 344-354.

BAIN, G., MULLER, T., WANG, X. & PAPKOFF, J. 2003. Activated beta-catenin induces osteoblast differentiation of C3H10T1/2 cells and participates in BMP2 mediated signal transduction. *Biochem Biophys Res Commun,* 301**,** 84-91.

BAJADA, S., HARRISON, P. E., ASHTON, B. A., CASSAR-PULLICINO, V. N., ASHAMMAKHI, N. & RICHARDSON, J. B. 2007. Successful treatment of refractory tibial nonunion using calcium sulphate and bone marrow stromal cell implantation. *J Bone Joint Surg Br,* 89**,** 1382-6.

BAKSH, D., BOLAND, G. M. & TUAN, R. S. 2007. Cross-talk between Wnt signaling pathways in human mesenchymal stem cells leads to functional antagonism during osteogenic differentiation. *J Cell Biochem,* 101**,** 1109-24.

BAKSH, D., SONG, L. & TUAN, R. S. 2004. Adult mesenchymal stem cells: characterization, differentiation, and application in cell and gene therapy. *Journal of Cellular and Molecular Medicine,* 8**,** 301-316.

BAKSH, D. & TUAN, R. S. 2007. Canonical and non-canonical wnts differentially affect the development potential of primary isolate of human bone marrow mesenchymal stem cells. *Journal of Cellular Physiology,* 212**,** 817-826.

BALEMANS, W., EBELING, M., PATEL, N., VAN HUL, E., OLSON, P., DIOSZEGI, M., LACZA, C., WUYTS, W., VAN DEN ENDE, J., WILLEMS, P., PAES-ALVES, A. F., HILL, S., BUENO, M., RAMOS, F. J., TACCONI, P., DIKKERS, F. G., STRATAKIS, C., LINDPAINTNER, K., VICKERY, B., FOERNZLER, D. & VAN HUL, W. 2001. Increased bone density in sclerosteosis is due to the deficiency of a novel secreted protein (SOST). *Hum Mol Genet,* 10**,** 537-43.

BANCROFT, G. N., SIKAVITSAS, V. I., VAN DEN DOLDER, J., SHEFFIELD, T. L., AMBROSE, C. G., JANSEN, J. A. & MIKOS, A. G. 2002. Fluid flow increases mineralized matrix deposition in 3D perfusion culture of marrow stromal osteoblasts in a dose-dependent manner. *Proc Natl Acad Sci U S A,* 99**,** 12600-5.

BAO, Y., WEN, T., SAMIA, A. C. S., KHANDHAR, A. & KRISHNAN, K. M. 2015. Magnetic nanoparticles: material engineering and emerging applications in lithography and biomedicine. *Journal of Materials Science,* 51**,** 513-553.

BARNES, G. L., KAKAR, S., VORA, S., MORGAN, E. F., GERSTENFELD, L. C. & EINHORN, T. A. 2008. Stimulation of fracture-healing with systemic intermittent parathyroid hormone treatment. *J Bone Joint Surg Am,* 90 Suppl 1**,** 120-7.

BARTHOLOMEW, A., STURGEON, C., SIATSKAS, M., FERRER, K., MCINTOSH, K., PATIL, S., HARDY, W., DEVINE, S., UCKER, D., DEANS, R., MOSELEY, A. & HOFFMAN, R. 2002. Mesenchymal stem cells suppress lymphocyte proliferation in vitro and prolong skin graft survival in vivo. *Exp Hematol,* 30**,** 42-8.

BEDNARSKA, K., KLINK, M. & SULOWSKA, Z. 2006. Application of Intracellular Alkaline Phosphatase Activity Measurement in Detection of Neutrophil Adherence In Vitro. *Mediators of Inflammation,* 2006**,** 8 Pages.

BELEMA BEDADA, F., TECHNAU, A., EBELT, H., SCHULZE, M. & BRAUN, T. 2005. Activation of myogenic differentiation pathways in adult bone marrow-derived stem cells. *Mol Cell Biol,* 25**,** 9509-19.

BELL, S. M., SCHREINER, C. M., WERT, S. E., MUCENSKI, M. L., SCOTT, W. J. & WHITSETT, J. A. 2008. R-spondin 2 is required for normal laryngeal-tracheal, lung and limb morphogenesis. *Development,* 135**,** 1049-58.

BENAUD, C. M. & DICKSON, R. B. 2001. Regulation of the expression of c-Myc by beta1 integrins in epithelial cells. *Oncogene,* 20**,** 759-68.

BENNETT, C. N., LONGO, K. A., WRIGHT, W. S., SUVA, L. J., LANE, T. F., HANKENSON, K. D. & MACDOUGALD, O. A. 2005. Regulation of osteoblastogenesis and bone mass by Wnt10b. *Proc Natl Acad Sci U S A,* 102**,** 3324-9.

BERIS, A. E., LYKISSAS, M. G., KOSTAS-AGNANTIS, I. & MANOUDIS, G. N. 2012. Treatment of full-thickness chondral defects of the knee with autologous chondrocyte implantation: a functional evaluation with long-term follow-up. *Am J Sports Med,* 40**,** 562-7.

BHANDARI, M., GUYATT, G. H., SWIONTKOWSKI, M. F. & SCHEMITSCH, E. H. 2001. Treatment of open fractures of the shaft of the tibia. *A SYSTEMATIC OVERVIEW AND META-ANALYSIS,* 83-B**,** 62-68.

BHOSALE, A. M., KUIPER, J. H., JOHNSON, W. E., HARRISON, P. E. & RICHARDSON, J. B. 2009. Midterm to long-term longitudinal outcome of autologous chondrocyte implantation in the knee joint: a multilevel analysis. *Am J Sports Med,* 37 Suppl 1**,** 131S-8S.

BILEZIKIAN, J. P., RAISZ, L. G. & MARTIN, T. J. 2008. *Principles of Bone Biology: Two-Volume Set*, Elsevier Science. Pages 85-88, 91-92, 160, 193

BINNERTS, M. E., KIM, K. A., BRIGHT, J. M., PATEL, S. M., TRAN, K., ZHOU, M., LEUNG, J. M., LIU, Y., LOMAS, W. E., 3RD, DIXON, M., HAZELL, S. A., WAGLE, M., NIE, W. S., TOMASEVIC, N., WILLIAMS, J., ZHAN, X., LEVY, M. D., FUNK, W. D. & ABO, A. 2007. R-Spondin1 regulates Wnt signaling by inhibiting internalization of LRP6. *Proc Natl Acad Sci U S A,* 104**,** 14700-5.

BIRMINGHAM, E., NIEBUR, G. L., MCHUGH, P. E., SHAW, G., BARRY, F. P. & MCNAMARA, L. M. 2012. Osteogenic differentiation of mesenchymal stem cells is regulated by osteocyte and osteoblast cells in a simplified bone niche. *Eur Cell Mater,* 23**,** 13-27.

BLANKESTEIJN WESSEL MATTHIJS, L. H., HACKENG TILMAN MATHIAS. 2010. *ANTAGONISTIC PEPTIDES FOR FRIZZLED-1 AND FRIZZLED-2*. European Patent Office. Patent application 09154475.9.

BLITZER, J. T. & NUSSE, R. 2006. A critical role for endocytosis in Wnt signaling. *BMC Cell Biology,* 7**,** 1-10.

BOLAND, G. M., PERKINS, G., HALL, D. J. & TUAN, R. S. 2004. Wnt 3a promotes proliferation and suppresses osteogenic differentiation of adult human mesenchymal stem cells. *J Cell Biochem,* 93**,** 1210-30.

BONGSO, A. & LEE, E. H. 2005. *Stem Cells: From Bench to Bedside*, World Scientific. Pages 2-5

BOSE, S., ROY, M. & BANDYOPADHYAY, A. 2012. Recent advances in bone tissue engineering scaffolds. *Trends in biotechnology,* 30**,** 546-554.

BOVOLENTA, P., ESTEVE, P., RUIZ, J. M., CISNEROS, E. & LOPEZ-RIOS, J. 2008. Beyond Wnt inhibition: new functions of secreted Frizzled-related proteins in development and disease. *J Cell Sci,* 121**,** 737-46.

BOXALL, S. A. & JONES, E. 2012. Markers for characterization of bone marrow multipotential stromal cells. *Stem Cells Int,* 2012**,** 12 pages.

BOYDEN, L. M., MAO, J., BELSKY, J., MITZNER, L., FARHI, A., MITNICK, M. A., WU, D., INSOGNA, K. & LIFTON, R. P. 2002. High bone density due to a mutation in LDL-receptor-related protein 5. *N Engl J Med,* 346**,** 1513-21.

BRINKLEY, M. 1992. A brief survey of methods for preparing protein conjugates with dyes, haptens, and cross-linking reagents. *Bioconjug Chem,* 3**,** 2-13.

BROWN, S. D., TWELLS, R. C., HEY, P. J., COX, R. D., LEVY, E. R., SODERMAN, A. R., METZKER, M. L., CASKEY, C. T., TODD, J. A. & HESS, J. F. 1998. Isolation and characterization of LRP6, a novel member of the low density lipoprotein receptor gene family. *Biochem Biophys Res Commun,* 248**,** 879-88.

BULLIONS, L. C. & LEVINE, A. J. 1998. The role of beta-catenin in cell adhesion, signal transduction, and cancer. *Curr Opin Oncol,* 10**,** 81-7.

CANADIAN ORTHOPAEDIC TRAUMA, S. 2003. Nonunion following intramedullary nailing of the femur with and without reaming. Results of a multicenter randomized clinical trial. *J Bone Joint Surg Am,* 85-A**,** 2093-6.

CAPLAN, A. I. 2010. Mesenchymal Stem Cells: The Past, the Present, the Future. *Cartilage,* 1**,** 6-9.

CAPLAN, A. I. & BRUDER, S. P. 2001. Mesenchymal stem cells: building blocks for molecular medicine in the 21st century. *Trends Mol Med,* 7**,** 259-64.

CARMON, K. S., GONG, X., LIN, Q., THOMAS, A. & LIU, Q. 2011. R-spondins function as ligands of the orphan receptors LGR4 and LGR5 to regulate Wnt/β-catenin signaling. *Proceedings of the National Academy of Sciences,* 108**,** 11452-11457.

CARRON, C., PASCAL, A., DJIANE, A., BOUCAUT, J. C., SHI, D. L. & UMBHAUER, M. 2003. Frizzled receptor dimerization is sufficient to activate the Wnt/beta-catenin pathway. *J Cell Sci,* 116**,** 2541-50.

CARTHY, J. M., GARMAROUDI, F. S., LUO, Z. & MCMANUS, B. M. 2011. Wnt3a induces myofibroblast differentiation by upregulating TGF-beta signaling through SMAD2 in a beta-catenin-dependent manner. *PLoS One,* 6**,** e19809.

CARTMELL, S. H., DOBSON, J., VERSCHUEREN, S. B. & EL HAJ, A. J. 2002. Development of magnetic particle techniques for long-term culture of bone cells with intermittent mechanical activation. *IEEE Trans Nanobioscience,* 1**,** 92-7.

CARTMELL, S. H., KERAMANE, A., KIRKHAM, G. R., VERSCHUEREN, S. B., MAGNAY, J. L., HAJ, A. J. E. & DOBSON, J. 2005. Use of magnetic particles to apply mechanical forces for bone tissue engineering purposes. *Journal of Physics: Conference Series,* 17**,** 77.

CASTRO-MALASPINA, H., GAY, R. E., RESNICK, G., KAPOOR, N., MEYERS, P., CHIARIERI, D., MCKENZIE, S., BROXMEYER, H. E. & MOORE, M. A. 1980. Characterization of human bone marrow fibroblast colony-forming cells (CFU-F) and their progeny. *Blood,* 56**,** 289-301.

CECCONI, C., SHANK, E. A., BUSTAMANTE, C. & MARQUSEE, S. 2005. Direct observation of the three-state folding of a single protein molecule. *Science,* 309**,** 2057-60.

CHACHISVILIS, M., ZHANG, Y.-L. & FRANGOS, J. A. 2006. G protein-coupled receptors sense fluid shear stress in endothelial cells. *Proceedings of the National Academy of Sciences,* 103**,** 15463-15468.

CHAKRABORTY, M., JAIN, S. & RANI, V. 2011. Nanotechnology: emerging tool for diagnostics and therapeutics. *Appl Biochem Biotechnol,* 165**,** 1178-87.

CHANG, J., SONOYAMA, W., WANG, Z., JIN, Q., ZHANG, C., KREBSBACH, P. H., GIANNOBILE, W., SHI, S. & WANG, C. Y. 2007. Noncanonical Wnt-4 signaling enhances bone regeneration of mesenchymal stem cells in craniofacial defects through activation of p38 MAPK. *J Biol Chem,* 282**,** 30938-48.

CHANG, J. T., ESUMI, N., MOORE, K., LI, Y., ZHANG, S., CHEW, C., GOODMAN, B., RATTNER, A., MOODY, S., STETTEN, G., CAMPOCHIARO, P. A. & ZACK, D. J. 1999. Cloning and characterization of a secreted frizzled-related protein that is expressed by the retinal pigment epithelium. *Hum Mol Genet,* 8**,** 575-83.

CHEN, B., DODGE, M. E., TANG, W., LU, J., MA, Z., FAN, C. W., WEI, S., HAO, W., KILGORE, J., WILLIAMS, N. S., ROTH, M. G., AMATRUDA, J. F., CHEN, C. & LUM, L. 2009. Small molecule-mediated disruption of Wnt-dependent signaling in tissue regeneration and cancer. *Nat Chem Biol,* 5**,** 100-7.

CHEN, J., FABRY, B., SCHIFFRIN, E. L. & WANG, N. 2001. Twisting integrin receptors increases endothelin-1 gene expression in endothelial cells. *Am J Physiol Cell Physiol,* 280**,** C1475-84.

CHEN, X. Y., ZHANG, X. Z., GUO, Y., LI, R. X., LIN, J. J. & WEI, Y. 2008. The establishment of a mechanobiology model of bone and functional adaptation in response to mechanical loading. *Clin Biomech (Bristol, Avon),* 23 Suppl 1**,** S88-95.

CHEN, Y., WHETSTONE, H. C., YOUN, A., NADESAN, P., CHOW, E. C., LIN, A. C. & ALMAN, B. A. 2007. Beta-catenin signaling pathway is crucial for bone morphogenetic protein 2 to induce new bone formation. *J Biol Chem,* 282**,** 526-33.

CHO, H. H., KIM, Y. J., KIM, S. J., KIM, J. H., BAE, Y. C., BA, B. & JUNG, J. S. 2006. Endogenous Wnt signaling promotes proliferation and suppresses osteogenic differentiation in human adipose derived stromal cells. *Tissue Eng,* 12**,** 111-21.

CHO, S. W., YANG, F., SON, S. M., PARK, H. J., GREEN, J. J., BOGATYREV, S., MEI, Y., PARK, S., LANGER, R. & ANDERSON, D. G. 2012. Therapeutic angiogenesis using genetically engineered human endothelial cells. *J Control Release,* 160**,** 515-24.

CLAES, L. & WILLIE, B. 2007. The enhancement of bone regeneration by ultrasound. *Prog Biophys Mol Biol,* 93**,** 384-98.

CLARKE, B. 2008. Normal Bone Anatomy and Physiology. *Clinical Journal of the American Society of Nephrology : CJASN,* 3**,** S131-S139.

CLEVERS, H. 2006. Wnt/β-Catenin Signaling in Development and Disease. *Cell,* 127**,** 469-480.

CLEVERS, H., LOH, K. M. & NUSSE, R. 2014. An integral program for tissue renewal and regeneration: Wnt signaling and stem cell control. *Science,* 346.

CONDE, J., DIAS, J. T., GRAZÚ, V., MOROS, M., BAPTISTA, P. V. & DE LA FUENTE, J. M. 2014. Revisiting 30 years of Biofunctionalization and Surface Chemistry of Inorganic Nanoparticles for Nanomedicine. *Frontiers in Chemistry,* 2.

CONG, F., SCHWEIZER, L., CHAMORRO, M. & VARMUS, H. 2003. Requirement for a nuclear function of beta-catenin in Wnt signaling. *Mol Cell Biol,* 23**,** 8462-70.

CONG, F., SCHWEIZER, L. & VARMUS, H. 2004. Wnt signals across the plasma membrane to activate the beta-catenin pathway by forming oligomers containing its receptors, Frizzled and LRP. *Development,* 131**,** 5103-15.

CONNOLLY, J. F. 1995. Injectable bone marrow preparations to stimulate osteogenic repair. *Clin Orthop Relat Res***,** 8-18.

COOK, D. A., FELLGETT, S. W., POWNALL, M. E., O'SHEA, P. J. & GENEVER, P. G. 2014. Wnt-dependent osteogenic commitment of bone marrow stromal cells using a novel GSK3beta inhibitor. *Stem Cell Res,* 12**,** 415-27.

CORES, J., CARANASOS, T. G. & CHENG, K. 2015. Magnetically Targeted Stem Cell Delivery for Regenerative Medicine. *Journal of Functional Biomaterials,* 6**,** 526-546.

COUDREUSE, D. & KORSWAGEN, H. C. 2007. The making of Wnt: new insights into Wnt maturation, sorting and secretion. *Development,* 134**,** 3-12.

CROCKETT, J. C., ROGERS, M. J., COXON, F. P., HOCKING, L. J. & HELFRICH, M. H. 2011. Bone remodelling at a glance. *Journal of Cell Science,* 124**,** 991-998.

CURREY, J. D. 2013. *Bones: Structure and Mechanics*, Princeton University Press. Page 6

DASARI, V. R., VEERAVALLI, K. K. & DINH, D. H. 2014. Mesenchymal stem cells in the treatment of spinal cord injuries: A review. *World Journal of Stem Cells,* 6**,** 120-133.

DAVIDSON, G., WU, W., SHEN, J., BILIC, J., FENGER, U., STANNEK, P., GLINKA, A. & NIEHRS, C. 2005. Casein kinase 1 gamma couples Wnt receptor activation to cytoplasmic signal transduction. *Nature,* 438**,** 867-72.

DAY, T. F., GUO, X., GARRETT-BEAL, L. & YANG, Y. 2005. Wnt/beta-catenin signaling in mesenchymal progenitors controls osteoblast and chondrocyte differentiation during vertebrate skeletogenesis. *Dev Cell,* 8**,** 739-50.

DE BOER, J., SIDDAPPA, R., GASPAR, C., VAN APELDOORN, A., FODDE, R. & VAN BLITTERSWIJK, C. 2004a. Wnt signaling inhibits osteogenic differentiation of human mesenchymal stem cells. *Bone,* 34**,** 818-826.

DE BOER, J., WANG, H. J. & VAN BLITTERSWIJK, C. 2004b. Effects of Wnt signaling on proliferation and differentiation of human mesenchymal stem cells. *Tissue Eng,* 10**,** 393-401.

DE PEPPO, G. M., MARCOS-CAMPOS, I., KAHLER, D. J., ALSALMAN, D., SHANG, L., VUNJAK-NOVAKOVIC, G. & MAROLT, D. 2013. Engineering bone tissue substitutes from human induced pluripotent stem cells. *Proc Natl Acad Sci U S A,* 110**,** 8680-5.

DEJMEK, J., SAFHOLM, A., KAMP NIELSEN, C., ANDERSSON, T. & LEANDERSSON, K. 2006. Wnt-5a/Ca2+-induced NFAT activity is counteracted by Wnt-5a/Yes-Cdc42-casein kinase 1alpha signaling in human mammary epithelial cells. *Mol Cell Biol,* 26**,** 6024-36.

DELA PAZ, N., MELCHIOR, B. & FRANGOS, J. 2015. Shear Stress Induces G Protein-Coupled Receptor (GPCR)-Independent Heterotrimeric G Protein Activation in Endothelial Cells. *The FASEB Journal,* 29**,** 1 Supplement 1029.7.

DELAINE-SMITH, R. M., MACNEIL, S. & REILLY, G. C. 2012. Matrix production and collagen structure are enhanced in two types of osteogenic progenitor cells by a simple fluid shear stress stimulus. *Eur Cell Mater,* 24**,** 162-74.

DESAI, M. P., LABHASETWAR, V., WALTER, E., LEVY, R. J. & AMIDON, G. L. 1997. The mechanism of uptake of biodegradable microparticles in Caco-2 cells is size dependent. *Pharm Res,* 14**,** 1568-73.

DI NICOLA, M., CARLO-STELLA, C., MAGNI, M., MILANESI, M., LONGONI, P. D., MATTEUCCI, P., GRISANTI, S. & GIANNI, A. M. 2002. Human bone marrow stromal cells suppress T-

lymphocyte proliferation induced by cellular or nonspecific mitogenic stimuli. *Blood,* 99**,** 3838-43.
DIMITRIOU, R., JONES, E., MCGONAGLE, D. & GIANNOUDIS, P. V. 2011. Bone regeneration: current concepts and future directions. *BMC Medicine,* 9**,** 1-10.
DOBSON, J. 2006. Gene therapy progress and prospects: magnetic nanoparticle-based gene delivery. *Gene Ther,* 13**,** 283-287.
DOBSON, J. 2008. Remote control of cellular behaviour with magnetic nanoparticles. *Nat Nanotechnol,* 3**,** 139-43.
DOBSON, J., CARTMELL, S. H., KERAMANE, A. & EL HAJ, A. J. 2006. Principles and design of a novel magnetic force mechanical conditioning bioreactor for tissue engineering, stem cell conditioning, and dynamic in vitro screening. *IEEE Trans Nanobioscience,* 5**,** 173-7.
DOMINICI, M., LE BLANC, K., MUELLER, I., SLAPER-CORTENBACH, I., MARINI, F., KRAUSE, D., DEANS, R., KEATING, A., PROCKOP, D. & HORWITZ, E. 2006. Minimal criteria for defining multipotent mesenchymal stromal cells. The International Society for Cellular Therapy position statement. *Cytotherapy,* 8**,** 315-7.
DUCY, P., ZHANG, R., GEOFFROY, V., RIDALL, A. L. & KARSENTY, G. 1997. Osf2/Cbfa1: A Transcriptional Activator of Osteoblast Differentiation. *Cell,* 89**,** 747-754.
DURÁN, M. C., WILLENBROCK, S., BARCHANSKI, A., MÜLLER, J.-M. V., MAIOLINI, A., SOLLER, J. T., BARCIKOWSKI, S., NOLTE, I., FEIGE, K. & MURUA ESCOBAR, H. 2011. Comparison of nanoparticle-mediated transfection methods for DNA expression plasmids: efficiency and cytotoxicity. *Journal of Nanobiotechnology,* 9**,** 1-11.
EHNINGER, A. & TRUMPP, A. 2011. The bone marrow stem cell niche grows up: mesenchymal stem cells and macrophages move in. *J Exp Med,* 208**,** 421-8.
EHRLICH, D., BRUDER, E., THOME, M. A., GUTT, C. N., VON KNEBEL DOEBERITZ, M., NIGGLI, F., PERANTONI, A. O. & KOESTERS, R. 2010. Nuclear accumulation of beta-catenin protein indicates activation of wnt signaling in chemically induced rat nephroblastomas. *Pediatr Dev Pathol,* 13**,** 1-8.
EIJKEN, M., MEIJER, I. M. J., WESTBROEK, I., KOEDAM, M., CHIBA, H., UITTERLINDEN, A. G., POLS, H. A. P. & VAN LEEUWEN, J. P. T. M. 2008. Wnt signaling acts and is regulated in a human osteoblast differentiation dependent manner. *Journal of Cellular Biochemistry,* 104**,** 568-579.
EL-SHERBINY, I. M. & YACOUB, M. H. 2013. Hydrogel scaffolds for tissue engineering: Progress and challenges. *Global Cardiology Science & Practice,* 2013(3)**,** 316-342.
EL HAJ, A. J., WOOD, M. A., THOMAS, P. & YANG, Y. 2005. Controlling cell biomechanics in orthopaedic tissue engineering and repair. *Pathol Biol (Paris),* 53**,** 581-9.
ELLEGAARD, M., JORGENSEN, N. R. & SCHWARZ, P. 2010. Parathyroid hormone and bone healing. *Calcif Tissue Int,* 87**,** 1-13.
ETHERIDGE, S. L., SPENCER, G. J., HEATH, D. J. & GENEVER, P. G. 2004. Expression profiling and functional analysis of wnt signaling mechanisms in mesenchymal stem cells. *Stem Cells,* 22**,** 849-60.
FARGE, E. 2003. Mechanical induction of Twist in the Drosophila foregut/stomodeal primordium. *Curr Biol,* 13**,** 1365-77.
FARRELL, E., WIELOPOLSKI, P., PAVLJASEVIC, P., VAN TIEL, S., JAHR, H., VERHAAR, J., WEINANS, H., KRESTIN, G., O'BRIEN, F. J., VAN OSCH, G. & BERNSEN, M. 2008. Effects of iron oxide incorporation for long term cell tracking on MSC differentiation in vitro and in vivo. *Biochem Biophys Res Commun,* 369**,** 1076-81.
FENG, L., XIA, Y., GARCIA, G. E., HWANG, D. & WILSON, C. B. 1995. Involvement of reactive oxygen intermediates in cyclooxygenase-2 expression induced by interleukin-1, tumor necrosis factor-alpha, and lipopolysaccharide. *J Clin Invest,* 95**,** 1669-75.
FILALI, M., CHENG, N., ABBOTT, D., LEONTIEV, V. & ENGELHARDT, J. F. 2002. Wnt-3A/beta-catenin signaling induces transcription from the LEF-1 promoter. *J Biol Chem,* 277**,** 33398-410.

FINK, M., DUPRAT, F., LESAGE, F., REYES, R., ROMEY, G., HEURTEAUX, C. & LAZDUNSKI, M. 1996. Cloning, functional expression and brain localization of a novel unconventional outward rectifier K+ channel. *EMBO J,* 15**,** 6854-62.

FOSTER, K. A., YAZDANIAN, M. & AUDUS, K. L. 2001. Microparticulate uptake mechanisms of in-vitro cell culture models of the respiratory epithelium. *J Pharm Pharmacol,* 53**,** 57-66.

FOURIKI, A., CLEMENTS, M. A., FARROW, N. & DOBSON, J. 2014. Efficient transfection of MG-63 osteoblasts using magnetic nanoparticles and oscillating magnetic fields. *Journal of Tissue Engineering and Regenerative Medicine,* 8**,** 169-175.

FOURIKI, A. & DOBSON, J. 2013. Oscillating magnet array-based nanomagnetic gene transfection of human mesenchymal stem cells. *Nanomedicine,* 9**,** 989-997.

FRAHER, L. J. 1993. Biochemical markers of bone turnover. *Clin Biochem,* 26**,** 431-2.

FRELAND, L. & BEAULIEU, J. M. 2012. Inhibition of GSK3 by lithium, from single molecules to signaling networks. *Front Mol Neurosci,* 5**,** 14.

FRIEDL, G., SCHMIDT, H., REHAK, I., KOSTNER, G., SCHAUENSTEIN, K. & WINDHAGER, R. 2007. Undifferentiated human mesenchymal stem cells (hMSCs) are highly sensitive to mechanical strain: transcriptionally controlled early osteo-chondrogenic response in vitro. *Osteoarthritis Cartilage,* 15**,** 1293-300.

GANG, E. J., JEONG, J. A., HONG, S. H., HWANG, S. H., KIM, S. W., YANG, I. H., AHN, C., HAN, H. & KIM, H. 2004. Skeletal myogenic differentiation of mesenchymal stem cells isolated from human umbilical cord blood. *Stem Cells,* 22**,** 617-24.

GARDNER, M. J., VAN DER MEULEN, M. C., DEMETRAKOPOULOS, D., WRIGHT, T. M., MYERS, E. R. & BOSTROM, M. P. 2006. In vivo cyclic axial compression affects bone healing in the mouse tibia. *J Orthop Res,* 24**,** 1679-86.

GATTAZZO, F., URCIUOLO, A. & BONALDO, P. 2014. Extracellular matrix: A dynamic microenvironment for stem cell niche(). *Biochimica et Biophysica Acta,* 1840**,** 2506-2519.

GAUR, T. E. A. 2005. Canonical WNT signaling promotes osteogenesis by directly stimulating Runx2 gene expression. *J Biol Chem,* 280**,** 33132-40.

GILBERT, S. F. 2000. *Developmental Biology, Volume 1* [Online]. http://www.ncbi.nlm.nih.gov/books/NBK10056/: Palgrave Macmillan. [Accessed Jan 2016.

GIULIANI, N., LISIGNOLI, G., MAGNANI, M., RACANO, C., BOLZONI, M., DALLA PALMA, B., SPOLZINO, A., MANFERDINI, C., ABATI, C., TOSCANI, D., FACCHINI, A. & AVERSA, F. 2013. New Insights into Osteogenic and Chondrogenic Differentiation of Human Bone Marrow Mesenchymal Stem Cells and Their Potential Clinical Applications for Bone Regeneration in Pediatric Orthopaedics. *Stem Cells International,* Vol. 2013**,** 11 pages.

GNEVECKOW, U., JORDAN, A., SCHOLZ, R., BRUSS, V., WALDOFNER, N., RICKE, J., FEUSSNER, A., HILDEBRANDT, B., RAU, B. & WUST, P. 2004. Description and characterization of the novel hyperthermia- and thermoablation-system MFH 300F for clinical magnetic fluid hyperthermia. *Med Phys,* 31**,** 1444-51.

GOLDSTEIN, S. A., BOCKENHAUER, D., O'KELLY, I. & ZILBERBERG, N. 2001. Potassium leak channels and the KCNK family of two-P-domain subunits. *Nat Rev Neurosci,* 2**,** 175-84.

GOMEZ-BENITO, M. J., GONZALEZ-TORRES, L. A., REINA-ROMO, E., GRASA, J., SERAL, B. & GARCIA-AZNAR, J. M. 2011. Influence of high-frequency cyclical stimulation on the bone fracture-healing process: mathematical and experimental models. *Philos Trans A Math Phys Eng Sci,* 369**,** 4278-94.

GONG, Y., SLEE, R. B., FUKAI, N., RAWADI, G., ROMAN-ROMAN, S., REGINATO, A. M., WANG, H., CUNDY, T., GLORIEUX, F. H., LEV, D., ZACHARIN, M., OEXLE, K., MARCELINO, J., SUWAIRI, W., HEEGER, S., SABATAKOS, G., APTE, S., ADKINS, W. N., ALLGROVE, J., ARSLAN-KIRCHNER, M., BATCH, J. A., BEIGHTON, P., BLACK, G. C., BOLES, R. G., BOON, L. M., BORRONE, C., BRUNNER, H. G., CARLE, G. F., DALLAPICCOLA, B., DE PAEPE, A., FLOEGE, B., HALFHIDE, M. L., HALL, B., HENNEKAM, R. C., HIROSE, T., JANS, A., JUPPNER, H., KIM, C. A.,

KEPPLER-NOREUIL, K., KOHLSCHUETTER, A., LACOMBE, D., LAMBERT, M., LEMYRE, E., LETTEBOER, T., PELTONEN, L., RAMESAR, R. S., ROMANENGO, M., SOMER, H., STEICHEN-GERSDORF, E., STEINMANN, B., SULLIVAN, B., SUPERTI-FURGA, A., SWOBODA, W., VAN DEN BOOGAARD, M. J., VAN HUL, W., VIKKULA, M., VOTRUBA, M., ZABEL, B., GARCIA, T., BARON, R., OLSEN, B. R., WARMAN, M. L. & OSTEOPOROSIS-PSEUDOGLIOMA SYNDROME COLLABORATIVE, G. 2001. LDL receptor-related protein 5 (LRP5) affects bone accrual and eye development. *Cell,* 107**,** 513-23.

GONSALVES, F. C., KLEIN, K., CARSON, B. B., KATZ, S., EKAS, L. A., EVANS, S., NAGOURNEY, R., CARDOZO, T., BROWN, A. M. & DASGUPTA, R. 2011. An RNAi-based chemical genetic screen identifies three small-molecule inhibitors of the Wnt/wingless signaling pathway. *Proc Natl Acad Sci U S A,* 108**,** 5954-63.

GOTHARD, D., SMITH, E. L., KANCZLER, J. M., RASHIDI, H., QUTACHI, O., HENSTOCK, J., ROTHERHAM, M., EL HAJ, A., SHAKESHEFF, K. M. & OREFFO, R. O. 2014. Tissue engineered bone using select growth factors: A comprehensive review of animal studies and clinical translation studies in man. *Eur Cell Mater,* 28**,** 166-207; discussion 207-8.

GRABAREK, Z. & GERGELY, J. 1990. Zero-length crosslinking procedure with the use of active esters. *Anal Biochem,* 185**,** 131-5.

GRONTHOS, S., ZANNETTINO, A. C., GRAVES, S. E., OHTA, S., HAY, S. J. & SIMMONS, P. J. 1999. Differential cell surface expression of the STRO-1 and alkaline phosphatase antigens on discrete developmental stages in primary cultures of human bone cells. *J Bone Miner Res,* 14**,** 47-56.

GRONTHOS, S., ZANNETTINO, A. C., HAY, S. J., SHI, S., GRAVES, S. E., KORTESIDIS, A. & SIMMONS, P. J. 2003. Molecular and cellular characterisation of highly purified stromal stem cells derived from human bone marrow. *J Cell Sci,* 116**,** 1827-35.

GRUBER, R., KOCH, H., DOLL, B. A., TEGTMEIER, F., EINHORN, T. A. & HOLLINGER, J. O. 2006. Fracture healing in the elderly patient. *Exp Gerontol,* 41**,** 1080-93.

GRUMOLATO, L., LIU, G., MONG, P., MUDBHARY, R., BISWAS, R., ARROYAVE, R., VIJAYAKUMAR, S., ECONOMIDES, A. N. & AARONSON, S. A. 2010. Canonical and noncanonical Wnts use a common mechanism to activate completely unrelated coreceptors. *Genes Dev,* 24**,** 2517-30.

GUJRAL, T. S. & MACBEATH, G. 2010. A system-wide investigation of the dynamics of Wnt signaling reveals novel phases of transcriptional regulation. *PLoS One,* 5**,** e10024.

GUPTA, A. K. & GUPTA, M. 2005. Synthesis and surface engineering of iron oxide nanoparticles for biomedical applications. *Biomaterials,* 26**,** 3995-4021.

HAASPER, C., JAGODZINSKI, M., DRESCHER, M., MELLER, R., WEHMEIER, M., KRETTEK, C. & HESSE, E. 2008. Cyclic strain induces FosB and initiates osteogenic differentiation of mesenchymal cells. *Exp Toxicol Pathol,* 59**,** 355-63.

HABIB, S. J., CHEN, B. C., TSAI, F. C., ANASTASSIADIS, K., MEYER, T., BETZIG, E. & NUSSE, R. 2013. A localized Wnt signal orients asymmetric stem cell division in vitro. *Science,* 339**,** 1445-8.

HADJIDAKIS, D. J. & ANDROULAKIS, II 2006. Bone remodeling. *Ann N Y Acad Sci,* 1092**,** 385-96.

HANINI, A., SCHMITT, A., KACEM, K., CHAU, F., AMMAR, S. & GAVARD, J. 2011. Evaluation of iron oxide nanoparticle biocompatibility. *International Journal of Nanomedicine,* 6**,** 787-794.

HARMEY, D., HESSLE, L., NARISAWA, S., JOHNSON, K. A., TERKELTAUB, R. & MILLAN, J. L. 2004. Concerted regulation of inorganic pyrophosphate and osteopontin by akp2, enpp1, and ank: an integrated model of the pathogenesis of mineralization disorders. *Am J Pathol,* 164**,** 1199-209.

HE, T. C., SPARKS, A. B., RAGO, C., HERMEKING, H., ZAWEL, L., DA COSTA, L. T., MORIN, P. J., VOGELSTEIN, B. & KINZLER, K. W. 1998. Identification of c-MYC as a target of the APC pathway. *Science,* 281**,** 1509-12.

HEINEKE, J. & MOLKENTIN, J. D. 2006. Regulation of cardiac hypertrophy by intracellular signalling pathways. *Nat Rev Mol Cell Biol,* 7**,** 589-600.

HEISENBERG, C. P. & BELLAICHE, Y. 2013. Forces in tissue morphogenesis and patterning. *Cell,* 153**,** 948-62.
HELLER, E. & FUCHS, E. 2015. Tissue patterning and cellular mechanics. *The Journal of Cell Biology,* 211**,** 219-231.
HELMICK, C. G., FELSON, D. T., LAWRENCE, R. C., GABRIEL, S., HIRSCH, R., KWOH, C. K., LIANG, M. H., KREMERS, H. M., MAYES, M. D., MERKEL, P. A., PILLEMER, S. R., REVEILLE, J. D., STONE, J. H. & NATIONAL ARTHRITIS DATA, W. 2008. Estimates of the prevalence of arthritis and other rheumatic conditions in the United States. Part I. *Arthritis Rheum,* 58**,** 15-25.
HENSTOCK, J. R., ROTHERHAM, M., RASHIDI, H., SHAKESHEFF, K. M. & EL HAJ, A. J. 2014. Remotely Activated Mechanotransduction via Magnetic Nanoparticles Promotes Mineralization Synergistically With Bone Morphogenetic Protein 2: Applications for Injectable Cell Therapy. *Stem Cells Translational Medicine,* 3**,** 1363-1374.
HENSTOCK, J. R., ROTHERHAM, M., ROSE, J. B. & EL HAJ, A. J. 2013. Cyclic hydrostatic pressure stimulates enhanced bone development in the foetal chick femur in vitro. *Bone,* 53**,** 468-77.
HERBST, A., JURINOVIC, V., KREBS, S., THIEME, S. E., BLUM, H., GÖKE, B. & KOLLIGS, F. T. 2014. Comprehensive analysis of β-catenin target genes in colorectal carcinoma cell lines with deregulated Wnt/β-catenin signaling. *BMC Genomics,* 15**,** 1-15.
HERR, P., HAUSMANN, G. & BASLER, K. 2012. WNT secretion and signalling in human disease. *Trends Mol Med,* 18**,** 483-93.
HILGER, I., HERGT, R. & KAISER, W. A. 2005. Towards breast cancer treatment by magnetic heating. *Journal of Magnetism and Magnetic Materials,* 293**,** 314-319.
HOEPPNER, L. H., SECRETO, F. J. & WESTENDORF, J. J. 2009. Wnt signaling as a therapeutic target for bone diseases. *Expert Opin Ther Targets,* 13**,** 485-96.
HOFFMAN, M. D. & BENOIT, D. S. 2015. Agonism of Wnt-beta-catenin signalling promotes mesenchymal stem cell (MSC) expansion. *J Tissue Eng Regen Med,* 9**,** E13-26.
HOGAN, B. L. 1996. Bone morphogenetic proteins: multifunctional regulators of vertebrate development. *Genes Dev,* 10**,** 1580-94.
HOLLINGER, J. O., EINHORN, T. A., DOLL, B. & SFEIR, C. 2004. *Bone Tissue Engineering*, CRC Press. Pages 4, 30, 35
HOLMEN, S. L., ROBERTSON, S. A., ZYLSTRA, C. R. & WILLIAMS, B. O. 2005. Wnt-independent activation of beta-catenin mediated by a Dkk1-Fz5 fusion protein. *Biochem Biophys Res Commun,* 328**,** 533-9.
HOLTORF, H. L., SHEFFIELD, T. L., AMBROSE, C. G., JANSEN, J. A. & MIKOS, A. G. 2005. Flow perfusion culture of marrow stromal cells seeded on porous biphasic calcium phosphate ceramics. *Ann Biomed Eng,* 33**,** 1238-48.
HORIE, M., CHOI, H., LEE, R. H., REGER, R. L., YLOSTALO, J., MUNETA, T., SEKIYA, I. & PROCKOP, D. J. 2012. Intra-articular injection of human mesenchymal stem cells (MSCs) promote rat meniscal regeneration by being activated to express Indian hedgehog that enhances expression of type II collagen. *Osteoarthritis and Cartilage,* 20**,** 1197-1207.
HORWITZ, E. M., PROCKOP, D. J., FITZPATRICK, L. A., KOO, W. W., GORDON, P. L., NEEL, M., SUSSMAN, M., ORCHARD, P., MARX, J. C., PYERITZ, R. E. & BRENNER, M. K. 1999. Transplantability and therapeutic effects of bone marrow-derived mesenchymal cells in children with osteogenesis imperfecta. *Nat Med,* 5**,** 309-13.
HOSKINS, C., CUSCHIERI, A. & WANG, L. 2012. The cytotoxicity of polycationic iron oxide nanoparticles: Common endpoint assays and alternative approaches for improved understanding of cellular response mechanism. *Journal of Nanobiotechnology,* 10**,** 1-11.
HOWE, L. R., SUBBARAMAIAH, K., CHUNG, W. J., DANNENBERG, A. J. & BROWN, A. M. 1999. Transcriptional activation of cyclooxygenase-2 in Wnt-1-transformed mouse mammary epithelial cells. *Cancer Res,* 59**,** 1572-7.

HSIEH, J. C., RATTNER, A., SMALLWOOD, P. M. & NATHANS, J. 1999. Biochemical characterization of Wnt-frizzled interactions using a soluble, biologically active vertebrate Wnt protein. *Proc Natl Acad Sci U S A,* 96**,** 3546-51.

HSIEH, Y. F. & TURNER, C. H. 2001. Effects of loading frequency on mechanically induced bone formation. *J Bone Miner Res,* 16**,** 918-24.

HU, B., DOBSON, J. & EL HAJ, A. J. 2014. Control of smooth muscle alpha-actin (SMA) up-regulation in HBMSCs using remote magnetic particle mechano-activation. *Nanomedicine,* 10**,** 45-55.

HU, B., EL HAJ, A. J. & DOBSON, J. 2013. Receptor-targeted, magneto-mechanical stimulation of osteogenic differentiation of human bone marrow-derived mesenchymal stem cells. *Int J Mol Sci,* 14**,** 19276-93.

HU, Y., BOCK, G., WICK, G. & XU, Q. 1998. Activation of PDGF receptor alpha in vascular smooth muscle cells by mechanical stress. *FASEB J,* 12**,** 1135-42.

HUANG, C. & OGAWA, R. 2010. Mechanotransduction in bone repair and regeneration. *FASEB J,* 24**,** 3625-32.

HUANG, D. M., HSIAO, J. K., CHEN, Y. C., CHIEN, L. Y., YAO, M., CHEN, Y. K., KO, B. S., HSU, S. C., TAI, L. A., CHENG, H. Y., WANG, S. W., YANG, C. S. & CHEN, Y. C. 2009. The promotion of human mesenchymal stem cell proliferation by superparamagnetic iron oxide nanoparticles. *Biomaterials,* 30**,** 3645-51.

HUBER, A. H., NELSON, W. J. & WEIS, W. I. 1997. Three-dimensional structure of the armadillo repeat region of beta-catenin. *Cell,* 90**,** 871-82.

HUGHES, S., DOBSON, J. & EL HAJ, A. J. 2007. Magnetic targeting of mechanosensors in bone cells for tissue engineering applications. *J Biomech,* 40 Suppl 1**,** S96-104.

HUGHES, S., EL HAJ, A. J. & DOBSON, J. 2005. Magnetic micro- and nanoparticle mediated activation of mechanosensitive ion channels. *Medical Engineering & Physics,* 27**,** 754-762.

HUGHES, S., MAGNAY, J., FOREMAN, M., PUBLICOVER, S. J., DOBSON, J. P. & EL HAJ, A. J. 2006. Expression of the mechanosensitive 2PK+ channel TREK-1 in human osteoblasts. *J Cell Physiol,* 206**,** 738-48.

HUGHES, S., MCBAIN, S., DOBSON, J. & EL HAJ, A. J. 2008. Selective activation of mechanosensitive ion channels using magnetic particles. *J R Soc Interface,* 5**,** 855-63.

HULL, K. L. 2011. *Human Form, Human Function: Essentials of Anatomy & Physiology*, Lippincott Williams & Wilkins. Page 111

HUMPHRIES, J. D., BYRON, A. & HUMPHRIES, M. J. 2006. Integrin ligands at a glance. *Journal of Cell Science,* 119**,** 3901-3903.

HUTMACHER, D. W. 2000. Scaffolds in tissue engineering bone and cartilage. *Biomaterials,* 21**,** 2529-2543.

HYNES, R. O. 2002. Integrins: bidirectional, allosteric signaling machines. *Cell,* 110**,** 673-87.

INGBER, D. E. 2006. Cellular mechanotransduction: putting all the pieces together again. *FASEB J,* 20**,** 811-27.

INOUE, T., OZ, H. S., WILAND, D., GHARIB, S., DESHPANDE, R., HILL, R. J., KATZ, W. S. & STERNBERG, P. W. 2004. C. elegans LIN-18 is a Ryk ortholog and functions in parallel to LIN-17/Frizzled in Wnt signaling. *Cell,* 118**,** 795-806.

ISHITANI, T., KISHIDA, S., HYODO-MIURA, J., UENO, N., YASUDA, J., WATERMAN, M., SHIBUYA, H., MOON, R. T., NINOMIYA-TSUJI, J. & MATSUMOTO, K. 2003. The TAK1-NLK mitogen-activated protein kinase cascade functions in the Wnt-5a/Ca(2+) pathway to antagonize Wnt/beta-catenin signaling. *Mol Cell Biol,* 23**,** 131-9.

ISHITANI, T., NINOMIYA-TSUJI, J., NAGAI, S., NISHITA, M., MENEGHINI, M., BARKER, N., WATERMAN, M., BOWERMAN, B., CLEVERS, H., SHIBUYA, H. & MATSUMOTO, K. 1999. The TAK1-NLK-MAPK-related pathway antagonizes signalling between beta-catenin and transcription factor TCF. *Nature,* 399**,** 798-802.

ITANO, N., OKAMOTO, S., ZHANG, D., LIPTON, S. A. & RUOSLAHTI, E. 2003. Cell spreading controls endoplasmic and nuclear calcium: a physical gene regulation pathway from the cell surface to the nucleus. *Proc Natl Acad Sci U S A,* 100**,** 5181-6.

ITASAKI, N., JONES, C. M., MERCURIO, S., ROWE, A., DOMINGOS, P. M., SMITH, J. C. & KRUMLAUF, R. 2003. Wise, a context-dependent activator and inhibitor of Wnt signalling. *Development,* 130**,** 4295-305.

ITO, A., KUGA, Y., HONDA, H., KIKKAWA, H., HORIUCHI, A., WATANABE, Y. & KOBAYASHI, T. 2004. Magnetite nanoparticle-loaded anti-HER2 immunoliposomes for combination of antibody therapy with hyperthermia. *Cancer Letters,* 212**,** 167-175.

JAISWAL, N., HAYNESWORTH, S. E., CAPLAN, A. I. & BRUDER, S. P. 1997. Osteogenic differentiation of purified, culture-expanded human mesenchymal stem cells in vitro. *J Cell Biochem,* 64**,** 295-312.

JAMBHRUNKAR, S., QU, Z., POPAT, A., YANG, J., NOONAN, O., ACAUAN, L., AHMAD NOR, Y., YU, C. & KARMAKAR, S. 2014. Effect of Surface Functionality of Silica Nanoparticles on Cellular Uptake and Cytotoxicity. *Molecular Pharmaceutics,* 11**,** 3642-3655.

JAMES, A. W. 2013. Review of Signaling Pathways Governing MSC Osteogenic and Adipogenic Differentiation. *Scientifica,* 2013**,** 17 pages.

JANECZEK, A. A., TARE, R. S., SCARPA, E., MORENO-JIMENEZ, I., ROWLAND, C. A., JENNER, D., NEWMAN, T. A., OREFFO, R. O. C. & EVANS, N. D. 2016. Transient Canonical Wnt Stimulation Enriches Human Bone Marrow Mononuclear Cell Isolates for Osteoprogenitors. *STEM CELLS,* 34**,** 418-430.

JASMIN, TORRES, A. L. M., NUNES, H. M., PASSIPIERI, J. A., JELICKS, L. A., GASPARETTO, E. L., SPRAY, D. C., CAMPOS DE CARVALHO, A. C. & MENDEZ-OTERO, R. 2011. Optimized labeling of bone marrow mesenchymal cells with superparamagnetic iron oxide nanoparticles and in vivo visualization by magnetic resonance imaging. *Journal of Nanobiotechnology,* 9**,** 1-13.

JAVAHERI, B., SUNTERS, A., ZAMAN, G., SUSWILLO, R. F., SAXON, L. K., LANYON, L. E. & PRICE, J. S. 2012. Lrp5 is not required for the proliferative response of osteoblasts to strain but regulates proliferation and apoptosis in a cell autonomous manner. *PLoS One,* 7**,** e35726.

JIANG, J. X. & CHENG, B. 2001. Mechanical stimulation of gap junctions in bone osteocytes is mediated by prostaglandin E2. *Cell Commun Adhes,* 8**,** 283-8.

JIANG, Y., HUO, S., MIZUHARA, T., DAS, R., LEE, Y.-W., HOU, S., MOYANO, D. F., DUNCAN, B., LIANG, X.-J. & ROTELLO, V. M. 2015. The Interplay of Size and Surface Functionality on the Cellular Uptake of Sub-10 nm Gold Nanoparticles. *ACS Nano,* 9**,** 9986-9993.

JIN, M., DU, X. & CHEN, L. 2012. Cross-talk between FGF and other cytokine signalling pathways during endochondral bone development. *Cell Biology International,* 36**,** 691-696.

JIN, Y., JIA, C., HUANG, S. W., O'DONNELL, M. & GAO, X. 2010. Multifunctional nanoparticles as coupled contrast agents. *Nat Commun,* 1**,** 41.

JIN, Z. G., UEBA, H., TANIMOTO, T., LUNGU, A. O., FRAME, M. D. & BERK, B. C. 2003. Ligand-independent activation of vascular endothelial growth factor receptor 2 by fluid shear stress regulates activation of endothelial nitric oxide synthase. *Circ Res,* 93**,** 354-63.

JUNQUEIRA, L. C., BIGNOLAS, G. & BRENTANI, R. R. 1979. Picrosirius staining plus polarization microscopy, a specific method for collagen detection in tissue sections. *Histochem J,* 11**,** 447-55.

JUNQUEIRA, L. C. U., BIGNOLAS, G. & BRENTANI, R. R. Picrosirius staining plus polarization microscopy, a specific method for collagen detection in tissue sections. *The Histochemical Journal,* 11**,** 447-455.

KAHLER, R. A., GALINDO, M., LIAN, J., STEIN, G. S., VAN WIJNEN, A. J. & WESTENDORF, J. J. 2006. Lymphocyte enhancer-binding factor 1 (Lef1) inhibits terminal differentiation of osteoblasts. *J Cell Biochem,* 97**,** 969-83.

KAHLER, R. A. & WESTENDORF, J. J. 2003. Lymphoid enhancer factor-1 and beta-catenin inhibit Runx2-dependent transcriptional activation of the osteocalcin promoter. *J Biol Chem,* 278**,** 11937-44.

KAHLER, R. A., YINGST, S. M., HOEPPNER, L. H., JENSEN, E. D., KRAWCZAK, D., OXFORD, J. T. & WESTENDORF, J. J. 2008. Collagen 11a1 is indirectly activated by lymphocyte enhancer-binding factor 1 (Lef1) and negatively regulates osteoblast maturation. *Matrix Biol,* 27**,** 330-8.

KANCZLER, J. M. & OREFFO, R. O. 2008. Osteogenesis and angiogenesis: the potential for engineering bone. *Eur Cell Mater,* 15**,** 100-14.

KANCZLER, J. M., SMITH, E. L., ROBERTS, C. A. & OREFFO, R. O. 2012. A novel approach for studying the temporal modulation of embryonic skeletal development using organotypic bone cultures and microcomputed tomography. *Tissue Eng Part C Methods,* 18**,** 747-60.

KANCZLER, J. M., SURA, H. S., MAGNAY, J., GREEN, D., OREFFO, R. O., DOBSON, J. P. & EL HAJ, A. J. 2010. Controlled differentiation of human bone marrow stromal cells using magnetic nanoparticle technology. *Tissue Eng Part A,* 16**,** 3241-50.

KANG, Q., SUN, M. H., CHENG, H., PENG, Y., MONTAG, A. G., DEYRUP, A. T., JIANG, W., LUU, H. H., LUO, J., SZATKOWSKI, J. P., VANICHAKARN, P., PARK, J. Y., LI, Y., HAYDON, R. C. & HE, T. C. 2004. Characterization of the distinct orthotopic bone-forming activity of 14 BMPs using recombinant adenovirus-mediated gene delivery. *Gene Ther,* 11**,** 1312-1320.

KANI, S., OISHI, I., YAMAMOTO, H., YODA, A., SUZUKI, H., NOMACHI, A., IOZUMI, K., NISHITA, M., KIKUCHI, A., TAKUMI, T. & MINAMI, Y. 2004. The receptor tyrosine kinase Ror2 associates with and is activated by casein kinase Iepsilon. *J Biol Chem,* 279**,** 50102-9.

KANNO, T., TAKAHASHI, T., TSUJISAWA, T., ARIYOSHI, W. & NISHIHARA, T. 2007. Mechanical stress-mediated Runx2 activation is dependent on Ras/ERK1/2 MAPK signaling in osteoblasts. *J Cell Biochem,* 101**,** 1266-77.

KATO, M., PATEL, M. S., LEVASSEUR, R., LOBOV, I., CHANG, B. H., GLASS, D. A., 2ND, HARTMANN, C., LI, L., HWANG, T. H., BRAYTON, C. F., LANG, R. A., KARSENTY, G. & CHAN, L. 2002. Cbfa1-independent decrease in osteoblast proliferation, osteopenia, and persistent embryonic eye vascularization in mice deficient in Lrp5, a Wnt coreceptor. *J Cell Biol,* 157**,** 303-14.

KAWANO, K. & MAITANI, Y. 2011. Effects of Polyethylene Glycol Spacer Length and Ligand Density on Folate Receptor Targeting of Liposomal Doxorubicin In Vitro. *Journal of Drug Delivery,* vol. 2011**,** 6 Pages.

KAZANSKAYA, O., GLINKA, A., DEL BARCO BARRANTES, I., STANNEK, P., NIEHRS, C. & WU, W. 2004. R-Spondin2 is a secreted activator of Wnt/beta-catenin signaling and is required for Xenopus myogenesis. *Dev Cell,* 7**,** 525-34.

KENGAKU, M., CAPDEVILA, J., RODRIGUEZ-ESTEBAN, C., DE LA PENA, J., JOHNSON, R. L., IZPISUA BELMONTE, J. C. & TABIN, C. J. 1998. Distinct WNT pathways regulating AER formation and dorsoventral polarity in the chick limb bud. *Science,* 280**,** 1274-7.

KETCHUM, K. A., JOINER, W. J., SELLERS, A. J., KACZMAREK, L. K. & GOLDSTEIN, S. A. 1995. A new family of outwardly rectifying potassium channel proteins with two pore domains in tandem. *Nature,* 376**,** 690-5.

KHAN, K. 2001. *Physical Activity and Bone Health*, Human Kinetics. Pages 24, 26, 32

KIKUCHI, A., YAMAMOTO, H. & KISHIDA, S. 2007. Multiplicity of the interactions of Wnt proteins and their receptors. *Cellular Signalling,* 19**,** 659-671.

KIM, J.-A., CHOI, H.-K., KIM, T.-M., LEEM, S.-H. & OH, I.-H. 2015. Regulation of mesenchymal stromal cells through fine tuning of canonical Wnt signaling. *Stem Cell Research,* 14**,** 356-368.

KIM, J.-B., LEUCHT, P., LAM, K., LUPPEN, C., TEN BERGE, D., NUSSE, R. & HELMS, J. A. 2007. Bone Regeneration Is Regulated by Wnt Signaling. *Journal of Bone and Mineral Research,* 22**,** 1913-1923.

KIM, K. A., KAKITANI, M., ZHAO, J., OSHIMA, T., TANG, T., BINNERTS, M., LIU, Y., BOYLE, B., PARK, E., EMTAGE, P., FUNK, W. D. & TOMIZUKA, K. 2005. Mitogenic influence of human R-spondin1 on the intestinal epithelium. *Science,* 309**,** 1256-9.

KIMELMAN, D. & XU, W. 2006. [beta]-Catenin destruction complex: insights and questions from a structural perspective. *Oncogene,* 25**,** 7482-7491.

KINI, U. & NANDEESH, B. N. 2012. *Physiology of Bone Formation, Remodeling, and Metabolism*, Springer Berlin Heidelberg. Pages 29-57

KIRBY, G. T. S., WHITE, L. J., RAHMAN, C. V., COX, H. C., QUTACHI, O., ROSE, F. R. A. J., HUTMACHER, D. W., SHAKESHEFF, K. M. & WOODRUFF, M. A. 2011. PLGA-Based Microparticles for the Sustained Release of BMP-2. *Polymers,* 3**,** 571-586.

KIRKHAM, G. R., ELLIOT, K. J., KERAMANE, A., SALTER, D. M., DOBSON, J. P., EL HAJ, A. J. & CARTMELL, S. H. 2010. Hyperpolarization of human mesenchymal stem cells in response to magnetic force. *IEEE Trans Nanobioscience,* 9**,** 71-4.

KITASE, Y., BARRAGAN, L., QING, H., KONDOH, S., JIANG, J. X., JOHNSON, M. L. & BONEWALD, L. F. 2010. Mechanical induction of PGE2 in osteocytes blocks glucocorticoid-induced apoptosis through both the β-catenin and PKA pathways. *Journal of Bone and Mineral Research,* 25**,** 2657-2668.

KLEIN-NULEND, J., BACABAC, R. G. & MULLENDER, M. G. 2005. Mechanobiology of bone tissue. *Pathol Biol (Paris),* 53**,** 576-80.

KNOTHE TATE, M. L., FALLS, T. D., MCBRIDE, S. H., ATIT, R. & KNOTHE, U. R. 2008. Mechanical modulation of osteochondroprogenitor cell fate. *Int J Biochem Cell Biol,* 40**,** 2720-38.

KOH, S. D., MONAGHAN, K., SERGEANT, G. P., RO, S., WALKER, R. L., SANDERS, K. M. & HOROWITZ, B. 2001. TREK-1 regulation by nitric oxide and cGMP-dependent protein kinase. An essential role in smooth muscle inhibitory neurotransmission. *J Biol Chem,* 276**,** 44338-46.

KOLBEN, T., PEROBNER, I., FERNSEBNER, K., LECHNER, F., GEISSLER, C., RUIZ-HEINRICH, L., CAPOVILLA, S., JOCHUM, M. & NETH, P. 2012. Dissecting the impact of Frizzled receptors in Wnt/beta-catenin signaling of human mesenchymal stem cells. *Biol Chem,* 393**,** 1433-47.

KOLF, C. M., CHO, E. & TUAN, R. S. 2007. Mesenchymal stromal cells: Biology of adult mesenchymal stem cells: regulation of niche, self-renewal and differentiation. *Arthritis Research & Therapy,* 9**,** 1-10.

KOLLAR, K., COOK, M. M., ATKINSON, K. & BROOKE, G. 2009. Molecular mechanisms involved in mesenchymal stem cell migration to the site of acute myocardial infarction. *Int J Cell Biol,* vol. 2009**,** 8 pages.

KOMEKADO, H., YAMAMOTO, H., CHIBA, T. & KIKUCHI, A. 2007. Glycosylation and palmitoylation of Wnt-3a are coupled to produce an active form of Wnt-3a. *Genes Cells,* 12**,** 521-34.

KON, E., FILARDO, G., DI MARTINO, A. & MARCACCI, M. 2012. ACI and MACI. *J Knee Surg,* 25**,** 17-22.

KOUASSI, G. K. & IRUDAYARAJ, J. 2006a. Magnetic and Gold-Coated Magnetic Nanoparticles as a DNA Sensor. *Analytical Chemistry,* 78**,** 3234-3241.

KOUASSI, G. K. & IRUDAYARAJ, J. 2006b. A nanoparticle-based immobilization assay for prion-kinetics study. *Journal of Nanobiotechnology,* 4**,** 1-10.

KRAMPERA, M., PIZZOLO, G., APRILI, G. & FRANCHINI, M. 2006. Mesenchymal stem cells for bone, cartilage, tendon and skeletal muscle repair. *Bone,* 39**,** 678-83.

KRATCHMAROVA, I., BLAGOEV, B., HAACK-SORENSEN, M., KASSEM, M. & MANN, M. 2005. Mechanism of divergent growth factor effects in mesenchymal stem cell differentiation. *Science,* 308**,** 1472-7.

KREKE, M. R., SHARP, L. A., LEE, Y. W. & GOLDSTEIN, A. S. 2008. Effect of intermittent shear stress on mechanotransductive signaling and osteoblastic differentiation of bone marrow stromal cells. *Tissue Eng Part A,* 14**,** 529-37.

KREMENEVSKAJA, N., VON WASIELEWSKI, R., RAO, A. S., SCHOFL, C., ANDERSSON, T. & BRABANT, G. 2005. Wnt-5a has tumor suppressor activity in thyroid carcinoma. *Oncogene,* 24**,** 2144-54.

KRUPNIK, V. E., SHARP, J. D., JIANG, C., ROBISON, K., CHICKERING, T. W., AMARAVADI, L., BROWN, D. E., GUYOT, D., MAYS, G., LEIBY, K., CHANG, B., DUONG, T., GOODEARL, A. D., GEARING, D. P., SOKOL, S. Y. & MCCARTHY, S. A. 1999. Functional and structural diversity of the human Dickkopf gene family. *Gene,* 238**,** 301-13.

KUHL, M., SHELDAHL, L. C., MALBON, C. C. & MOON, R. T. 2000a. Ca(2+)/calmodulin-dependent protein kinase II is stimulated by Wnt and Frizzled homologs and promotes ventral cell fates in Xenopus. *J Biol Chem,* 275**,** 12701-11.

KUHL, M., SHELDAHL, L. C., PARK, M., MILLER, J. R. & MOON, R. T. 2000b. The Wnt/Ca2+ pathway: a new vertebrate Wnt signaling pathway takes shape. *Trends Genet,* 16**,** 279-83.

KULTERER, B., FRIEDL, G., JANDROSITZ, A., SANCHEZ-CABO, F., PROKESCH, A., PAAR, C., SCHEIDELER, M., WINDHAGER, R., PREISEGGER, K.-H. & TRAJANOSKI, Z. 2007. Gene expression profiling of human mesenchymal stem cells derived from bone marrow during expansion and osteoblast differentiation. *BMC Genomics,* 8**,** 1-15.

KUMAR, A. & BORIEK, A. M. 2003. Mechanical stress activates the nuclear factor-kappaB pathway in skeletal muscle fibers: a possible role in Duchenne muscular dystrophy. *FASEB J,* 17**,** 386-96.

KUMAR, C. S. S. R. 2009. *Magnetic Nanomaterials*, Wiley. Pages 56-57, 79

KUNNEL, J. G., GILBERT, J. L. & STERN, P. H. 2002. In vitro mechanical and cellular responses of neonatal mouse bones to loading using a novel micromechanical-testing device. *Calcif Tissue Int,* 71**,** 499-507.

KYRTATOS, P. G., LEHTOLAINEN, P., JUNEMANN-RAMIREZ, M., GARCIA-PRIETO, A., PRICE, A. N., MARTIN, J. F., GADIAN, D. G., PANKHURST, Q. A. & LYTHGOE, M. F. 2009. Magnetic tagging increases delivery of circulating progenitors in vascular injury. *JACC Cardiovasc Interv,* 2**,** 794-802.

LAEREMANS, H., HACKENG, T. M., VAN ZANDVOORT, M. A., THIJSSEN, V. L., JANSSEN, B. J., OTTENHEIJM, H. C., SMITS, J. F. & BLANKESTEIJN, W. M. 2011. Blocking of frizzled signaling with a homologous peptide fragment of wnt3a/wnt5a reduces infarct expansion and prevents the development of heart failure after myocardial infarction. *Circulation,* 124**,** 1626-35.

LAKO, M., STRACHAN, T., BULLEN, P., WILSON, D. I., ROBSON, S. C. & LINDSAY, S. 1998. Isolation, characterisation and embryonic expression of WNT11, a gene which maps to 11q13.5 and has possible roles in the development of skeleton, kidney and lung. *Gene,* 219**,** 101-10.

LALANDE, C., MIRAUX, S., DERKAOUI, S. M., MORNET, S., BAREILLE, R., FRICAIN, J. C., FRANCONI, J. M., LE VISAGE, C., LETOURNEUR, D., AMEDEE, J. & BOUZIER-SORE, A. K. 2011. Magnetic resonance imaging tracking of human adipose derived stromal cells within three-dimensional scaffolds for bone tissue engineering. *Eur Cell Mater,* 21**,** 341-54.

LANGENBACH, F. & HANDSCHEL, J. 2013. Effects of dexamethasone, ascorbic acid and β-glycerophosphate on the osteogenic differentiation of stem cells in vitro. *Stem Cell Research & Therapy,* 4**,** 1-7.

LANZA, R. & ATALA, A. 2013. *Essentials of Stem Cell Biology*, Elsevier Science. Pages 7-9

LANZA, R., BLAU, H., GEARHART, J., HOGAN, B., MELTON, D., MOORE, M., PEDERSEN, R., THOMAS, E. D., THOMSON, J. A. & VERFAILLIE, C. 2004. *Handbook of Stem Cells, Two-Volume Set: Volume 1-Embryonic Stem Cells; Volume 2-Adult & Fetal Stem Cells*, Elsevier Science. Page 13

LAURSEN, M., HOY, K., HANSEN, E. S., GELINECK, J., CHRISTENSEN, F. B. & BUNGER, C. E. 1999. Recombinant bone morphogenetic protein-7 as an intracorporal bone growth stimulator in unstable thoracolumbar burst fractures in humans: preliminary results. *Eur Spine J,* 8**,** 485-90.

LEIMEISTER, C., BACH, A. & GESSLER, M. 1998. Developmental expression patterns of mouse sFRP genes encoding members of the secreted frizzled related protein family. *Mech Dev,* 75**,** 29-42.

LEMKE, A. J., SENFFT VON PILSACH, M. I., LÜBBE, A., BERGEMANN, C., RIESS, H. & FELIX, R. 2004. MRI after magnetic drug targeting in patients with advanced solid malignant tumors. *European Radiology,* 14**,** 1949-1955.

LEMMON, M. A. & SCHLESSINGER, J. 2010. Cell signaling by receptor tyrosine kinases. *Cell,* 141**,** 1117-34.

LENDECKEL, S., JODICKE, A., CHRISTOPHIS, P., HEIDINGER, K., WOLFF, J., FRASER, J. K., HEDRICK, M. H., BERTHOLD, L. & HOWALDT, H. P. 2004. Autologous stem cells (adipose) and fibrin glue used to treat widespread traumatic calvarial defects: case report. *J Craniomaxillofac Surg,* 32**,** 370-3.

LESAGE, F. & LAZDUNSKI, M. 2000. Molecular and functional properties of two-pore-domain potassium channels. *Am J Physiol Renal Physiol,* 279**,** F793-801.

LETAMENDIA, A., LABBE, E. & ATTISANO, L. 2001. Transcriptional regulation by Smads: crosstalk between the TGF-beta and Wnt pathways. *J Bone Joint Surg Am,* 83-A Suppl 1**,** S31-9.

LEUCHT, P., MINEAR, S., TEN BERGE, D., NUSSE, R. & HELMS, J. A. 2008. Translating insights from development into regenerative medicine: the function of Wnts in bone biology. *Semin Cell Dev Biol,* 19**,** 434-43.

LEVY, R. M. 2012. *Principles of Solid State Physics*, Elsevier Science. Pages 193-194

LI, S. M. D. & SIEGAL, G. P. M. D. P. 2010. Small Cell Tumors of Bone. *Advances in Anatomic Pathology,* 17**,** 1-11.

LICHTMAN, M. A. 1981. The ultrastructure of the hemopoietic environment of the marrow: a review. *Exp Hematol,* 9**,** 391-410.

LIEDERT, A., KASPAR, D., BLAKYTNY, R., CLAES, L. & IGNATIUS, A. 2006. Signal transduction pathways involved in mechanotransduction in bone cells. *Biochem Biophys Res Commun,* 349**,** 1-5.

LIN, M. M., KIM DO, K., EL HAJ, A. J. & DOBSON, J. 2008. Development of superparamagnetic iron oxide nanoparticles (SPIONS) for translation to clinical applications. *IEEE Trans Nanobioscience,* 7**,** 298-305.

LING, L., NURCOMBE, V. & COOL, S. M. 2009. Wnt signaling controls the fate of mesenchymal stem cells. *Gene,* 433**,** 1-7.

LITTLE, R. D., CARULLI, J. P., DEL MASTRO, R. G., DUPUIS, J., OSBORNE, M., FOLZ, C., MANNING, S. P., SWAIN, P. M., ZHAO, S. C., EUSTACE, B., LAPPE, M. M., SPITZER, L., ZWEIER, S., BRAUNSCHWEIGER, K., BENCHEKROUN, Y., HU, X., ADAIR, R., CHEE, L., FITZGERALD, M. G., TULIG, C., CARUSO, A., TZELLAS, N., BAWA, A., FRANKLIN, B., MCGUIRE, S., NOGUES, X., GONG, G., ALLEN, K. M., ANISOWICZ, A., MORALES, A. J., LOMEDICO, P. T., RECKER, S. M., VAN EERDEWEGH, P., RECKER, R. R. & JOHNSON, M. L. 2002. A mutation in the LDL receptor-related protein 5 gene results in the autosomal dominant high-bone-mass trait. *Am J Hum Genet,* 70**,** 11-19.

LIU, C., ABEDIAN, R., MEISTER, R., HAASPER, C., HURSCHLER, C., KRETTEK, C., VON LEWINSKI, G. & JAGODZINSKI, M. 2012. Influence of perfusion and compression on the proliferation and differentiation of bone mesenchymal stromal cells seeded on polyurethane scaffolds. *Biomaterials,* 33**,** 1052-64.

LIU, G., VIJAYAKUMAR, S., GRUMOLATO, L., ARROYAVE, R., QIAO, H., AKIRI, G. & AARONSON, S. A. 2009. Canonical Wnts function as potent regulators of osteogenesis by human mesenchymal stem cells. *J Cell Biol,* 185**,** 67-75.

LOEBINGER, M. R., KYRTATOS, P. G., TURMAINE, M., PRICE, A. N., PANKHURST, Q., LYTHGOE, M. F. & JANES, S. M. 2009. Magnetic resonance imaging of mesenchymal stem cells homing to pulmonary metastases using biocompatible magnetic nanoparticles. *Cancer Res,* 69**,** 8862-7.

LOGAN, C. Y. & NUSSE, R. 2004. The Wnt signaling pathway in development and disease. *Annu Rev Cell Dev Biol,* 20**,** 781-810.

LU, J., MA, Z., HSIEH, J. C., FAN, C. W., CHEN, B., LONGGOOD, J. C., WILLIAMS, N. S., AMATRUDA, J. F., LUM, L. & CHEN, C. 2009. Structure-activity relationship studies of small-molecule inhibitors of Wnt response. *Bioorg Med Chem Lett,* 19**,** 3825-7.

LUU, Y. K., CAPILLA, E., ROSEN, C. J., GILSANZ, V., PESSIN, J. E., JUDEX, S. & RUBIN, C. T. 2009. Mechanical stimulation of mesenchymal stem cell proliferation and differentiation promotes osteogenesis while preventing dietary-induced obesity. *J Bone Miner Res,* 24**,** 50-61.

M. HOFMANN-AMTENBRINK, B. V. R., H. HOFMANN 2009. *Superparamagnetic nanoparticles for biomedical applications*, Transworld Research Network. Pages 121-122

MA, L. & WANG, H. Y. 2006. Suppression of cyclic GMP-dependent protein kinase is essential to the Wnt/cGMP/Ca2+ pathway. *J Biol Chem,* 281**,** 30990-1001.

MACDONALD, B. T., TAMAI, K. & HE, X. 2009. Wnt/beta-catenin signaling: components, mechanisms, and diseases. *Dev Cell,* 17**,** 9-26.

MACMULL, S., JAISWAL, P. K., BENTLEY, G., SKINNER, J. A., CARRINGTON, R. W. & BRIGGS, T. W. 2012. The role of autologous chondrocyte implantation in the treatment of symptomatic chondromalacia patellae. *Int Orthop,* 36**,** 1371-7.

MAHMOUDI, M., SANT, S., WANG, B., LAURENT, S. & SEN, T. 2011. Superparamagnetic iron oxide nanoparticles (SPIONs): development, surface modification and applications in chemotherapy. *Adv Drug Deliv Rev,* 63**,** 24-46.

MAMMOTO, A., MAMMOTO, T. & INGBER, D. E. 2012. Mechanosensitive mechanisms in transcriptional regulation. *J Cell Sci,* 125**,** 3061-73.

MANIOTIS, A. J., CHEN, C. S. & INGBER, D. E. 1997. Demonstration of mechanical connections between integrins, cytoskeletal filaments, and nucleoplasm that stabilize nuclear structure. *Proceedings of the National Academy of Sciences of the United States of America,* 94**,** 849-854.

MAO, B. & NIEHRS, C. 2003. Kremen2 modulates Dickkopf2 activity during Wnt/LRP6 signaling. *Gene,* 302**,** 179-83.

MAO, B., WU, W., DAVIDSON, G., MARHOLD, J., LI, M., MECHLER, B. M., DELIUS, H., HOPPE, D., STANNEK, P., WALTER, C., GLINKA, A. & NIEHRS, C. 2002. Kremen proteins are Dickkopf receptors that regulate Wnt/beta-catenin signalling. *Nature,* 417**,** 664-7.

MAO, B., WU, W., LI, Y., HOPPE, D., STANNEK, P., GLINKA, A. & NIEHRS, C. 2001. LDL-receptor-related protein 6 is a receptor for Dickkopf proteins. *Nature,* 411**,** 321-5.

MAQUET, P., WOLFF, J. & FURLONG, R. 2012. *The Law of Bone Remodelling*, Springer Berlin Heidelberg. Pages 4-5

MARCOS-CAMPOS, I., ASIN, L., TORRES, T. E., MARQUINA, C., TRES, A., IBARRA, M. R. & GOYA, G. F. 2011. Cell death induced by the application of alternating magnetic fields to nanoparticle-loaded dendritic cells. *Nanotechnology,* 22**,** 205101.

MARKIDES, H., KEHOE, O., MORRIS, R. H. & EL HAJ, A. J. 2013. Whole body tracking of superparamagnetic iron oxide nanoparticle-labelled cells – a rheumatoid arthritis mouse model. *Stem Cell Research & Therapy,* 4**,** 1-14.

MARKIDES, H., MCLAREN, J. S. & EL HAJ, A. J. 2015. Overcoming translational challenges - The delivery of mechanical stimuli in vivo. *Int J Biochem Cell Biol,* 69**,** 162-72.

MARKIDES, H., ROTHERHAM, M. & EL HAJ, A. J. 2012. Biocompatibility and Toxicity of Magnetic Nanoparticles in Regenerative Medicine. *Journal of Nanomaterials,* 2012**,** 11 pages.

MAROM, R., SHUR, I., SOLOMON, R. & BENAYAHU, D. 2005. Characterization of adhesion and differentiation markers of osteogenic marrow stromal cells. *Journal of Cellular Physiology,* 202**,** 41-48.

MAROTO, R., RASO, A., WOOD, T. G., KUROSKY, A., MARTINAC, B. & HAMILL, O. P. 2005. TRPC1 forms the stretch-activated cation channel in vertebrate cells. *Nat Cell Biol,* 7**,** 179-85.

MARTIN, C. R., PREEDY, V. R. & HUNTER, R. J. 2012. *Nanomedicine and the Nervous System*, CRC Press. Page 212

MARTIN, G. R. 1998. The roles of FGFs in the early development of vertebrate limbs. *Genes Dev,* 12**,** 1571-86.

MARUYAMA, T., MIRANDO, A. J., DENG, C.-X. & HSU, W. 2010. The Balance of WNT and FGF Signaling Influences Mesenchymal Stem Cell Fate During Skeletal Development. *Science Signaling,* 3**,** ra40-ra40.

MATTHEWS, B. D., OVERBY, D. R., MANNIX, R. & INGBER, D. E. 2006. Cellular adaptation to mechanical stress: role of integrins, Rho, cytoskeletal tension and mechanosensitive ion channels. *J Cell Sci,* 119**,** 508-18.

MCBAIN, S. C., YIU, H. H. & DOBSON, J. 2008. Magnetic nanoparticles for gene and drug delivery. *Int J Nanomedicine,* 3**,** 169-80.

MEDEROS Y SCHNITZLER, M., STORCH, U., MEIBERS, S., NURWAKAGARI, P., BREIT, A., ESSIN, K., GOLLASCH, M. & GUDERMANN, T. 2008. Gq-coupled receptors as mechanosensors mediating myogenic vasoconstriction. *EMBO J,* 27**,** 3092-103.

MEDHURST, A. D., RENNIE, G., CHAPMAN, C. G., MEADOWS, H., DUCKWORTH, M. D., KELSELL, R. E., GLOGER, II & PANGALOS, M. N. 2001. Distribution analysis of human two pore domain potassium channels in tissues of the central nervous system and periphery. *Brain Res Mol Brain Res,* 86**,** 101-14.

MEHVAR, R. 2000. Dextrans for targeted and sustained delivery of therapeutic and imaging agents. *Journal of Controlled Release,* 69**,** 1-25.

MEIJER, L., SKALTSOUNIS, A. L., MAGIATIS, P., POLYCHRONOPOULOS, P., KNOCKAERT, M., LEOST, M., RYAN, X. P., VONICA, C. A., BRIVANLOU, A., DAJANI, R., CROVACE, C., TARRICONE, C., MUSACCHIO, A., ROE, S. M., PEARL, L. & GREENGARD, P. 2003. GSK-3-selective inhibitors derived from Tyrian purple indirubins. *Chem Biol,* 10**,** 1255-66.

MENG, J., FAN, J., GALIANA, G., BRANCA, R. T., CLASEN, P. L., MA, S., ZHOU, J., LEUSCHNER, C., KUMAR, C. S. S. R., HORMES, J., OTITI, T., BEYE, A. C., HARMER, M. P., KIELY, C. J., WARREN, W., HAATAJA, M. P. & SOBOYEJO, W. O. 2009. LHRH-functionalized superparamagnetic iron oxide nanoparticles for breast cancer targeting and contrast enhancement in MRI. *Materials Science and Engineering: C,* 29**,** 1467-1479.

MENG LIN, M., KIM, H. H., KIM, H., MUHAMMED, M. & KYUNG KIM, D. 2010. Iron oxide-based nanomagnets in nanomedicine: fabrication and applications. *Nano Rev,* 1.

MERCADER, N., LEONARDO, E., PIEDRA, M. E., MARTINEZ-A, C., ROS, M. A. & TORRES, M. 2000. Opposing RA and FGF signals control proximodistal vertebrate limb development through regulation of Meis genes. *Development,* 127**,** 3961-3970.

MERCURIO, F. & MANNING, A. M. 1999. NF-kappaB as a primary regulator of the stress response. *Oncogene,* 18**,** 6163-71.

MESCHER, A. 2009. *Junqueira's Basic Histology: Text and Atlas, 12th Edition*, McGraw-Hill Education. Pages 121-139

MILAT, F. & NG, K. W. 2009. Is Wnt signalling the final common pathway leading to bone formation? *Molecular and Cellular Endocrinology,* 310**,** 52-62.

MINEAR, S., LEUCHT, P., JIANG, J., LIU, B., ZENG, A., FUERER, C., NUSSE, R. & HELMS, J. A. 2010. Wnt proteins promote bone regeneration. *Sci Transl Med,* 2**,** 29ra30.

MONAGHAN, A. P., KIOSCHIS, P., WU, W., ZUNIGA, A., BOCK, D., POUSTKA, A., DELIUS, H. & NIEHRS, C. 1999. Dickkopf genes are co-ordinately expressed in mesodermal lineages. *Mech Dev,* 87**,** 45-56.

MONTALBETTI, C. A. G. N. & FALQUE, V. 2005. Amide bond formation and peptide coupling. *Tetrahedron,* 61**,** 10827-10852.

MORAES, L., VASCONCELOS-DOS-SANTOS, A., SANTANA, F. C., GODOY, M. A., ROSADO-DE-CASTRO, P. H., JASMIN, AZEVEDO-PEREIRA, R. L., CINTRA, W. M., GASPARETTO, E. L., SANTIAGO, M. F. & MENDEZ-OTERO, R. 2012. Neuroprotective effects and magnetic

resonance imaging of mesenchymal stem cells labeled with SPION in a rat model of Huntington's disease. *Stem Cell Research,* 9**,** 143-155.
MORTENSEN, A. 2006. *Concise Encyclopedia of Composite Materials*, Elsevier Science. Pages 59-62
MOSLEY, J. R. & LANYON, L. E. 1998. Strain rate as a controlling influence on adaptive modeling in response to dynamic loading of the ulna in growing male rats. *Bone,* 23**,** 313-8.
MULLENDER, M., EL HAJ, A. J., YANG, Y., VAN DUIN, M. A., BURGER, E. H. & KLEIN-NULEND, J. 2004. Mechanotransduction of bone cells in vitro: mechanobiology of bone tissue. *Med Biol Eng Comput,* 42**,** 14-21.
NALESSO, G., SHERWOOD, J., BERTRAND, J., PAP, T., RAMACHANDRAN, M., DE BARI, C., PITZALIS, C. & DELL'ACCIO, F. 2011. WNT-3A modulates articular chondrocyte phenotype by activating both canonical and noncanonical pathways. *J Cell Biol,* 193**,** 551-64.
NAM, J. S., TURCOTTE, T. J., SMITH, P. F., CHOI, S. & YOON, J. K. 2006. Mouse cristin/R-spondin family proteins are novel ligands for the Frizzled 8 and LRP6 receptors and activate beta-catenin-dependent gene expression. *J Biol Chem,* 281**,** 13247-57.
NETH, P., CICCARELLA, M., EGEA, V., HOELTERS, J., JOCHUM, M. & RIES, C. 2006. Wnt signaling regulates the invasion capacity of human mesenchymal stem cells. *Stem Cells,* 24**,** 1892-903.
NG, F., BOUCHER, S., KOH, S., SASTRY, K. S., CHASE, L., LAKSHMIPATHY, U., CHOONG, C., YANG, Z., VEMURI, M. C., RAO, M. S. & TANAVDE, V. 2008. PDGF, TGF-beta, and FGF signaling is important for differentiation and growth of mesenchymal stem cells (MSCs): transcriptional profiling can identify markers and signaling pathways important in differentiation of MSCs into adipogenic, chondrogenic, and osteogenic lineages. *Blood,* 112**,** 295-307.
NISWANDER, L., TICKLE, C., VOGEL, A., BOOTH, I. & MARTIN, G. R. 1993. FGF-4 replaces the apical ectodermal ridge and directs outgrowth and patterning of the limb. *Cell,* 75**,** 579-87.
NORVELL, S. M., ALVAREZ, M., BIDWELL, J. P. & PAVALKO, F. M. 2004. Fluid shear stress induces beta-catenin signaling in osteoblasts. *Calcif Tissue Int,* 75**,** 396-404.
NOWLAN, N. C., MURPHY, P. & PRENDERGAST, P. J. 2007. Mechanobiology of embryonic limb development. *Ann N Y Acad Sci,* 1101**,** 389-411.
NUÑEZ, F., BRAVO, S., CRUZAT, F., MONTECINO, M. & DE FERRARI, G. V. 2011. Wnt/β-Catenin Signaling Enhances Cyclooxygenase-2 (COX2) Transcriptional Activity in Gastric Cancer Cells. *PLoS ONE,* 6**,** e18562.
NUSSE, R. 1999. WNT targets. Repression and activation. *Trends Genet,* 15**,** 1-3.
NUSSE, R. 2008. Wnt signaling and stem cell control. *Cell Res,* 18**,** 523-7.
OISHI, I., SUZUKI, H., ONISHI, N., TAKADA, R., KANI, S., OHKAWARA, B., KOSHIDA, I., SUZUKI, K., YAMADA, G., SCHWABE, G. C., MUNDLOS, S., SHIBUYA, H., TAKADA, S. & MINAMI, Y. 2003. The receptor tyrosine kinase Ror2 is involved in non-canonical Wnt5a/JNK signalling pathway. *Genes Cells,* 8**,** 645-54.
OKOYE, U. C., MALBON, C. C. & WANG, H. Y. 2008. Wnt and Frizzled RNA expression in human mesenchymal and embryonic (H7) stem cells. *J Mol Signal,* 3**,** 16.
OREFFO, R. O., COOPER, C., MASON, C. & CLEMENTS, M. 2005. Mesenchymal stem cells: lineage, plasticity, and skeletal therapeutic potential. *Stem Cell Rev,* 1**,** 169-78.
ORIMO, H. 2010. The mechanism of mineralization and the role of alkaline phosphatase in health and disease. *J Nippon Med Sch,* 77**,** 4-12.
OSWALD, J., BOXBERGER, S., JORGENSEN, B., FELDMANN, S., EHNINGER, G., BORNHAUSER, M. & WERNER, C. 2004. Mesenchymal stem cells can be differentiated into endothelial cells in vitro. *Stem Cells,* 22**,** 377-84.
PAK, J. 2012. Autologous adipose tissue-derived stem cells induce persistent bone-like tissue in osteonecrotic femoral heads. *Pain Physician,* 15**,** 75-85.

PANYAM, J., ZHOU, W. Z., PRABHA, S., SAHOO, S. K. & LABHASETWAR, V. 2002. Rapid endo-lysosomal escape of poly(DL-lactide-co-glycolide) nanoparticles: implications for drug and gene delivery. *FASEB J,* 16**,** 1217-26.

PARK, J. 2012. *Biomaterials: An Introduction*, Springer US. Pages 1-5, 188-198

PATEL, A. J. & HONORE, E. 2001. Properties and modulation of mammalian 2P domain K+ channels. *Trends Neurosci,* 24**,** 339-46.

PATEL, A. J., HONORÉ, E., MAINGRET, F., LESAGE, F., FINK, M., DUPRAT, F. & LAZDUNSKI, M. 1998. A mammalian two pore domain mechano-gated S-like K+ channel. *The EMBO Journal,* 17**,** 4283-4290.

PATWARI, P. & LEE, R. T. 2008. Mechanical control of tissue morphogenesis. *Circ Res,* 103**,** 234-43.

PEROBNER, I., KAROW, M., JOCHUM, M. & NETH, P. 2012. LRP6 mediates Wnt/beta-catenin signaling and regulates adipogenic differentiation in human mesenchymal stem cells. *Int J Biochem Cell Biol,* 44**,** 1970-82.

PITTENGER, M. F., MACKAY, A. M., BECK, S. C., JAISWAL, R. K., DOUGLAS, R., MOSCA, J. D., MOORMAN, M. A., SIMONETTI, D. W., CRAIG, S. & MARSHAK, D. R. 1999. Multilineage potential of adult human mesenchymal stem cells. *Science,* 284**,** 143-7.

POLYAK, B., FISHBEIN, I., CHORNY, M., ALFERIEV, I., WILLIAMS, D., YELLEN, B., FRIEDMAN, G. & LEVY, R. J. 2008. High field gradient targeting of magnetic nanoparticle-loaded endothelial cells to the surfaces of steel stents. *Proceedings of the National Academy of Sciences of the United States of America,* 105**,** 698-703.

POMMERENKE, H., SCHREIBER, E., DURR, F., NEBE, B., HAHNEL, C., MOLLER, W. & RYCHLY, J. 1996. Stimulation of integrin receptors using a magnetic drag force device induces an intracellular free calcium response. *Eur J Cell Biol,* 70**,** 157-64.

POTIER, E., NOAILLY, J. & ITO, K. 2010. Directing bone marrow-derived stromal cell function with mechanics. *J Biomech,* 43**,** 807-17.

POWNALL, M. E. & ISAACS, H. V. 2010. *FGF Signalling in Vertebrate Development*, Morgan & Claypool. Pages 46-50

PRABHA, S., ZHOU, W. Z., PANYAM, J. & LABHASETWAR, V. 2002. Size-dependency of nanoparticle-mediated gene transfection: studies with fractionated nanoparticles. *Int J Pharm,* 244**,** 105-15.

PREMARATNE, G., NERIMETLA, R., MATLOCK, R., SUNDAY, L., HIKKADUWA KORALEGE, R. S., RAMSEY, J. D. & KRISHNAN, S. 2016. Stability, scalability, and reusability of a volume efficient biocatalytic system constructed on magnetic nanoparticles. *Catalysis Science & Technology,* 6**,** 2361-2369.

PROCKOP, D. J. 1997. Marrow stromal cells as stem cells for nonhematopoietic tissues. *Science,* 276**,** 71-4.

PUCHTLER, H., MELOAN, S. N. & TERRY, M. S. 1969. On the history and mechanism of alizarin and alizarin red S stains for calcium. *J Histochem Cytochem,* 17**,** 110-24.

PUERTAS, S., MOROS, M., FERNÁNDEZ-PACHECO, R., IBARRA, M. R., GRAZÚ, V. & FUENTE, J. M. D. L. 2010. Designing novel nano-immunoassays: antibody orientation versus sensitivity. *Journal of Physics D: Applied Physics,* 43**,** 474012.

Q A PANKHURST, J. C., S K JONES AND J DOBSON 2003. Applications of magnetic nanoparticles in biomedicine. *Journal of Physics D: Applied Physics,* 36**,** R167 - R 181.

QIANG, Y. W., SHAUGHNESSY, J. D., JR. & YACCOBY, S. 2008. Wnt3a signaling within bone inhibits multiple myeloma bone disease and tumor growth. *Blood,* 112**,** 374-82.

QIU, W., ANDERSEN, T. E., BOLLERSLEV, J., MANDRUP, S., ABDALLAH, B. M. & KASSEM, M. 2007. Patients with high bone mass phenotype exhibit enhanced osteoblast differentiation and inhibition of adipogenesis of human mesenchymal stem cells. *J Bone Miner Res,* 22**,** 1720-31.

QUARTO, N., BEHR, B. & LONGAKER, M. T. 2010. Opposite spectrum of activity of canonical Wnt signaling in the osteogenic context of undifferentiated and differentiated mesenchymal cells: implications for tissue engineering. *Tissue Eng Part A,* 16**,** 3185-97.

QUARTO, R., MASTROGIACOMO, M., CANCEDDA, R., KUTEPOV, S. M., MUKHACHEV, V., LAVROUKOV, A., KON, E. & MARCACCI, M. 2001. Repair of large bone defects with the use of autologous bone marrow stromal cells. *N Engl J Med,* 344**,** 385-6.

RADZICKA, A. & WOLFENDEN, R. 1996. Rates of Uncatalyzed Peptide Bond Hydrolysis in Neutral Solution and the Transition State Affinities of Proteases. *Journal of the American Chemical Society,* 118**,** 6105-6109.

RAISZ, L. G. 1999. Physiology and pathophysiology of bone remodeling. *Clin Chem,* 45**,** 1353-8.

RALPHS, J. R., WAGGETT, A. D. & BENJAMIN, M. 2002. Actin stress fibres and cell–cell adhesion molecules in tendons: organisation in vivo and response to mechanical loading of tendon cells in vitro. *Matrix Biology,* 21**,** 67-74.

RAMASWAMY, S., GRECO, J. B., ULUER, M. C., ZHANG, Z., ZHANG, Z., FISHBEIN, K. W. & SPENCER, R. G. 2009. Magnetic resonance imaging of chondrocytes labeled with superparamagnetic iron oxide nanoparticles in tissue-engineered cartilage. *Tissue Eng Part A,* 15**,** 3899-910.

RAO, T. P. & KUHL, M. 2010. An updated overview on Wnt signaling pathways: a prelude for more. *Circ Res,* 106**,** 1798-806.

RATTNER, A., HSIEH, J. C., SMALLWOOD, P. M., GILBERT, D. J., COPELAND, N. G., JENKINS, N. A. & NATHANS, J. 1997. A family of secreted proteins contains homology to the cysteine-rich ligand-binding domain of frizzled receptors. *Proc Natl Acad Sci U S A,* 94**,** 2859-63.

RAWADI, G., VAYSSIERE, B., DUNN, F., BARON, R. & ROMAN-ROMAN, S. 2003. BMP-2 controls alkaline phosphatase expression and osteoblast mineralization by a Wnt autocrine loop. *J Bone Miner Res,* 18**,** 1842-53.

REGARD, J. B., ZHONG, Z., WILLIAMS, B. O. & YANG, Y. 2012. Wnt signaling in bone development and disease: making stronger bone with Wnts. *Cold Spring Harb Perspect Biol,* 4.

RICKARD, D. J., SULLIVAN, T. A., SHENKER, B. J., LEBOY, P. S. & KAZHDAN, I. 1994. Induction of rapid osteoblast differentiation in rat bone marrow stromal cell cultures by dexamethasone and BMP-2. *Dev Biol,* 161**,** 218-28.

RIDDLE, R. C., TAYLOR, A. F., GENETOS, D. C. & DONAHUE, H. J. 2006. MAP kinase and calcium signaling mediate fluid flow-induced human mesenchymal stem cell proliferation. *Am J Physiol Cell Physiol,* 290**,** C776-84.

RIDDLE, R. D., ENSINI, M., NELSON, C., TSUCHIDA, T., JESSELL, T. M. & TABIN, C. 1995. Induction of the LIM homeobox gene Lmx1 by WNT7a establishes dorsoventral pattern in the vertebrate limb. *Cell,* 83**,** 631-40.

RIEHEMANN, K., SCHNEIDER, S. W., LUGER, T. A., GODIN, B., FERRARI, M. & FUCHS, H. 2009. Nanomedicine--challenge and perspectives. *Angew Chem Int Ed Engl,* 48**,** 872-97.

RIVELINE, D., ZAMIR, E., BALABAN, N. Q., SCHWARZ, U. S., ISHIZAKI, T., NARUMIYA, S., KAM, Z., GEIGER, B. & BERSHADSKY, A. D. 2001. Focal contacts as mechanosensors: externally applied local mechanical force induces growth of focal contacts by an mDia1-dependent and ROCK-independent mechanism. *J Cell Biol,* 153**,** 1175-86.

ROACH, H. I. 1990. Long-term organ culture of embryonic chick femora: a system for investigating bone and cartilage formation at an intermediate level of organization. *J Bone Miner Res,* 5**,** 85-100.

ROACH, H. I. 1997. New aspects of endochondral ossification in the chick: chondrocyte apoptosis, bone formation by former chondrocytes, and acid phosphatase activity in the endochondral bone matrix. *J Bone Miner Res,* 12**,** 795-805.

ROBERTS, S., MCCALL, I. W., DARBY, A. J., MENAGE, J., EVANS, H., HARRISON, P. E. & RICHARDSON, J. B. 2003. Autologous chondrocyte implantation for cartilage repair: monitoring its success by magnetic resonance imaging and histology. *Arthritis Res Ther,* 5**,** R60-73.

ROBINSON, J. A., CHATTERJEE-KISHORE, M., YAWORSKY, P. J., CULLEN, D. M., ZHAO, W., LI, C., KHARODE, Y., SAUTER, L., BABIJ, P., BROWN, E. L., HILL, A. A., AKHTER, M. P., JOHNSON, M. L., RECKER, R. R., KOMM, B. S. & BEX, F. J. 2006. Wnt/beta-catenin signaling is a normal physiological response to mechanical loading in bone. *J Biol Chem,* 281**,** 31720-8.

ROBLING, A. G., NIZIOLEK, P. J., BALDRIDGE, L. A., CONDON, K. W., ALLEN, M. R., ALAM, I., MANTILA, S. M., GLUHAK-HEINRICH, J., BELLIDO, T. M., HARRIS, S. E. & TURNER, C. H. 2008. Mechanical Stimulation of Bone in Vivo Reduces Osteocyte Expression of Sost/Sclerostin. *Journal of Biological Chemistry,* 283**,** 5866-5875.

ROHRS, S., KUTZNER, N., VLAD, A., GRUNWALD, T., ZIEGLER, S. & MULLER, O. 2009. Chronological expression of Wnt target genes Ccnd1, Myc, Cdkn1a, Tfrc, Plf1 and Ramp3. *Cell Biol Int,* 33**,** 501-8.

ROOSE, J., HULS, G., VAN BEEST, M., MOERER, P., VAN DER HORN, K., GOLDSCHMEDING, R., LOGTENBERG, T. & CLEVERS, H. 1999. Synergy between tumor suppressor APC and the beta-catenin-Tcf4 target Tcf1. *Science,* 285**,** 1923-6.

ROSHAN-GHIAS, A., LAMBERS, F. M., GHOLAM-REZAEE, M., MULLER, R. & PIOLETTI, D. P. 2011. In vivo loading increases mechanical properties of scaffold by affecting bone formation and bone resorption rates. *Bone,* 49**,** 1357-64.

ROSS, A. J., MAY-SIMERA, H., EICHERS, E. R., KAI, M., HILL, J., JAGGER, D. J., LEITCH, C. C., CHAPPLE, J. P., MUNRO, P. M., FISHER, S., TAN, P. L., PHILLIPS, H. M., LEROUX, M. R., HENDERSON, D. J., MURDOCH, J. N., COPP, A. J., ELIOT, M.-M., LUPSKI, J. R., KEMP, D. T., DOLLFUS, H., TADA, M., KATSANIS, N., FORGE, A. & BEALES, P. L. 2005. Disruption of Bardet-Biedl syndrome ciliary proteins perturbs planar cell polarity in vertebrates. *Nat Genet,* 37**,** 1135-1140.

ROSS, C. L., SIRIWARDANE, M., ALMEIDA-PORADA, G., PORADA, C. D., BRINK, P., CHRIST, G. J. & HARRISON, B. S. 2015. The effect of low-frequency electromagnetic field on human bone marrow stem/progenitor cell differentiation. *Stem Cell Research,* 15**,** 96-108.

RUBIN, C. T., SOMMERFELDT, D. W., JUDEX, S. & QIN, Y. 2001. Inhibition of osteopenia by low magnitude, high-frequency mechanical stimuli. *Drug Discov Today,* 6**,** 848-858.

RUOSLAHTI, E. 1996. RGD and other recognition sequences for integrins. *Annu Rev Cell Dev Biol,* 12**,** 697-715.

SADER, M., COULEAUD, P., CARPENTIER, G., GILLES, M.-E., BOUSSERRHINE, N., LIVET, A., CASCONE, I., DESTOUCHES, D., CORTAJARENA, A. L. & COURTY, J. 2015. Functionalization of Iron Oxide Magnetic Nanoparticles with the Multivalent Pseudopeptide N6l for Breast Tumor Targeting. *Journal of Nanomedicine & Nanotechnology,* 6.

SAFHOLM, A., LEANDERSSON, K., DEJMEK, J., NIELSEN, C. K., VILLOUTREIX, B. O. & ANDERSSON, T. 2006. A formylated hexapeptide ligand mimics the ability of Wnt-5a to impair migration of human breast epithelial cells. *J Biol Chem,* 281**,** 2740-9.

SALATA, O. 2004. Applications of nanoparticles in biology and medicine. *Journal of Nanobiotechnology,* 2**,** 1-6.

SANTOS, A., BAKKER, A. D., WILLEMS, H. M., BRAVENBOER, N., BRONCKERS, A. L. & KLEIN-NULEND, J. 2011. Mechanical loading stimulates BMP7, but not BMP2, production by osteocytes. *Calcif Tissue Int,* 89**,** 318-26.

SANTOS, A., BAKKER, A. D., ZANDIEH-DOULABI, B., SEMEINS, C. M. & KLEIN-NULEND, J. 2009. Pulsating fluid flow modulates gene expression of proteins involved in Wnt signaling pathways in osteocytes. *J Orthop Res,* 27**,** 1280-7.

SATOH, A., MAKANAE, A. & WADA, N. 2010. The apical ectodermal ridge (AER) can be re-induced by wounding, wnt-2b, and fgf-10 in the chicken limb bud. *Dev Biol,* 342**,** 157-68.

SATOH, W., MATSUYAMA, M., TAKEMURA, H., AIZAWA, S. & SHIMONO, A. 2008. Sfrp1, Sfrp2, and Sfrp5 regulate the Wnt/beta-catenin and the planar cell polarity pathways during early trunk formation in mouse. *Genesis,* 46**,** 92-103.

SAWAKAMI, K., ROBLING, A. G., AI, M., PITNER, N. D., LIU, D., WARDEN, S. J., LI, J., MAYE, P., ROWE, D. W., DUNCAN, R. L., WARMAN, M. L. & TURNER, C. H. 2006. The Wnt co-receptor LRP5 is essential for skeletal mechanotransduction but not for the anabolic bone response to parathyroid hormone treatment. *J Biol Chem,* 281**,** 23698-711.

SAXON, S. V., MARY JEAN ETTEN, E. D. G. N. P. F. T. & DR. ELIZABETH A. PERKINS, P. D. R. 2014. *Physical Change and Aging, Sixth Edition: A Guide for the Helping Professions*, Springer Publishing Company. Pages 37-49

SCHÄFER, R., BANTLEON, R., KEHLBACH, R., SIEGEL, G., WISKIRCHEN, J., WOLBURG, H., KLUBA, T., EIBOFNER, F., NORTHOFF, H., CLAUSSEN, C. D. & SCHLEMMER, H.-P. 2010. Functional investigations on human mesenchymal stem cells exposed to magnetic fields and labeled with clinically approved iron nanoparticles. *BMC Cell Biology,* 11**,** 1-17.

SCHERER, F., ANTON, M., SCHILLINGER, U., HENKE, J., BERGEMANN, C., KRUGER, A., GANSBACHER, B. & PLANK, C. 2002. Magnetofection: enhancing and targeting gene delivery by magnetic force in vitro and in vivo. *Gene Ther,* 9**,** 102-9.

SCHMIDT, C., POMMERENKE, H., DURR, F., NEBE, B. & RYCHLY, J. 1998. Mechanical stressing of integrin receptors induces enhanced tyrosine phosphorylation of cytoskeletally anchored proteins. *J Biol Chem,* 273**,** 5081-5.

SCHOFIELD, R. 1978. The relationship between the spleen colony-forming cell and the haemopoietic stem cell. *Blood Cells,* 4**,** 7-25.

SCHROEDER, T. M., JENSEN, E. D. & WESTENDORF, J. J. 2005. Runx2: a master organizer of gene transcription in developing and maturing osteoblasts. *Birth Defects Res C Embryo Today,* 75**,** 213-25.

SCHUIJERS, J., MOKRY, M., HATZIS, P., CUPPEN, E. & CLEVERS, H. 2014. Wnt-induced transcriptional activation is exclusively mediated by TCF/LEF. *EMBO J,* 33**,** 146-56.

SCHULTE, G. 2010. International Union of Basic and Clinical Pharmacology. LXXX. The Class Frizzled Receptors. *Pharmacological Reviews,* 62**,** 632-667.

SCHWARTZ, M. A. 1997. Integrins, Oncogenes, and Anchorage Independence. *The Journal of Cell Biology,* 139**,** 575-578.

SEMENOV, M., TAMAI, K. & HE, X. 2005. SOST is a ligand for LRP5/LRP6 and a Wnt signaling inhibitor. *J Biol Chem,* 280**,** 26770-5.

SEMENOV, M. V., TAMAI, K., BROTT, B. K., KUHL, M., SOKOL, S. & HE, X. 2001. Head inducer Dickkopf-1 is a ligand for Wnt coreceptor LRP6. *Curr Biol,* 11**,** 951-61.

SEMENOV, M. V., ZHANG, X. & HE, X. 2008. DKK1 antagonizes Wnt signaling without promotion of LRP6 internalization and degradation. *J Biol Chem,* 283**,** 21427-32.

SFEIR, C., HO, L., DOLL, B. A., AZARI, K. & HOLLINGER, J. O. 2005. Fracture Repair. *In:* LIEBERMAN, J. R. & FRIEDLAENDER, G. E. (eds.) *Bone Regeneration and Repair: Biology and Clinical Applications.* Totowa, NJ: Humana Press. Pages 21-44

SHAY-SALIT, A., SHUSHY, M., WOLFOVITZ, E., YAHAV, H., BREVIARIO, F., DEJANA, E. & RESNICK, N. 2002. VEGF receptor 2 and the adherens junction as a mechanical transducer in vascular endothelial cells. *Proc Natl Acad Sci U S A,* 99**,** 9462-7.

SHI, S. & GRONTHOS, S. 2003. Perivascular niche of postnatal mesenchymal stem cells in human bone marrow and dental pulp. *J Bone Miner Res,* 18**,** 696-704.

SHTUTMAN, M., ZHURINSKY, J., SIMCHA, I., ALBANESE, C., D'AMICO, M., PESTELL, R. & BEN-ZE'EV, A. 1999. The cyclin D1 gene is a target of the beta-catenin/LEF-1 pathway. *Proc Natl Acad Sci U S A,* 96**,** 5522-7.

SHUBAYEV, V. I., PISANIC, T. R., 2ND & JIN, S. 2009. Magnetic nanoparticles for theragnostics. *Adv Drug Deliv Rev,* 61**,** 467-77.

SIBOV, T. T., MIYAKI, L. A., MAMANI, J. B., MARTI, L. C., SARDINHA, L. R., PAVON, L. F., OLIVEIRA, D. M., CARDENAS, W. H. & GAMARRA, L. F. 2012. Evaluation of umbilical cord mesenchymal stem cell labeling with superparamagnetic iron oxide nanoparticles coated with dextran and complexed with Poly-L-lysine. *Einstein (Sao Paulo),* 10**,** 180-8.

SIMMONS, C. A., MATLIS, S., THORNTON, A. J., CHEN, S., WANG, C. Y. & MOONEY, D. J. 2003. Cyclic strain enhances matrix mineralization by adult human mesenchymal stem cells via the extracellular signal-regulated kinase (ERK1/2) signaling pathway. *J Biomech,* 36**,** 1087-96.

SINGH, V. 2014. *General Anatomy*, Elsevier Health Sciences APAC. Pages 70-81

SINHA, K. M. & ZHOU, X. 2013. Genetic and molecular control of Osterix in skeletal formation. *Journal of cellular biochemistry,* 114**,** 975-984.

SLUSARSKI, D. C., CORCES, V. G. & MOON, R. T. 1997a. Interaction of Wnt and a Frizzled homologue triggers G-protein-linked phosphatidylinositol signalling. *Nature,* 390**,** 410-3.

SLUSARSKI, D. C., YANG-SNYDER, J., BUSA, W. B. & MOON, R. T. 1997b. Modulation of embryonic intracellular Ca2+ signaling by Wnt-5A. *Dev Biol,* 182**,** 114-20.

SMITH, E. L., KANCZLER, J. M., GOTHARD, D., ROBERTS, C. A., WELLS, J. A., WHITE, L. J., QUTACHI, O., SAWKINS, M. J., PETO, H., RASHIDI, H., ROJO, L., STEVENS, M. M., EL HAJ, A. J., ROSE, F. R., SHAKESHEFF, K. M. & OREFFO, R. O. 2014a. Evaluation of skeletal tissue repair, part 1: assessment of novel growth-factor-releasing hydrogels in an ex vivo chick femur defect model. *Acta Biomater,* 10**,** 4186-96.

SMITH, E. L., KANCZLER, J. M., GOTHARD, D., ROBERTS, C. A., WELLS, J. A., WHITE, L. J., QUTACHI, O., SAWKINS, M. J., PETO, H., RASHIDI, H., ROJO, L., STEVENS, M. M., EL HAJ, A. J., ROSE, F. R., SHAKESHEFF, K. M. & OREFFO, R. O. 2014b. Evaluation of skeletal tissue repair, part 2: enhancement of skeletal tissue repair through dual-growth-factor-releasing hydrogels within an ex vivo chick femur defect model. *Acta Biomater,* 10**,** 4197-205.

SMITH, E. L., KANCZLER, J. M. & OREFFO, R. O. 2013. A new take on an old story: chick limb organ culture for skeletal niche development and regenerative medicine evaluation. *Eur Cell Mater,* 26**,** 91-106; discussion 106.

SMITH, E. L., KANCZLER, J. M., ROBERTS, C. A. & OREFFO, R. O. 2012. Developmental cues for bone formation from parathyroid hormone and parathyroid hormone-related protein in an ex vivo organotypic culture system of embryonic chick femora. *Tissue Eng Part C Methods,* 18**,** 984-94.

SMITH, E. L., RASHIDI, H., KANCZLER, J. M., SHAKESHEFF, K. M. & OREFFO, R. O. C. 2015. The Effects of 1α, 25-dihydroxyvitamin D3 and Transforming Growth Factor-β3 on Bone Development in an Ex Vivo Organotypic Culture System of Embryonic Chick Femora. *PLoS ONE,* 10**,** e0121653.

STAAL, F. J. T., VAN NOORT, M., STROUS, G. J. & CLEVERS, H. C. 2002. Wnt signals are transmitted through N-terminally dephosphorylated [beta]-catenin. *EMBO Rep,* 3**,** 63-68.

STANNARD, J. P., SCHMIDT, A. H. & KREGOR, P. J. 2007. *Surgical Treatment of Orthopaedic Trauma*, Thieme. Pages 59-64, 70-73, 77-82, 84-93

STEELE, D. G. & BRAMBLETT, C. A. 1988. *The Anatomy and Biology of the Human Skeleton*, Texas A&M University Press. Pages 4-5, 10-15

STEINAUER, K. K., GIBBS, I., NING, S., FRENCH, J. N., ARMSTRONG, J. & KNOX, S. J. 2000. Radiation induces upregulation of cyclooxygenase-2 (COX-2) protein in PC-3 cells. *Int J Radiat Oncol Biol Phys,* 48**,** 325-8.

STEVENS, M. M. 2008. Biomaterials for bone tissue engineering. *Materials Today,* 11**,** 18-25.

STEWART, K., WALSH, S., SCREEN, J., JEFFERISS, C. M., CHAINEY, J., JORDAN, G. R. & BERESFORD, J. N. 1999. Further characterization of cells expressing STRO-1 in cultures of adult human bone marrow stromal cells. *J Bone Miner Res,* 14**,** 1345-56.

STIEHLER, M., BUNGER, C., BAATRUP, A., LIND, M., KASSEM, M. & MYGIND, T. 2009. Effect of dynamic 3-D culture on proliferation, distribution, and osteogenic differentiation of human mesenchymal stem cells. *J Biomed Mater Res A,* 89**,** 96-107.

SUI, Y., CUI, Y., NIE, Y., XIA, G.-M., SUN, G.-X. & HAN, J.-T. 2012. Surface modification of magnetite nanoparticles using gluconic acid and their application in immobilized lipase. *Colloids and Surfaces B: Biointerfaces,* 93**,** 24-28.

SUKHAREV, S. & COREY, D. P. 2004. Mechanosensitive Channels: Multiplicity of Families and Gating Paradigms. *Science Signaling,* 2004**,** re4.
TAKAHASHI, K., SHANAHAN, M. D., COULTON, L. A. & DUCKWORTH, T. 1991. Fracture healing of chick femurs in tissue culture. *Acta Orthop Scand,* 62**,** 352-5.
TALELLI, M., RIJCKEN, C. J., LAMMERS, T., SEEVINCK, P. R., STORM, G., VAN NOSTRUM, C. F. & HENNINK, W. E. 2009. Superparamagnetic iron oxide nanoparticles encapsulated in biodegradable thermosensitive polymeric micelles: toward a targeted nanomedicine suitable for image-guided drug delivery. *Langmuir,* 25**,** 2060-7.
TALLQUIST, M. & KAZLAUSKAS, A. 2004. PDGF signaling in cells and mice. *Cytokine Growth Factor Rev,* 15**,** 205-13.
TAMAI, K., ZENG, X., LIU, C., ZHANG, X., HARADA, Y., CHANG, Z. & HE, X. 2004. A mechanism for Wnt coreceptor activation. *Mol Cell,* 13**,** 149-56.
TAN, S. D., DE VRIES, T. J., KUIJPERS-JAGTMAN, A. M., SEMEINS, C. M., EVERTS, V. & KLEIN-NULEND, J. 2007. Osteocytes subjected to fluid flow inhibit osteoclast formation and bone resorption. *Bone,* 41**,** 745-51.
TANABE, Y., SAITO, M., UENO, A., NAKAMURA, M., TAKEISHI, K. & NAKAYAMA, K. 2000. Mechanical stretch augments PDGF receptor beta expression and protein tyrosine phosphorylation in pulmonary artery tissue and smooth muscle cells. *Mol Cell Biochem,* 215**,** 103-13.
TANAKA, Y., NAKAYAMADA, S. & OKADA, Y. 2005. Osteoblasts and osteoclasts in bone remodeling and inflammation. *Curr Drug Targets Inflamm Allergy,* 4**,** 325-8.
TERSTAPPEN, G. C., GAVIRAGHI, G. & CARICASOLE, A. 2006. The Wnt signaling pathway as a target for the treatment of neurodegenerative disorders. *IDrugs,* 9**,** 35-8.
THANH, N. T. K. 2012. *Magnetic Nanoparticles: From Fabrication to Clinical Applications : Theory to Therapy, Chemistry to Clinic, Bench to Bedside*, CRC PressINC. Pages 480-498
THOMPSON, W. R., RUBIN, C. T. & RUBIN, J. 2012. Mechanical regulation of signaling pathways in bone. *Gene,* 503**,** 179-93.
TODT, W. L. & FALLON, J. F. 1984. Development of the apical ectodermal ridge in the chick wing bud. *J Embryol Exp Morphol,* 80**,** 21-41.
TOLWINSKI, N. S., WEHRLI, M., RIVES, A., ERDENIZ, N., DINARDO, S. & WIESCHAUS, E. 2003. Wg/Wnt signal can be transmitted through arrow/LRP5,6 and Axin independently of Zw3/Gsk3beta activity. *Dev Cell,* 4**,** 407-18.
TU, X., RHEE, Y., CONDON, K. W., BIVI, N., ALLEN, M. R., DWYER, D., STOLINA, M., TURNER, C. H., ROBLING, A. G., PLOTKIN, L. I. & BELLIDO, T. 2012. Sost downregulation and local Wnt signaling are required for the osteogenic response to mechanical loading. *Bone,* 50**,** 209-17.
TULLBERG-REINERT, H. & JUNDT, G. 1999. In situ measurement of collagen synthesis by human bone cells with a sirius red-based colorimetric microassay: effects of transforming growth factor beta2 and ascorbic acid 2-phosphate. *Histochem Cell Biol,* 112**,** 271-6.
TZIMA, E., IRANI-TEHRANI, M., KIOSSES, W. B., DEJANA, E., SCHULTZ, D. A., ENGELHARDT, B., CAO, G., DELISSER, H. & SCHWARTZ, M. A. 2005. A mechanosensory complex that mediates the endothelial cell response to fluid shear stress. *Nature,* 437**,** 426-431.
UMBHAUER, M., DJIANE, A., GOISSET, C., PENZO-MENDEZ, A., RIOU, J. F., BOUCAUT, J. C. & SHI, D. L. 2000. The C-terminal cytoplasmic Lys-thr-X-X-X-Trp motif in frizzled receptors mediates Wnt/beta-catenin signalling. *EMBO J,* 19**,** 4944-54.
VAES, B. L., DECHERING, K. J., VAN SOMEREN, E. P., HENDRIKS, J. M., VAN DE VEN, C. J., FEIJEN, A., MUMMERY, C. L., REINDERS, M. J., OLIJVE, W., VAN ZOELEN, E. J. & STEEGENGA, W. T. 2005. Microarray analysis reveals expression regulation of Wnt antagonists in differentiating osteoblasts. *Bone,* 36**,** 803-11.
VAN AMERONGEN, R., MIKELS, A. & NUSSE, R. 2008. Alternative Wnt Signaling Is Initiated by Distinct Receptors. *Science Signaling,* 1**,** re9.

VAN HIEL, M. B., VANDERSMISSEN, H. P., VAN LOY, T. & VANDEN BROECK, J. 2012. An evolutionary comparison of leucine-rich repeat containing G protein-coupled receptors reveals a novel LGR subtype. *Peptides,* 34**,** 193-200.

VAN LOY, T., VANDERSMISSEN, H. P., VAN HIEL, M. B., POELS, J., VERLINDEN, H., BADISCO, L., VASSART, G. & VANDEN BROECK, J. 2008. Comparative genomics of leucine-rich repeats containing G protein-coupled receptors and their ligands. *General and Comparative Endocrinology,* 155**,** 14-21.

VARASTEH, Z., ROSENSTRÖM, U., VELIKYAN, I., MITRAN, B., ALTAI, M., HONARVAR, H., ROSESTEDT, M., LINDEBERG, G., SÖRENSEN, J., LARHED, M., TOLMACHEV, V. & ORLOVA, A. 2014. The Effect of Mini-PEG-Based Spacer Length on Binding and Pharmacokinetic Properties of a 68Ga-Labeled NOTA-Conjugated Antagonistic Analog of Bombesin. *Molecules,* 19**,** 10455-10472.

VODYANIK, M. A., YU, J., ZHANG, X., TIAN, S., STEWART, R., THOMSON, J. A. & SLUKVIN, II 2010. A mesoderm-derived precursor for mesenchymal stem and endothelial cells. *Cell Stem Cell,* 7**,** 718-29.

VORONKOV, A. E., BASKIN, II, PALYULIN, V. A. & ZEFIROV, N. S. 2008. Molecular model of the Wnt protein binding site on the surface of dimeric CRD domain of the hFzd8 receptor. *Dokl Biochem Biophys,* 419**,** 75-8.

WAGNER, E. R., ZHU, G., ZHANG, B. Q., LUO, Q., SHI, Q., HUANG, E., GAO, Y., GAO, J. L., KIM, S. H., RASTEGAR, F., YANG, K., HE, B. C., CHEN, L., ZUO, G. W., BI, Y., SU, Y., LUO, J., LUO, X., HUANG, J., DENG, Z. L., REID, R. R., LUU, H. H., HAYDON, R. C. & HE, T. C. 2011. The therapeutic potential of the Wnt signaling pathway in bone disorders. *Curr Mol Pharmacol,* 4**,** 14-25.

WALKER, L. M., HOLM, A., COOLING, L., MAXWELL, L., OBERG, A., SUNDQVIST, T. & EL HAJ, A. J. 1999. Mechanical manipulation of bone and cartilage cells with 'optical tweezers'. *FEBS Lett,* 459**,** 39-42.

WANG, H.-Y., LIU, T. & MALBON, C. C. 2006. Structure-function analysis of Frizzleds. *Cellular Signalling,* 18**,** 934-941.

WANG, N., BUTLER, J. P. & INGBER, D. E. 1993. Mechanotransduction across the cell surface and through the cytoskeleton. *Science,* 260**,** 1124-7.

WANG, T.-H. & LEE, W.-C. 2003. Immobilization of proteins on magnetic nanoparticles. *Biotechnology and Bioprocess Engineering,* 8**,** 263-267.

WARD, D. F., JR., SALASZNYK, R. M., KLEES, R. F., BACKIEL, J., AGIUS, P., BENNETT, K., BOSKEY, A. & PLOPPER, G. E. 2007. Mechanical strain enhances extracellular matrix-induced gene focusing and promotes osteogenic differentiation of human mesenchymal stem cells through an extracellular-related kinase-dependent pathway. *Stem Cells Dev,* 16**,** 467-80.

WEI, Q., YOKOTA, C., SEMENOV, M. V., DOBLE, B., WOODGETT, J. & HE, X. 2007. R-spondin1 is a high affinity ligand for LRP6 and induces LRP6 phosphorylation and beta-catenin signaling. *J Biol Chem,* 282**,** 15903-11.

WHITE, A. P., VACCARO, A. R., HALL, J. A., WHANG, P. G., FRIEL, B. C. & MCKEE, M. D. 2007. Clinical applications of BMP-7/OP-1 in fractures, nonunions and spinal fusion. *Int Orthop,* 31**,** 735-41.

WILLERT, K., BROWN, J. D., DANENBERG, E., DUNCAN, A. W., WEISSMAN, I. L., REYA, T., YATES, J. R., 3RD & NUSSE, R. 2003. Wnt proteins are lipid-modified and can act as stem cell growth factors. *Nature,* 423**,** 448-52.

WILLERT, K. & NUSSE, R. 2012. Wnt proteins. *Cold Spring Harb Perspect Biol,* 4**,** a007864.

WIMPENNY, I., MARKIDES, H. & EL HAJ, A. J. 2012. Orthopaedic applications of nanoparticle-based stem cell therapies. *Stem Cell Research & Therapy,* 3**,** 1-12.

WOHL, G. R., TOWLER, D. A. & SILVA, M. J. 2009. Stress fracture healing: fatigue loading of the rat ulna induces upregulation in expression of osteogenic and angiogenic genes that mimic the intramembranous portion of fracture repair. *Bone,* 44**,** 320-30.

WONG, H. C., BOURDELAS, A., KRAUSS, A., LEE, H. J., SHAO, Y., WU, D., MLODZIK, M., SHI, D. L. & ZHENG, J. 2003. Direct binding of the PDZ domain of Dishevelled to a conserved internal sequence in the C-terminal region of Frizzled. *Mol Cell,* 12**,** 1251-60.

WU, G., XU, G., SCHULMAN, B. A., JEFFREY, P. D., HARPER, J. W. & PAVLETICH, N. P. 2003. Structure of a beta-TrCP1-Skp1-beta-catenin complex: destruction motif binding and lysine specificity of the SCF(beta-TrCP1) ubiquitin ligase. *Mol Cell,* 11**,** 1445-56.

WU, R., LIU, G., BHARADWAJ, S. & ZHANG, Y. 2013. Isolation and myogenic differentiation of mesenchymal stem cells for urologic tissue engineering. *Methods Mol Biol,* 1001**,** 65-80.

XU, Q., WANG, Y., DABDOUB, A., SMALLWOOD, P. M., WILLIAMS, J., WOODS, C., KELLEY, M. W., JIANG, L., TASMAN, W., ZHANG, K. & NATHANS, J. 2004. Vascular development in the retina and inner ear: control by Norrin and Frizzled-4, a high-affinity ligand-receptor pair. *Cell,* 116**,** 883-95.

YAMAMOTO, A., NAGANO, T., TAKEHARA, S., HIBI, M. & AIZAWA, S. 2005. Shisa promotes head formation through the inhibition of receptor protein maturation for the caudalizing factors, Wnt and FGF. *Cell,* 120**,** 223-35.

YAMAMOTO, H., KOMEKADO, H. & KIKUCHI, A. 2006. Caveolin is necessary for Wnt-3a-dependent internalization of LRP6 and accumulation of beta-catenin. *Dev Cell,* 11**,** 213-23.

YASHIRO, K., ZHAO, X., UEHARA, M., YAMASHITA, K., NISHIJIMA, M., NISHINO, J., SAIJOH, Y., SAKAI, Y. & HAMADA, H. 2004. Regulation of retinoic acid distribution is required for proximodistal patterning and outgrowth of the developing mouse limb. *Dev Cell,* 6**,** 411-22.

YIU, H. H. 2011. Engineering the multifunctional surface on magnetic nanoparticles for targeted biomedical applications: a chemical approach. *Nanomedicine (Lond),* 6**,** 1429-46.

YONEI-TAMURA, S., ENDO, T., YAJIMA, H., OHUCHI, H., IDE, H. & TAMURA, K. 1999. FGF7 and FGF10 directly induce the apical ectodermal ridge in chick embryos. *Dev Biol,* 211**,** 133-43.

YOSHIKAWA, S., MCKINNON, R. D., KOKEL, M. & THOMAS, J. B. 2003. Wnt-mediated axon guidance via the Drosophila Derailed receptor. *Nature,* 422**,** 583-8.

YOU, L., TEMIYASATHIT, S., LEE, P., KIM, C. H., TUMMALA, P., YAO, W., KINGERY, W., MALONE, A. M., KWON, R. Y. & JACOBS, C. R. 2008. Osteocytes as Mechanosensors in the Inhibition of Bone Resorption Due to Mechanical Loading. *Bone,* 42**,** 172-179.

YOUREK, G., MCCORMICK, S. M., MAO, J. J. & REILLY, G. C. 2010. Shear stress induces osteogenic differentiation of human mesenchymal stem cells. *Regen Med,* 5**,** 713-24.

ZAMAN, G., DALLAS, S. L. & LANYON, L. E. 1992. Cultured embryonic bone shafts show osteogenic responses to mechanical loading. *Calcif Tissue Int,* 51**,** 132-6.

ZAMANI, A., OMRANI, G. R. & NASAB, M. M. 2009. Lithium's effect on bone mineral density. *Bone,* 44**,** 331-4.

ZENG, X., TAMAI, K., DOBLE, B., LI, S., HUANG, H., HABAS, R., OKAMURA, H., WOODGETT, J. & HE, X. 2005. A dual-kinase mechanism for Wnt co-receptor phosphorylation and activation. *Nature,* 438**,** 873-7.

ZHOU, H., MAK, W., KALAK, R., STREET, J., FONG-YEE, C., ZHENG, Y., DUNSTAN, C. R. & SEIBEL, M. J. 2009. Glucocorticoid-dependent Wnt signaling by mature osteoblasts is a key regulator of cranial skeletal development in mice. *Development,* 136**,** 427-36.

ZHU, K., ZHANG, Y., HE, S., CHEN, W., SHEN, J., WANG, Z. & JIANG, X. 2012. Quantification of proteins by functionalized gold nanoparticles using click chemistry. *Anal Chem,* 84**,** 4267-70.

ZIROS, P. G., BASDRA, E. K. & PAPAVASSILIOU, A. G. 2008. Runx2: of bone and stretch. *Int J Biochem Cell Biol,* 40**,** 1659-63.

Appendix A: hMSC characterisation

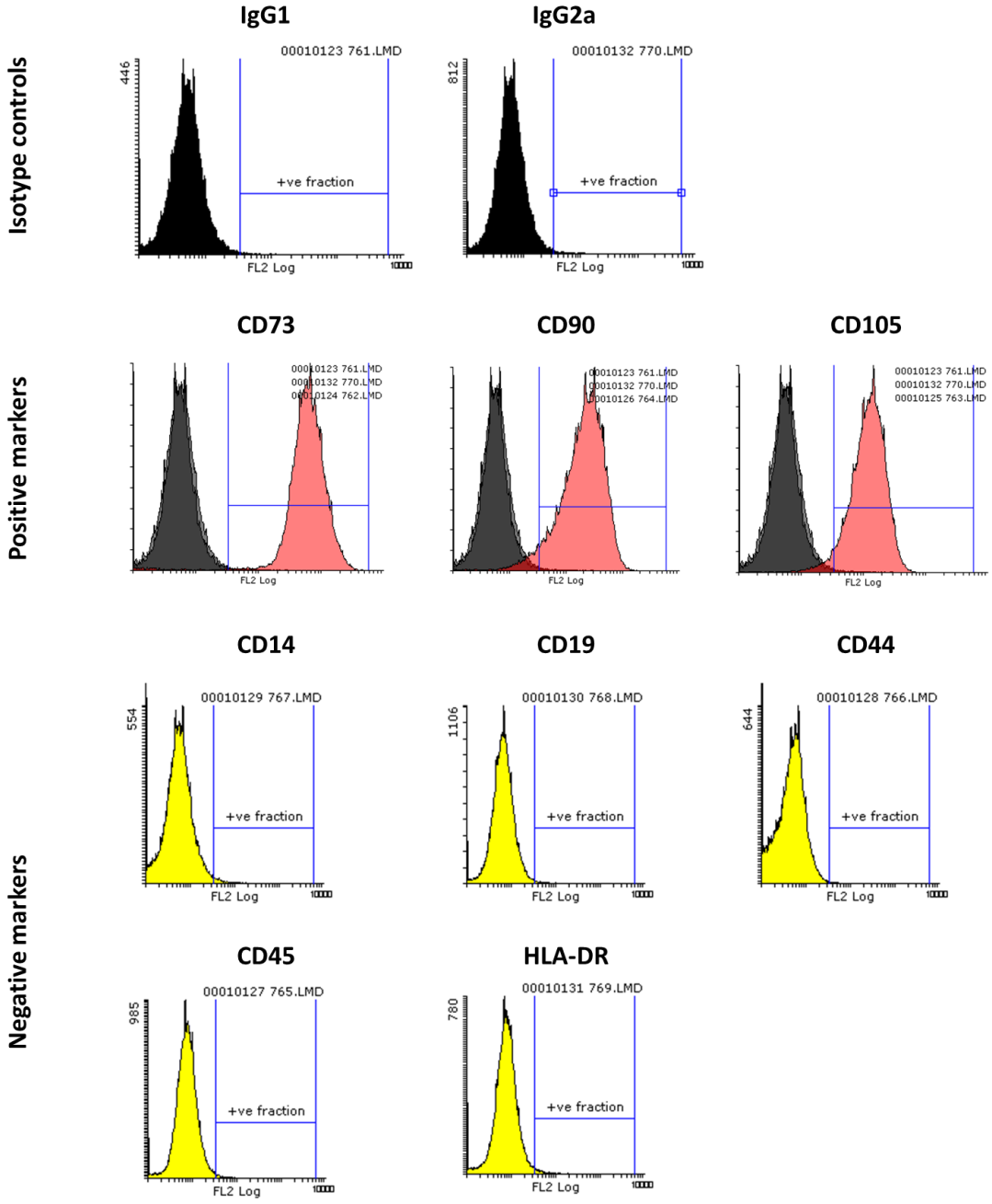

Figure A.1. hMSC surface marker characterisation.
MSC surface marker expression was analysed by flow cytometry to confirm the presence of MSC markers CD73, CD90 and CD105 and the absence of CD14, CD19, CD44, CD45 and HLA-DR. Each marker displays the result of a minimum of $5X10^4$ events. This experiment was performed by J. Price (Keele University)

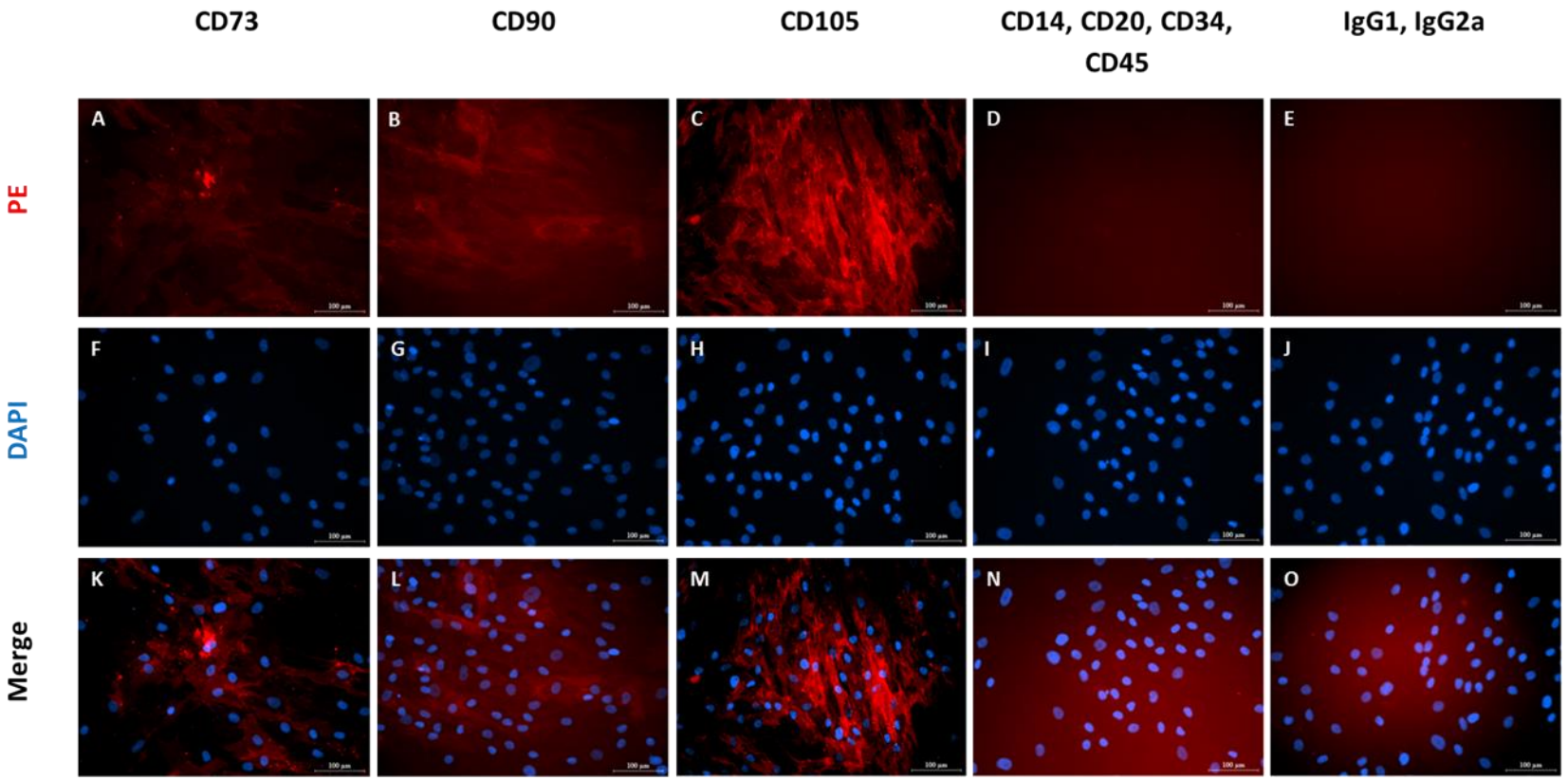

Figure A.2. hMSC marker expression.
Immunofluorescence images for CD marker expression showing bone-marrow derived hMSC are positive for hMSC markers CD73 (A), CD90 (B) and CD105 (C). Cells were negative for haematopoietic markers CD14, CD20, CD34 and CD45 (D). IgG Isotype controls were also negative (E). Cells nuclei are shown by DAPI staining (F-J), Merged images are shown K-O. Representative images of n=3 shown, scale bar represents 100µm.

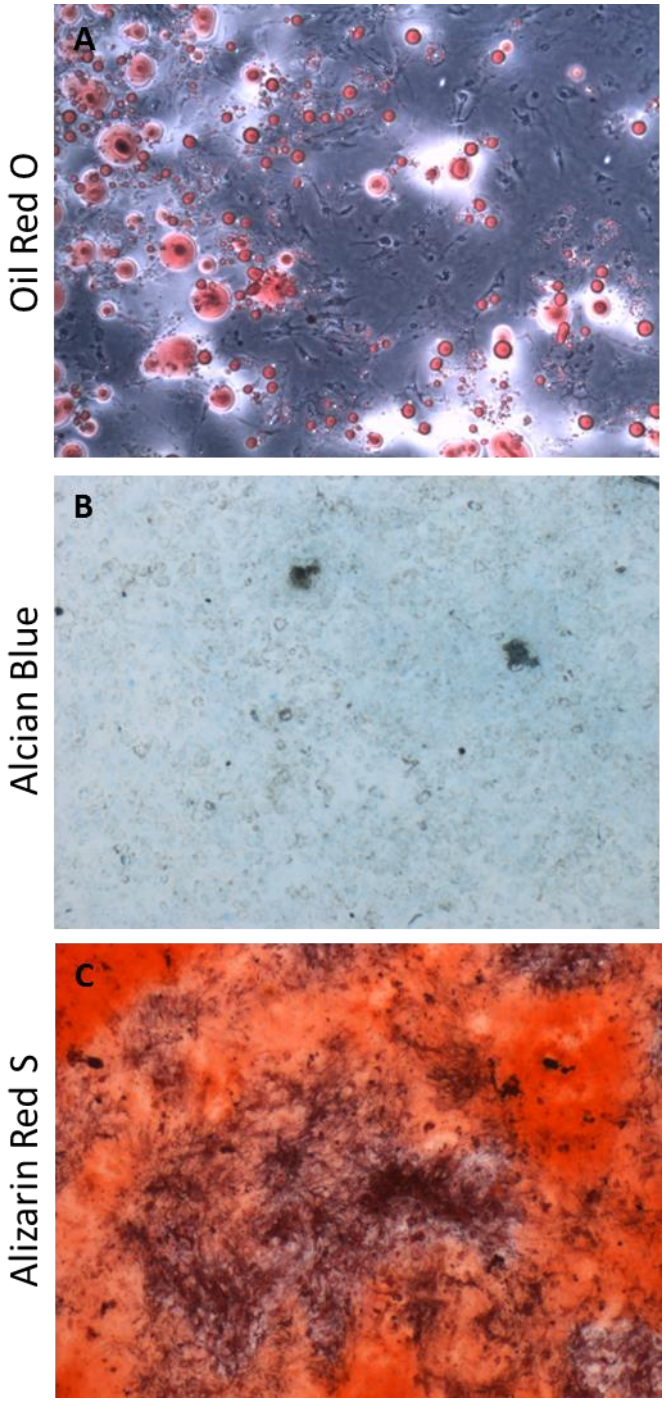

Figure A.3. hMSC tri-lineage histological staining.
Histological staining of hMSC after 21 days culture in differentiation media. Cells cultured in adipogenic differentiation media were positive for lipid droplets as shown by Oil red O staining (A). Cells cultured in chondrogenic media were positive for GAG's as shown by Alcian blue staining (B). Cells cultured in osteogenic media were positive for calcium as shown by Alizarin Red S staining (C). Representative images of n=3 shown. This experiment was performed by S. Moise (Keele University).

Appendix B: Standard curves

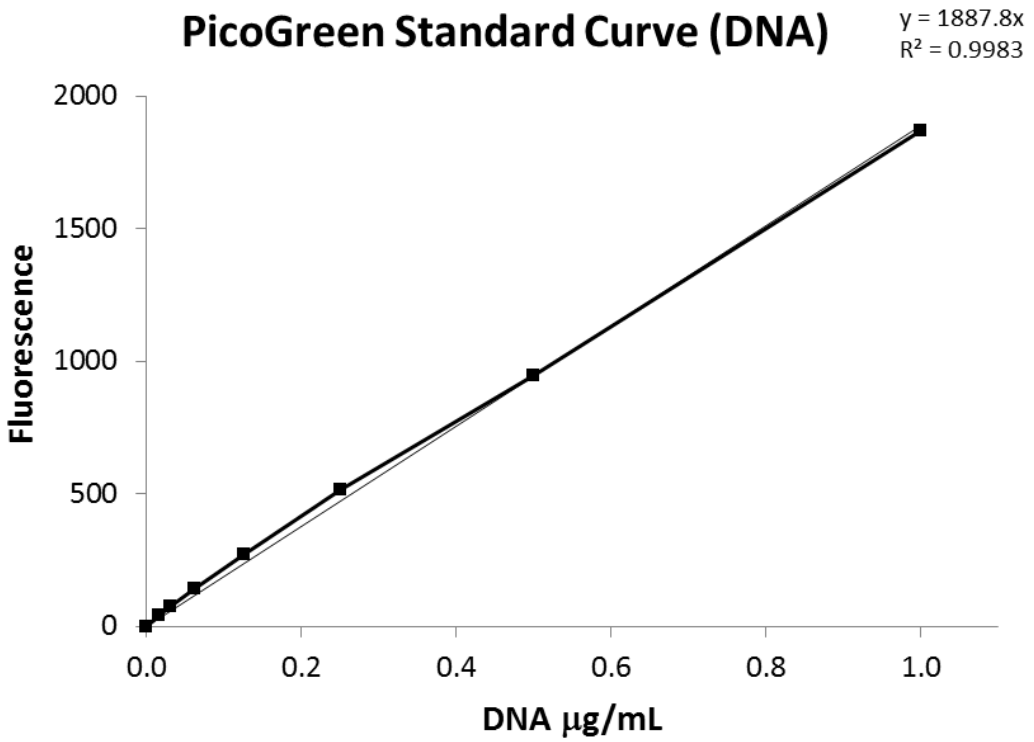

Figure B.1. Standard curve for DNA in TE buffer using PicoGreen assay.

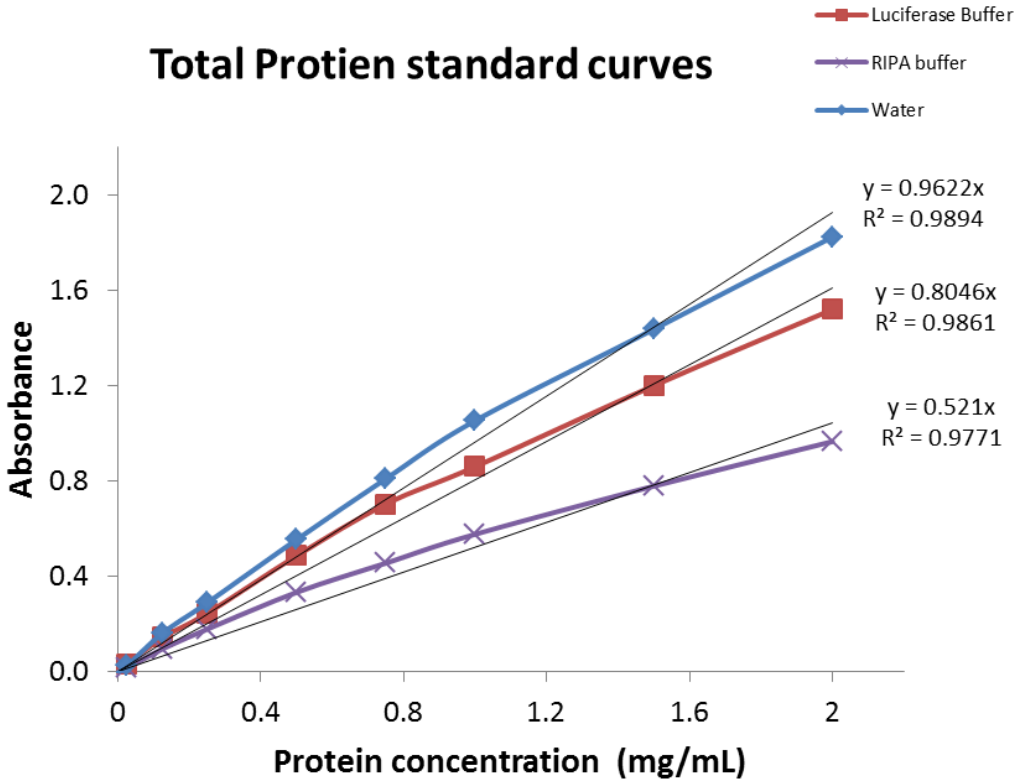

Figure B.2. Standard curves of Bovine Serum Albumin acquired in different buffers.

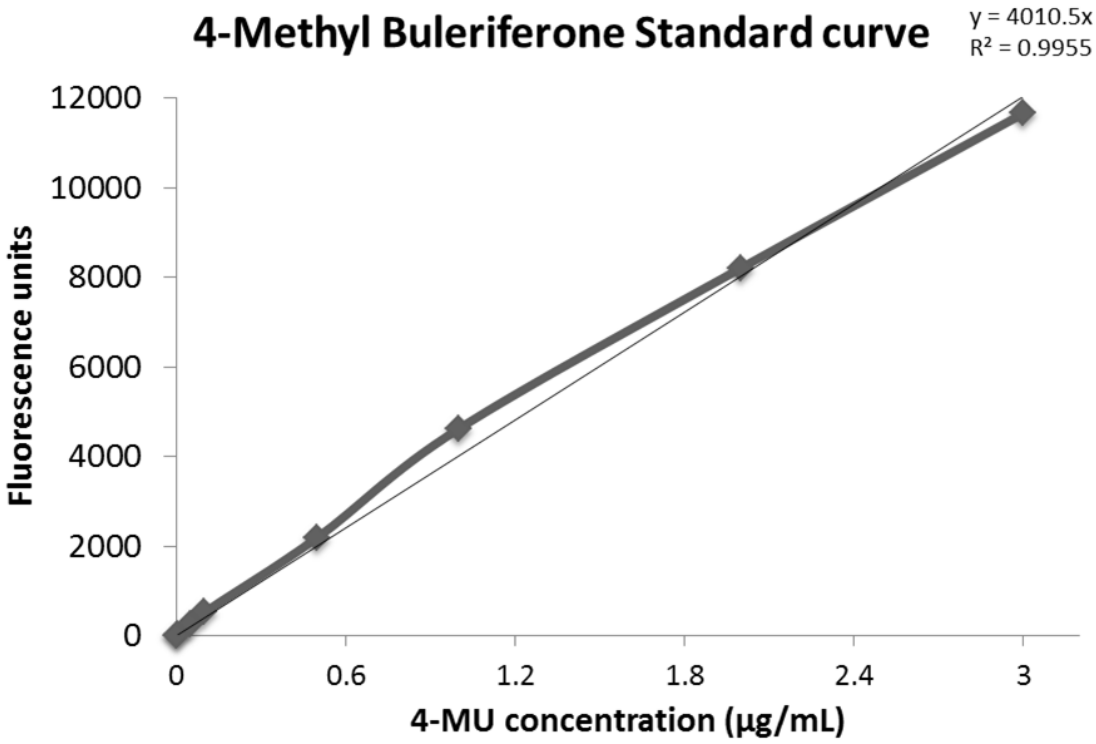

Figure B.3. Standard curve of 4-Methylumbelliferone in Diethanolamine buffer for the quantification of Alkaline Phosphatase activity.

Appendix C: Extended Methods

Extraction of total RNA using RNAeasy kit

Cells were lysed with addition of 350µL of buffer RLT for 10mins. 350µL of 70% EtOH was added to each well and mixed. Lysates were then transferred to RNAeasy mini-spin columns and centrifuged at 8000g for 15s, the flow through was discarded. 700µL of Buffer RW1 was added to the columns and samples centrifuged at 8000gfor 15s, the flow through was discarded. 500µL of Buffer RPE was added to each column and samples centrifuged at 8000gfor 15s, the flow through was discarded. Another 500µL of Buffer RPE was added to each column and samples were centrifuged at 8000g for 2mins, the flow through was discarded. Centrifugation was repeated at 12,000rpm for 1mins, the flow through was discarded. 17µL of H_20 was added to each column and centrifuged at 8000g for 1min to elute the RNA. The flow through was added back to the column and re-centrifuged at 8000g for 1min to complete RNA elution. RNA quality and concentration was determined by spectrophotometric analysis using absorbance at 260 nm and 280 nm respectively.

Extraction of total RNA using TRI reagent

Cells were lysed using 1mL of Tri reagent per well for 10mins. Lysate was homogenised by passing through a pipette several times collected in sample tubes and vortexed for 15s. Samples were incubated for 5mins. 0.2mL of chloroform was added to each sample then vortexed for 15s. Samples were incubated for 5mins then centrifuged at 12000g for 15mins at 4^oC. The upper colourless aqueous phase was transferred to a new sample tube. RNA was precipitated with the addition of 0.5mL of 2-Propanol per sample. Samples were incubated 10mins then centrifuged at 12000g for 10mins at 4^oC. The supernatant

was removed and the RNA pellet was washed with 1mL of 75% EtOH. Samples were mixed then centrifuged at 12000g for 5mins at 4^{o}C. The supernatant was removed and samples allowed to air dry for 5mins. RNA was dissolved in 17µL H_2O. RNA quality and concentration was determined by spectrophotometric analysis using absorbance at 260 nm and 280 nm respectively.

cDNA synthesis using High capacity cDNA Reverse transcription kit (Applied Biosystems)

A reverse transcription (RT) master mix was prepared on ice as detailed below:

Component	Volume per reaction (µL)
10x Reverse Transcription buffer	2
25x dNTP mix	0.8
10x Reverse Transcription random primers	2
Reverse Transcriptase	1
H_20	4.2
Total	10

Table C.1. Reverse Transcription master mix components

10µL of RT master mix was aliquoted into reaction tubes. The appropriate amounts of extracted RNA were added to the RT master mix. Tubes were sealed and samples kept on ice until thermocycling. Reverse transcription was performed under the conditions detailed below. Samples were stored at -20^{o}C until further use.

	Step 1	Step 2	Step 3	Step 4
Temperature (°C)	25	37	85	4
Time (mins)	10	120	5	Hold

Table C.2. Reverse Transcription thermocycling conditions

RT-PCR and qPCR primer details

Primer	**Catalogue no.**	**Gene**	**Detected Transcript**	**Amplicon length**
Hs_FZD2_1_SG	QT00208208	FZD2	NM_001466 (3834 bp)	141 bp
Hs_GAPDH_2_SG	QT01192646	GAPDH	NM_002046 (1421 bp) NM_001289745 (1513 bp)	119 bp 211 bp
Hs_PTGS2_1_SG	QT00040586	PTGS2	NM_000963 (4507 bp)	68 bp
Hs_MYC_1_SG	QT00035406	MYC	NM_002467 (2379 bp)	129 bp
Hs_NFKB1_1_SG	QT00063791	NFKB1	NM_001165412 (4090 bp) NM_003998 (4093 bp) XM_005263029 (4007 bp) XM_006714229 (3642 bp)	68 bp 68 bp 68 bp 68 bp

Table C.3. Qiagen primer details

Western blotting lysis buffer recipe

Component	Working Concentration
Pepstatin A (Sigma)	1µM
PMSF (Sigma)	1mM
Protease inhibitor cocktail mix (Sigma)	1x
Sodium vanadate	1mM
Sodium Fluoride	40mM
RIPA buffer (Sigma)	1x

Table C.4. Western blotting cell lysis buffer components

Preparation of Wnt 3A conditioned media

Mouse L-M(TK-) cells that overexpress Wnt 3A (LGC standards) were seeded into T75 flasks and cultured in 10mL of basal media (High Glucose DMEM, 10% FBS, 1% Pen/Strep, 1% L-Glutamine) until confluent. The media was then removed and stored. 10mL of fresh media was added to the flasks and cells cultured for a further 3 days. The media was removed, mixed with the first batch of media 1:1, sterile filtered and stored at -20^{o}C until further use.